604261
p. 188

R82AEB406

NASA CR-168289

NASA

National Aeronautics and
Space Administration

NASA Lewis Research Center

P-173
#304579

ENERGY EFFICIENT ENGINE
HIGH PRESSURE TURBINE COMPONENT TEST PERFORMANCE REPORT

By

L.P. TIMKO

GENERAL ELECTRIC COMPANY

Contract NAS3-20643

Prepared for

National Aeronautics and Space Administration

1. Report No.
NASA CR-168289

2. Government Accession No.

3. Recipient's Catalog No.

4. Title and Subtitle
Energy Efficient Engine
High Pressure Turbine Component Test
Performance Report

5. Report Date

6. Performing Organization Code

7. Author(s)
L. P. Timko

8. Performing Organization Report No.
R82AEB406

9. Performing Organization Name and Address
General Electric Company
Aircraft Engine Group
Cincinnati, Ohio 45215

10. Work Unit No.

11. Contract or Grant No.
NAS3-20643

12. Sponsoring Agency Name and Address
NASA-Lewis Research Center
21000 Brookpark Road
Cleveland, Ohio 44135

13. Type of Report and Period Covered

14. Sponsoring Agency Code

15. Supplementary Notes
NASA Project Manager - Mr. C.C. Ciepluch
NASA Project Engineer - Mr. R.P. Dengler
G.E. Project Manager - Mr. R.W. Bucy

16. Abstract

The high pressure turbine for the General Electric Energy Efficient Engine is a two stage design of moderate loading. Results of detailed system studies led to selection of this configuration as the most appropriate in meeting the efficiency goals of the component development program.

To verify the design features of the high pressure turbine, a full scale warm air turbine test rig with cooling flows simulated was run. Prior to this testing, an annular cascade test was run to select vane unguided turn for the first stage nozzle. Results of this test showed the base configuration to exceed the lower unguided turning configuration by 0.48 percent in vane kinetic energy efficiency.

The air turbine test program, consisting of extensive mapping and cooling flow variation as well as design point evaluation, demonstrated a design point efficiency level of 90.0% based on the thermodynamic definition. In terms of General Electric cycle definition, this efficiency was 92.5%. Based on this test, it is concluded that efficiency goals for the Flight Propulsion System have been met.

17. Key Words (Suggested by Author(s))
Vane Annular Cascade Test
Air Turbine Test
Two Stage, Cooled Vane

18. Distribution Statement
[redacted]

[redacted]

19. Security Classif. (of this report)	20. Security Classif. (of this page)	21. No. of Pages	22. Price*
Unclassified	Unclassified.		

[redacted]

TABLE OF CONTENTS

LIST OF ILLUSTRATIONS

LIST OF ILLUSTRATIONS (Continued)

LIST OF ILLUSTRATIONS (Continued)

LIST OF ILLUSTRATIONS (Continued)

LIST OF TABLES

LIST OF SYMBOLS

C_o	Theoretical velocity obtained by expanding flow from turbine inlet total enthalpy to ideal exit enthalpy, m/sec (ft/sec)
C_p	Specific heat at constant pressure, Joules/(kgK), (Btu/(lbm °R))
g	Gravitational constant, 32.2 (lbm ft)/(lbf sec^2)
H	Turbine shaft power, Watts (Btu/sec)
H'	Power to pump rotor coolant, Watts (Btu/sec)
h	Specific enthalpy, Joules/kg, (Btu/lbm)
J	Joule's constant, 778.2 ft-lbf/Btu
l	Characteristic length, Cm, (in.)
M	Mach number
N	Rotational speed, radians/sec. (rpm)
P	Pressure, Pascals (psia)
r	Radius, cm, (in.)
Re	Reynolds Number
Rx	Reaction
T	Temperature, K (°R)
TQ	Shaft torque, Joules (Btu)
U	Wheel speed, m/sec (ft/sec)
V	Velocity, m/sec (ft/sec)
W	Mainstream flow rate, kg/sec (lbm/sec)
W_c	Coolant flow rate, kg/sec (lbm/sec)
X	Axial distance, cm, (in.)
Y	Tangential distance, cm, (in.)
Γ	Turbine exit absolute flow angle, degrees
γ	Ratio of specific heats
η_v	Efficiency, Nozzle, local
$\bar{\eta}_v$	Efficiency, Nozzle, average
η_{GE}	Efficiency, General Electric
η_{TH}	Efficiency, Thermodynamic
η_{THP}	Efficiency, Thermodynamic with rotor coolant pump power
μ	Absolute viscosity, kg/(sec. m), (lbm/(sec.ft))
ρ	Mass density, kg/cm^3, (lbm/in^3)
ψ_p	Aerodynamic loading at pitchline, $(\Delta h)/(2\Sigma U_p^{\,2})$

Subscripts

a	Isentropic available
c	Coolant
CDL	Simulated Compressor Discharge
equ	Equivalent
h	Hub
IND,ind	Inducer (tangential accelerator)
NC	Non-chargeable (flow going through stage one vane throat)
OB2	Stage two outer band
p	Pitchline, peak
S	Static conditions
T	Total conditions
t	Tip
u	Tangential component
0,4	Turbine inlet plane
1,41	Rotor inlet plane
2	Stage exit plane, airfoil exit plane
42	Turbine exit plane

1.0 SUMMARY

The high pressure turbine for the General Electric Energy Efficient Engine is a two stage, low thru-flow design of moderate loading. Results of detailed system studies led to selection of this configuration as the most appropriate in meeting the efficiency goals of the component development program.

To verify the design features of the high pressure turbine, a full scale warm air turbine test rig with cooling flows simulated was run. Prior to this testing, an annular cascade test was run to select vane unguided turning for the first stage nozzle. Results of this test showed the base configuration of 8.4 degrees to exceed the lower unguided turning configuration by 0.48 percent in vane kinetic energy efficiency.

The air turbine test program, consisting of extensive mapping and cooling flow variation as well as design point evaluation, demonstrated a design point efficiency level of 90.0% based on the thermodynamic definition with pump power credited to the turbine. In terms of General Electric cycle definition, efficiency was 92.5%. Based on this test, it is concluded that efficiency goals for the Flight Propulsion System (FPS) have been met.

2.0 INTRODUCTION

The NASA/GE Energy efficient Engine (E^3) Component Development and Integration Program was initiated on January 2, 1978. The program objective is to develop technology that will improve the energy efficiency of propulsion systems for subsonic commercial aircraft of the late 1980's or early 1990's.

The goals of the program are: a reduction in Flight Propulsion System (FPS) cruise installed sfc of at least 12% compared to the reference CF6-50C engine; a reduction in direct operating cost (DOC) of at least 5% based on advanced aircraft with E^3-type improvements compared to a scaled CF6-50C; to meet noise and emissions standards per FAR-Part 36 (as amended July 1978) and EPA new engine standards for January, 1981 respectively.

Four major technical tasks have been established for the E^3 program. Task 1 addresses the design and evaluation of the E^3 Flight Propulsion System; this propulsion system and associated flight nacelle is designed to meet the requirements for commercial service. The Task 1 results will establish the requirements for the experimental test hardware including the components, core, and integrated core/low spool. Task 2 consists of the design, fabrication, and testing of the components and includes supporting technology efforts. The supporting technology efforts are to be performed where required to provide verification of advanced concepts included in the propulsion system design. In addition, more advanced technologies that are not specifically included in the propulsion system design but which provide the potential for added performance improvements are to be explored also. Task 3 involves the design, fabrication, and test evaluation of a core engine consisting of the compressor, combustor, and high pressure turbine. Integration of the core with the low spool components and test evaluation of the integrated core/low spool (ICLS) comprise the Task 4 efforts. At the conclusion of the program, all performance data obtained for the experimental hardware (ICLS, core and component efforts) will be appraised and factored into a final propulsion system/aircraft design (as part of continual, ongoing evaluations in Task 1) to ascertain achievable performance as compared to program goals.

One major element of Task 2 was the aerodynamic evaluation of the high pressure turbine. This evaluation consisted of full scale, warm air annular cascade testing of the stage one vane and warm air turbine testing of the two stage group.

The objective of the stage one nozzle annular cascade program was to select a vane configuration for the air turbine rig. This selection was based on efficiency level determined by cascade testing. To this purpose, two vane configurations were designed to the same vector diagrams and flowpath. The primary difference between the two vanes was the amount of unguided turning. The base vane had a nominal value of 8.4° at the pitch-line. The alternate candidate had a lower unguided turning (LUT) of 5.5°. Each airfoil configuration was tested over a range of pressure ratios to determine the performance characteristics. Since the base vane exhibited a higher performance at design pressure ratio, it was selected for the air turbine rig and the ICLS.

The objective of the air turbine rig test was to evaluate the aerodynamic performance of the high pressure turbine. This was accomplished by determining the design point efficiency and by mapping the turbine over a large range of operation extending into the sub-idle, starting regions of the engine. Additional testing included blade tip clearance variation, Reynolds number variation, and cooling flow variation. Rig hardware was full scale at rig running conditions.

This report presents the results of the annular cascade and two-stage turbine rig testing.

3.0 TURBINE DESCRIPTION

3.1 Turbine Aerodynamic Design

To meet the requirements of the E^3 engine cycle, a two stage, low thru-flow high pressure turbine design of moderate loading was selected. Aerodynamic design point was the integrated core/low spool (ICLS) cycle point at maximum climb (M .8, 10.67km (35,000 ft)). These design reguirements are presented in Table I.

The turbine flowpath geometry and number of airfoils per stage were determined from preliminary design and subsequent trade studies. These trade studies also provided data and information for the selection of annulus area and the work split for the two stages. Details of these studies are found in Reference 1. Stage reaction levels were initially set consistent with other GE commercial engines with final values reflecting adjustment to trim rotor thrust balance. A summary of stage aerodynamic parameters is presented in Table II. The final hot flowpath developed is shown in Figure 1. The hot radii dimensions are the same for both the engine and rig designs.

The through-flow analysis was performed using a method that solves the full three-dimensional, radial equilibrium equation for circumferentially averaged flow. The procedure accounts for streamline slope and curvature, effect of radial blade force component due to airfoil sweep and dihedral, airfoil blockage, and radial gradients of flow properties. Calculations were made with radial gradients of blading losses, and also with local flow addition to simulate cooling flow injection. Temperature dilution, and momentum mixing losses associated with coolant addition were accounted for. Airfoil inlet angle selection considered mixing between streamtubes, combustor temperature profile and secondary flow effects. Final blading flow angles and Mach numbers are presented in Table III and the radial distributions are shown in Figure 2.

Airfoil cascade analysis was accomplished by a streamtube curvature method which calculated along a stream surface determined from the through-flow analysis, accounting for variations in streamtube thickness. Airfoil

Table I. Turbine Design Requirements at ICLS Max Climb (M0.8, 10.67 km (35000 ft))

Item	Units		ICLS	
Rotor Inlet Temperature, $T_{T,41}$	K ,	(°R)	1588	(2858)
Flow Function, $W_{41}\sqrt{T_{T,41}}\ P_{T,4}$	$\frac{kg\sqrt{K}}{sec\ kPa}$,	$\left(\frac{lbm\sqrt{°R}}{sec\ psia}\right)$	0.866	(17.66)
Corrected Speed, $N\sqrt{T_{T,41}}$	$\frac{rad}{sec\ \sqrt{K}}$,	$\left(\frac{rpm}{\sqrt{°R}}\right)$	33.19	(236.2)
Energy Function $\Delta h/T_{T,41}$	$\frac{Joules}{kg\ K}$,	$\left(\frac{Btu}{lbm\ °R}\right)$	353.3	(0.0844)
Pressure Ratio, $P_{T,4}/P_{T,42}$	-		4.933	
Pitchline Loading $\Delta h/2U^2$	-		0.65	

Table II. Stage Aerodynamic Parameters (ICLS at M0.8, 10.67 km (35000 ft) Max Climb Condition)

Stage		1		2
$P_{T,4}/P_{T,2}$, $P_{T,2}/P_{T,42}$		2.25		2.11
Pitchline $\Delta h/2U^2$		0.74		0.56
Tip Speed (takeoff) m/sec (ft/sec)	514	(1686)	535	(1756)
Exit Mach Number, M_2, M_{42}		0.34		0.42
Reaction, Rx		0.34		0.33
Swirl, Γ		16°		0°
No. of Vanes		46		48
No. of Blades		76		70
Radius Ratio, (r_h/r_t)		0.88		0.82
Tip Clearance, (% of blade height)		1.0		0.6
Work Fraction, (Stage Δh)/(Total Δh)		0.57		0.43

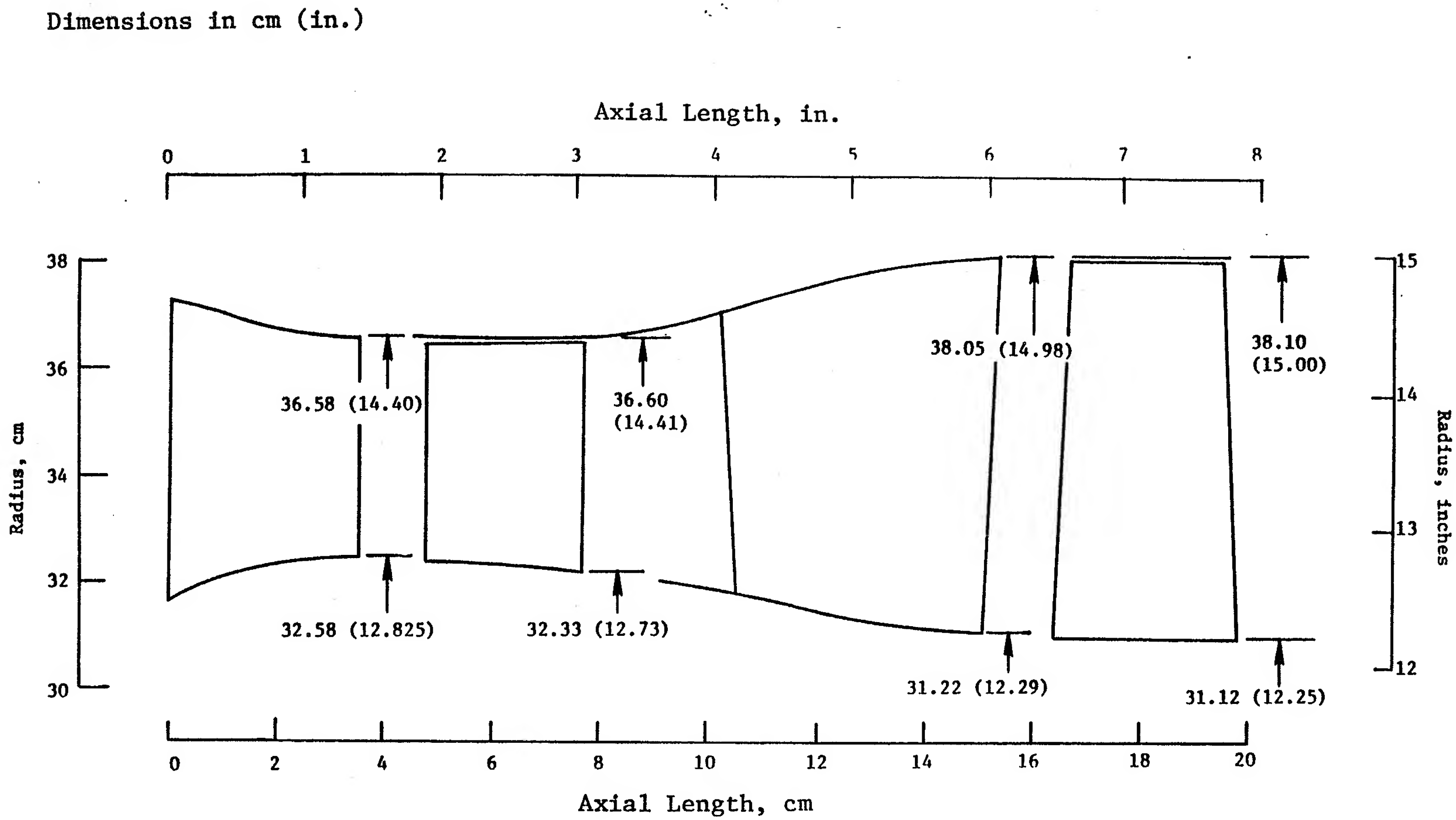

Figure 1. High Pressure Turbine Aerodynamic Flowpath.

Table III. Final Design Vector Diagram Angles and Mach Numbers

	Stage 1			Stage 2		
Streamline	Tip	Mean	Hub	Tip	Mean	Hub
Stator inlet absolute flow angle	0.0	0.0	0.0	7.4	21.8	11.5
Stator exit absolute flow angle	75.4	74.2	73.1	69.0	69.0	69.0
Rotor inlet relative flow angle	29.7	43.2	38.6	-18.2	17.0	31.5
Rotor exit relative flow angle	64.4	66.9	65.6	59.8	59.8	59.9
Stage exit absolute flow angle	5.2	17.7	9.7	-1.0	1.5	-4.6
Stator inlet absolute Mach No.	.084	.109	.114	.249	.276	.269
Stator exit absolute Mach No.	.815	.878	.910	.728	.828	.892
Rotor inlet relative Mach No.	.220	.324	.343	.286	.306	.339
Rotor exit relative Mach No.	.822	.819	.745	.934	.836	.724
Stage exit absolute Mach No.	.357	.338	.314	.469	.421	.365

o All Flow Angles are in Degrees.

a. Flow Angles

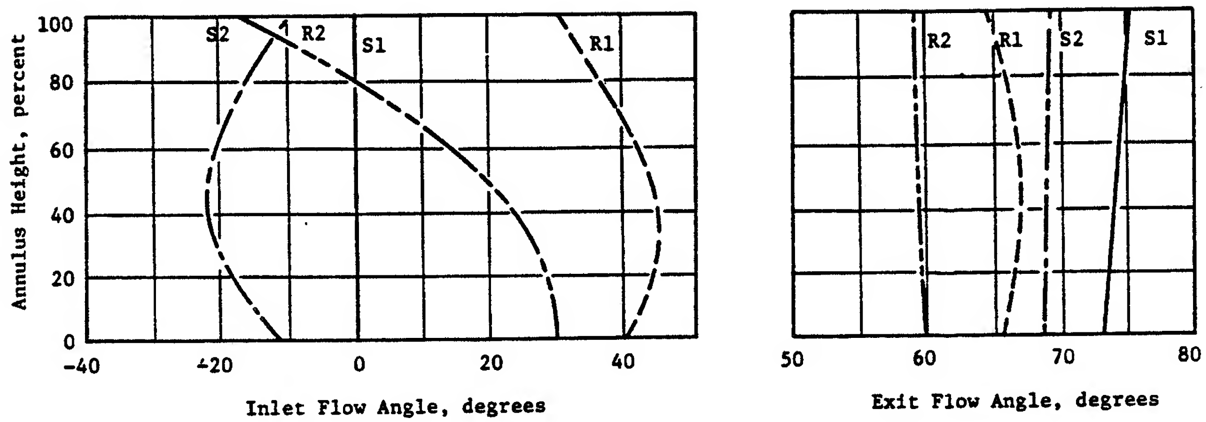

b. Mach Numbers

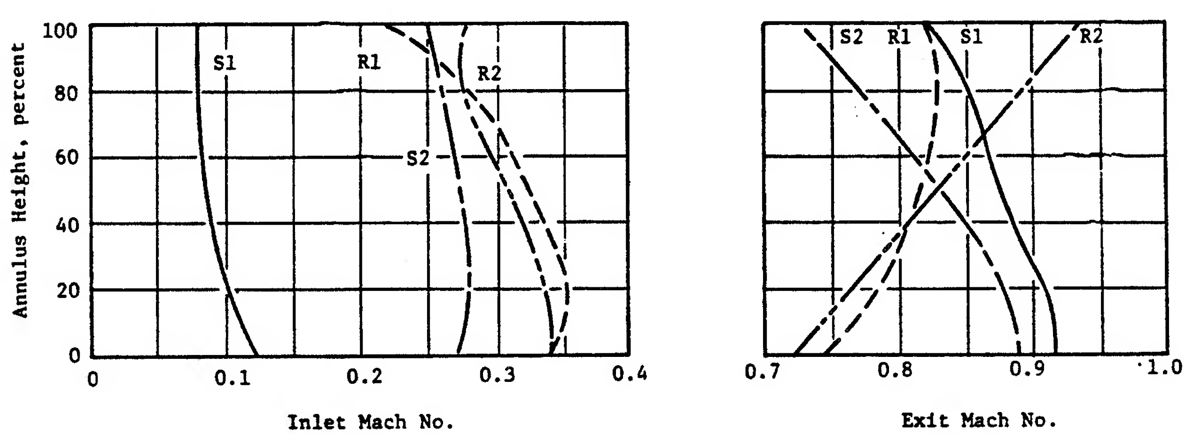

Figure 2. Blading Flow Angles and Mach Numbers.

contours and velocity distributions are shown in Figures 3 and 4. The stage one vane in Figure 3 is the base configuration. Section design data are presented in Tables IV thru VII. Airfoil coordinate data are provided in Appendix A.

Airfoil cooling hole definition for the base stage one vane is illustrated in Figure 5. The forward cavity is fed from the inner coolant supply circuit, while the aft cavity is supplied from the outer circuit. A photograph of a section of the rig nozzle is presented in Figure 6 where the vane cooling holes for the base vane are evident. The alternate, low unguided turning (LUT) stage one vane cooling hole definition is shown in Figure 7, where it is seen to be similar to the base vane. Stage one nozzle band cooling hole definitions for both base and LUT configurations are shown in Figures 8 and 9 for inner and outer band respectively. Stage one blade cooling hole definition is presented in Figure 10. A photograph of the blade showing these holes is found in Figure 11. The stage two vane cooling geometry is described in Figure 12. Figure 13 shows the arrangement of the trailing edge cooling holes and slots. Cooling hole geometry for the stage two blade is shown in Figure 14. All cooling air is supplied through the forward cavity with crossover slots connecting to the aft cavity. Flow in the aft cavity is discharged through the blade tip. A photograph of the blade showing the two pressure side slots is shown in Figure 11. The cooling hole geometries for the air turbine rig and annular cascade airfoils matched the engine design at the time the rig design was performed. Subsequently, some changes were made in the engine design involving number and size of the holes. Details of the engine design can be found in Reference 1.

3.2 Annular Cascade

The annular cascade consisted of a single row of forty-six stage one vane airfoils of two types differing in the level of unguided turning. The base vane had an unguided turning of 8.4° while the alternate candidate had a lower unguided turning (LUT) of 5.5°. The test philosophy of the annular cascade was to match the ICLS aerodynamic and cooling geometry as closely as practicable. The engine nozzle flowpath was used, vane and band cooling hole patterns matched then-current engine design. Test hardware was full scale.

o Linear Scale, Each Division Equals 0.508 cm (0.2 in.)

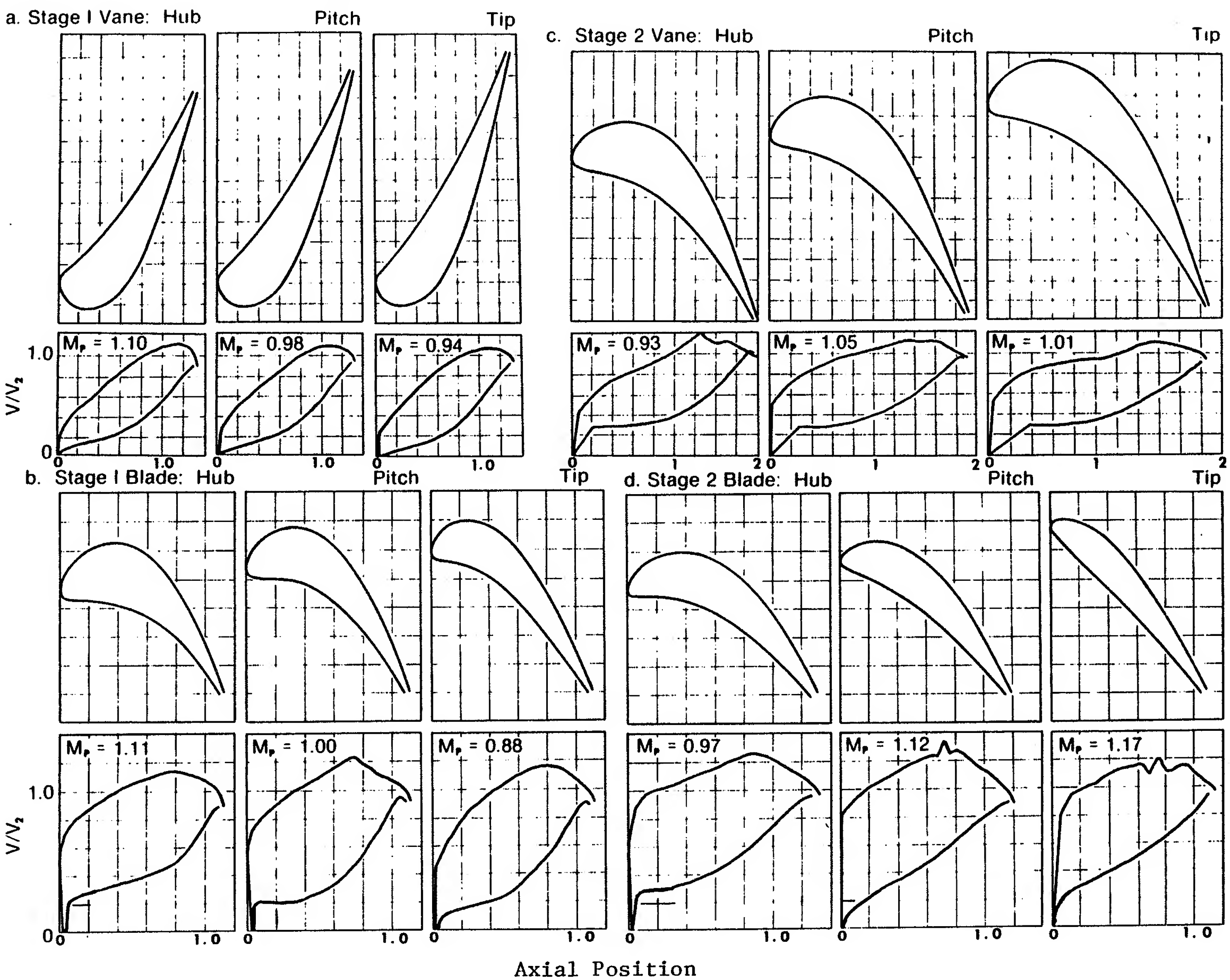

Figure 3. Final Airfoil Shapes and Velocity Distributions with Peak Mach Number Specified.

o Linear Scale, Each Division Equals
0.508 cm (0.2 in.)

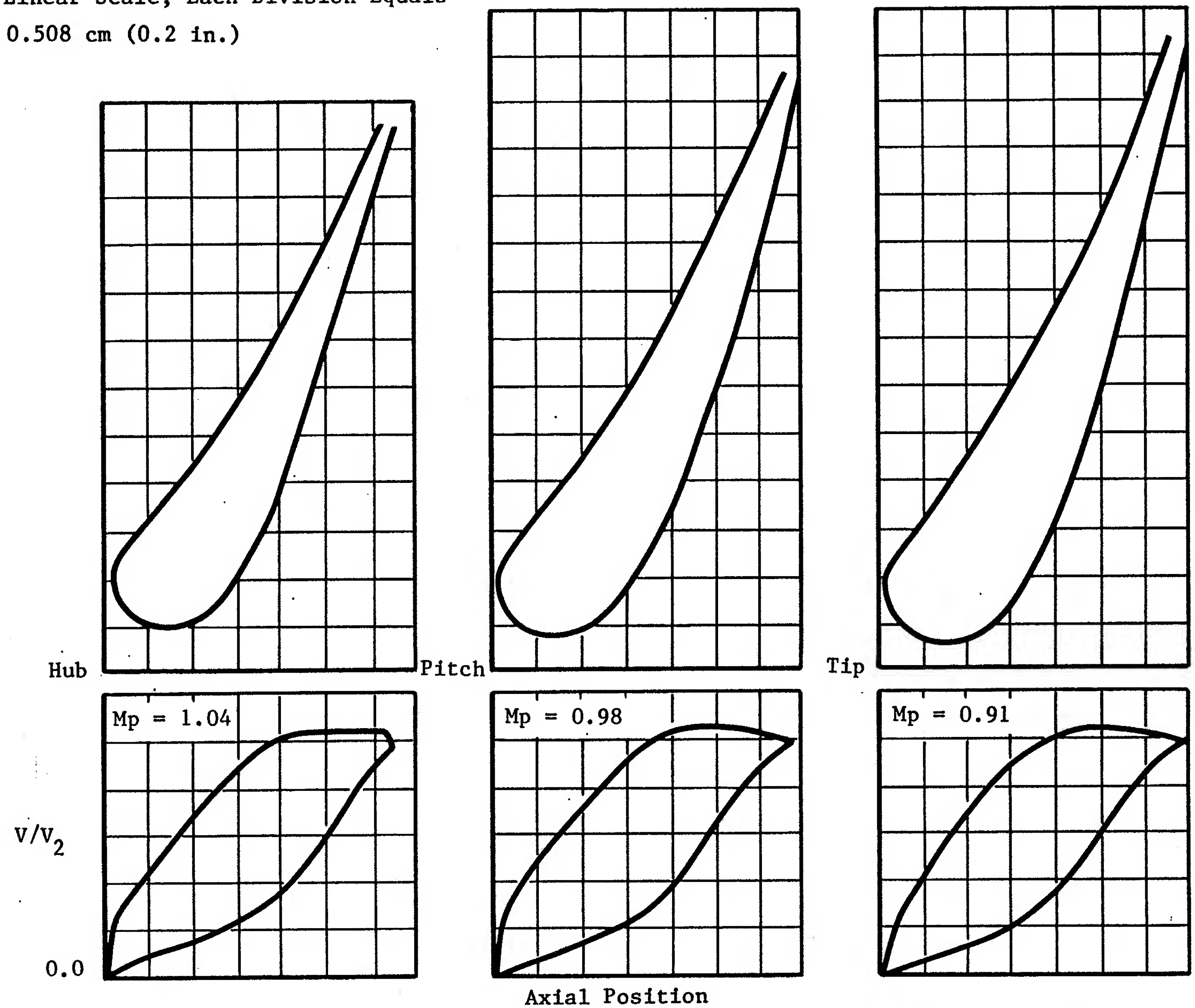

Figure 4. Airfoil Contour and Velocity Distribution for LUT Vane with Peak Mach Number Specified.

Table IV. Stage 1 Vane Section Design Data

	Base			Low Unguided Turning		
	Hub	Pitch	Tip	Hub	Pitch	Tip
Number	46			46		
Radius, cm	32.5755	34.576	36.576	32.5755	34.576	36.576
(in.)	(12.825)	(13.6125)	(14.400)	(12.825)	(13.6125)	(14.400)
Axial Width, cm	3.376	3.378	3.383	3.373	3.421	3.470
(in.)	(1.329)	(1.330)	(1.332)	(1.328)	(1.347)	(1.366)
Trailing Edge Thickness, cm	0.0965	0.0965	0.0965	0.0965	0.0965	0.0965
(in.)	(0.038)	(0.038)	(0.038)	(0.038)	(0.038)	(0.038)
Uncovered Turning, degrees	9.2	8.4	8.7	4.9	5.5	5.2
Trailing Edge Wedge Angle, degrees	10.2	9.2	9.0	9.0	9.0	9.3

Table V. Stage 1 Blade Section Design Data

	Hub	Pitch	Tip
Number		76	
Radius, cm	32.337	34.468	36.601
(in.)	(12.731)	(13.570)	(14.410)
Axial Width, cm	2.87	2.87	2.87
(in.)	(1.13)	(1.13)	(1.13)
Trailing Edge Thickness, cm	0.0965	0.0965	0.0965
(in.)	(0.038)	(0.038)	(0.038)
Uncovered Turning, degrees	13.0	13.0	13.0
Trailing Edge Wedge Angle, degrees	12.5	12.5	12.5

Table VI. Stage 2 Vane Section Design Data

	Hub	Pitch	Tip
Number		48	
Radius, cm	31.217	34.633	38.049
(in.)	(12.290)	(13.635)	(14.980)
Axial Width, cm	4.503	4.905	5.309
(in.)	(1.773)	(1.931)	(2.090)
Trailing Edge Thickness, cm	0.0965	0.0965	0.0965
(in.)	(0.038)	(0.038)	(0.038)
Uncovered Turning, degrees	10.5	11.0	11.5
Trailing Edge Wedge Angle, degrees	9.0	9.5	10.0

Table VII. Stage 2 Blade Section Design Data

	Hub	Pitch	Tip
Number		70	
Radius, cm	31.115	34.6075	38.100
(in.)	(12.25)	(13.625)	(15.000)
Axial Width, cm	3.353	3.073	2.794
(in.)	(1.32)	(1.21)	(1.10)
Trailing Edge Thickness, cm	0.1575	0.1118	0.1270
(in.)	(0.062)	(0.044)	(0.050)
Uncovered Turning, degrees	14.5	15.5	12.0
Trailing Edge Wedge Angle, degrees	14.0	14.0	9.0

Row	Number of Holes	Hole Diameter cm (in.)	Type
1	22	.061 (.024)	Axial, Shaped
2	23	.061 (.024)	Axial, Shaped
3	12	.048 (.019)	Radial
4	12	.048 (.019)	Radial
5	12	.048 (.019)	Radial
6	12	.048 (.019)	Radial
7	12	.048 (.019)	Radial
8	12	.048 (.019)	Radial
9	12	.048 (.019)	Radial
10	20	.036 (.014)	Compound Angle
11	19	.061 (.024)	Compound Angle
12	16	.061 (.024)	Compound Angle
13	16	.048 (.019)	Axial
14	18	.061 x .155 (.024 x .061)	Pressure Side Slot

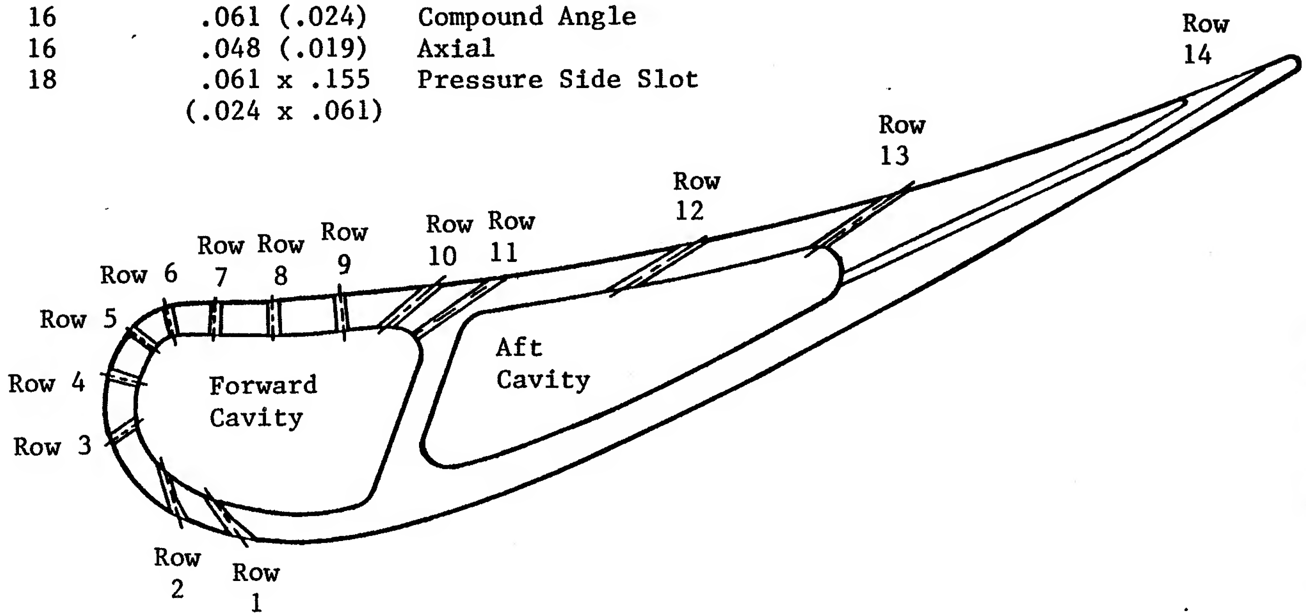

Figure 5. Base Stage 1 Vane Cooling Hole Definition.

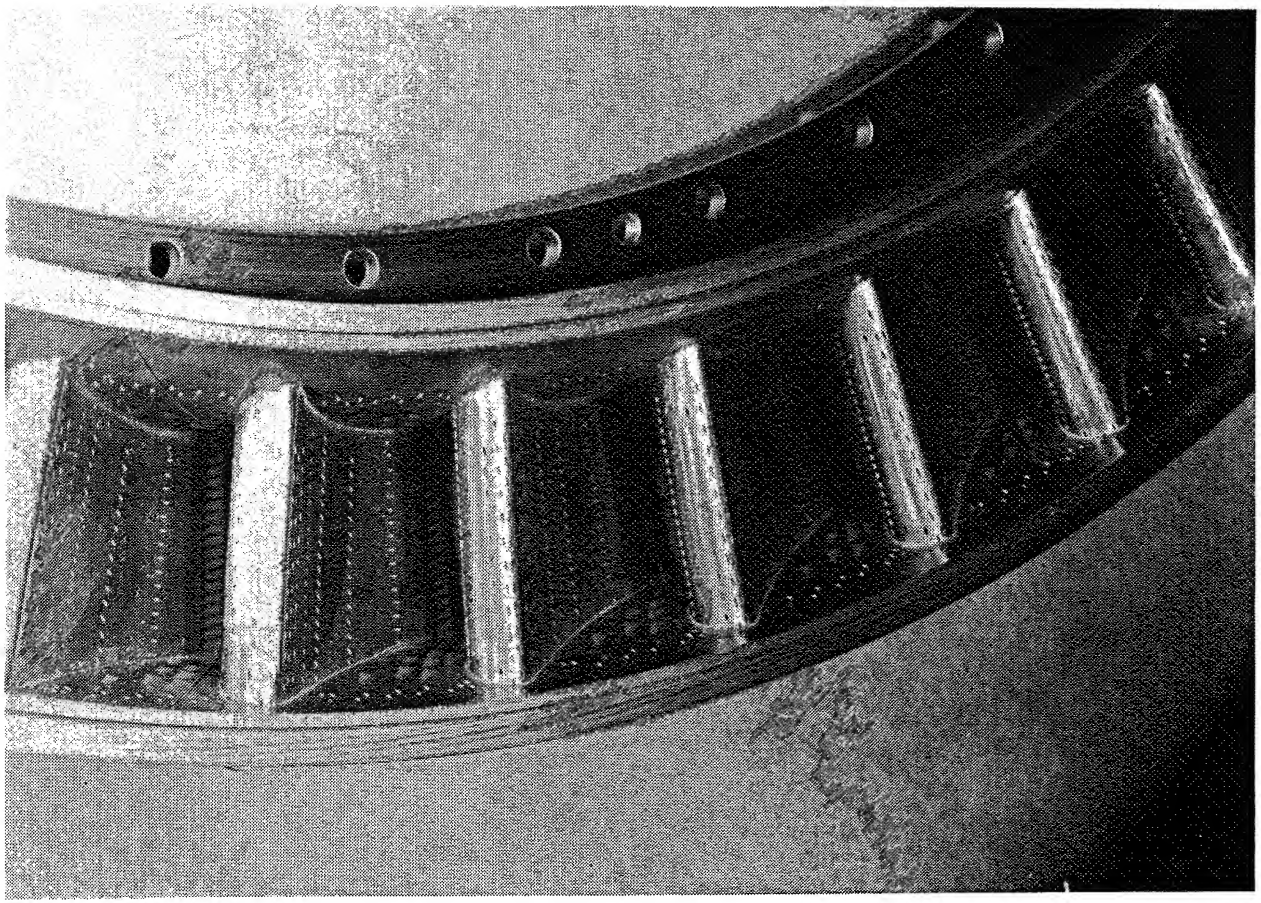

Figure 6. Stage 1 Nozzle with Base Vane Showing Cooling Holes and Band Saw-Cuts.

Row	Number of Holes	Hole Diameter cm (in.)	Type
1	22	.058 (.023)	Axial, Shaped
2	23	.058 (.023)	Axial, Shaped
3	12	.048 (.019)	Radial
4	11	.048 (.019)	Radial
5	12	.048 (.019)	Radial
6	11	.048 (.019)	Radial
7	12	.048 (.019)	Radial
8	11	.048 (.019)	Radial
9	12	.048 (.019)	Radial
10	20	.036 (.014)	Compound Angle
11	19	.064 (.065)	Compound Angle
12	16	.066 (.026)	Compound Angle
13	16	.048 (.019)	Compound Angle
14	18	.061 x .155 (.024 x .061)	Pressure Side Slot

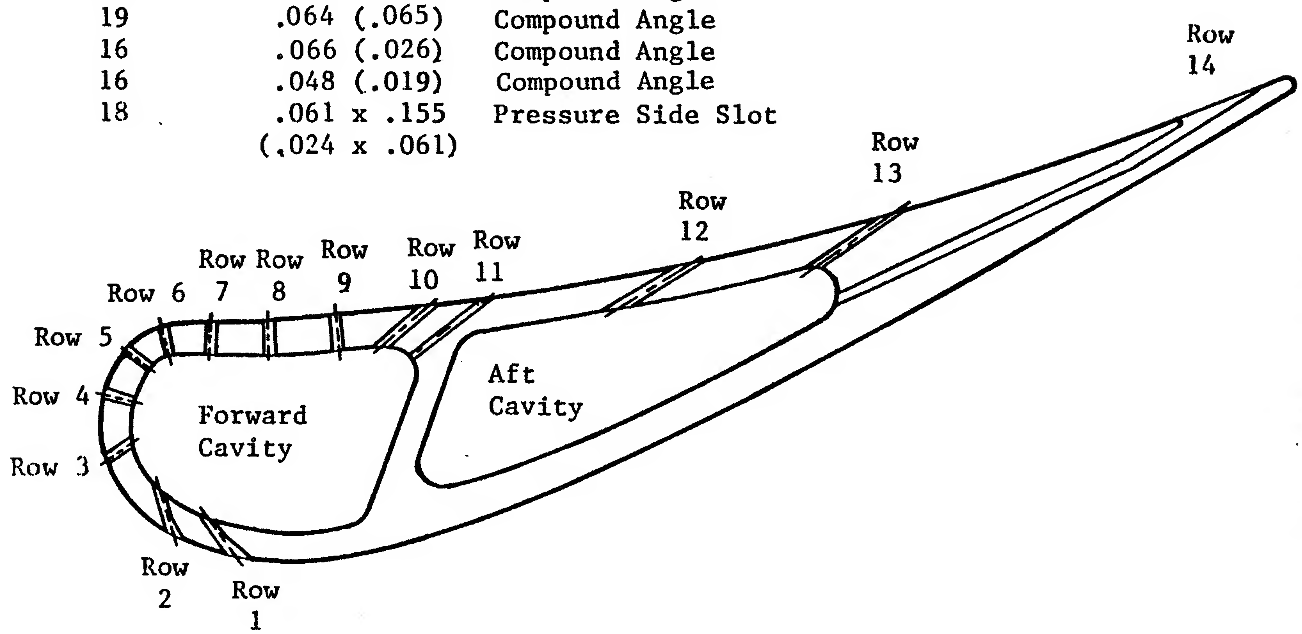

Figure 7. LUT Stage 1 Vane Cooling Hole Definition.

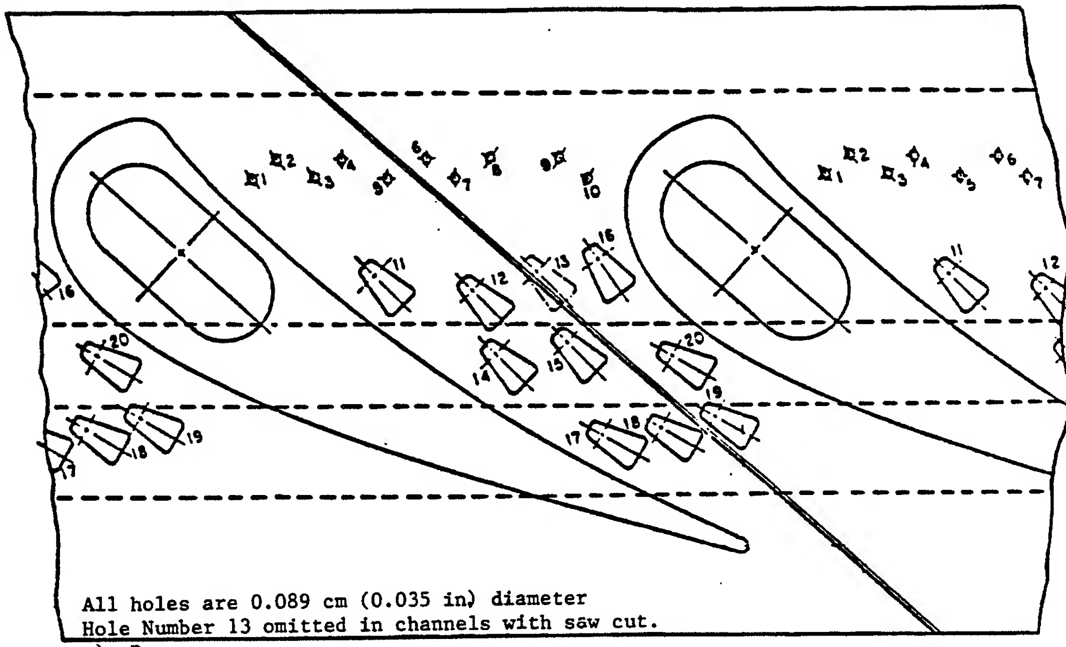

a) Base

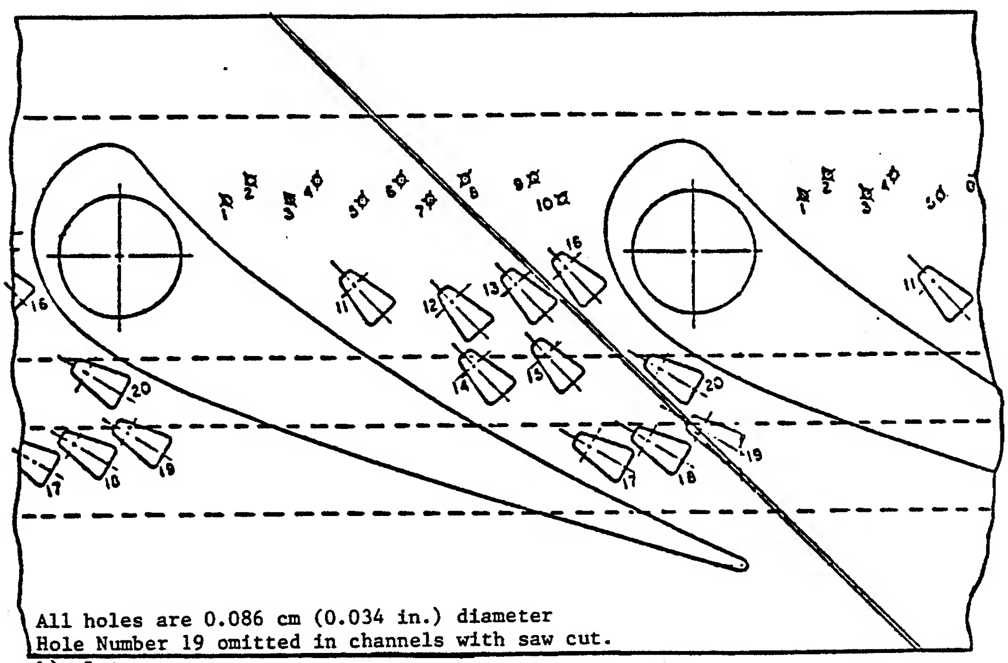

b) Lut

Figure 8. Stage 1 Nozzle Inner Band Cooling Hole Definition.

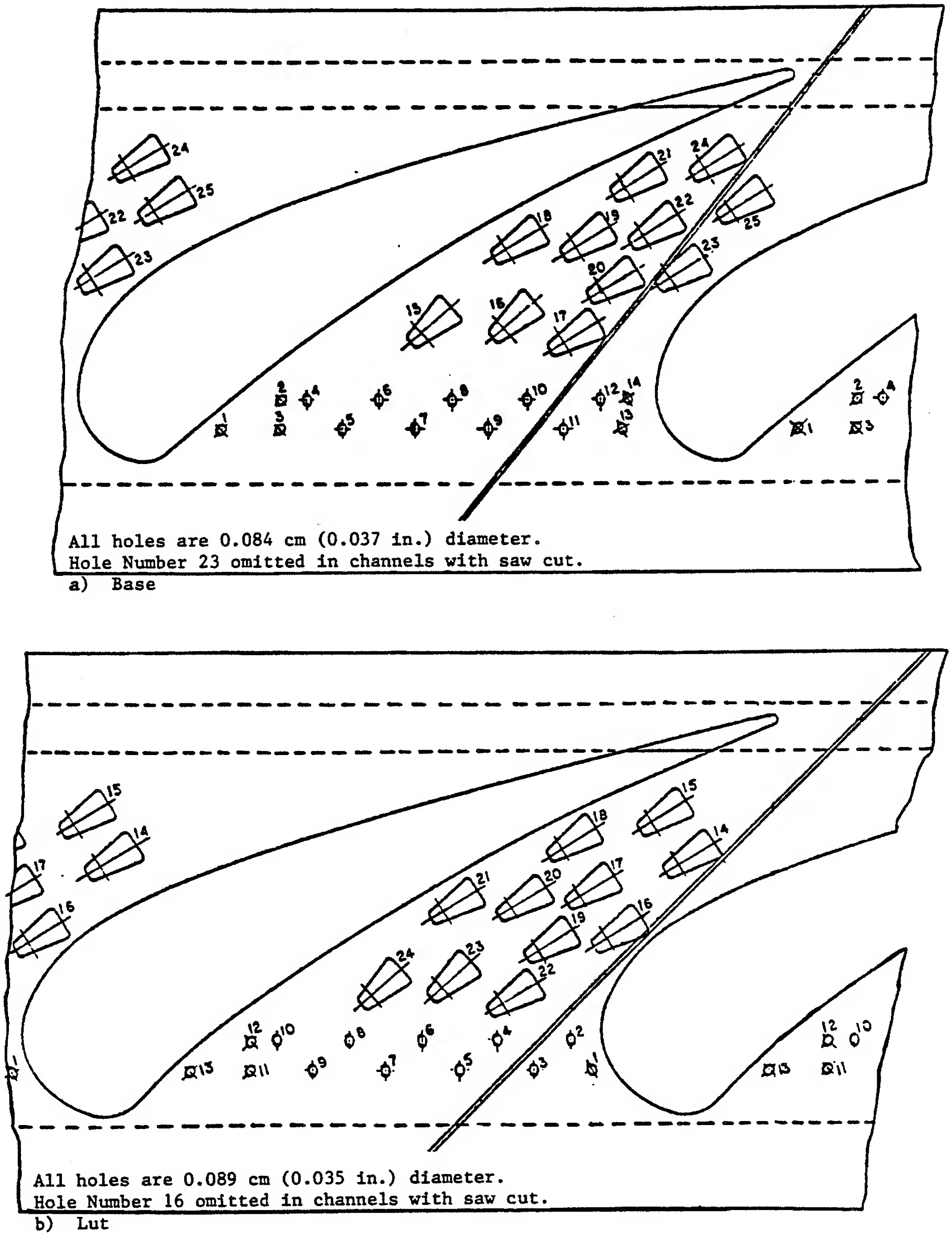

Figure 9. Stage 1 Nozzle Outer Band Cooling Hole Definition.

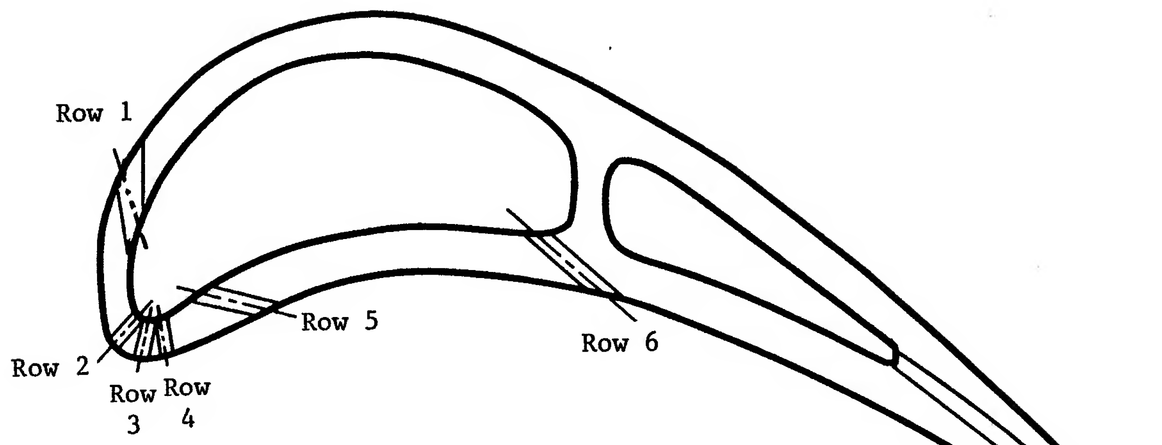

Row	Number of Holes	Hole Diameter cm (in.)	Type
1	25	.036 (.014)	Axial, Shaped
2	11	.036 (.014)	Radial
3	10	.036 (.014)	Radial
4	11	.036 (.014)	Radial
5	22	.036 (.014)	Axial
6	17	.036 (.014)	Compound Angle
7	11	.048 x .152 (.019 x .060)	Pressure Side Slot

Figure 10. Stage 1 Blade Cooling Hole Definition.

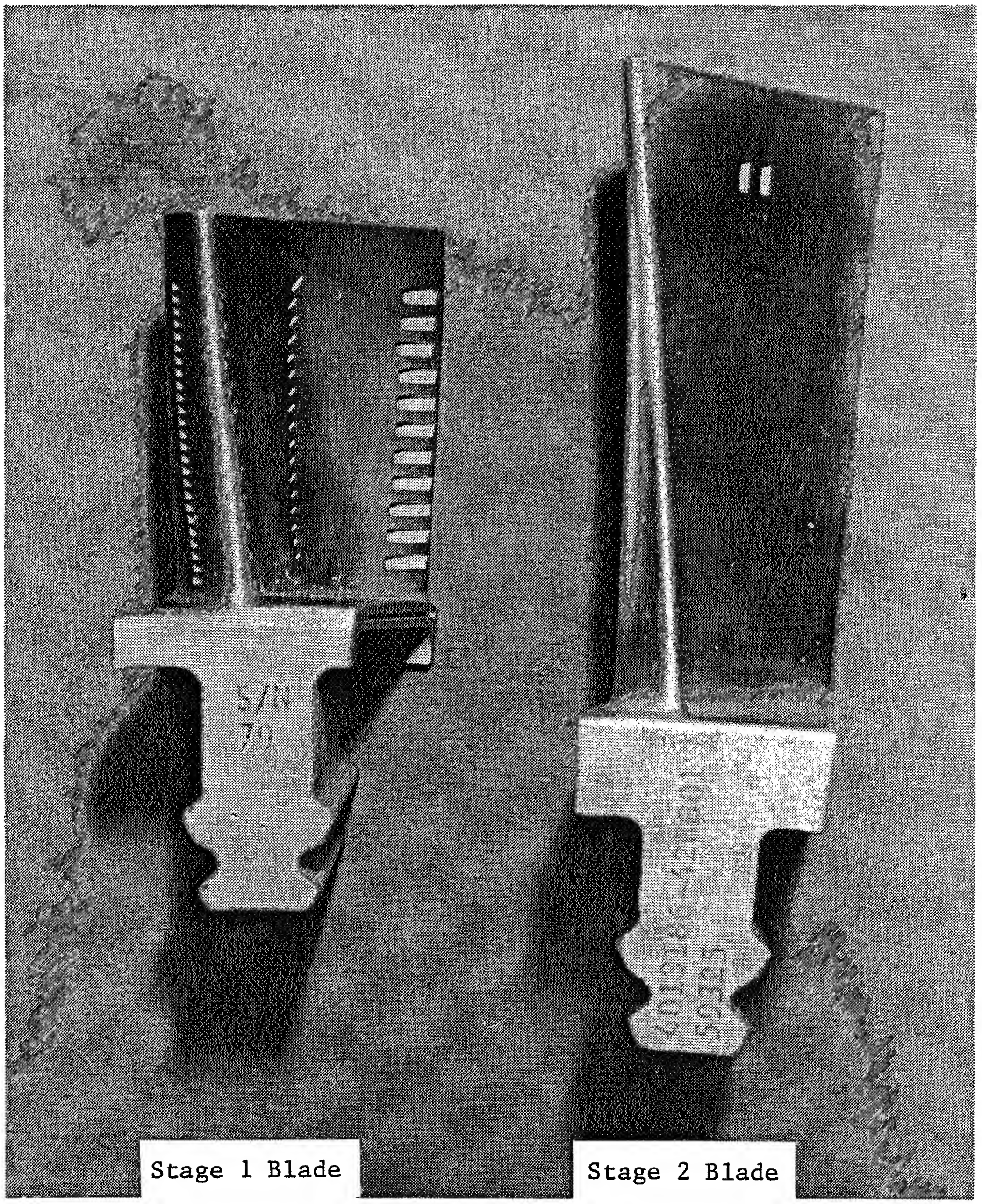

Figure 11. Stage 1 and Stage 2 Blades.

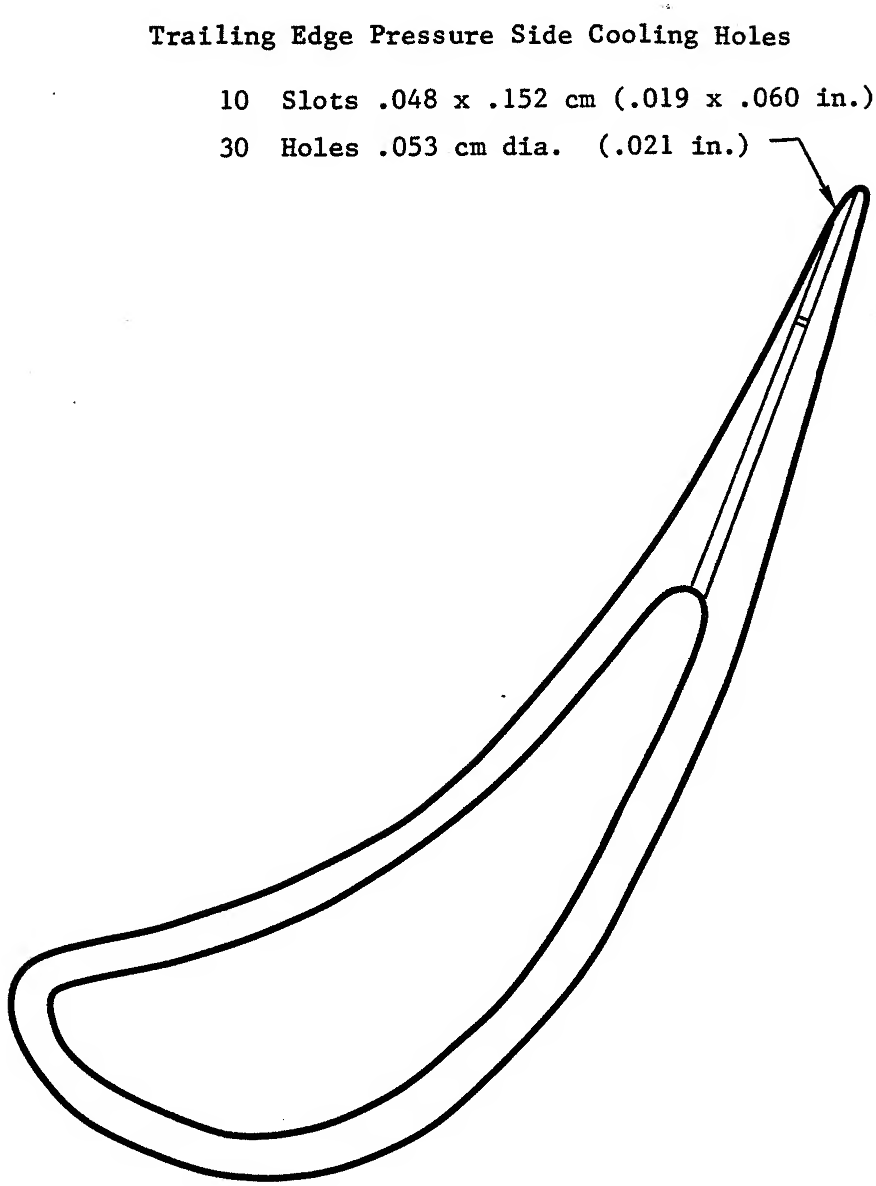

Figure 12. Stage 2 Vane Cooling Hole Definition.

ORIGINAL PAGE IS
OF POOR QUALITY

ORIGINAL PAGE
BLACK AND WHITE PHOTOGRAPH

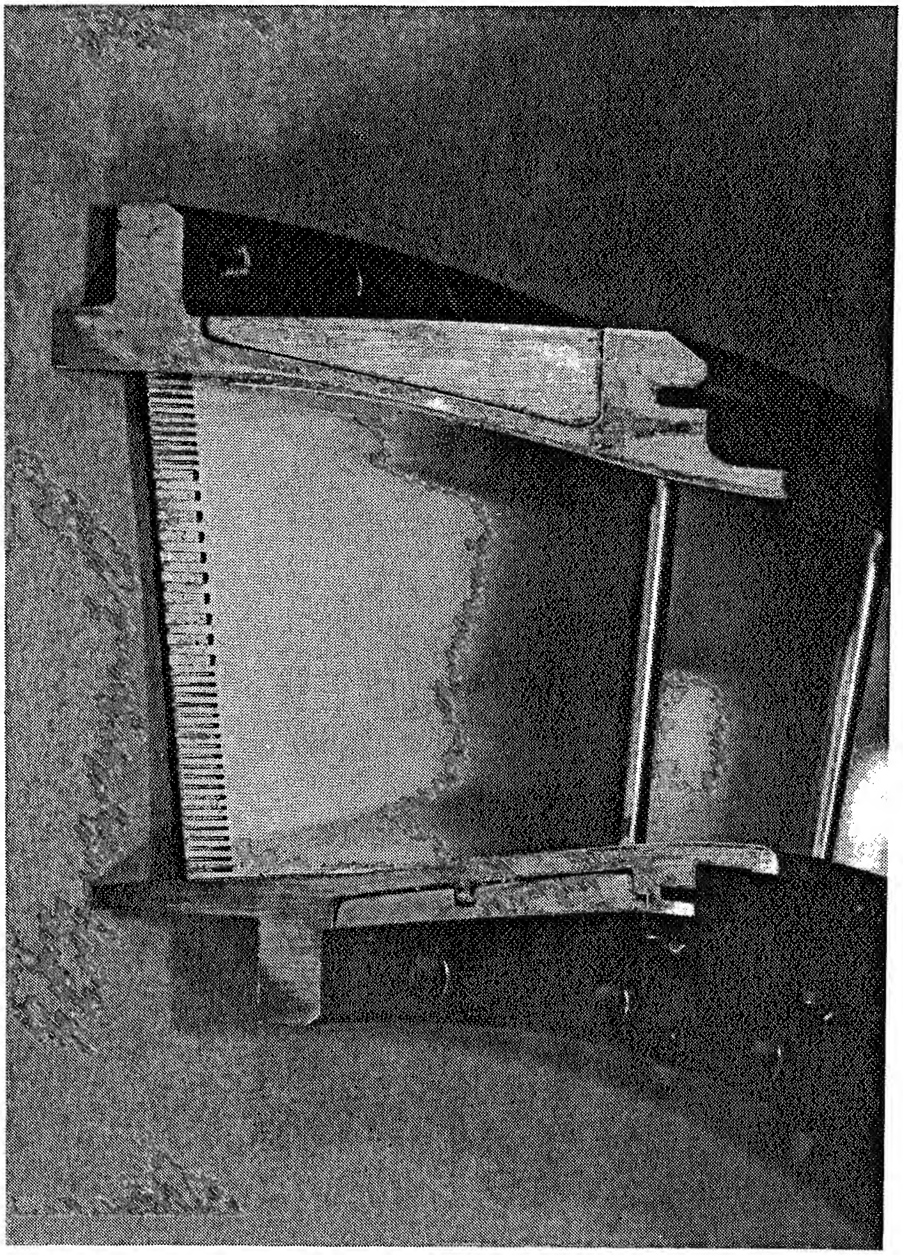

Figure 13. Stage 2 Nozzle Showing Trailing Edge Cooling Holes.

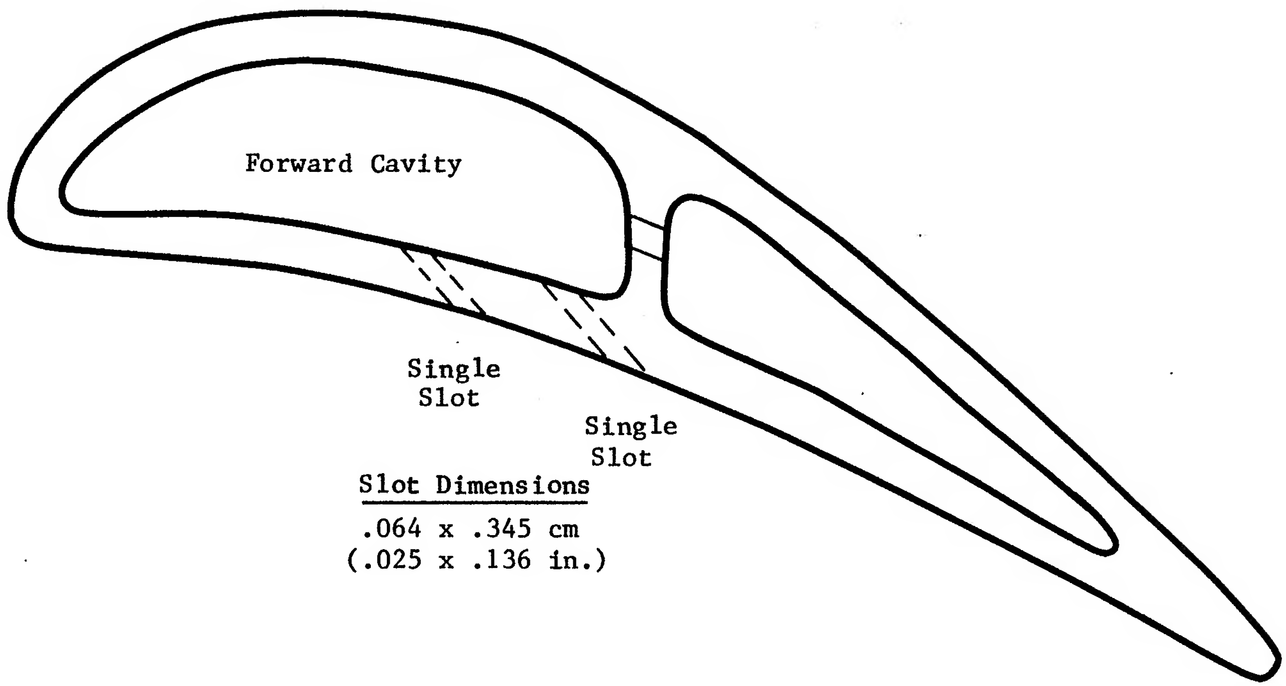

Figure 14. Stage 2 Blade Cooling Hole Definition.

In an effort to simulate the flowpath gaps between the two-vane segmented engine stator, saw cuts were made in both the outer and inner bands of the 360° annular cascade nozzle. These saw cuts are evident in Figure 6. Leakage flows between segments were not simulated. A cross-sectional view of the annular cascade rig is shown in Figure 15.

As stated previously, both base and LUT vanes were installed in the same nozzle ring. Thirty-four of the vanes were the base configuration which occupied a 266^{o} sector; the twelve LUT vanes covered the remaining 94^{o}. For reduced cost, only seven of the base vanes and five of the LUT vanes were cooled. The remaining airfoils were solid. In similar fashion, band cooling holes were drilled only in the cooled vane sectors. The arrangement of vane configurations is shown schematically in Figure 16. This technique of having several vane configurations in a single nozzle had been used in other cascade test programs and considered acceptable in determining total pressure losses.

3.3 Air Turbine Rig

The air turbine rig was a full scale design of the two stage high pressure turbine and fully cooled. The intent of the rig design was to match the ICLS aerodynamic and cooling geometry. As in the annular cascade, flowpath and cooling hole patterns matched the then-current engine design. Inter-blade row leakage and purge flows were also simulated including arrangement and type of seals used. In addition, wheel space geometry was matched in order to simulate windage effects. The cooling system film hole aerodynamic geometry was matched. The inducer (tangential accelerator) for rotor coolant delivery was at the same diameter and geometry as in the engine to give similar pumping characteristics. Stage one and two shrouds are segmented as is the engine design. Stage one nozzle is a continuous ring; in order to facilitate assembly, stage two nozzle is a split ring. To simulate the segmented construction, saw cuts were made in both nozzle bands. Leakage flow between segments was not simulated however, since the cost of drilling the necessarily large number of very small diameter holes was prohibitive. Endwall axial gap geometry was matched. Independent blade tip clearance control was provided for each stage. A cross-section of the rig is shown in Figure 17.

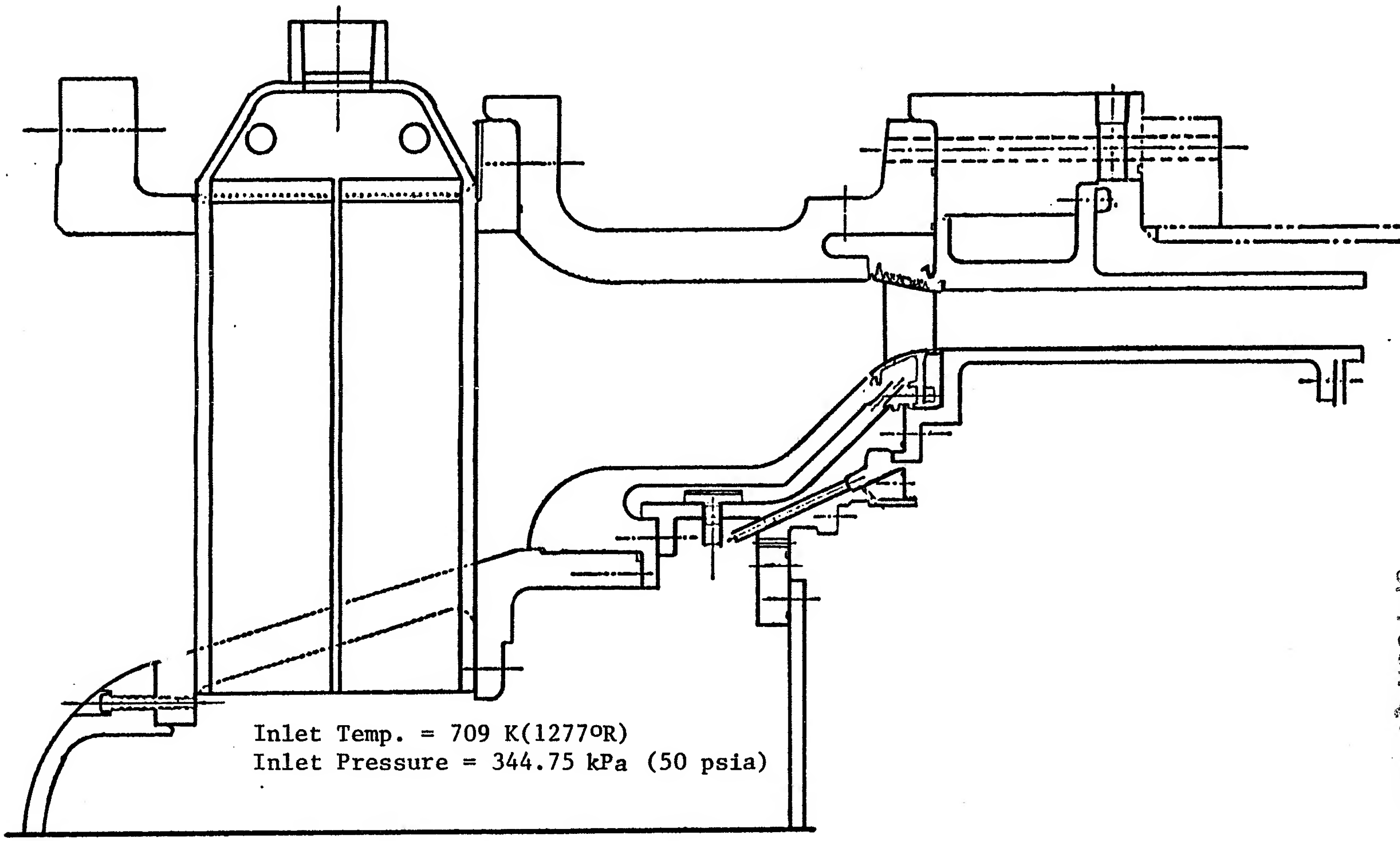

Figure 15. Annular Cascade Test Rig.

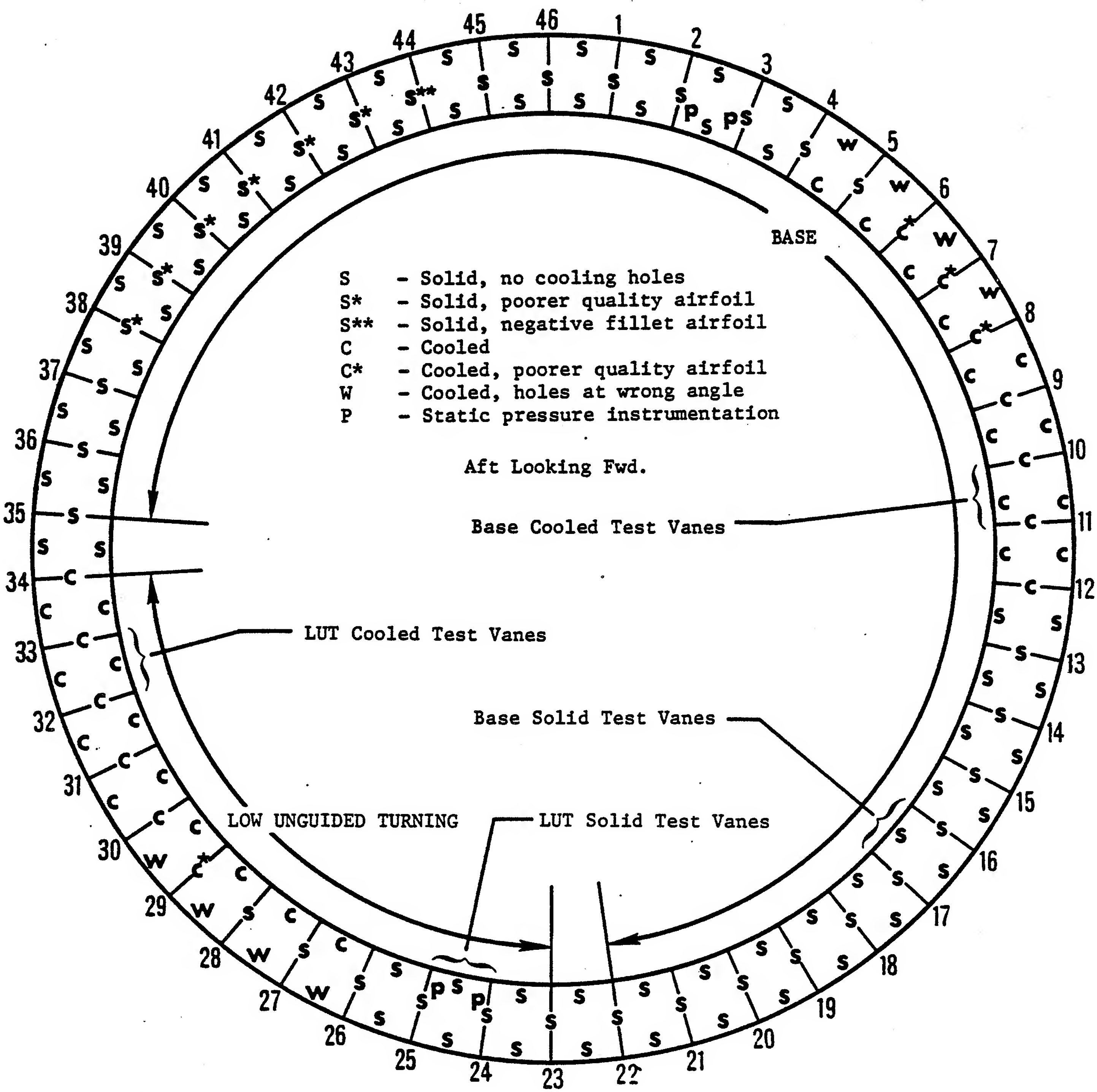

Figure 16. Vane Arrangement for Annular Cascade Nozzle.

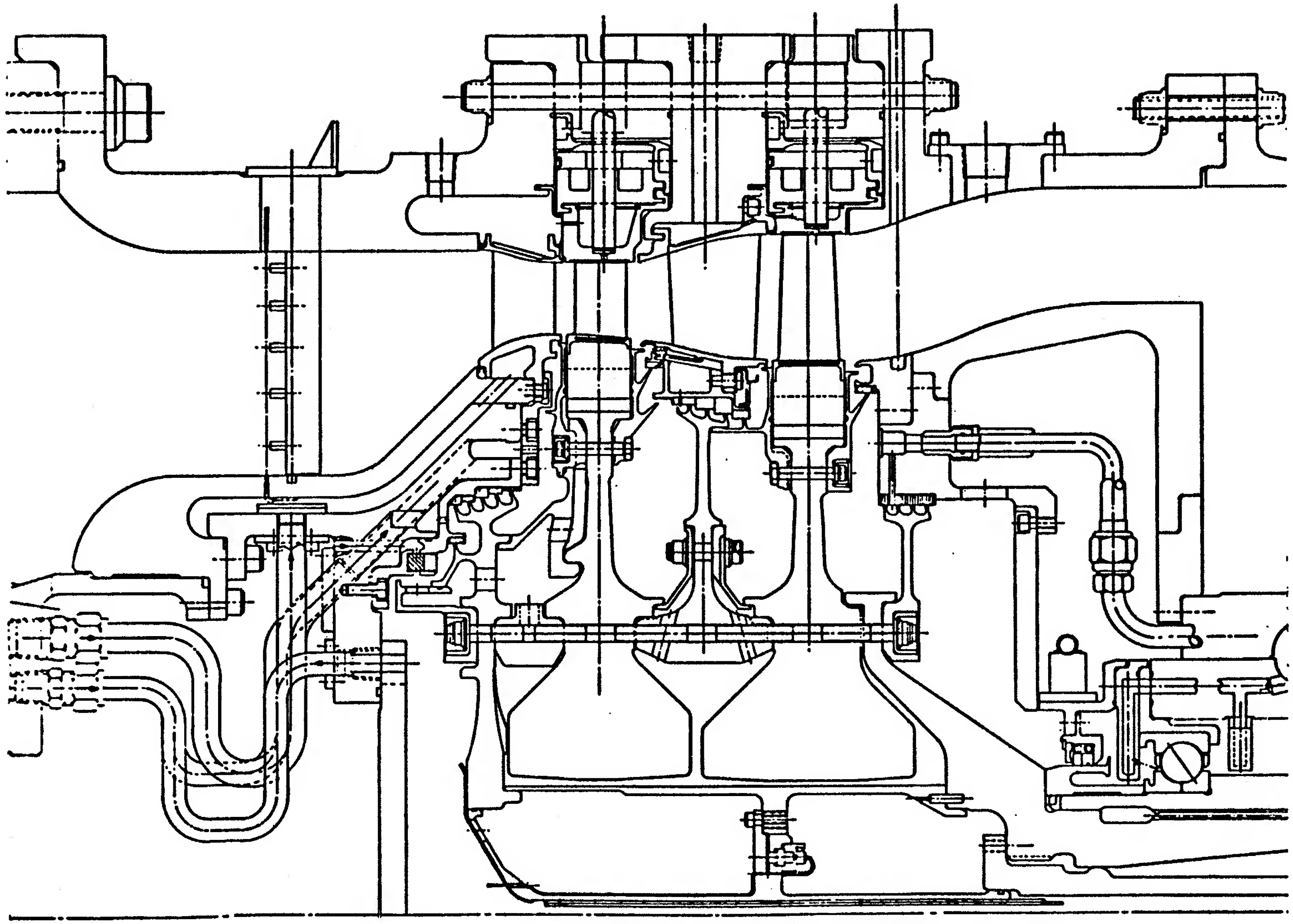

Figure 17. Warm Air Turbine Rig.

All rotor parts including blades were machined from 410 stainless steel. The stators were of the same material. Casings were nickel plated carbon steel. Standard facility frames and bearing cartridge were used.

Photographs of major rig sub-assemblies are presented in Figures 18 through 24.

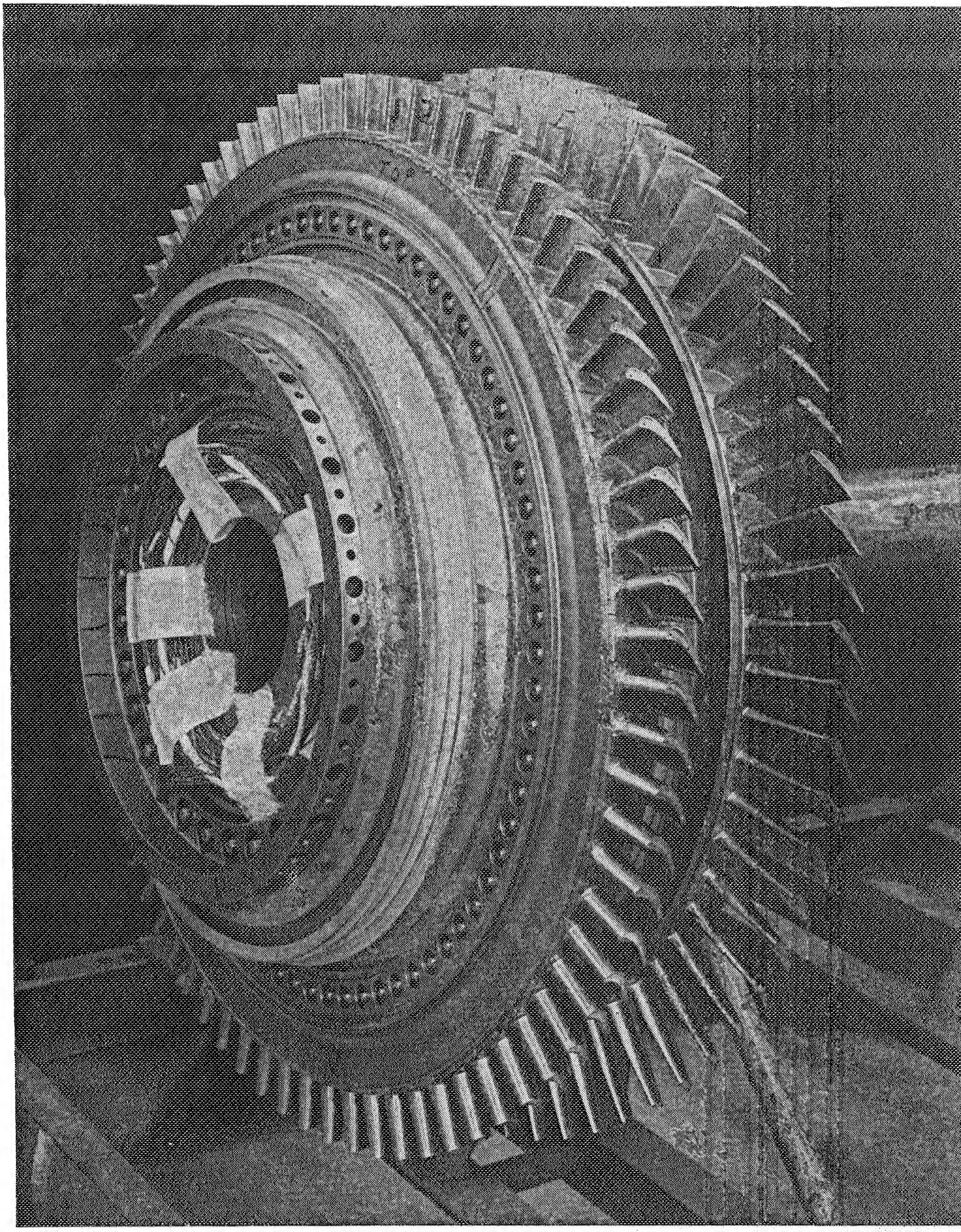

Figure 18. Two-Stage Rotor Assembly.

ORIGINAL PAGE
BLACK AND WHITE PHOTOGRAPH

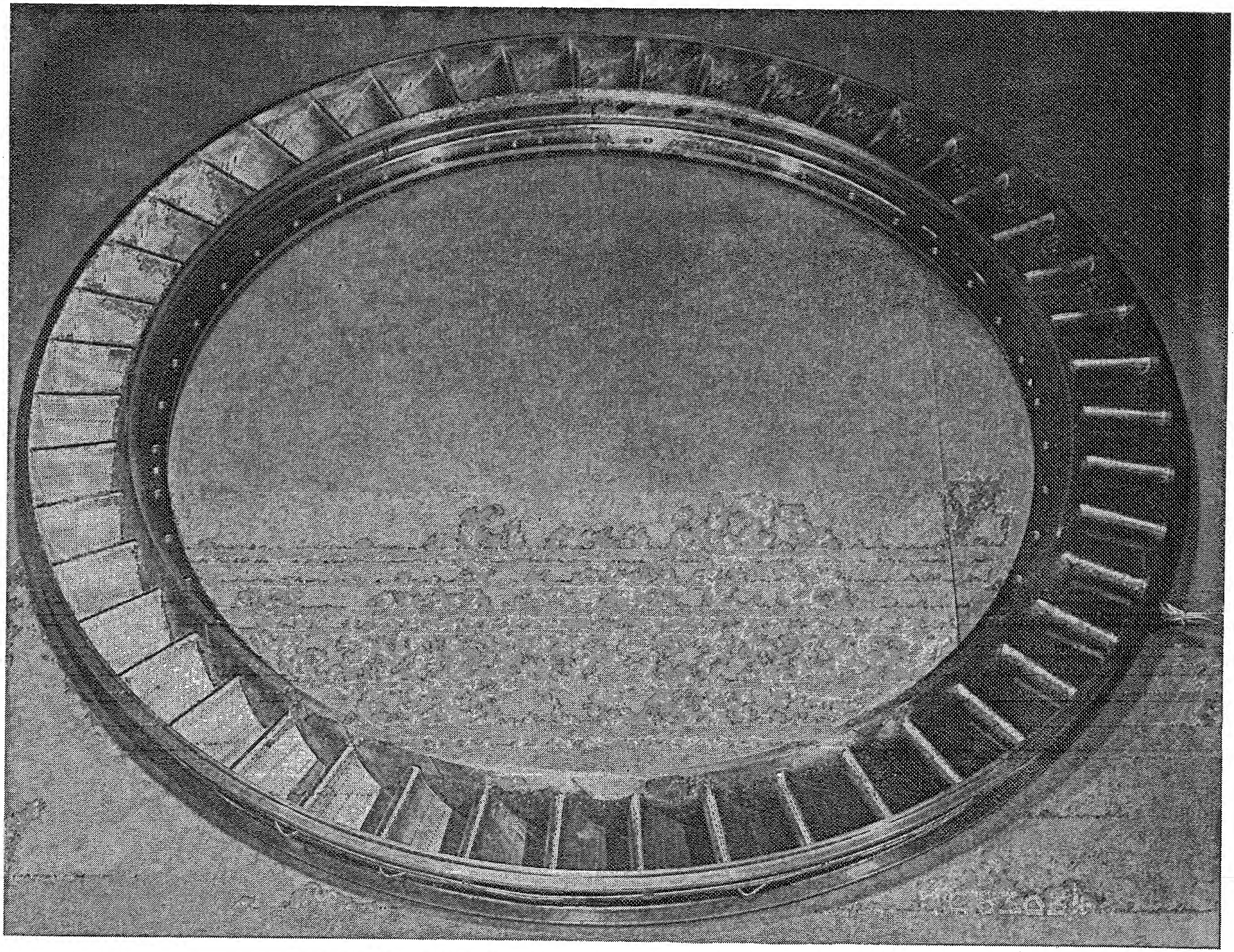

Figure 19. Stage 1 Nozzle Assembly (Forward Looking Aft)

ORIGINAL PAGE IS
OF POOR QUALITY

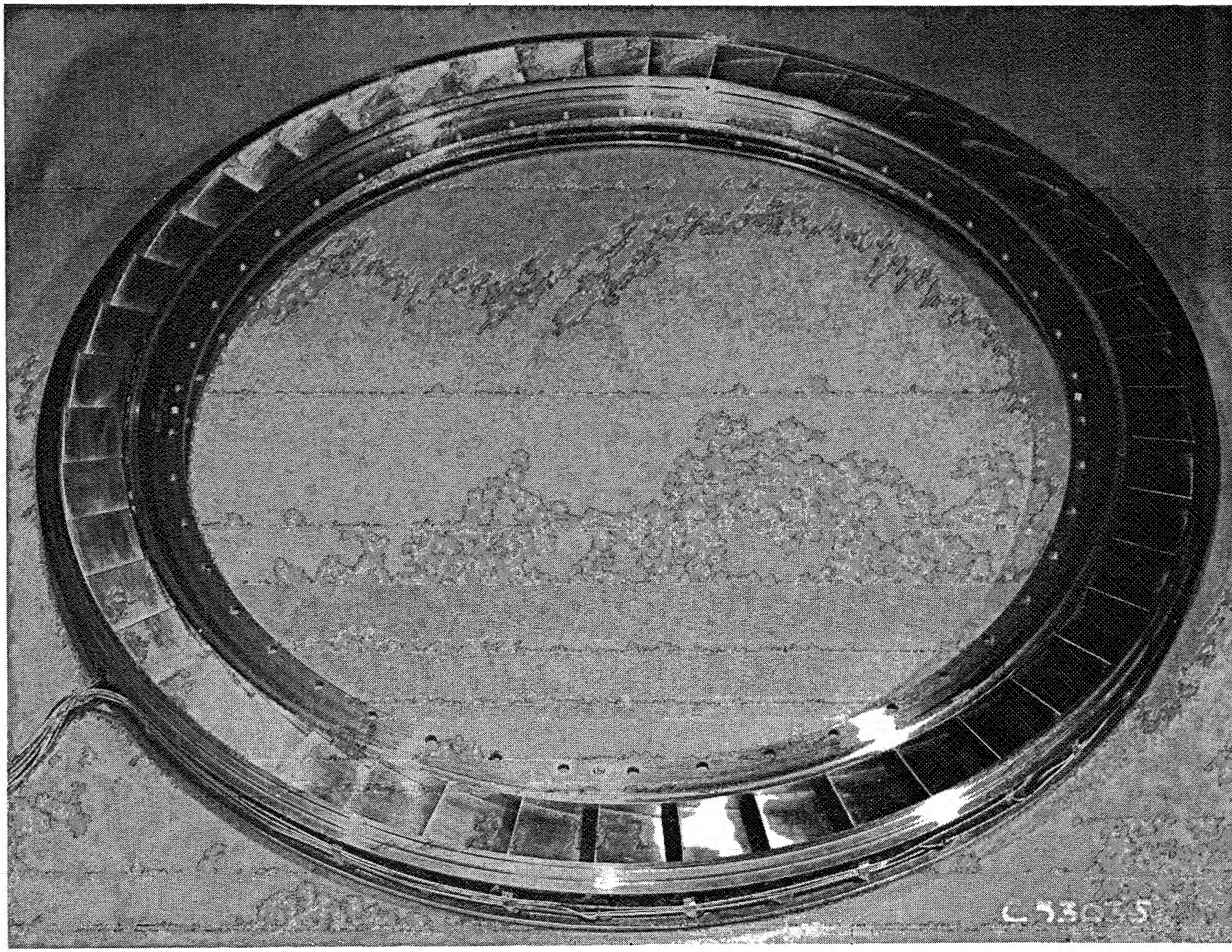

Figure 20. Stage 1 Nozzle Assembly (Aft Looking Forward)

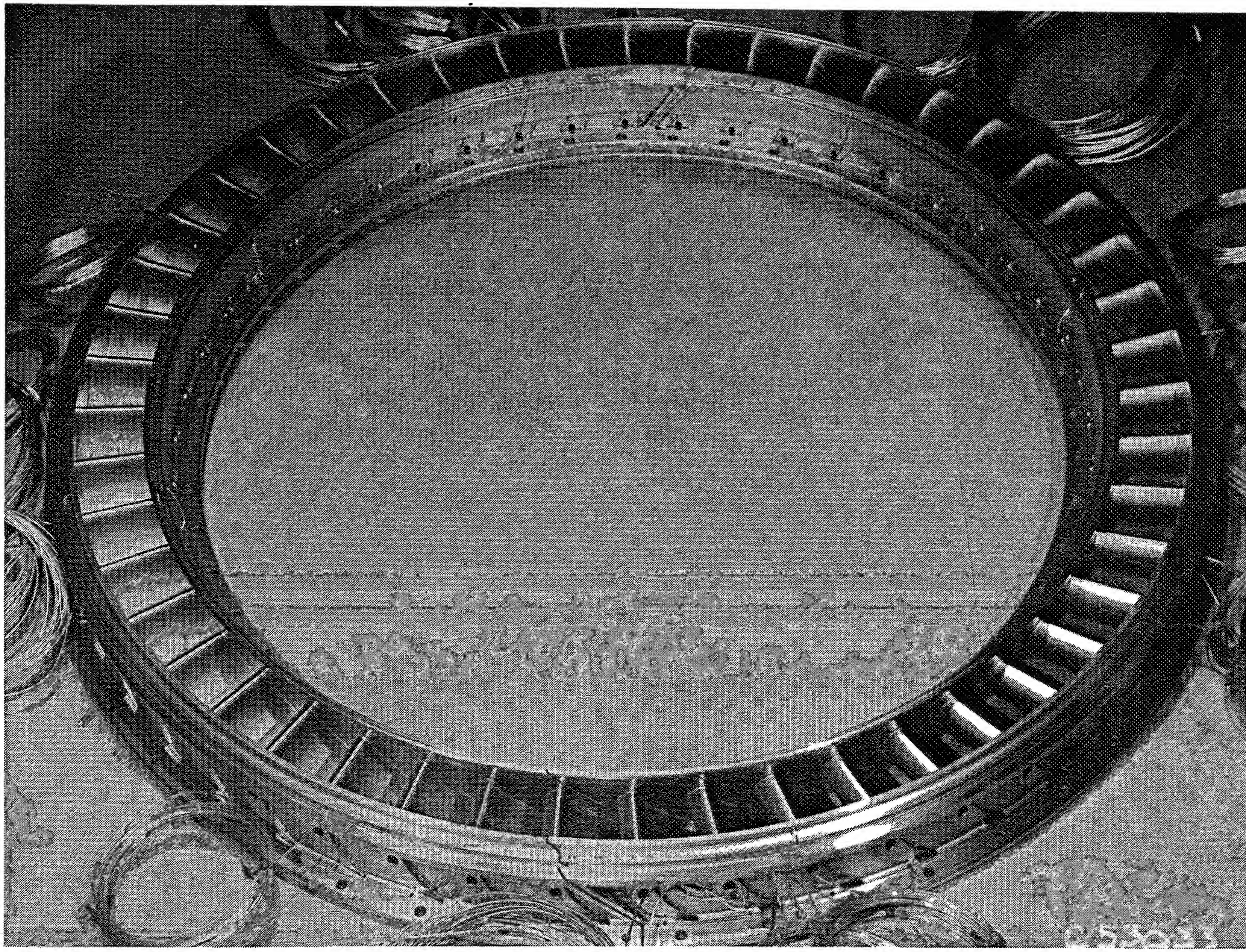

Figure 21. Stage 2 Nozzle Assembly (Forward Looking Aft)

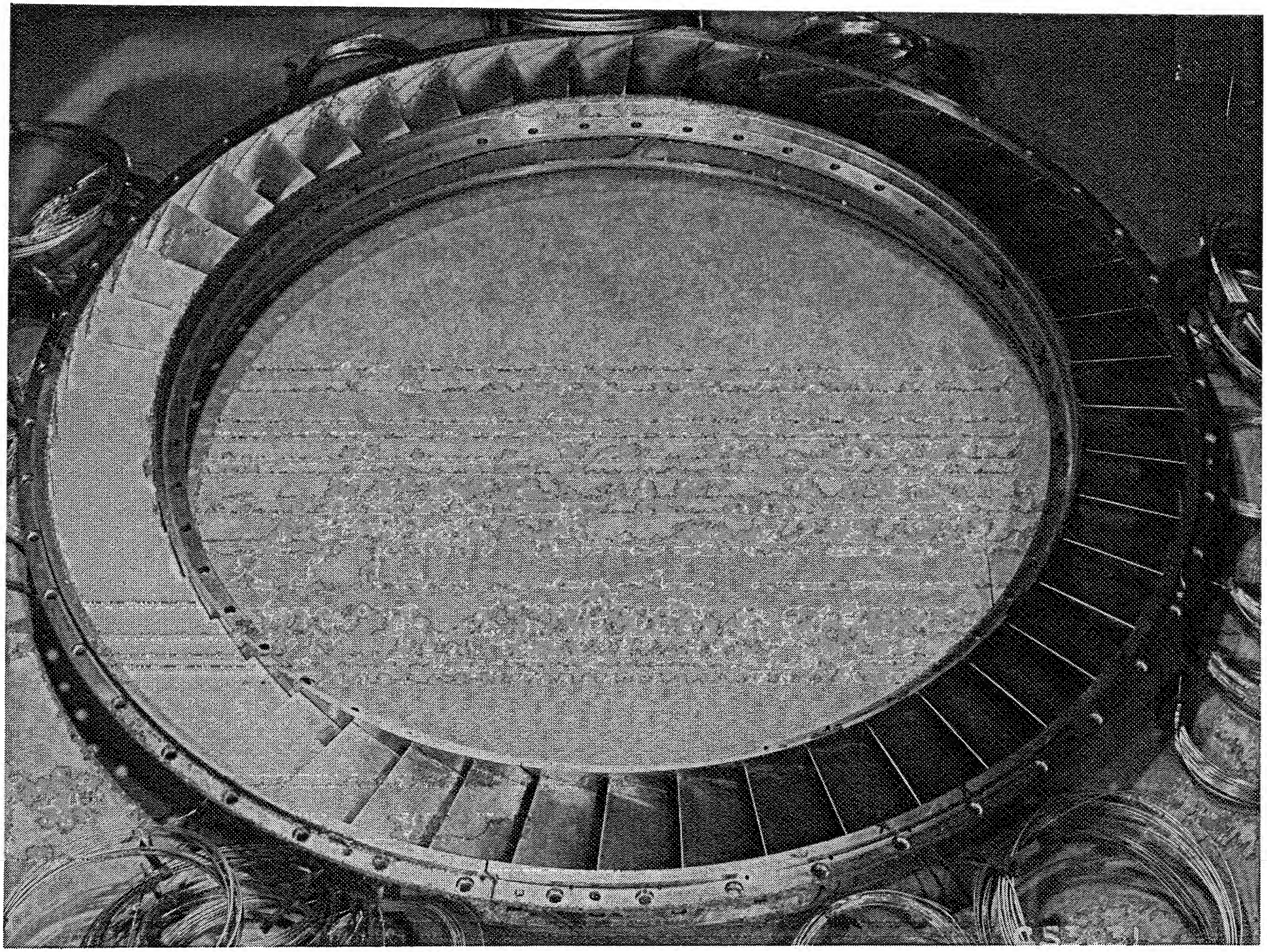

Figure 22. Stage 2 Nozzle Assembly (Aft Looking Forward)

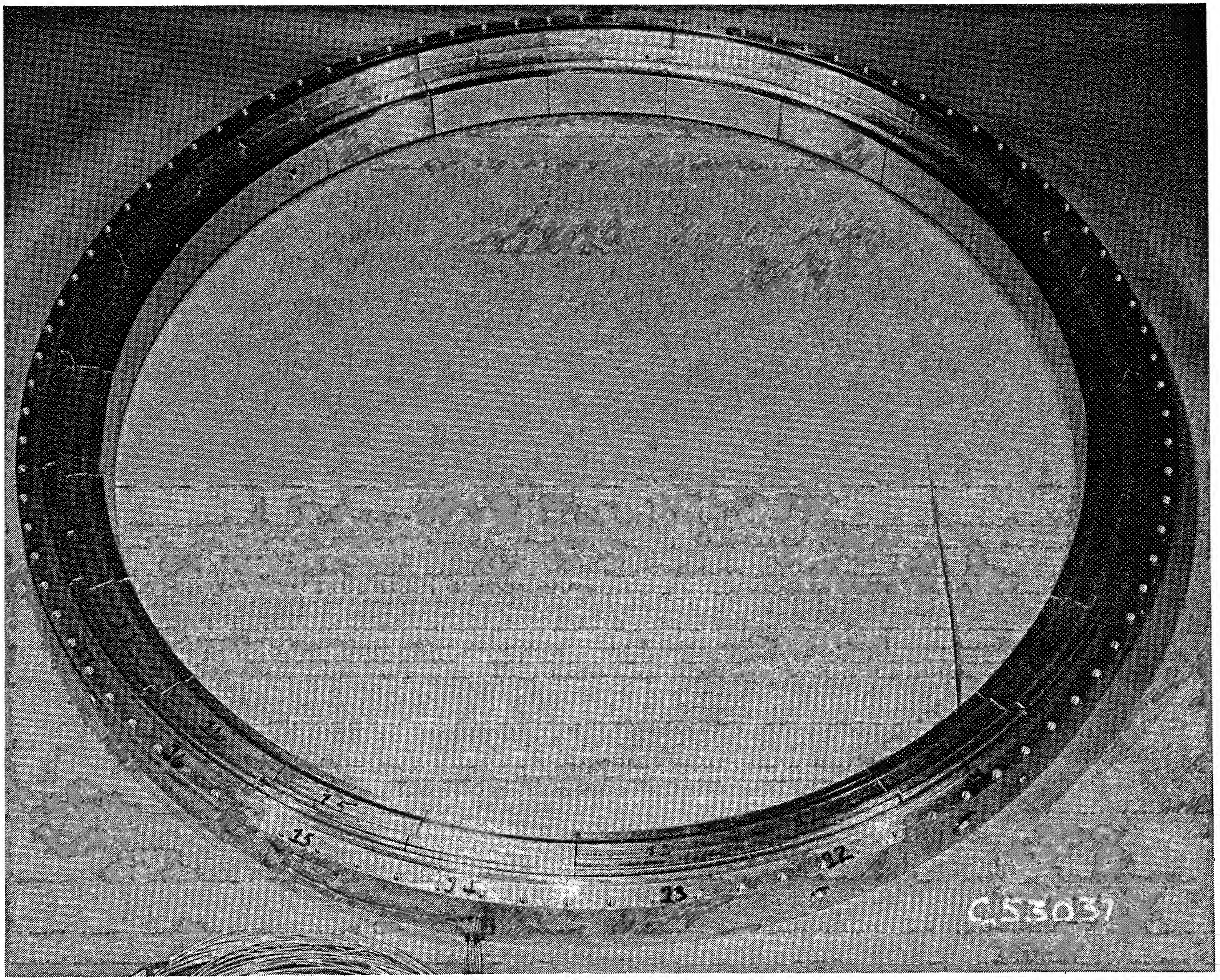

Figure 23. Stage 1 Shroud Assembly.

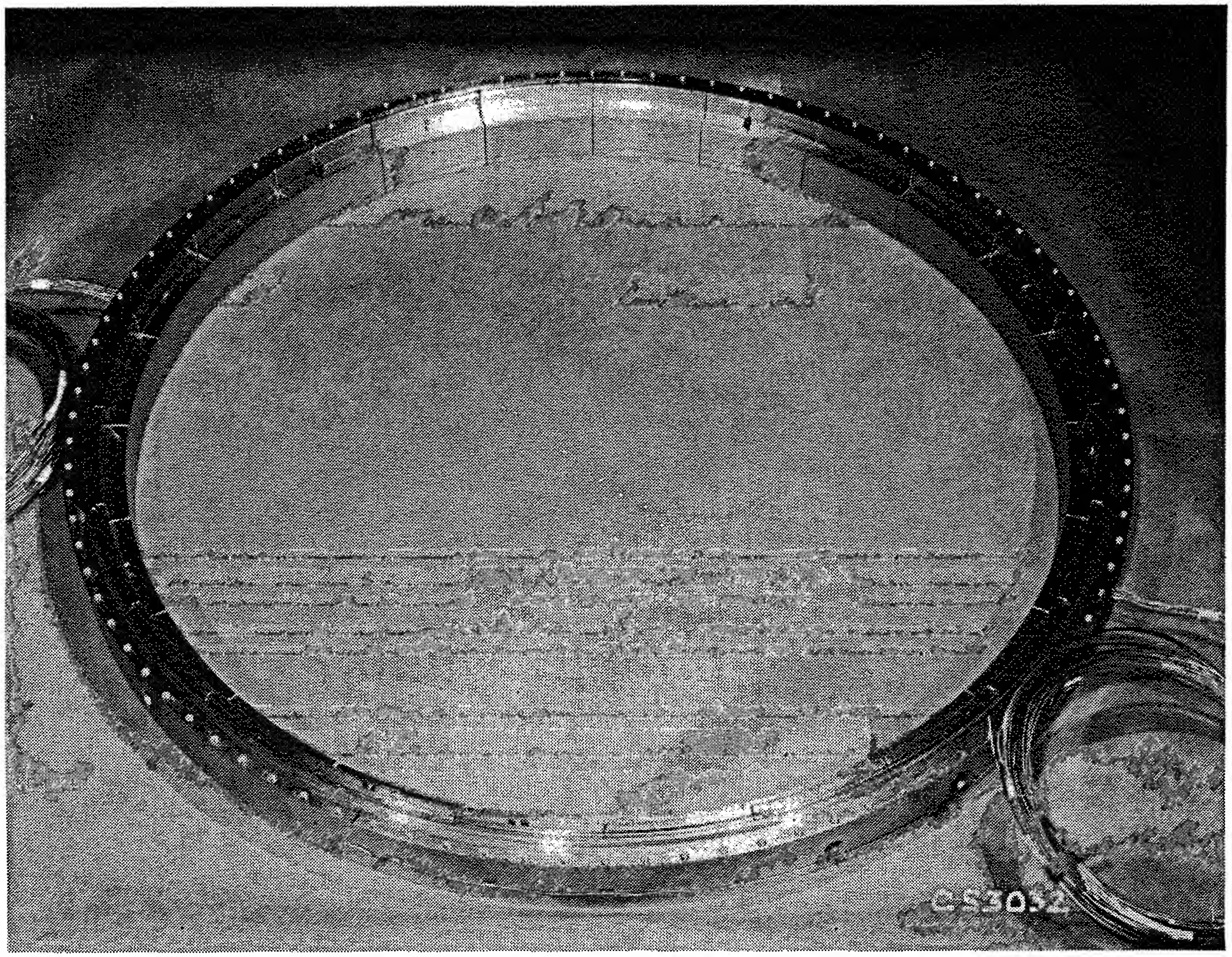

Figure 24. Stage 2 Shroud Assembly.

4.0 INSTRUMENTATION

4.1 Annular Cascade

Instrumentation for the annular cascade provided for the measurement of mainstream flow, cooling flow, inlet total pressure and temperature, coolant supply pressure and temperature, discharge total pressure and temperature, static pressure, flow angle, and airfoil surface static pressures. A summary of the instrumentation is presented in Table VIII. A schematic is shown in Figure 25.

Airflow measurements were made with choked, circular arc venturis. Inlet total pressure and temperature were measured by five radial rakes, each having a combination of five pressure and five temperature elements. These rakes were 12.7 cm (5.0 inches) upstream of the vane leading edge plane. Rake elements were located radially at the centers of equal flow streamtubes, determined by axisymmetric analysis. A schematic of the annular cascade inlet radial rakes is shown in Figure 26 where their location is shown relative to the six struts of the inlet frame.

Discharge total pressure and temperature were measured using a radially and circumferentially traversing sting probe. A schematic of the sting probe is shown in Figure 27. The sting sensing element was located 1.016 cm (0.4 inches) axially aft of the vane trailing edge and had 18^{o} of circumferential travel.

Flow angle measurements were made with a self-nulling cobra probe. A schematic of this probe is shown in Figure 28. This probe used the same casing slot as the sting probe. Consequently, its sensing element was 2.464 cm (0.97 inches) aft of the vane trailing edge. With the probe element in this axial position, a precise angle measurement was not expected.

Discharge static pressure was measured by forty-two taps in the plane of the sting sensing element. Twenty-one were on the inner case and twenty-one on the outer case.

Table VIII. Annular Cascade Instrumentation

LOCATION	MEASUREMENT	QUANTITY
Inlet	P_T, T_T	25 each (5 radial rakes, 5 dual elements per rake)
Inlet	P_S	10 total (5 each wall)
Vane Outer Cavity	P_S	3 total
Vane Outer Coolant Supply	T_T	3 total
Vane Surface	P_S	45 total (10 suction surface, 5 pressure surface 3 radial locations)
Bands	P_S	12 total (6 each wall, between two trailing edges)
Exit	P_S	42 total (21 each wall)
Exit	P_T, T_T	1 radially and circumferentially traversing sting probe
Exit	Flow Angle	1 radially and circumferentially traversing cobra probe

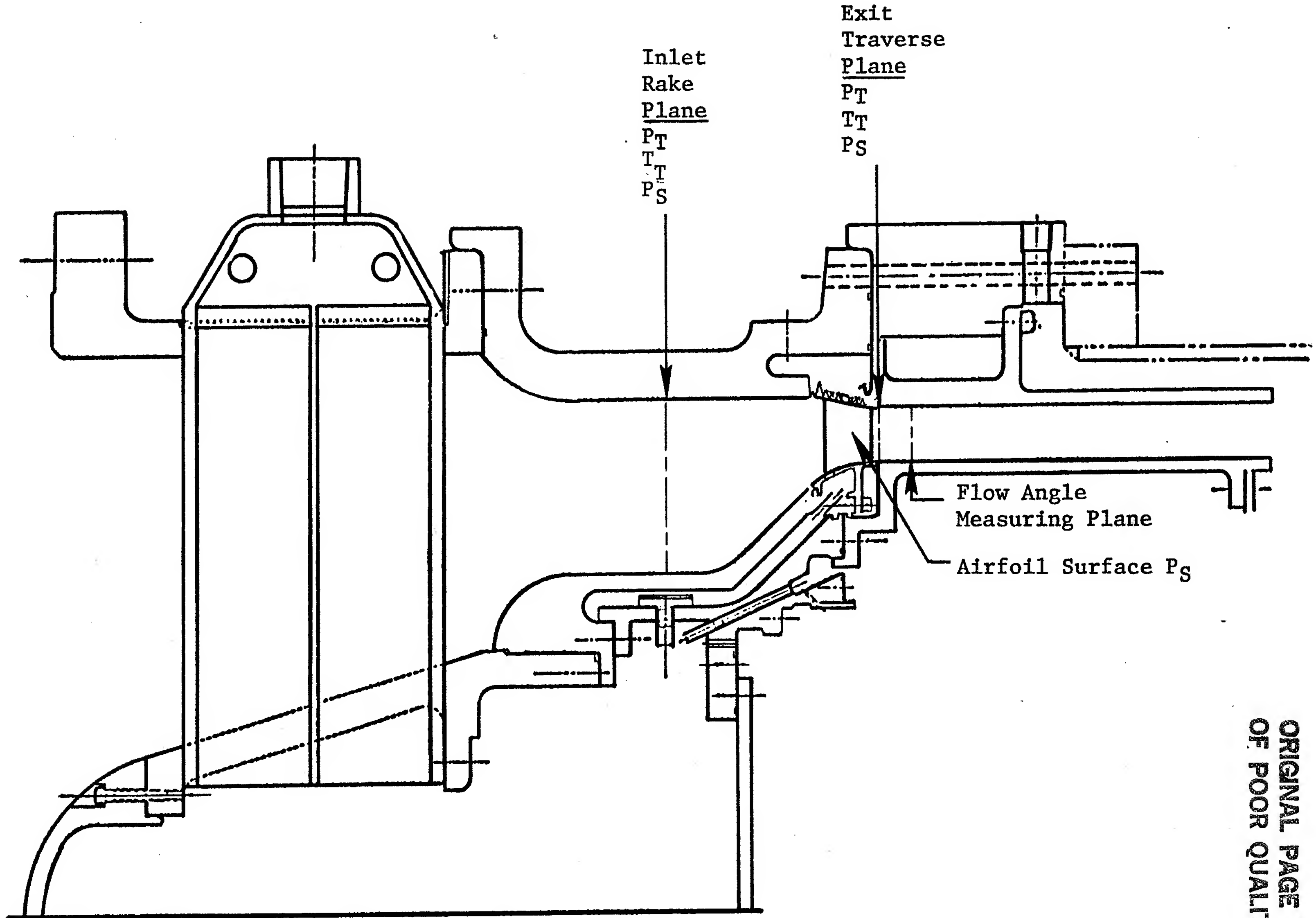

Figure 25. Schematic of Annular Cascade Instrumentation

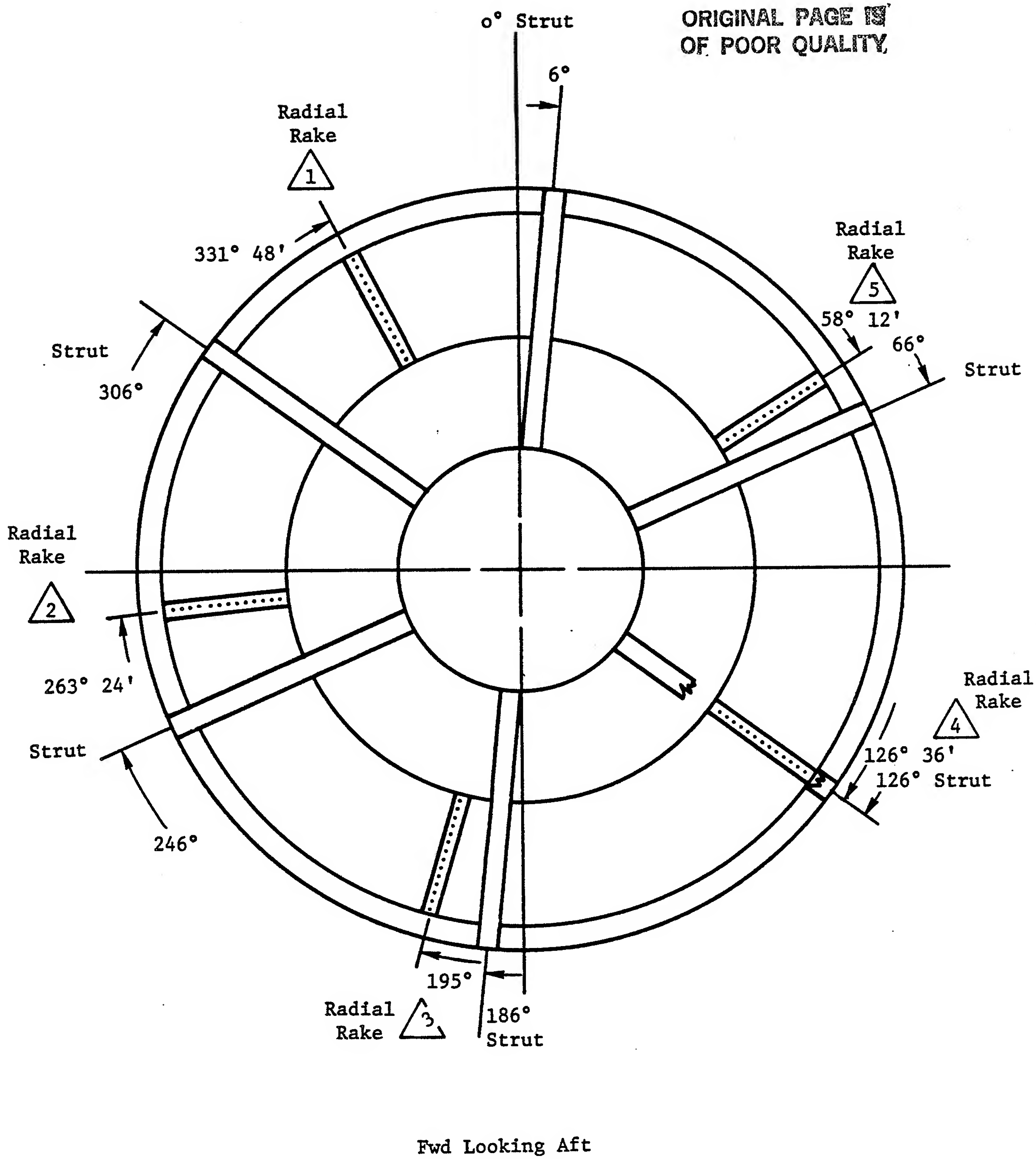

Figure 26. Schematic of Annular Cascade Inlet Radial Rake Showing Relative Location to Inlet Frame Struts

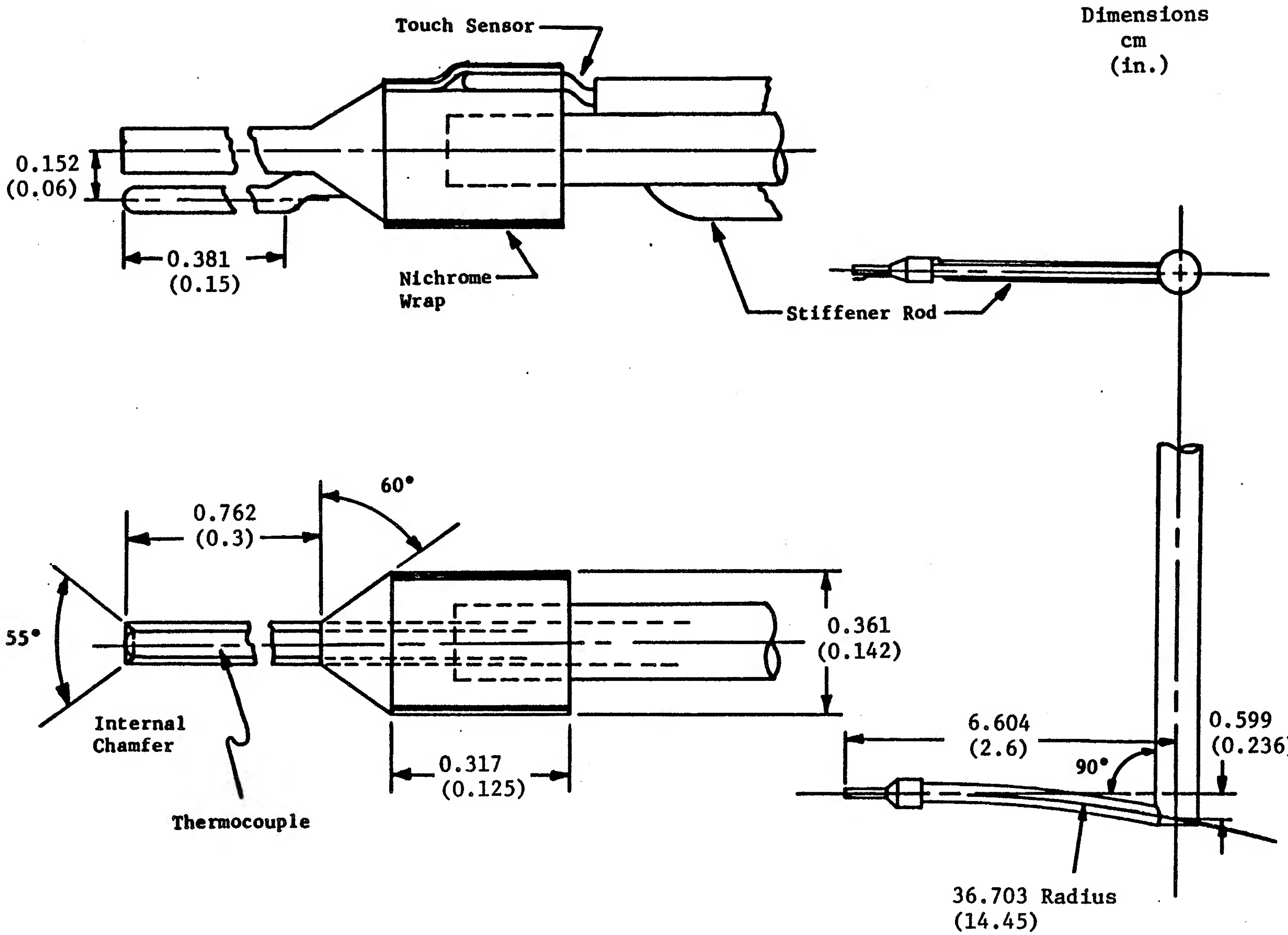

Figure 27. Sting Probe Schematic

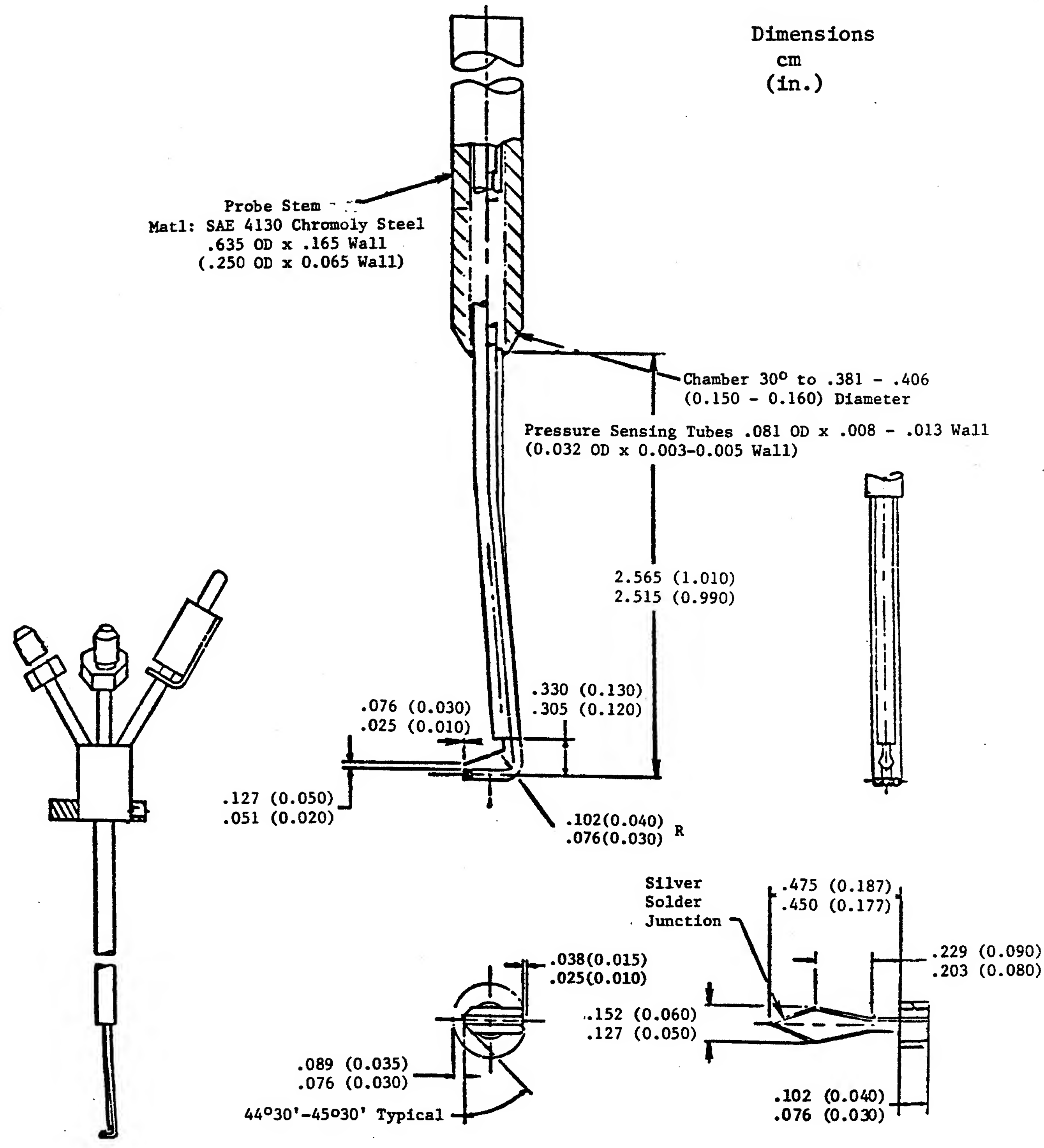

Figure 28. Cobra Probe Schematic.

Airfoil static pressure taps were installed at three radial locations, 0.254 cm (0.1 inch) from both walls and at the meanline. Ten taps were used on the suction surfaces and five on the pressure surfaces. The relative location of these taps on the airfoil surface are shown in Figure 29. Static pressures in the plane of the trailing edge on both walls are also depicted.

4.2 Rotating Rig

Instrumentation was provided to measure flows, pressures, temperatures, shaft speed, torque, tip clearance and exit flow angle. A schematic of the rig instrumentation is presented in Figure 30. The instrumentation is summarized in Table IX.

Main airflow was measured with a choked, circular arc venturi. Coolant flows were measured with choked or calibrated venturis and each coolant circuit had its own venturi.

Two independent strain gage torque meters mounted in the turbine shafting for direct readout were used as the primary torque measurement. This instrumentation provided the prime measurement of turbine power output in evaluating performance.

Speed measurements were made by an indicating system consisting of a 60-tooth gear attached to the turbine drive shaft and a stationary magnetic sensor mounted with its sensing head very close to the gear teeth. Electrical impulses resulting from the passing of each tooth yield an electrical frequency proportional to speed.

Inlet temperature and pressure were measured with the same radial rakes as used in the annular cascade. These provide twenty-five elements each for inlet total presure and total temperature. A frontal view of the rotating rig is shown in Figure 31, where the inlet rakes are seen in relation to the ten struts of the inlet frame.

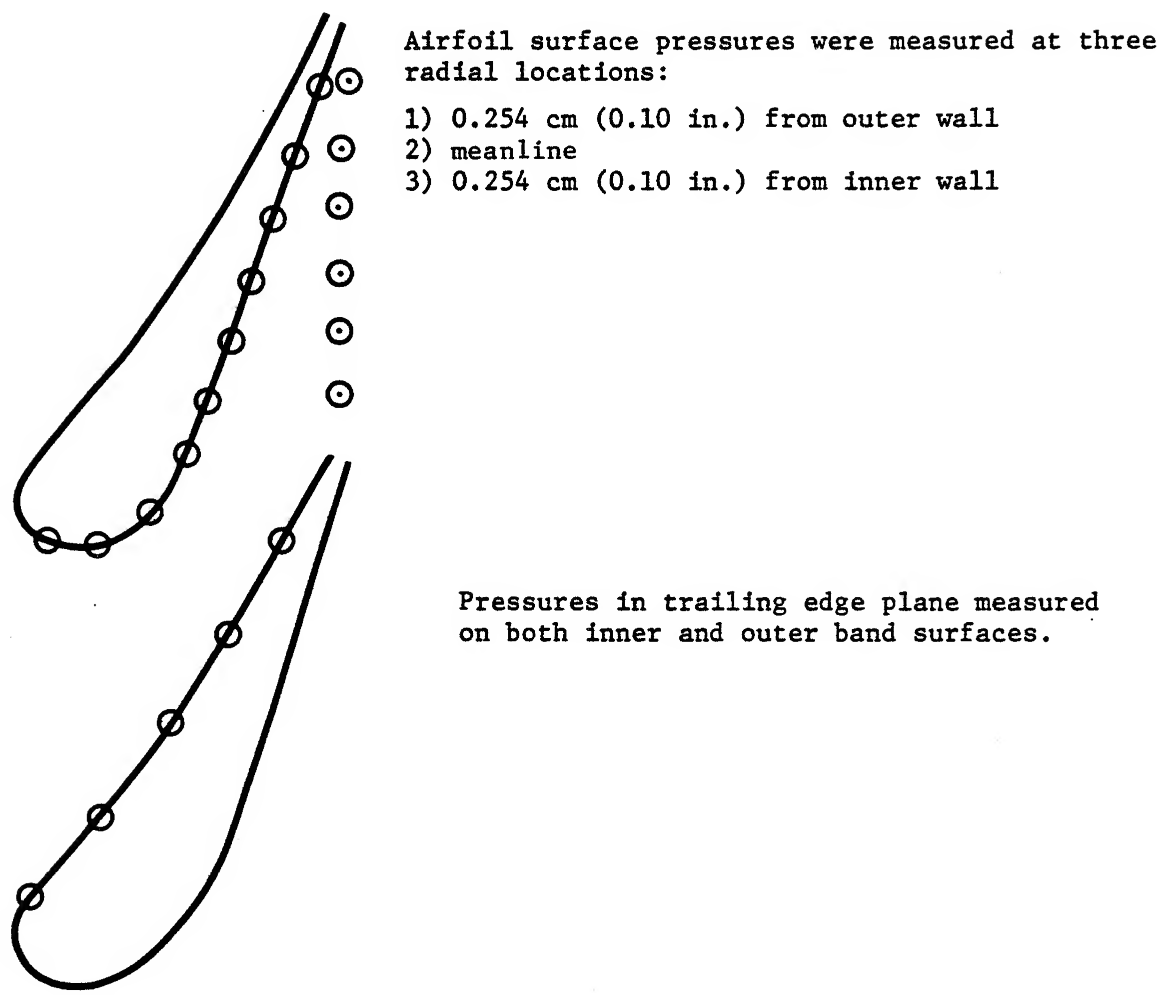

Figure 29. Location of Airfoil Surface and Band Static Pressure Taps in Annular Cascade.

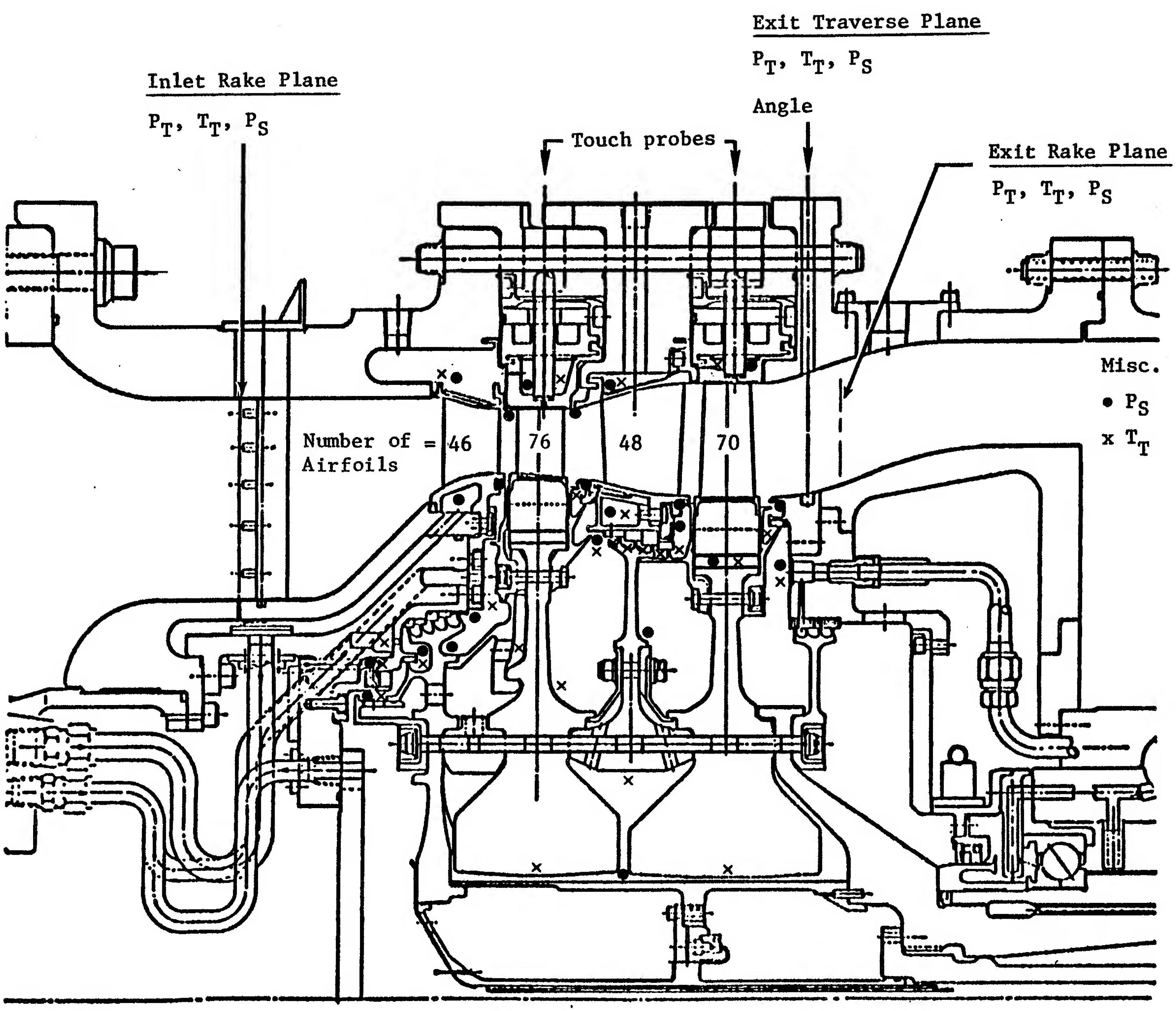

Figure 30. Schematic of Turbine Rig Instrumentation.

Table IX. Two Stage Rotating Rig Instrumentation.

LOCATION	MEASUREMENT	QUANTITY
Inlet	P_T, T_T	25 Each (5 radial rakes, 5 dual elements per rake)
Inlet	P_S	10 total (5 each wall)
Vane 1 Exit	P_S	8 total (4 in each cavity, outer and inner)
Blade 1 Exit	P_S	8 total (4 in each cavity, outer and inner)
Vane 2 Exit	P_S	4 in vane inner cavity
Blade 2 Exit	P_S	8 total (4 in each cavity, outer and inner)
Exit	P_T, T_T	72 total each (12 element, combination arc rakes at 6 radial locations)
Exit	P_S	12 total (6 each wall in rake plane)
Exit	P_S	8 total (4 each wall in traverse plane)
Exit	Flow Angle, P_T, T_T	Radially and circumferentially traversing cobra probe
Outer Case	Tip Clearance	8 wire brush touch probes (4 each stage)
Various Cavities	P_S, T_T	~200 for setting coolant conditions and monitoring coolant paths
Vehicle Shafting	Torque	2 independent strain gage torque meters
Inlet Piping	Flow	1 circular arc venturi
Coolant Piping	Flow	5 circular arc venturis (1 for each circuit)

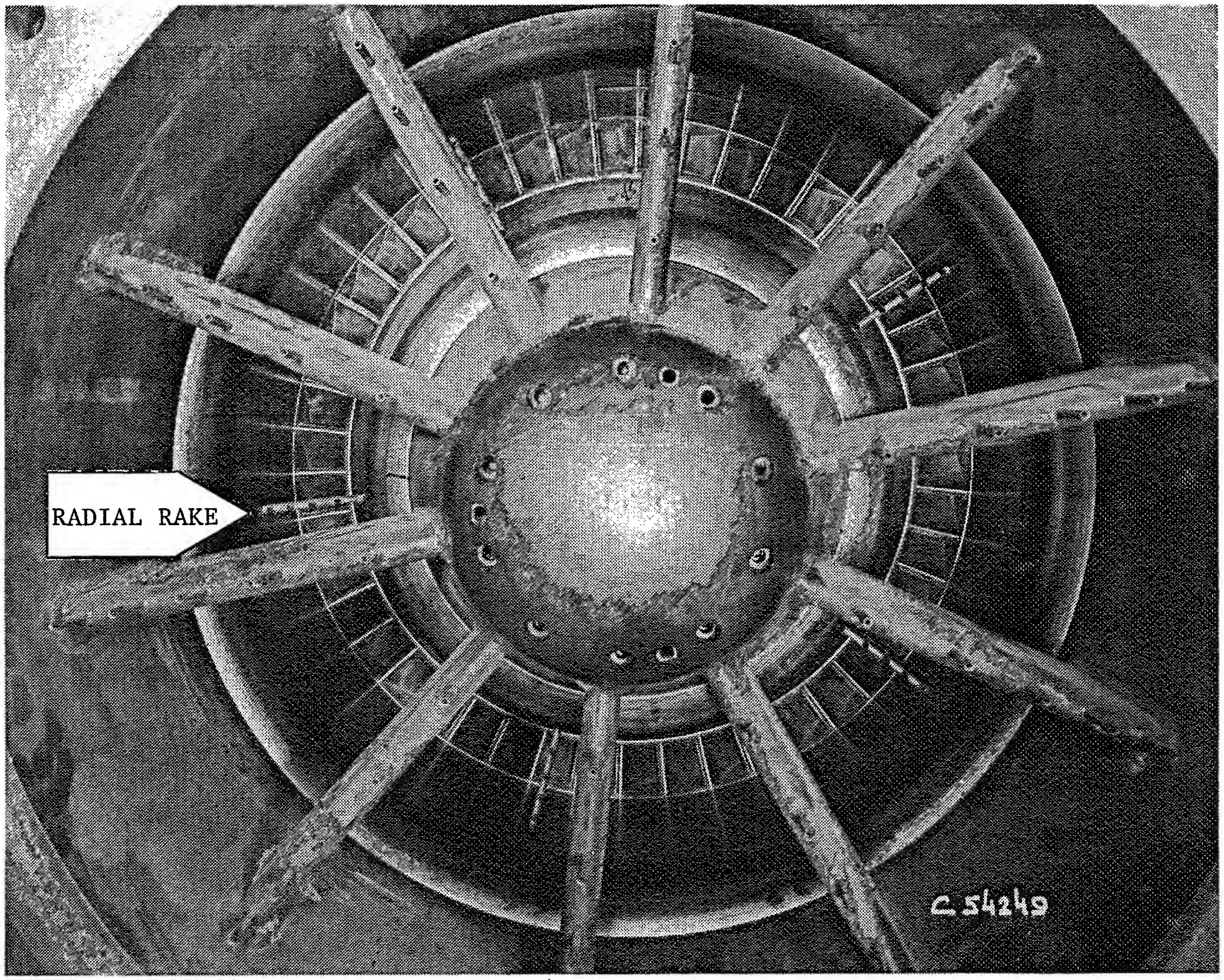

Figure 31. Front View of Turbine Rig Showing Location of Inlet Radial Rakes Relative to Inlet Frame Struts.

Turbine discharge total pressure and temperature were measured by arc rakes located 5.08 cm (2.0 inches) downstream of last bladerow. Six combination type arc rakes of twelve elements each were employed. A schematic of this rake is presented in Figure 32.

Turbine discharge static pressure was measured by twelve taps (six on outer wall, six on inner wall) in the plane of the exit arc rakes.

Stage exit flow angle was measured using a traversing cobra probe. This probe was located 3.02 cm (1.19 inches) aft of the stage two blade. The circumferential travel was 18° of arc. A schematic of this probe was shown previously in Figure 28.

Blade tip clearance measurements were obtained by means of wire brush touch probes. Four touch probes were used for each rotor. These probes physically contact the blade tips; an electrical signal indicates actual contact. The depth of the probe was determined from prior calibration of a radial motion actuator holding the probe. Rotor running tip clearance was determined from the difference between the rotor touch reading and a shroud reference point touch reading.

In addition to the primary performance instrumentation, the rig was heavily instrumented to obtain pressure and temperature data along the various coolant paths to the flowpath and interstage locations. The total number of these type items is on the order of 200 pieces of instrumentation.

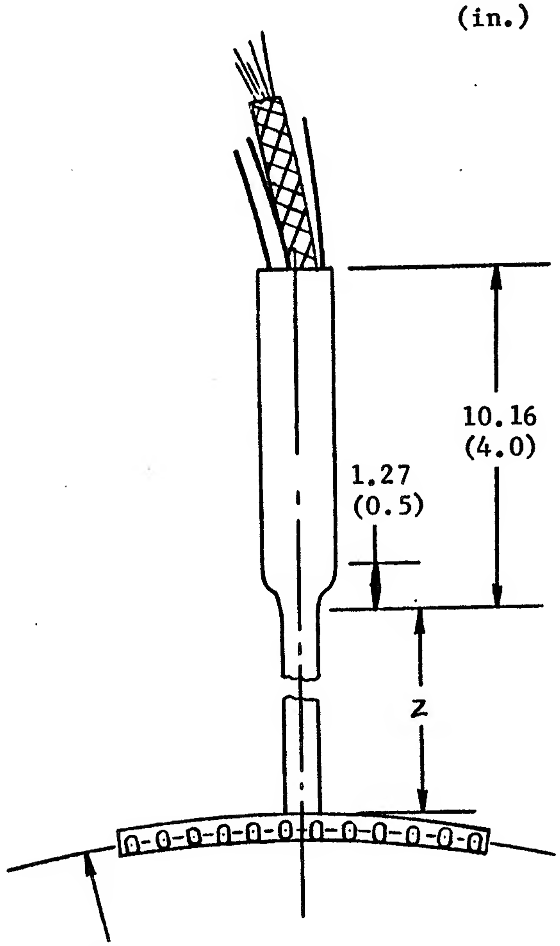

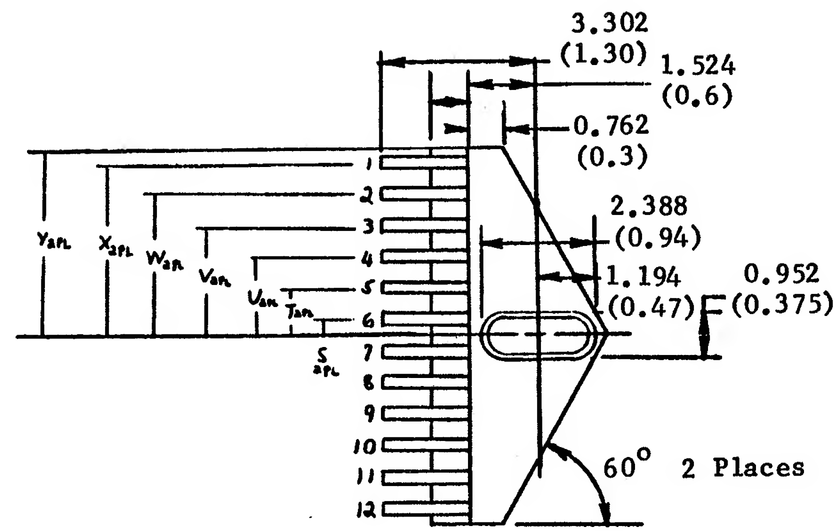

RAKE	GROUP	S	T	U	V	W	X	Y	Z
A	G01	.422 (.166)	1.270 (.500)	2.113 (.832)	2.960 (1.165)	3.805 (1.498)	4.651 (1.831)	4.928 (1.940)	1.016 (.400)
B	G02	.409 (.161)	1.277 (.483)	2.045 (.805)	2.863 (1.127)	3.680 (1.149)	4.498 (1.771)	4.775 (1.880)	2.210 (.870)
C	G03	.396 (.156)	1.189 (.468)	1.981 (.780)	2.774 (1.092)	3.566 (1.404)	4.359 (1.716)	4.636 (1.825)	3.429 (1.350)
D	G04	.381 (.150)	1.146 (.451)	1.910 (.752)	2.675 (1.053)	3.439 (1.354)	4.204 (1.655)	4.483 (1.765)	4.674 (1.840)
E	G05	.368 (.145)	1.105 (.435)	1.842 (.725)	2.578 (1.015)	3.315 (1.305)	4.051 (1.595)	4.331 (1.705)	5.994 (2.360)
F	G06	.353 (.139)	1.059 (.417)	1.765 (.695)	2.471 (.973)	3.178 (1.251)	3.884 (1.529)	4.166 (1.640)	7.341 (2.890)

Figure 32. Arc Rake Schematic.

5.0 TEST PROCEDURES

5.1 Annular Cascade

Test conditions for the annular cascade were intended to simulate the engine conditions at the maximum climb aerodynamic design point. Vane pressure ratio (upstream total to downstream static), ratio of cooling air supply pressure to mainstream pressure, and ratio of cooling air temperature to mainstream temperature were to be the same as in the engine. Coolant supply pressure was selected so that the pressure in the vane internal cavities would correspond to the pressure between the impingement insert and vane shell in the engine design.

Initially, vane coolant was supplied from both the outer and inner band circuits. The first run of the cascade however, revealed that too much heat was picked up by the inner circuit cooling air. The inner circuit cooling air was delivered through the inlet frame struts and dumped into the bullet nose region of the test vehicle. The air flow rate was low since only twelve of the forty-six vanes and thirty-five percent of the bands were cooled. The inlet struts and bullet nose were exposed to the mainstream temperature; this coupled with the low flow (high residence time) allowed a large heat pick-up by the cooling flow. This resulted in the inner circuit coolant flow to be significantly lower than design intent. In order to alleviate this condition, the inner circuit was blocked and the outer circuit was then used to supply all the cooling flow which required a slight increase in the outer circuit coolant pressure. A cavity pressure of 350.95 kPa (50.9 psia) was set to get a design intent flow of 0.3509 kg/sec (0.7736 lbs/sec). Setting cooling flow in this manner caused a slight over-pressure on the outer band and a similar under pressure on the inner band. The coolant supply scheme is illustrated in Figure 33.

Test point was established by setting cascade inlet pressure and temperature, coolant pressure and temperature, and total-to-static pressure ratio across the cascade. The test point schedule is presented in Table X.

ORIGINAL PAGE IS
OF POOR QUALITY

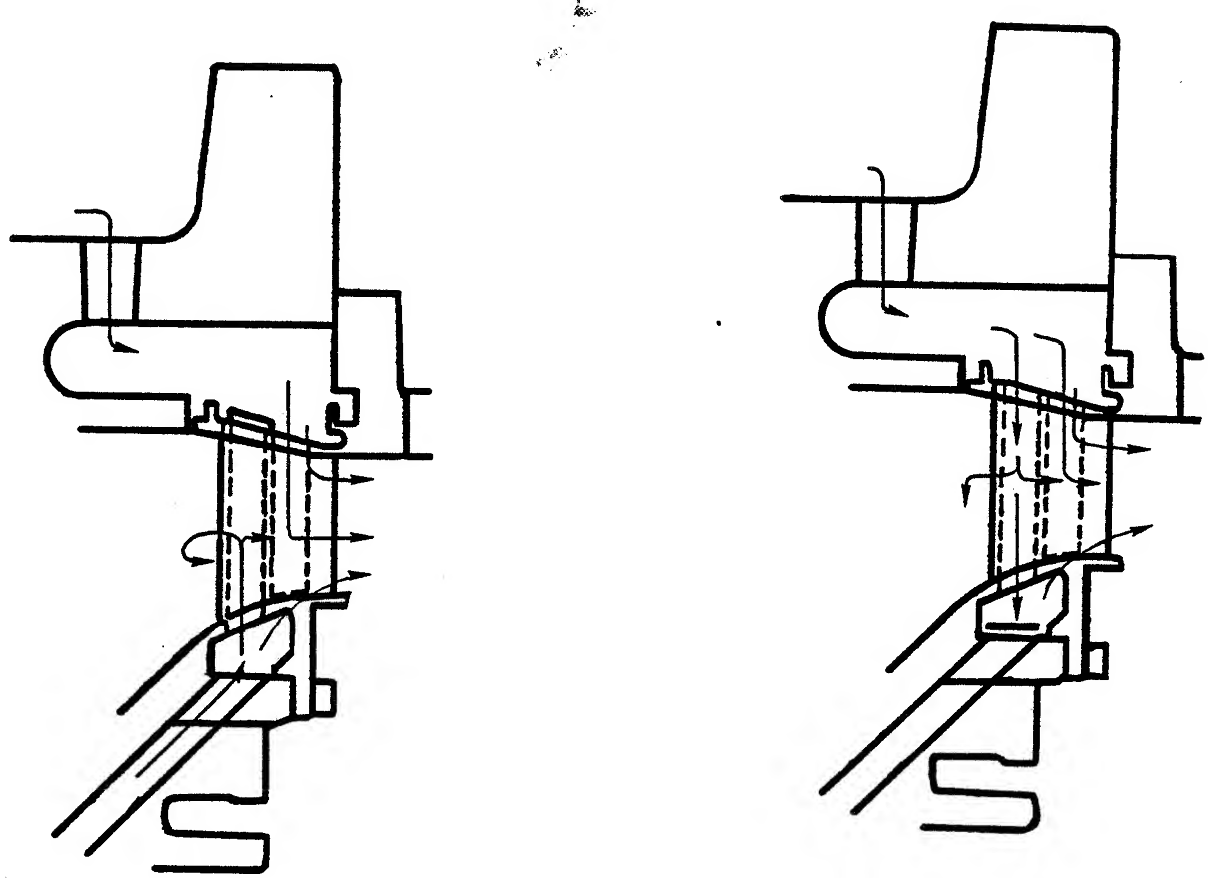

Original Cooling
Supply Scheme

Revised Cooling
Supply Scheme

Figure 33. Annular Cascade Coolant Supply Schematic.

Table X. Annular Cascade Test Conditions

$P_{T,0}/P_{S,1}$	$P_{T,0}$ Pa (psia)	$T_{T,0}$ K (°R)	P_c Pa (psia)	$T_{T,c}$ K (°R)	Traverse Type
1.5	3.4474×10^5	709	3.5095×10^5	339	B
1.67*	(50.0)	(1277)	(50.9)	(611)	A
1.8					B
1.9					B
2.0					A
2.1					B
2.2					B
2.3					B
2.5					A
2.7					B

* Design point conditions.

A = Circumferential traverses at 15 radial locations.

B = Circumferential traverses at pitchline.

In addition to testing the two vane configurations, several diagnostic runs were made. The purpose of these runs was to isolate the source of some larger than expected pitchline losses. The following configurations were tested:

Base vane	–	fully cooled
LUT vane	–	fully cooled
Base vane	–	solid vanes and bands
Base vane	–	last row of suction side holes sealed
Base vane	–	trailing edge sealed (1st test)
Base vane	–	trailing edge sealed (2nd test)

For the last three configurations, data were taken only at design pressure ratio.

5.2 Rotating Rig

In order to account for the hot-gas to warm-air difference in specific heat ratio (γ) in determining the equivalent aerodynamic operating point of the air turbine rig, a series of vector diagram calculations were made at rig test conditions from which plots of stage reaction*, bladerow inlet angles and stage loadings were prepared. From these plots, turbine pressure ratio and corrected speed were selected that resulted in minimum deviation of the three named parameters from engine turbine design values. As in past experience, the resultant operating point ($P_{T,4}/P_{T,42}$ and $N/\sqrt{T_{T,41}}$) closely matches the engine turbine design point value of energy function ($\Delta h/T_{T,41}$). A comparison of design point parameters for ICLS with those of the rig at facility inlet conditions is shown in Table XI. A comparison of blading inlet angles and stage hub reaction is presented in Table XII.

---

*Reaction is defined as the ratio of static enthalpy drop across the rotor to the total-to-static drop across the stage. For the first stage, this can be approximated as

$$Rx = 1 - \left\{ \left[1 - \left(\frac{P_{S,1}}{P_{T,0}} \right)^{\frac{\gamma-1}{\gamma}} \right] \Bigg/ \left[1 - \left(\frac{P_{S,2}}{P_{T,0}} \right)^{\frac{\gamma-1}{\gamma}} \right] \right\}.$$

Table XI. Design Point Parameters Compared, ICLS vs. Two Stage Rig

ITEM	UNITS	MAX CLIMB ICLS	MAX CLIMB RIG
Rotor Inlet Temperature, $T_{T,41}$	K °R	1588 2858	683 1230
Energy Extraction, $\Delta h/T_{T,41}$	Joules/kg/K Btu/lbm/°R	340.74 0.0814	339.90 0.0812
Corrected Speed, $N/\sqrt{T_{T,41}}$	rad/s/$\sqrt{K}$ rpm/$\sqrt{°R}$	33.19	33.19
Flow Function, $W_{41}\sqrt{T_{T,41}}/P_{T,4}$	kg$\sqrt{K}$/sec/kPa lbm$\sqrt{°R}$/sec/psia	0.867 17.678	0.885 18.026
Pressure Ration, Total-to-Total, $P_{T,4}/P_{T,42}$	-	4.933	5.04
Pressure Ratio, Total-to-Static, $P_{T,4}/P_{S,42}$	-	5.289	5.66
Velocity Ratio, U/C_o	-	0.575	0.575
Pitchline Aerodynamic Loading, ψ_p	-	0.648	0.646

Table XII. Comparison of Inlet Angles, Reaction, and Loading, for ICLS and Two Stage Rig.

	Inlet Gas Angle At Pitchline, Degrees		Stage Reaction, Rx				Aerodynamic Loading at Pitchline, ψ_p	
			HUB		TIP			
	ICLS	RIG	ICLS	RIG	ICLS	RIG	ICLS	RIG
Vane 1	0	0	---	---	---	---	---	---
Blade 1	46.2	46.7	0.345	0.337	0.467	0.460	0.746	0.748
Vane 2	20.3	19.9	---	---	---	---	---	---
Blade 2	18.8	17.9	0.330	0.334	0.513	0.516	0.550	0.545

Rig inlet temperature and pressure were set at 709K (1277°R) and 344.74 kPa (50 psia) respectively, as in the annular cascade. Ratio of cooling air temperature to mainstream temperature were maintained at engine levels. Pressures and temperatures to be set for each cooling circuit along with predicted cooling flows at design point were:

a) Stage 1 Outer Band, Vane and Shroud

$P_c = 3.4667 \times 10^5$ Pa (50.28 psia)
$T_{T,c} = 352$K (633°R)
$W_c = 0.656$ kg/sec (1.447 lb/sec)

b) Stage 1 Inner Band and Vane

$P_c = 3.5019 \times 10^5$ Pa (50.79 psia)
$T_{T,c} = 352$K (633°R)
$W_c = 0.598$ kg/sec (1.318 lb/sec)

c) Inducer

$P_c = 3.4660 \times 10^5$ Pa (50.27 psia)
$T_{T,c} = 344$K (620°R)
$W_c = 0.586$ kg/sec (1.293 lb/sec)

d) CDP Seal Leakage

$P_c = 2.6642 \times 10^5$ Pa (38.64 psia)
$T_{T,c} = 361$K (649°R)
$W_c = 0.176$ kg/sec (0.388 lb/sec)

e) Stage 2 Vane and Shroud

$P_c = 1.6327 \times 10^5$ Pa (23.68 psia) (at des. pt.),
will be set to give W_c/W_{41} = constant
$T_{T,c} = 300$K (540°R)
$W_c = 0.28$ kg/sec (0.617 lb/sec) (at des. pt.)

These flows are illustrated schematically in Figure 34.

Cooling Flow Legend	Design Intent Flows kg/sec	(lb/sec)	W_c/W_{41}
1) Outer Band, Aft Vane	0.656	(1.447)	0.0565
2) Inner Band, Fwd Vane	0.598	(1.318)	0.0511
3) Inducer, Blade 1 & 2	0.586	(1.293)	0.0503
4) Compressor Discharge Leakage	0.176	(0.388)	0.0151
5) Stage 2 Nozzle	0.280	(0.617)	0.0236

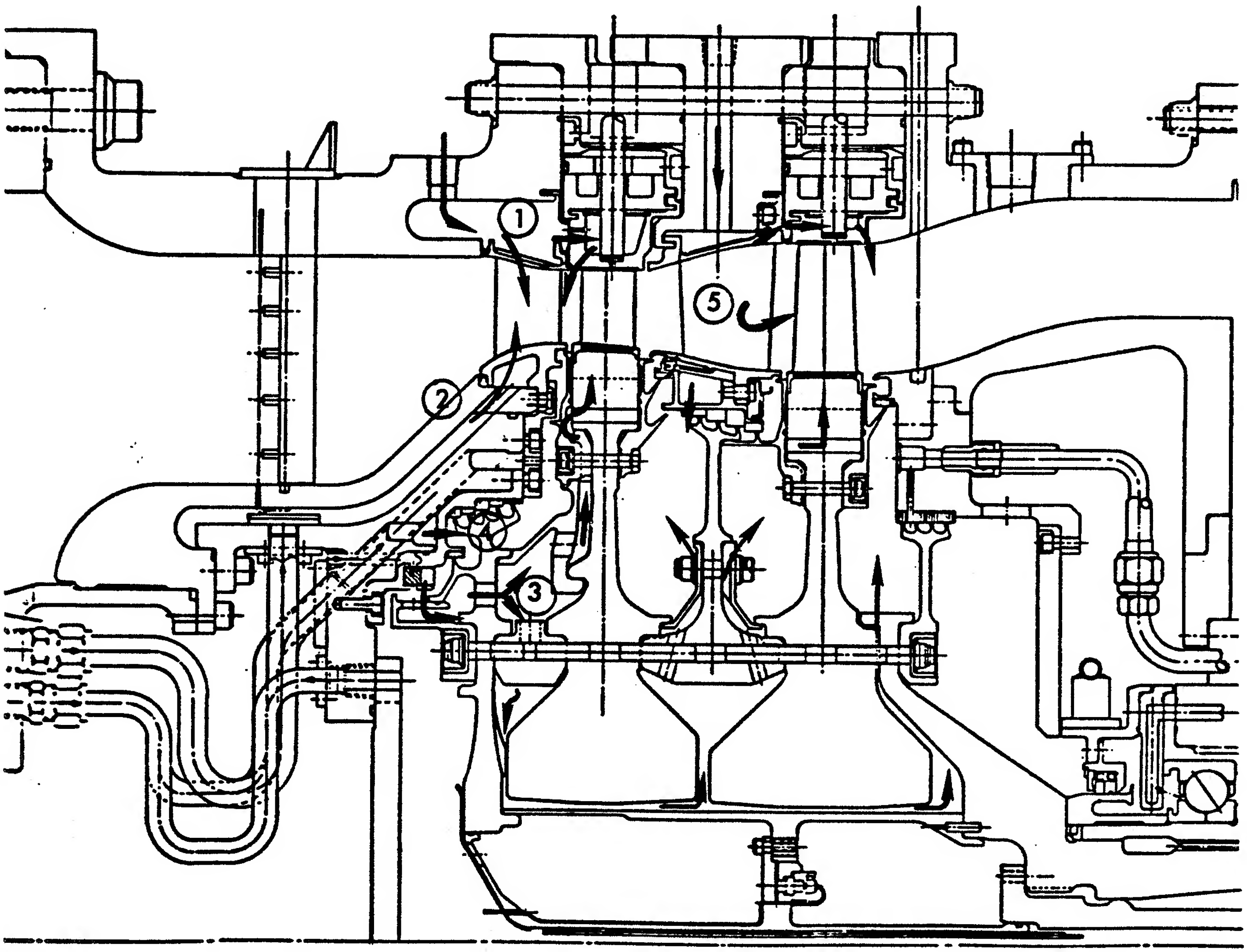

Figure 34. Turbine Rig Cooling Schematic.

Test points were established by setting turbine inlet total-to-exit static pressure ratio, inlet temperature, speed, tip clearance and coolant circuits. The turbine pressure ratio was measured for inlet rakes to discharge rake plane statics. Cooling flows were established by setting pressure and temperature in the various cavities and thus allowing flow rate to fall out. If flows deviated from design intent, no attempt was made to adjust the pressure to get the design intent flow. This criterion was followed since in an engine, the supply pressure and temperature are fixed. Furthermore, for small deviations on the order of 0 to 5%, the flowrate mismatch is more readily reconciled analytically than a mismatch in coolant source pressure or temperature.

In addition to design point operation, performance mapping, clearance variation, cooling flow variation, and Reynolds number excursion were accomplished. Details of these tests are discussed below.

Performance Map

The test plan was defined to include off-design performance mapping covering a wide range of operation. The test matrix was defined by specifying values of turbine total-to-static pressure ratio and blade-jet speed ratio, U/C_o. These parameters are independent dimensionless variables. They are independent in the sense that they are not functions of how the turbine performs. Further, total-to-static pressure ratio can be set directly by the cell operator, whereas total-to-total cannot. The pressure ratio is defined from inlet rake total pressure to static pressure at the exit rake plane. Lines of constant U/C_o are roughly parallel to the turbine operating line on a Δ/T vs $N/\sqrt{T}$ map. The definition and significance of blade-jet speed ratio are presented in Appendix B. The test matrix selected for the two stage group is shown graphically in Figure 35.

Reynolds Number Excursion

In addition to performance mapping, a Reynolds number excursion was made. This was accomplished by modulating inlet pressure at design point values of pressure ratio and speed to change flow density and thereby Reynolds

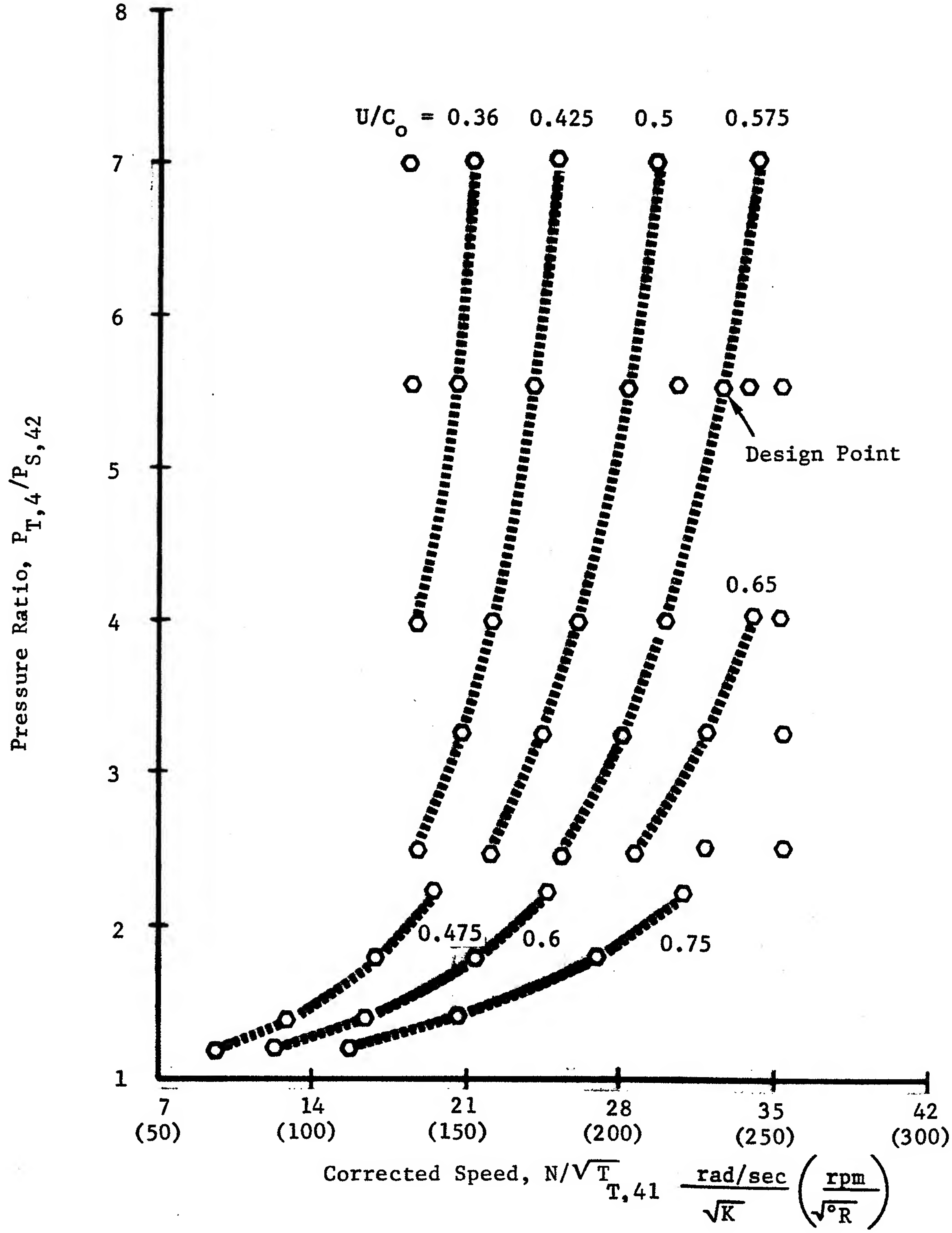

Figure 35. Turbine Rig Test Matrix

number. Sufficient points were taken to define efficiency variation with Reynolds number. In particular, it was intended to define the transition point where efficiency becomes independent of Reynolds number. The definition of Reynolds number used in this report is detailed in Appendix C.

Clearance Variation

Turbine efficiency as a function of blade clearance was determined by varying the radial clearance over each rotor separately. Clearance was varied by heating (or cooling) the shroud support, to control shroud diameter. Nominal running clearance was 0.041 cm (0.016 inches). The clearance variation was accomplished at design point conditions. In order to achieve the desired range of variation, it was necessary to reduce the temperature of the rotor coolant from 344K (620°R) to 317K (570°R).

Cooling Flow Variation

Effect of cooling flow variation on turbine performance was investigated by varying total flow to the first stage vane and flow to the following three circuits separately: compressor discharge leakage, rotor, and stage 2 nozzle. This variation was done at design speed and pressure ratio by increasing or decreasing the particular coolant supply pressure. The primary objective of the coolant flow variation tests was the acquisition of data for use in comparing with coolant effects prediction procedures.

6.0 RESULTS

6.1 Annular Cascade

As stated previously, the purpose of the annular cascade test was to evaluate the two vane configurations over a range of pressure ratios and select one for use in the air turbine and engine. The results of this testing are shown in Figure 36, where vane cascade efficiency is plotted versus cascade total-to-static pressure ratio. The definition of vane efficiency is presented in Appendix D. Pitchline efficiency is plotted in Figure 36a and overall efficiency in 36b. At the pitchline, base vane efficiency is 0.14% better than the LUT at design pressure ratio of 1.67. Overall efficiency of the base design is 93.59%, while that of the LUT design is 93.14% from which it follows that the base vane shows an advantage of 0.48% in vane efficiency at design conditions. At higher than design pressure ratios, the LUT design has better performance, probably due to less recompression shock loss. Because of its higher performance at design pressure ratio, the base vane was selected for air turbine evaluation and in the engine.

In Figure 37, the radial variations of efficiency and temperature for the two configurations are compared. From this figure it is seen that the base vane outperforms the LUT vane by about 1 point for the lower half of the annulus. Off-design performance in the spanwise direction is compared in Figure 38. Measured vane exit flow angle was adjusted to satisfy continuity using measured flow, pressure and temperature. Adjusted values are compared to design intent in Figure 39. Since this measurement was made relatively far downstream, the gradient shown is not necessarily considered indicative of that at the trailing edge. No flow angle measurement was made for the LUT vane.

The effect of reduced cooling flow was investigated for the base vane. This was accomplished by reducing the coolant supply pressure from 1.6% greater than inlet pressure to 0.2% greater. This brought about a reduction in total coolant flow to the nozzle assembly from 4.28% of inlet flow to 2.72%. The effect on vane efficiency is shown in Figure 40, where it is seen that while the integrated mass averaged efficiency did not change, there was a general increase in the outer annulus and decrease in the inner. Although the

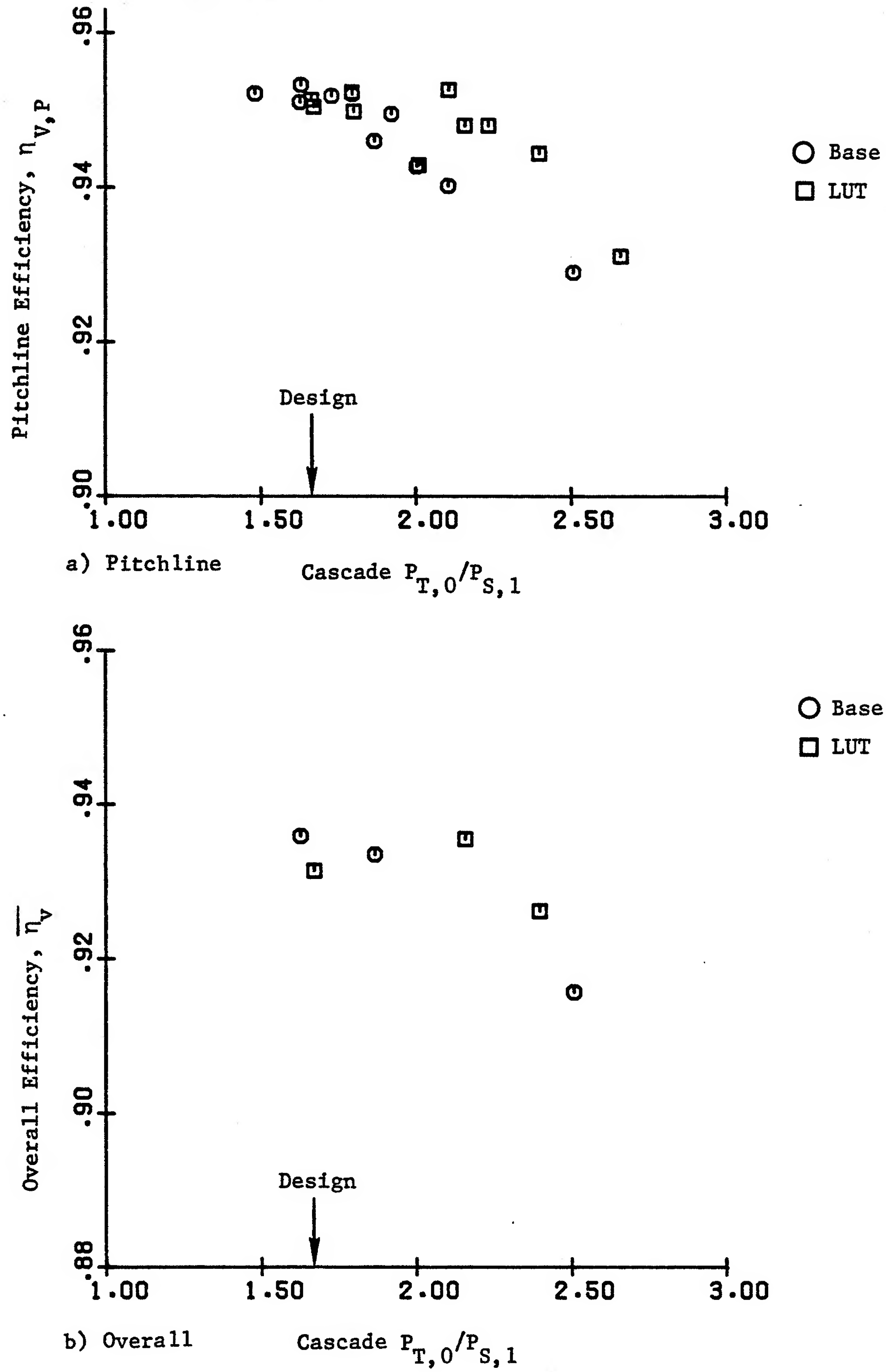

Figure 36. Vane Efficiency Versus Cascade Pressure Ratio, Base vs. LUT.

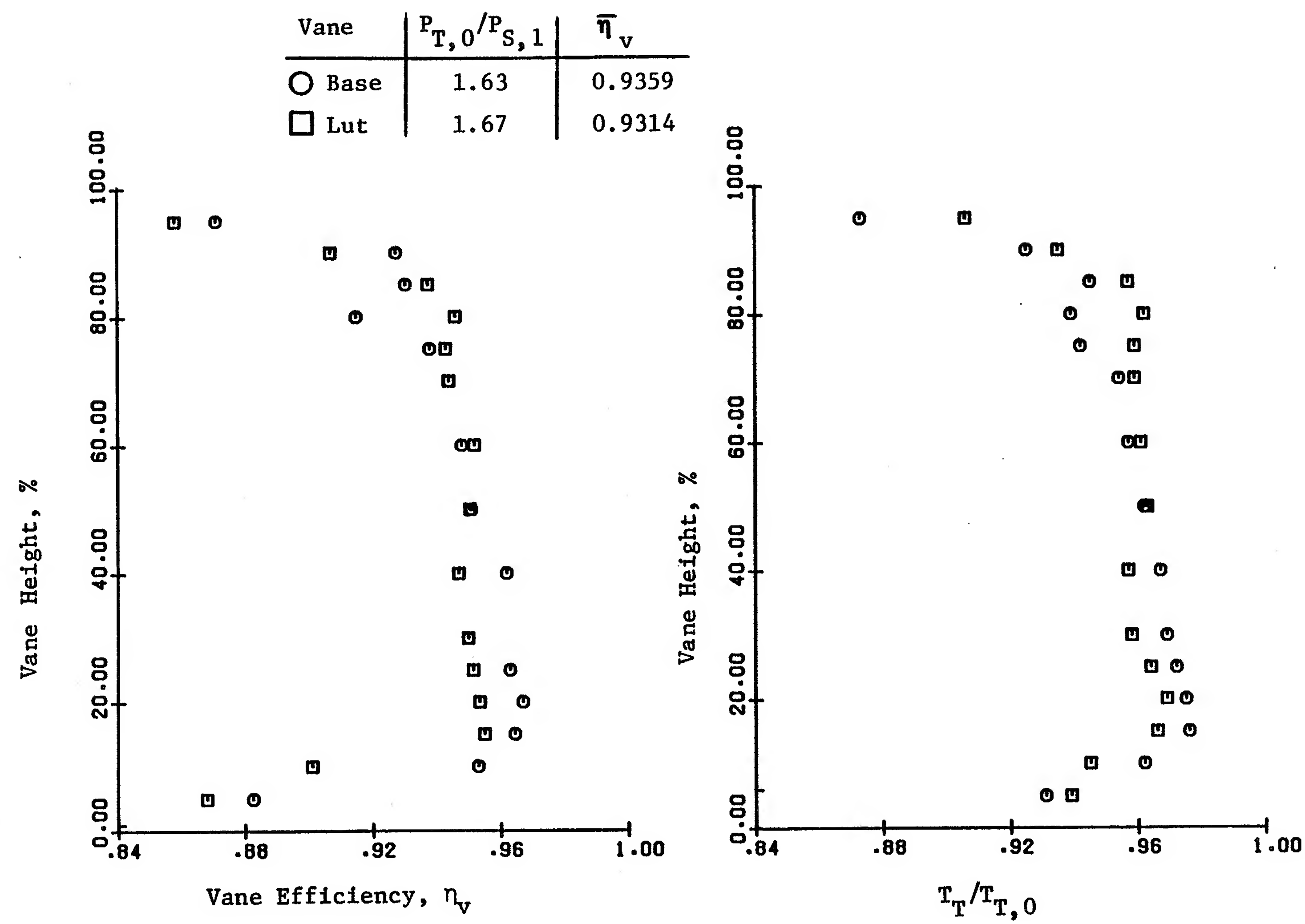

Figure 37. Radial Variation of Vane Efficiency and Temperature Ratio at Design Point, Base vs. LUT.

Vane	$P_{T,0}/P_{S,1}$	$\overline{\eta_v}$
△ Base	1.87	0.9335
◇ Base	2.51	0.9157
+ LUT	2.16	0.9355
× LUT	2.40	0.9262

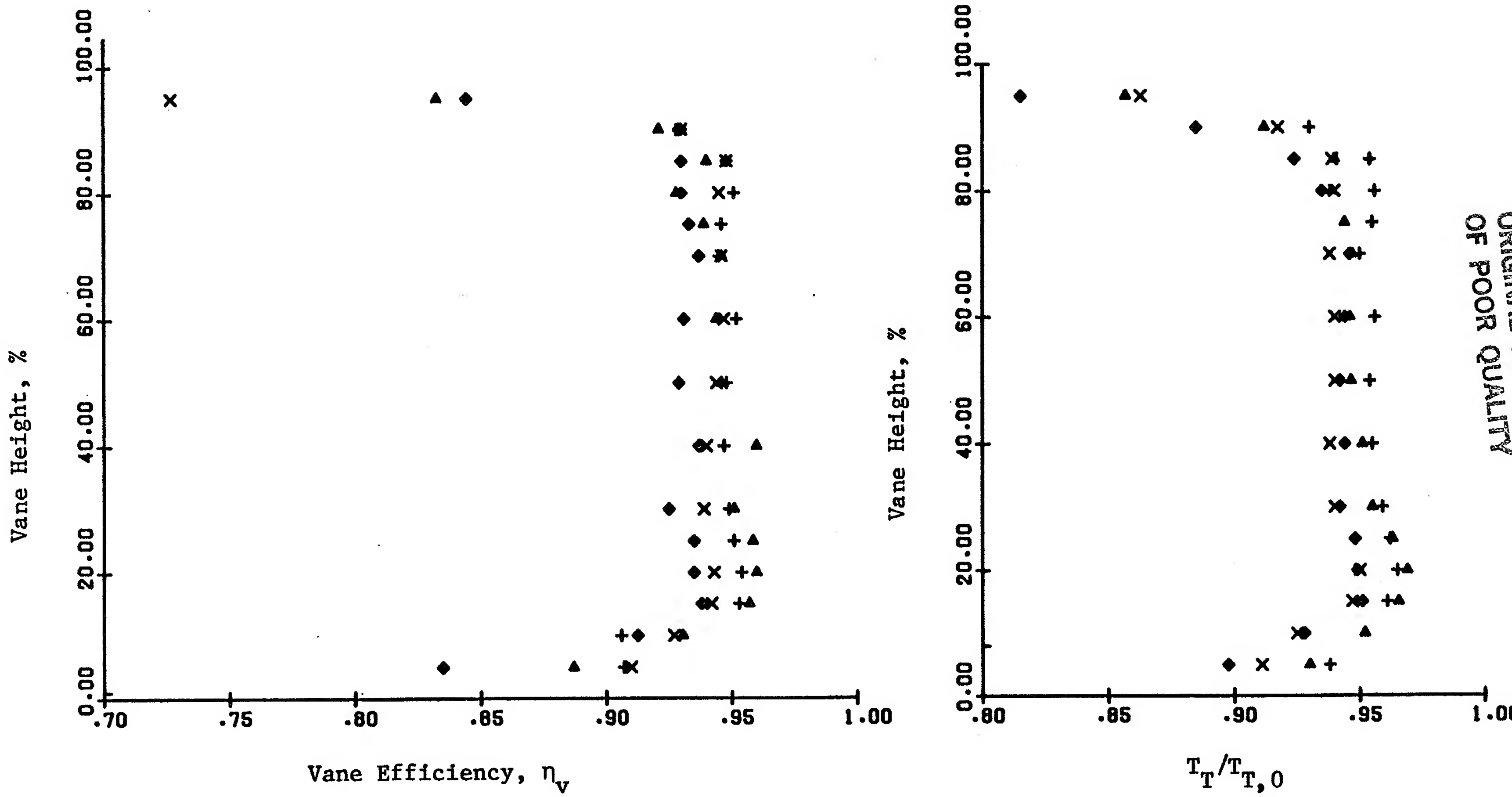

Figure 38. Radial Variation of Vane Efficiency and Temperature Ratio at Off Design Pressure Ratios, Base vs. LUT.

ORIGINAL PAGE IS
OF POOR QUALITY

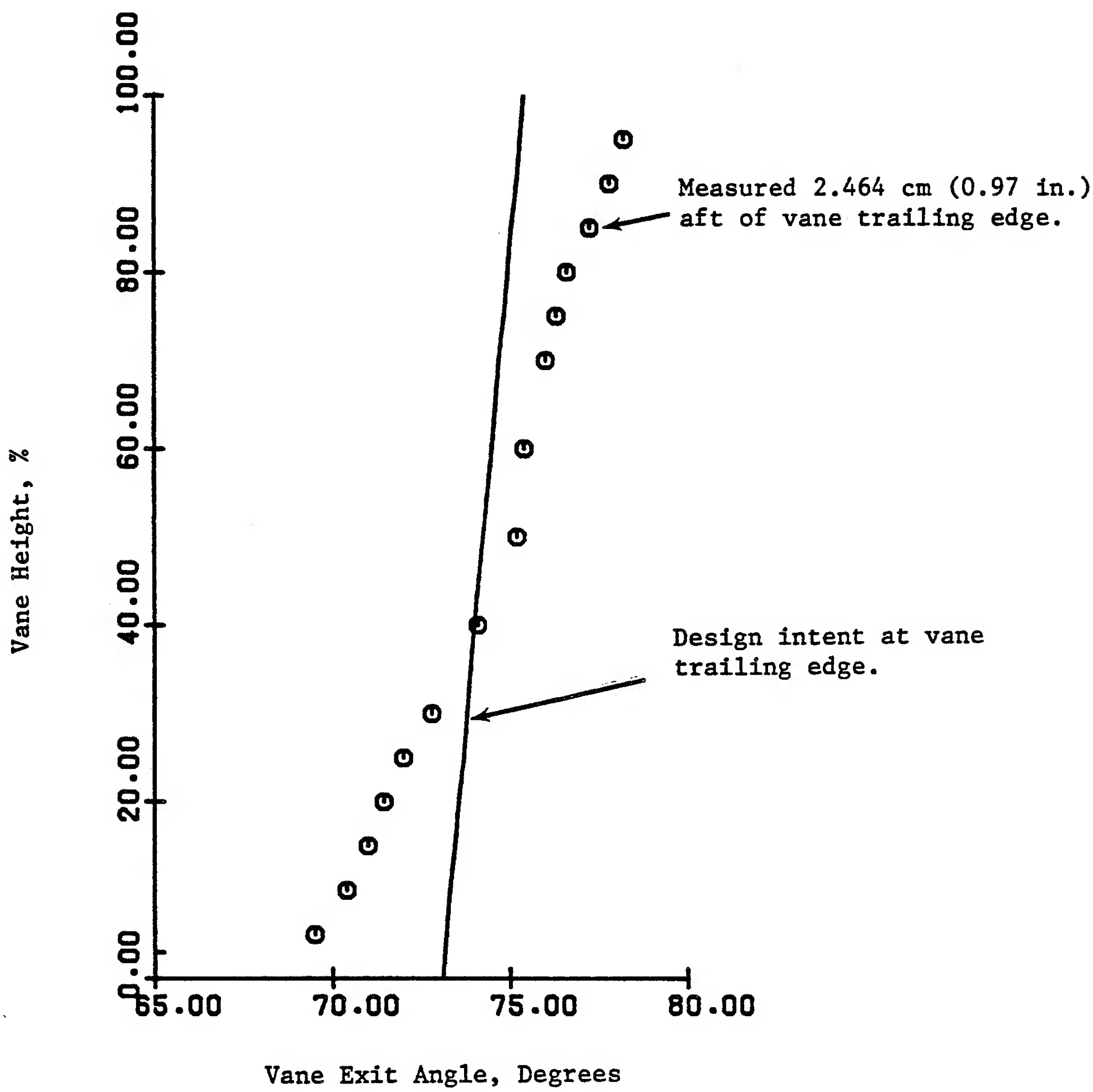

Figure 39. Base Vane Flow Angle.

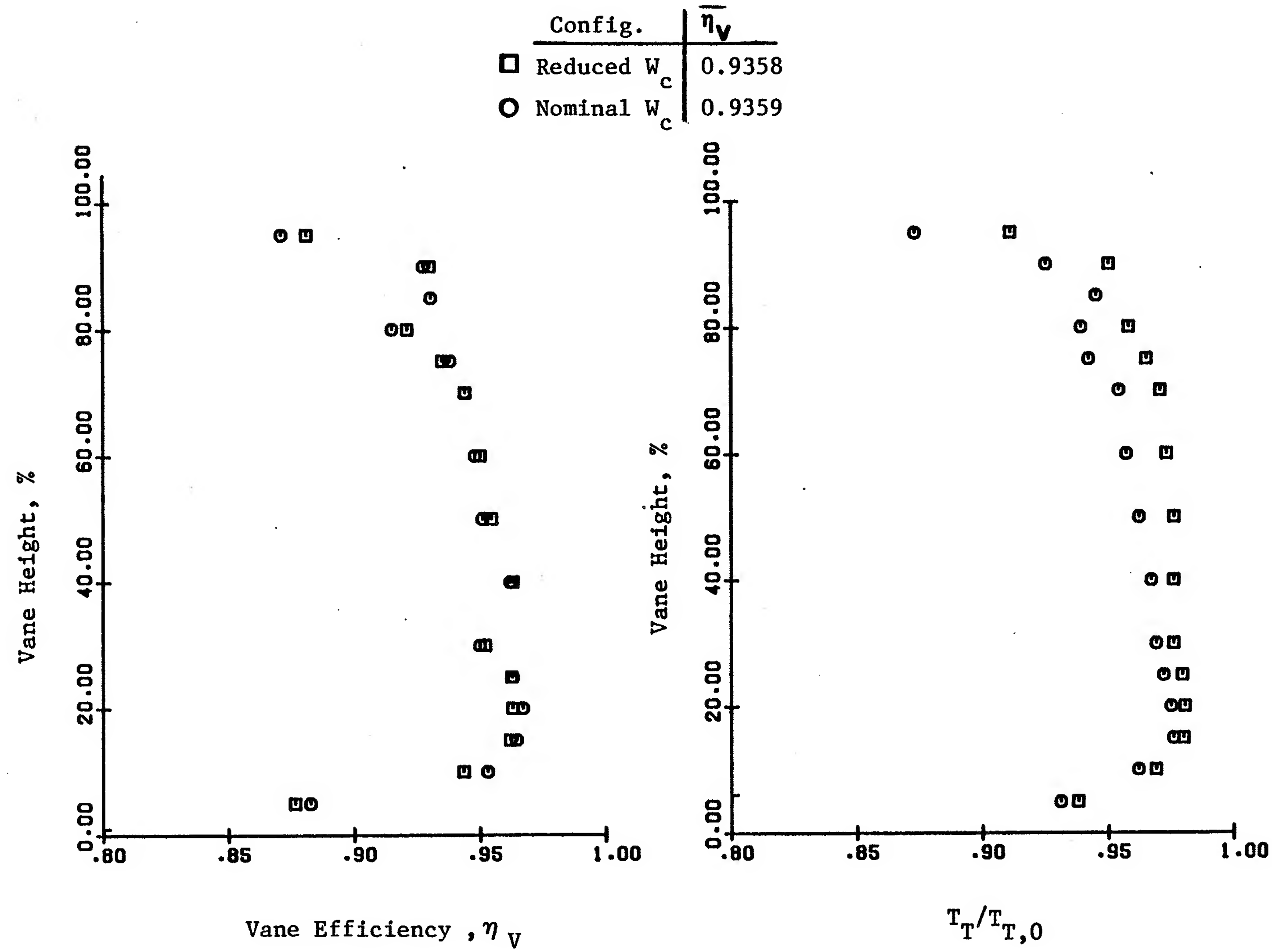

Figure 40. Effect of Reducing Cooling Flow on Base Vane Efficiency and Temperature Ratio.

result of no efficiency change is possible, and increase in efficiency was expected, that is the increase in efficiency due to reduced coolant flow was expected to be greater than the decrease due to reduced coolant pressure. The effect of the reduced cooling flow was also reflected in the higher temperature of the flow at the stator exit. In connection with the radial variation in efficiency change, it is noted that there is a gradient in temperature change, indicating that the cooling flow change tended to be concentrated toward the outer wall.

Results of base vane testing indicated that pitchline efficiency was lower than previous experience which prompted additional, diagnostic testing of the base design. The first diagnostic test was to determine whether this deficit was due to aerodynamics or cooling. This was done by traversing behind an all-solid base vane sector with solid bands.

This test of solid hardware showed a pitchline efficiency of 97.66% and an overall efficiency of 96.67%; these values are considered to be in the range of normal expectation of similar applications. Figure 41 compares the spanwise variation in efficiency and temperature for the solid and fully cooled base vanes. Secondary flow effects are confined to the inner and outer 10% of the annulus. It must also be pointed out that, during testing of the solid vane, cooling air was still being supplied to the rest of the nozzle assembly. This accounts,in part,for the temperature gradient at the outer wall of the solid vane in Figure 41. There was also evidence of a small leak where the vane was brazed to the outer band, thus allowing the lower temperature coolant from the supply cavity into the flowpath. This would also contribute to the temperature gradient. It is also observed that temperature ratios are greater than 1.0 for the solid vane. A reason for this is that the inlet temperature used for normalizing is a spanwise average of the inlet rakes. Since the average is less than the peak of the profile, temperature ratios greater than one can occur. Also, the inlet temperature level was observed to increase during the course of the traversing. This increase was observed in the inlet reference temperature which was recorded during each traverse and is most obvious at the four lowest traverse locations.* Solid vane performance at higher pressure ratios is shown in Figure 42. No temperature data were

*Efficiency results are not effected by the temperature anomally

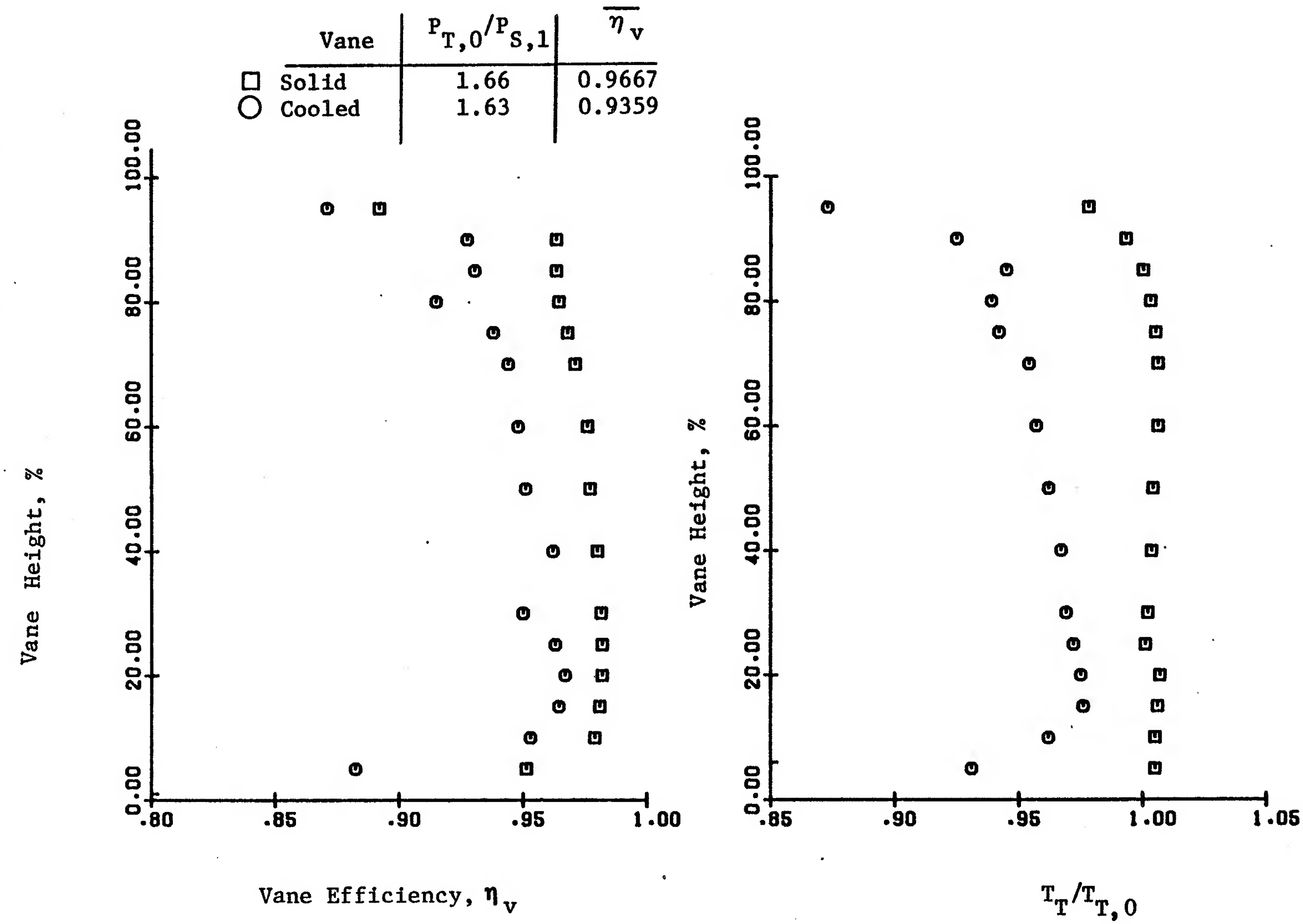

Figure 41. Radial Variation of Vane Efficiency and Temperature Ratio at Design Pressure Ratio for Base Vane, Cooled vs. Solid.

ORIGINAL PAGE IS
OF POOR QUALITY

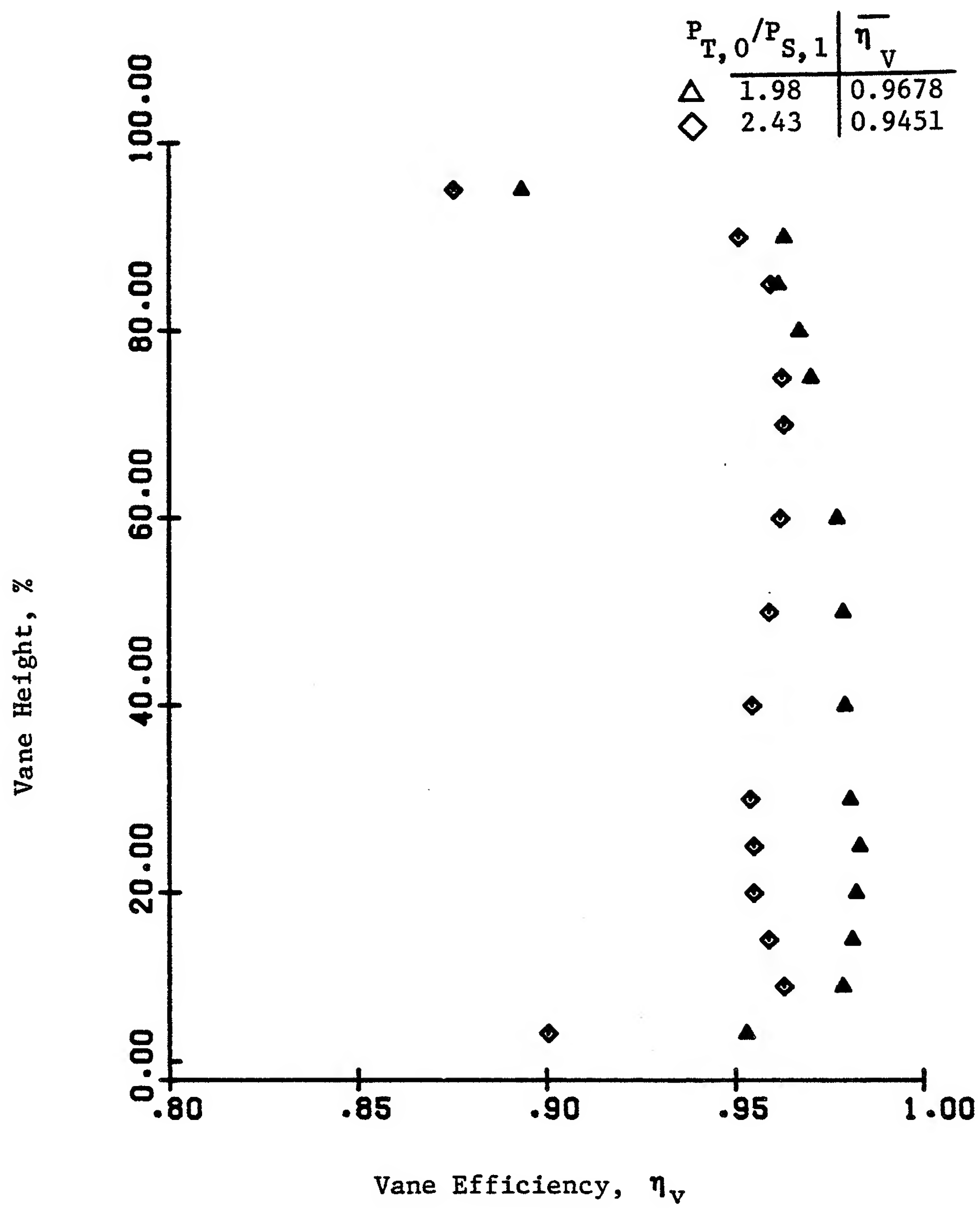

Figure 42. Radial Variation of Vane Efficiency at Off-Design Pressure Ratios for Solid Base Vane

taken at higher pressure ratios due to failure of the probe thermocouple. Solid vane performance as a function of total-to-static pressure ratio across the vane is presented in Figure 43 for both pitchline and overall vane efficiency. It is observed that efficiency is constant up to a pressure ratio of 2.0, then decreases with increasing pressure ratio.

Results of the solid vane test indicate that the higher-than-predicted loss obtained with the cooled vane was due to cooling flow effects. The largest cooling flow mixing losses are predicted for the suction side shaped holes and the trailing edge slots (These holes were shown in Figure 5). In an effort to identify the region of high loss, two tests were planned. The first of these tests was to determine the effect of sealing only the aft row of suction side holes. The second test was to determine the effect of sealing the trailing edge slots. Two attempts were made for the latter test. The first attempt yielded unsatisfactory results as some of the slots opened up. A second attempt provided a better test except near the endwalls where some of the cement had eroded and possible pinhole size leaks were noted.

The results of these tests are presented in Figure 44 where comparisons to the fully cooled and solid vanes are made. The mass averaged loss associated with the aft row of suction surface shaped holes was 0.7 points in vane efficiency, which agrees with prediction for this hole geometry. The predicted loss for the trailing edge slots was 0.9 points in vane efficiency; the indicated loss from Figure 44 substantially exceeds this predicted value. An inspection of the trailing edge slots revealed most to be tapered (small end upstream) and oversized. The resultant loss in coolant total pressure causes greater mixing loss and tends to account for the larger than expected loss in the cooled base vane.

Surface static pressure measurements were taken for the base vane. Taps were installed at hub, pitch, and tip of a solid vane and pitchline of a cooled vane. Results are compared to design intent in Figure 45. Surface taps on the LUT vane were installed but not hooked up for data acquisition in order to expedite testing.

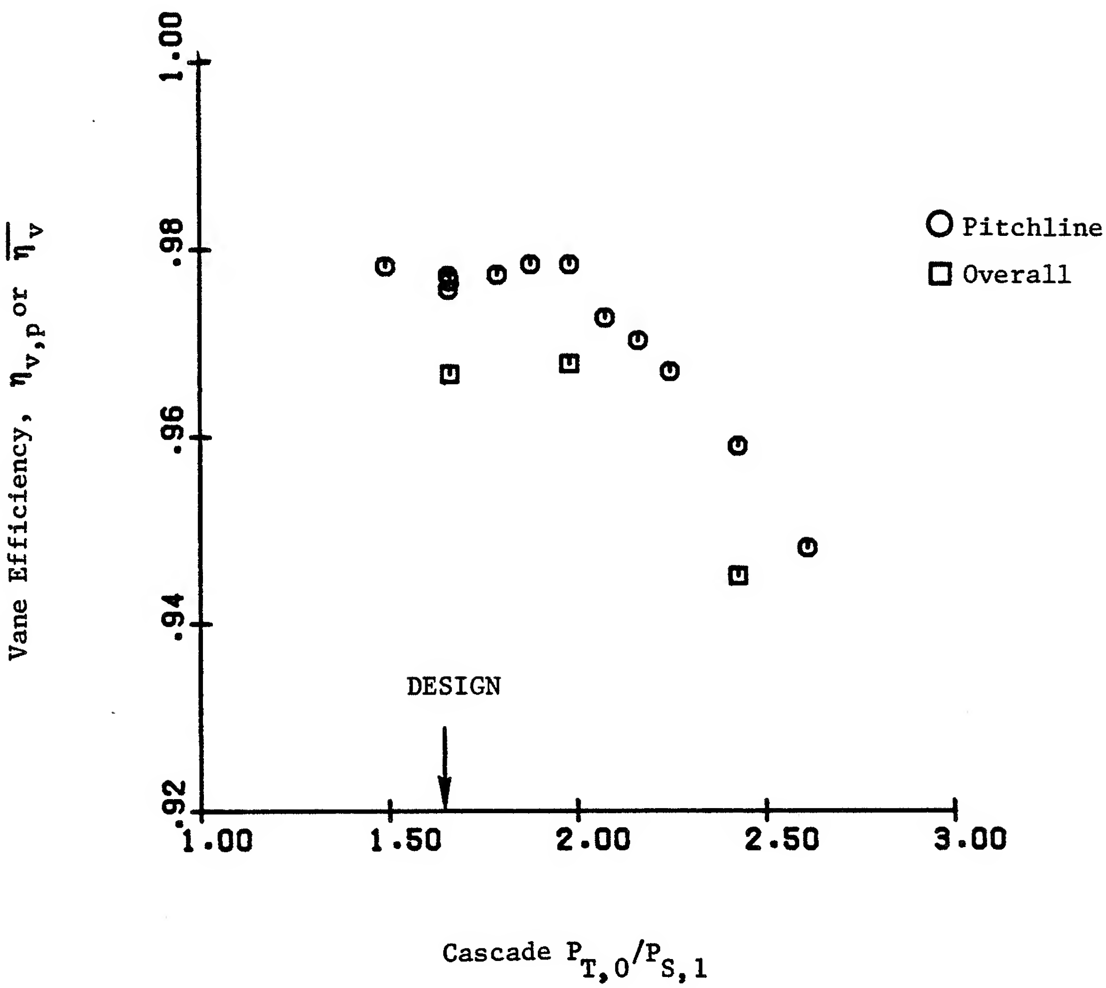

Figure 43. Vane Efficiency vs. Cascade Pressure Ratio for Solid Base Vane.

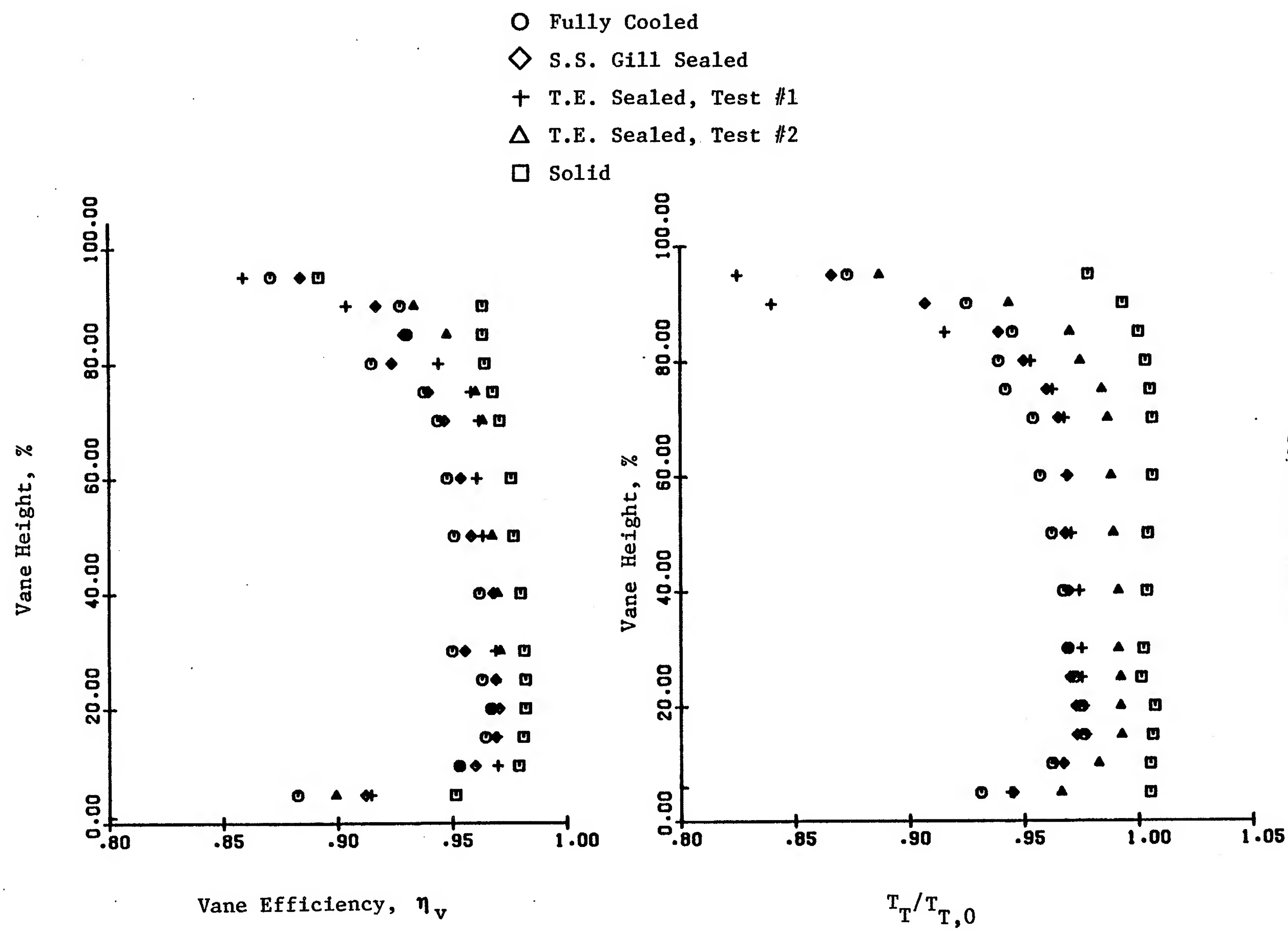

Figure 44. Radial Variation of Vane Efficiency and Temperature Ratio for Cooling Flow Diagnostic Test

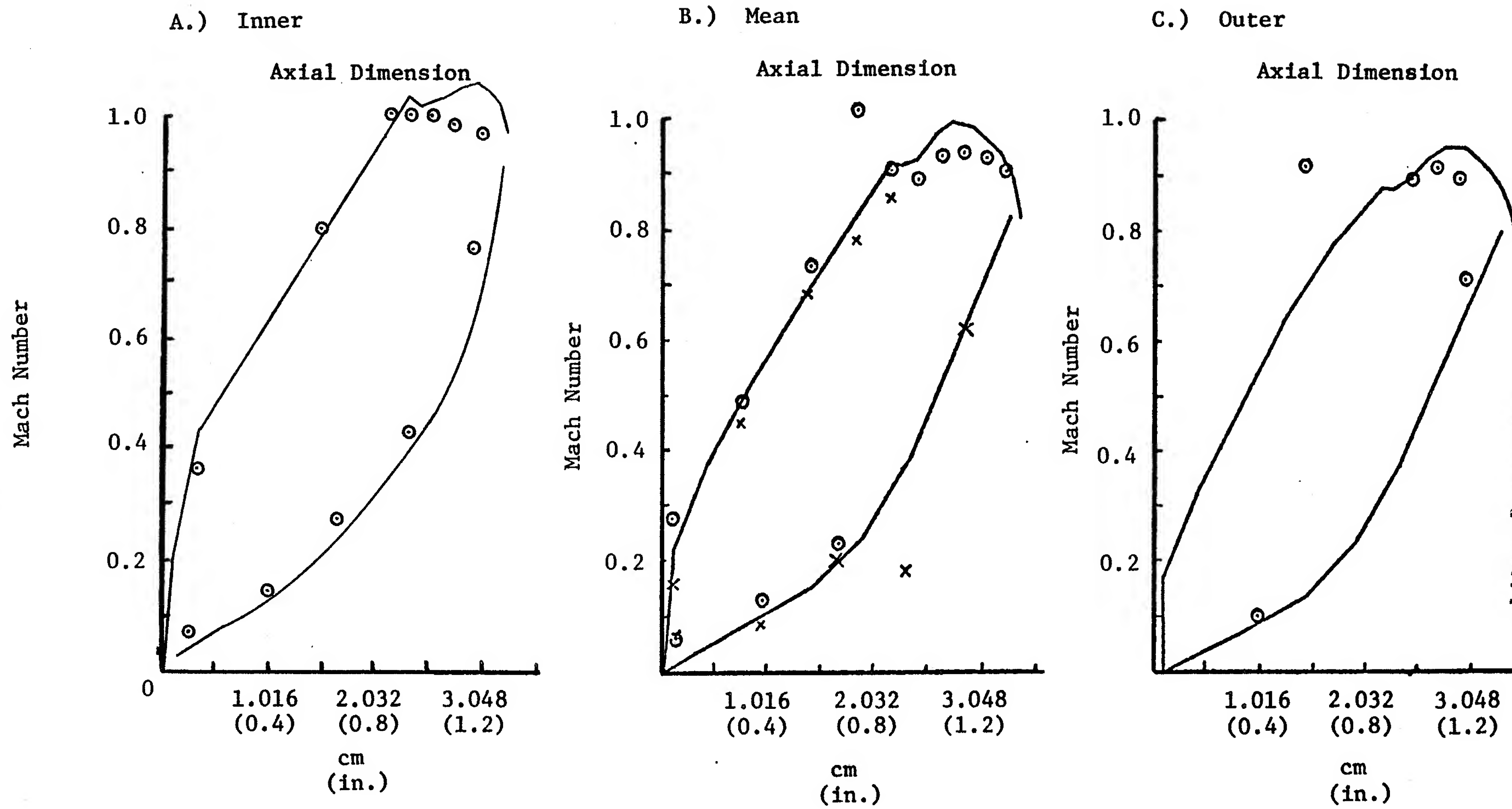

Design Intent
○ Test Measurements (Solid Vane)
× Test Measurements (Cooled Vane)

Figure 45. Base Vane - Surface Mach Number Distributions

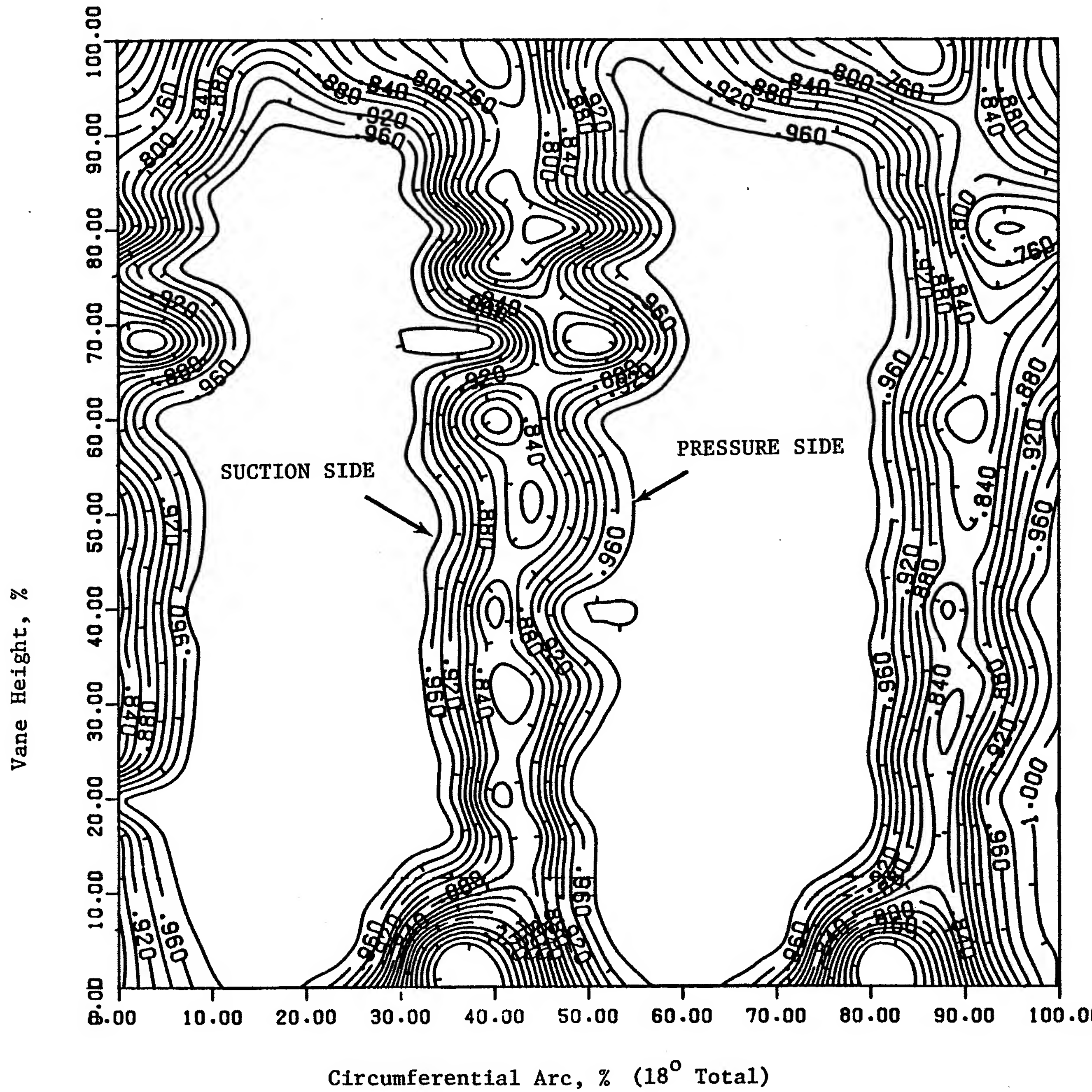

Figure 46. Efficiency Contours For Base Vane (Cooled)

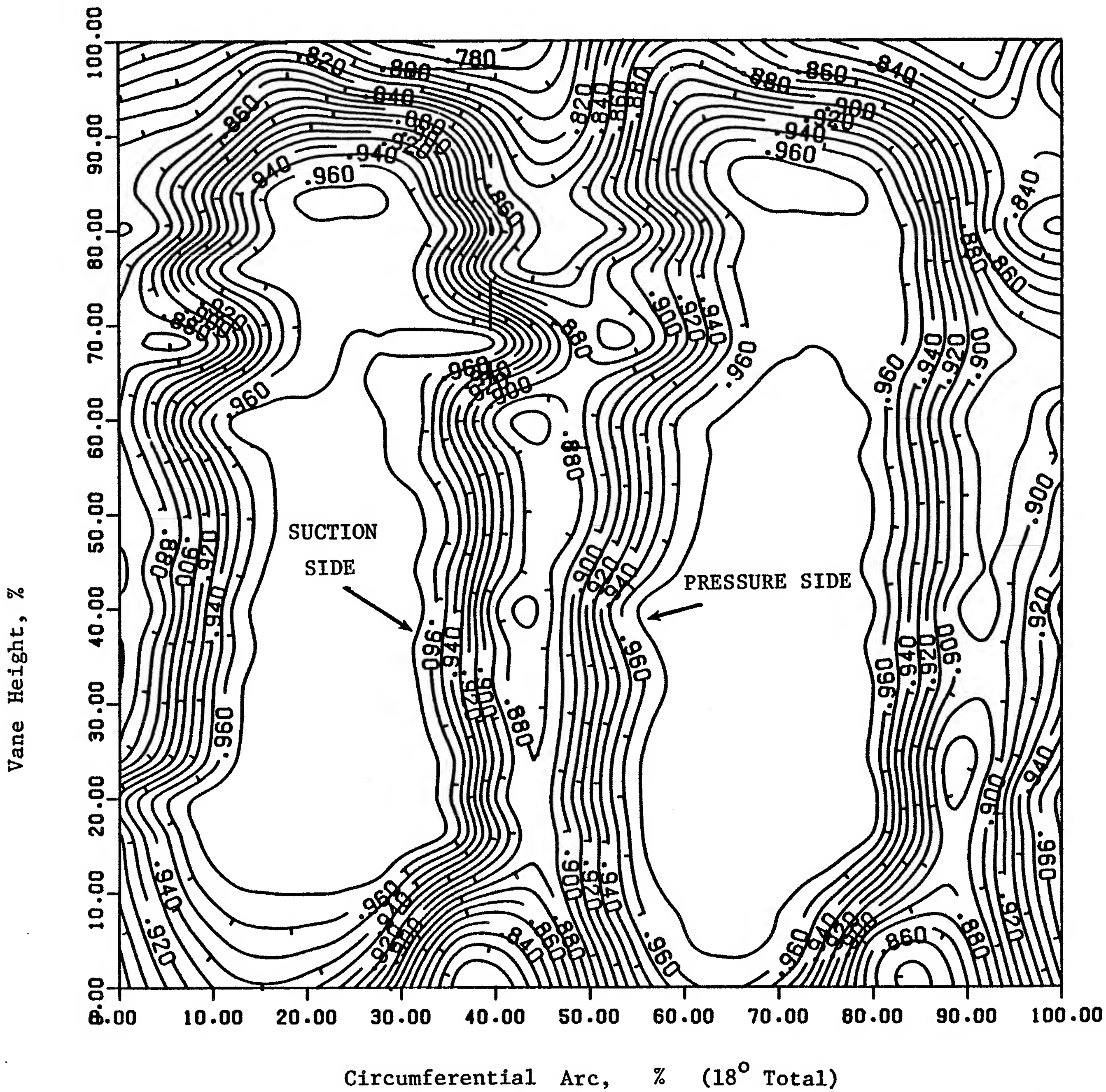

Figure 47. Temperature Contours For Base Vane (Cooled)

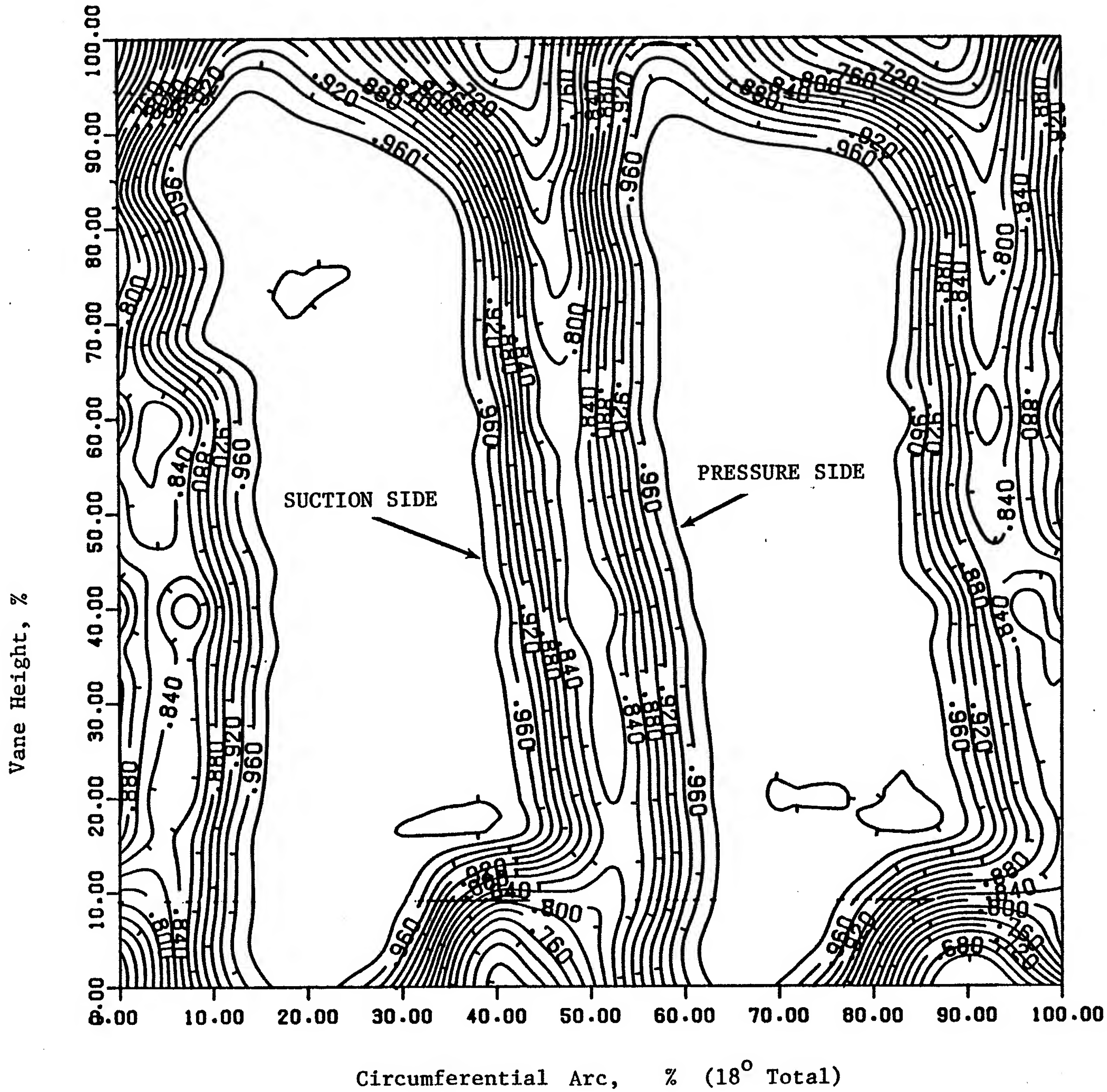

Figure 48. Efficiency Contours For LUT Vane (Cooled)

Vane Height, %

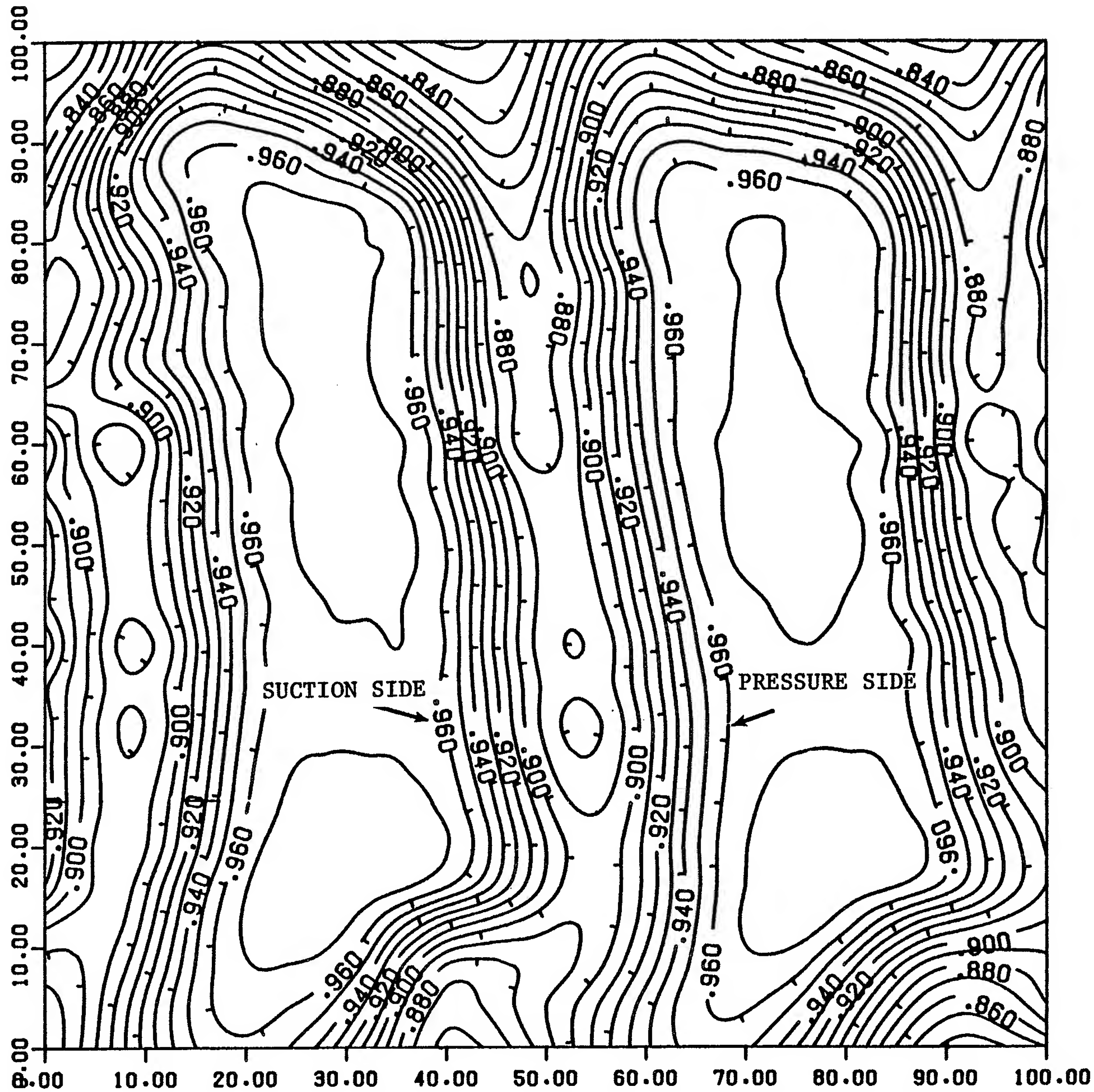

Circumferential Arc, % (18^{o} Total)

Figure 49. Temperature Contours For LUT Vane (Cooled)

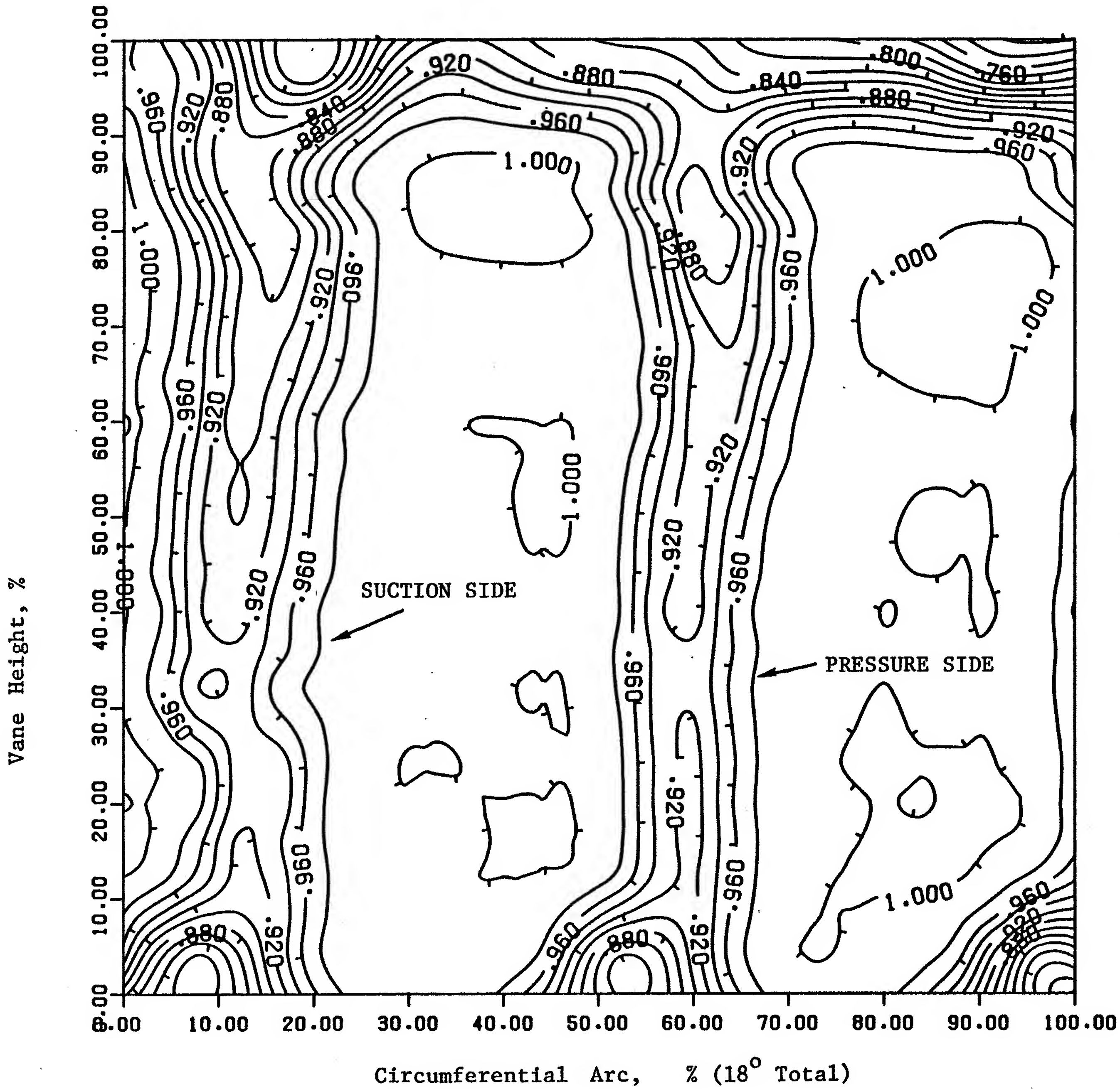

Figure 50. Efficiency Contours For Base Vane (Solid)

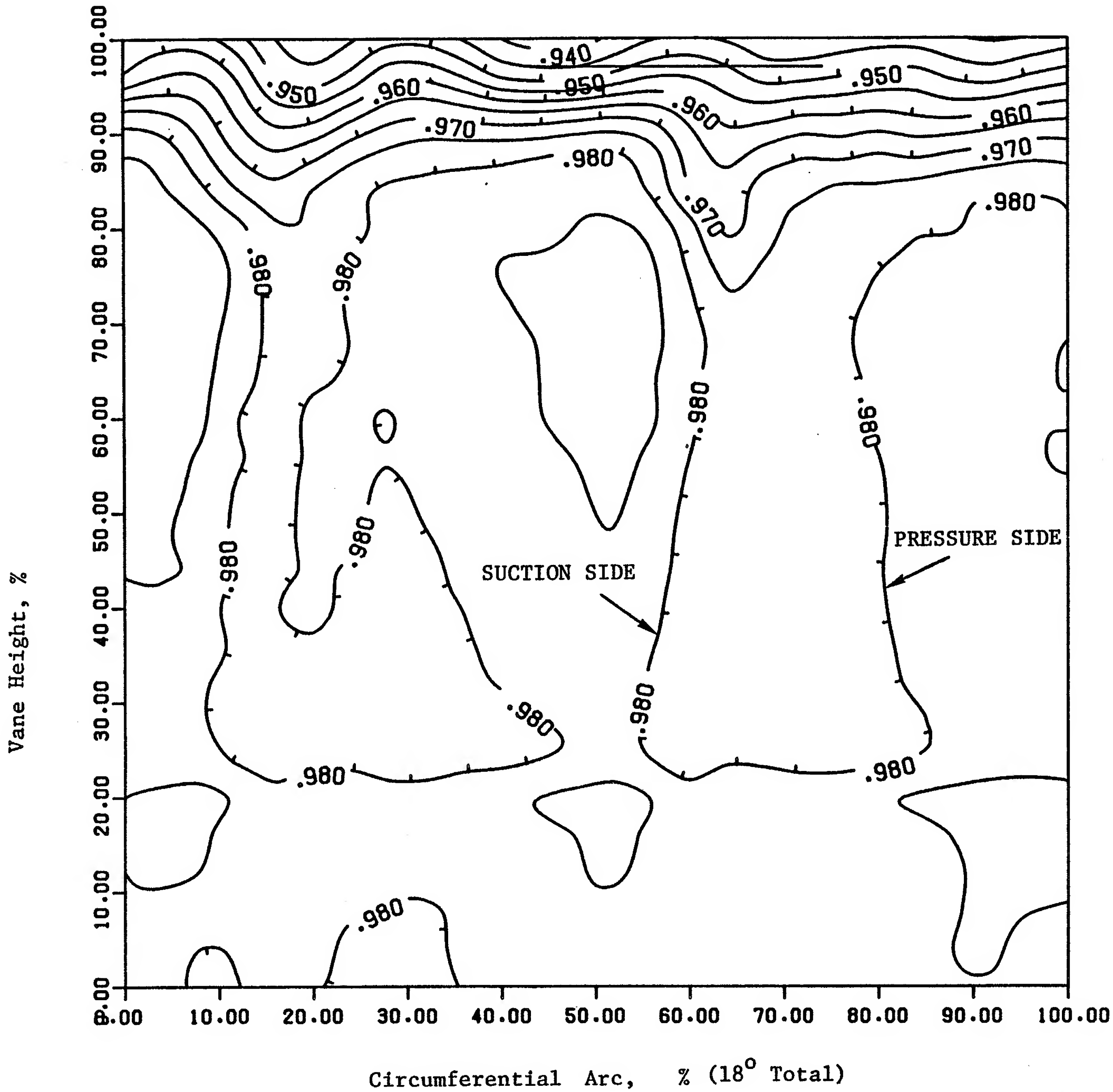

Figure 51. Temperature Contours For Base Vane (Solid)

Contour plots of vane efficiency and exit temperature ratio are presented in Figures 46 through 51 for the base cooled, LUT cooled and base solid configurations. These countours were constructed from circumferential traverses covering two nozzle passages at fifteen radial locations.

A tabulation of test readings is presented in Appendix E.

6.2. Air Turbine Rig

6.2.1 Performance

A summary of the air turbine performance parameters at design operating point is shown in Table XIII compared to E^3 program goals and pre-test predictions. Here it is seen that the E^3 FPS efficiency goal was met during this first test, exceeding expectations for the component test phase of the E^3 program. A comparison of efficiency definitions is presented in Appendix F.

Coolant flowrates were obtained by setting pressure and temperature in the various coolant supply circuits. A comparison of design intent vs measured flows and temperature is presented in Table XIV. Actual flows are close to design intent with the exception of two circuits, vane one forward and the inducer (rotor) circuit. A schematic of the cooling circuits was shown in Figure 34.

In the case of the rotor circuit, the higher than intended flowrate is believed to be due to a larger inducer (tangential accelerator) flow area than design intent and a higher resulting flow coefficient than assumed in sizing the inducer. For the vane forward cavity, the lower flowrate is probably due to heat pick-up from the inlet frame struts. The impact of these on performance will be discussed in Section 6.2.5.

In Table XIV it is also observed that the stage two vane coolant temperature is 56K (100°R) hotter than design intent. This is due to heat pick-up from the clearance control air circuits which supply hot air to the shroud housing to maintain blade tip clearances.

Table XIII. Summary of Turbine Performance Parameters at Design Operating Point

	ICLS	FPS	PREDICTION (1)	TEST
$P_{T,4}/P_{T,42}$	4.933	4.897	5.04	5.01
ψ_P	0.648	0.635	0.646	0.657
η_{GE}	0.919	0.924	0.916	0.925
$W_{41}\sqrt{T_{T,41}}/P_{T,4}$ $\frac{kg\sqrt{K}}{sec\ kP_a}$ $\left(\frac{lbs\ \sqrt{°R}}{sec\ psia}\right)$	0.866 (17.66)	0.865 (17.64)	0.844 (18.03)	0.892 (18.19)

(1) Corrected to rig conditions.

Table XIV. Comparison of Coolant Flow Ratios and Temperatures at Two Stage Rig Design Point Condition.

Coolant Circuit	Flow Ratio, W_c/W_{41}		Temperature, K (^oR)	
	Test	Design Intent	Test	Design Intent
Vane 1 Fwd Cavity and Inner Band	0.0332	0.0511	328 (590)	352 (633)
Vane 1 Aft Cavity	0.0528	0.0565		
Outer Band, and Stage 1 Shroud	0.0478*	0.0500*	352 (633)	352 (633)
Rotor	0.0642	0.0503	346 (622)	344 (620)
Simulated Compressor Discharge Leakage	0.0140	0.0151	344 (620)	361 (649)
Vane 2 and Stage 2 Shroud	0.0224	0.0236	356 (640)	300 (540)

* = Excluding Shroud air

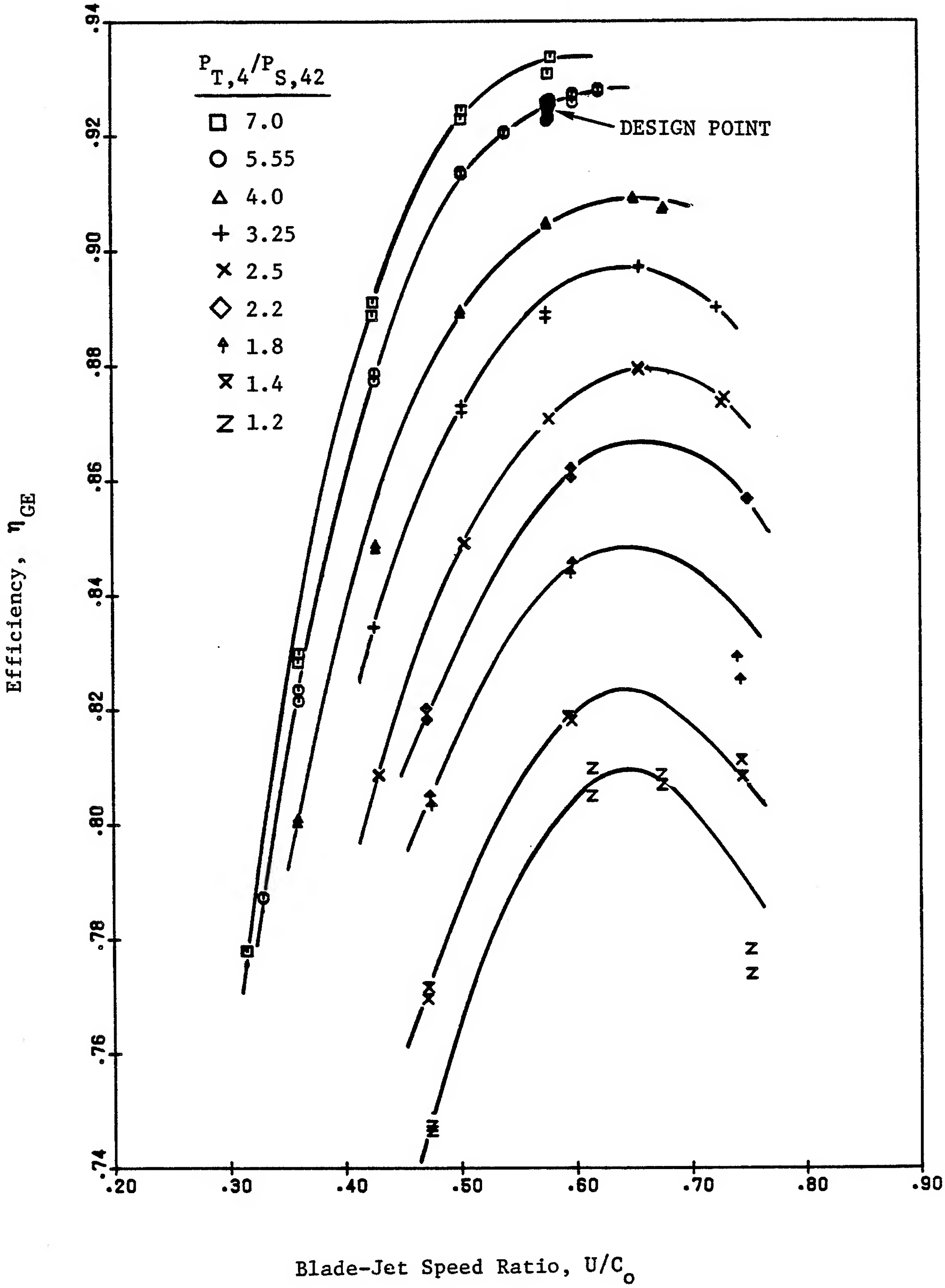

Figure 52. Efficiency (GE) vs. Blade-Jet Speed Ratio (Power from Shaft Torque)

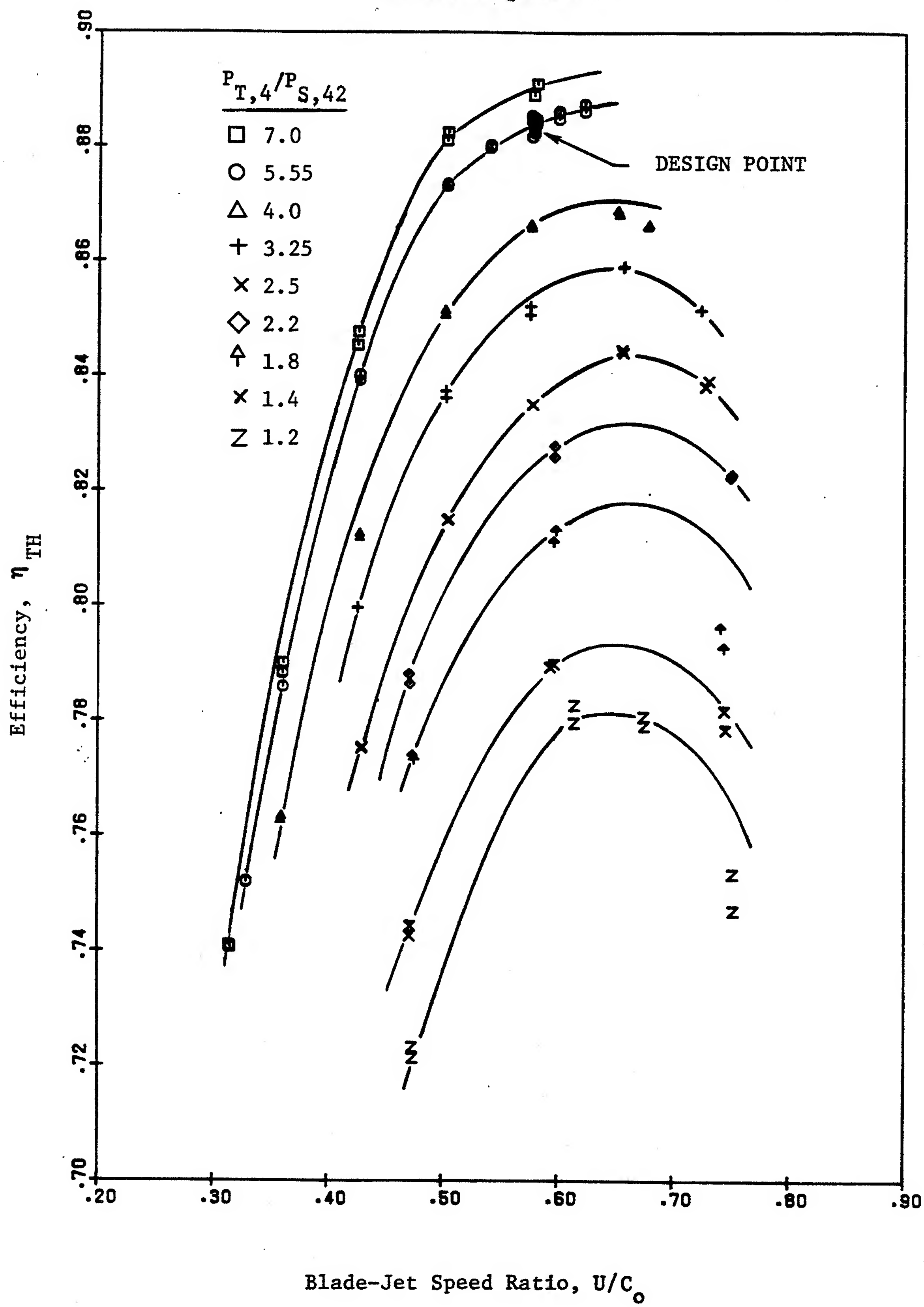

Figure 53. Efficiency (Thermo) vs. Blade-Jet Speed Ratio (Power from Shaft Torque)

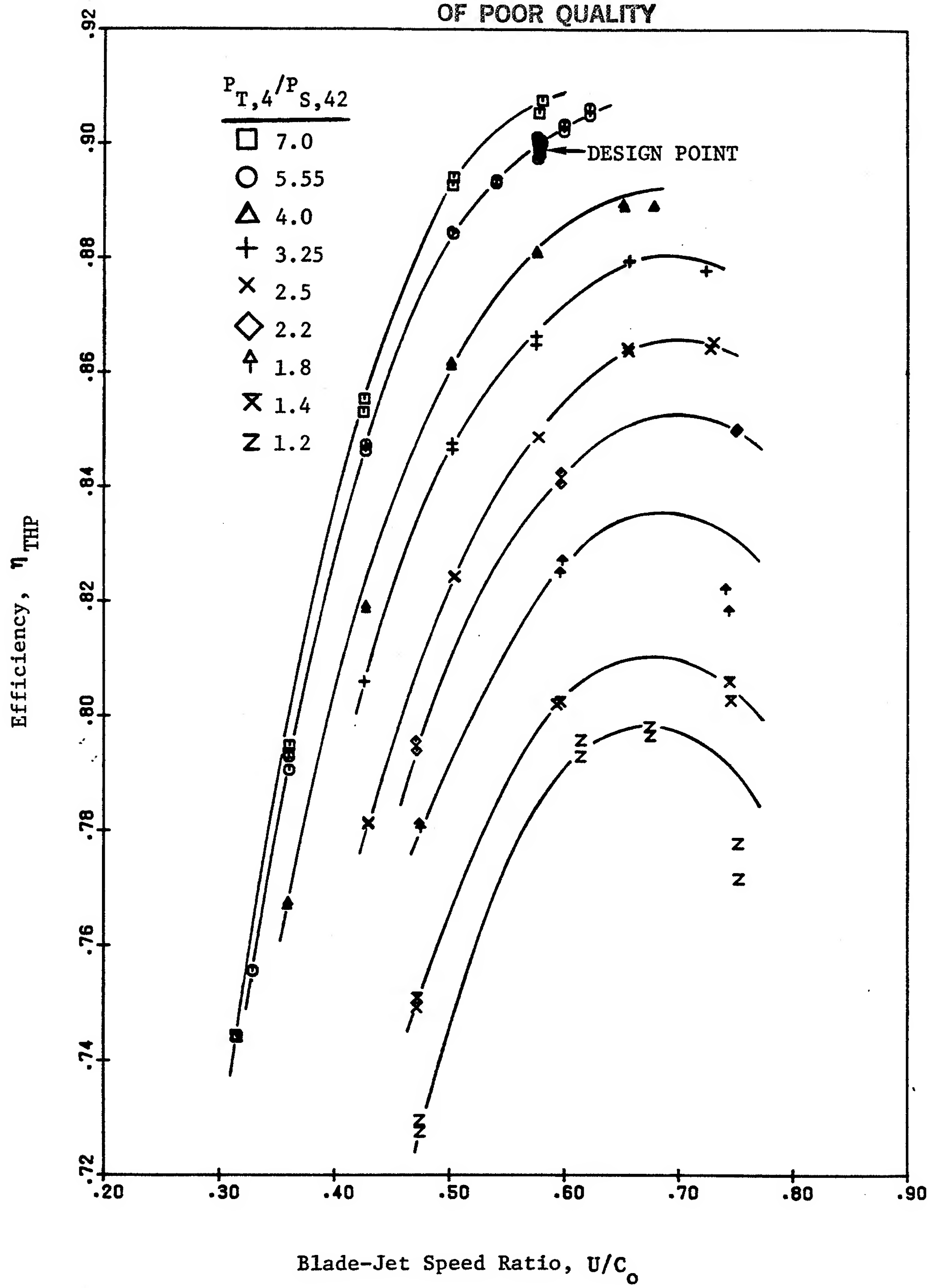

Figure 54. Efficiency (Thermo) vs. Blade-Jet Speed Ratio (Power from shaft torque plus rotor coolant pumping)

Results of the turbine mapping are presented in plots of efficiency versus blade-jet speed ratio. These are shown in Figures 52 to 54 for GE torque efficiency, torque thermodynamic efficiency and torque-plus-pumping thermodynamic efficiency respectively. These same efficiencies are also plotted versus group pitchline loading in Figures 55 to 57. At design point operation, $P_{T,4}/P_{S,42}$ =5.55, U/C =0.575, the following efficiencies are noted:

GE,	η_{GE}	92.5%
Thermo,	η_{TH}	88.4%
Thermo plus Pumping,	η_{THP}	90.0%

At design pressure ratio, efficiency is seen to be increasing as loading is decreasing below design point level, indicating normal off-design trend and incidence tolerance of the blading. Less incidence tolerant blading would exhibit a tendency for efficiency to peak at or near design point and then decrease with decreasing loading.

Energy extraction as a function of corrected speed is shown in Figure 58 for shaft torque and in Figure 59 for torque with pump work included. A comparison of the two figures shows the effect of including the pumping term in the power output. A shift in level is observed and this delta is seen to increase with speed. This increase with speed is because the pumping power term is a function of speed squared.

The torque characteristics (expressed as torque divided by inlet total pressure) of the turbine are presented in Figure 60. The torque parameter includes the additional torque due to pumping the rotor coolant. In addition to the quantitative aspects, this plot can also be used to judge the quality of the torque measurement. The plot shows a smooth family of curves, as expected. This gives credibility that the torque measurements are consistent over the range of conditions investigated.

Turbine total-to-total pressure ratio as a function of corrected speed and total-to-static pressure ratio is shown in Figure 61. The total pressures are determined with measurements obtained from inlet and exit rakes. This figure is included mainly to present the total-to-total pressure ratio data in a graphical form for those who use total-to-total pressure ratio rather than total-to-static in defining a test map matrix.

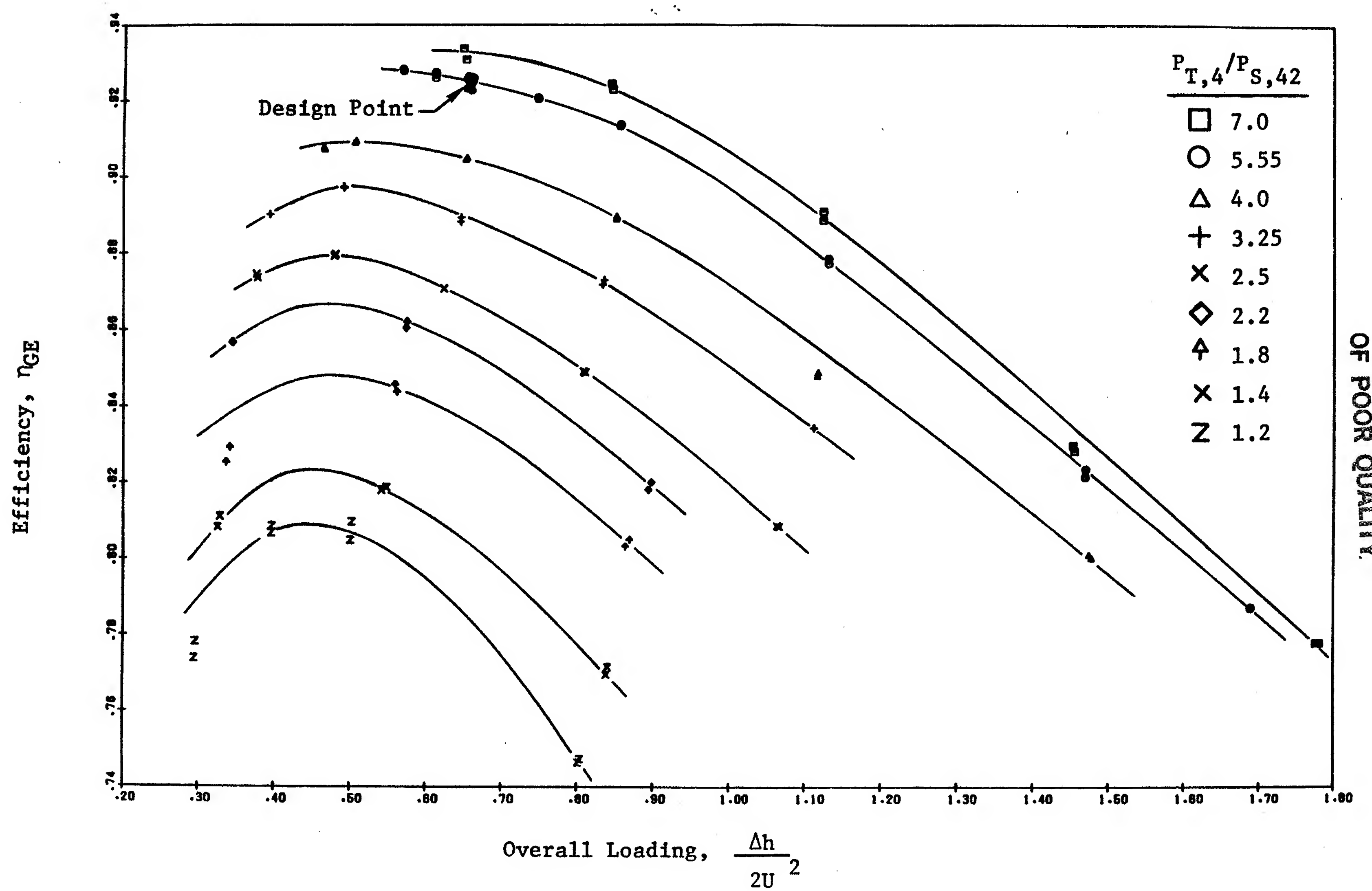

Figure 55. Efficiency (GE) vs. Loading.

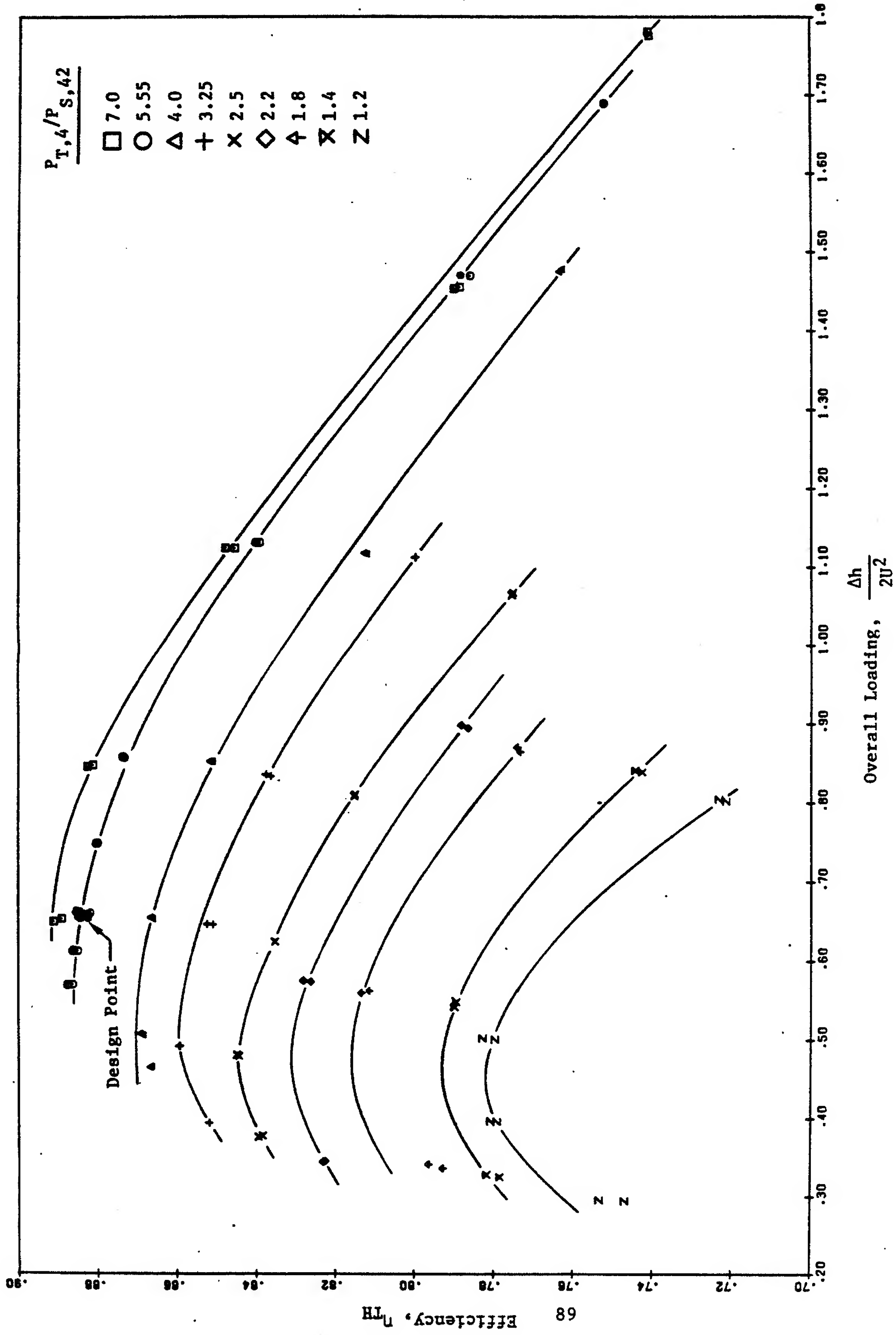

Figure 56. Efficiency (Thermo) vs. Loading (Power based on shaft torgue).

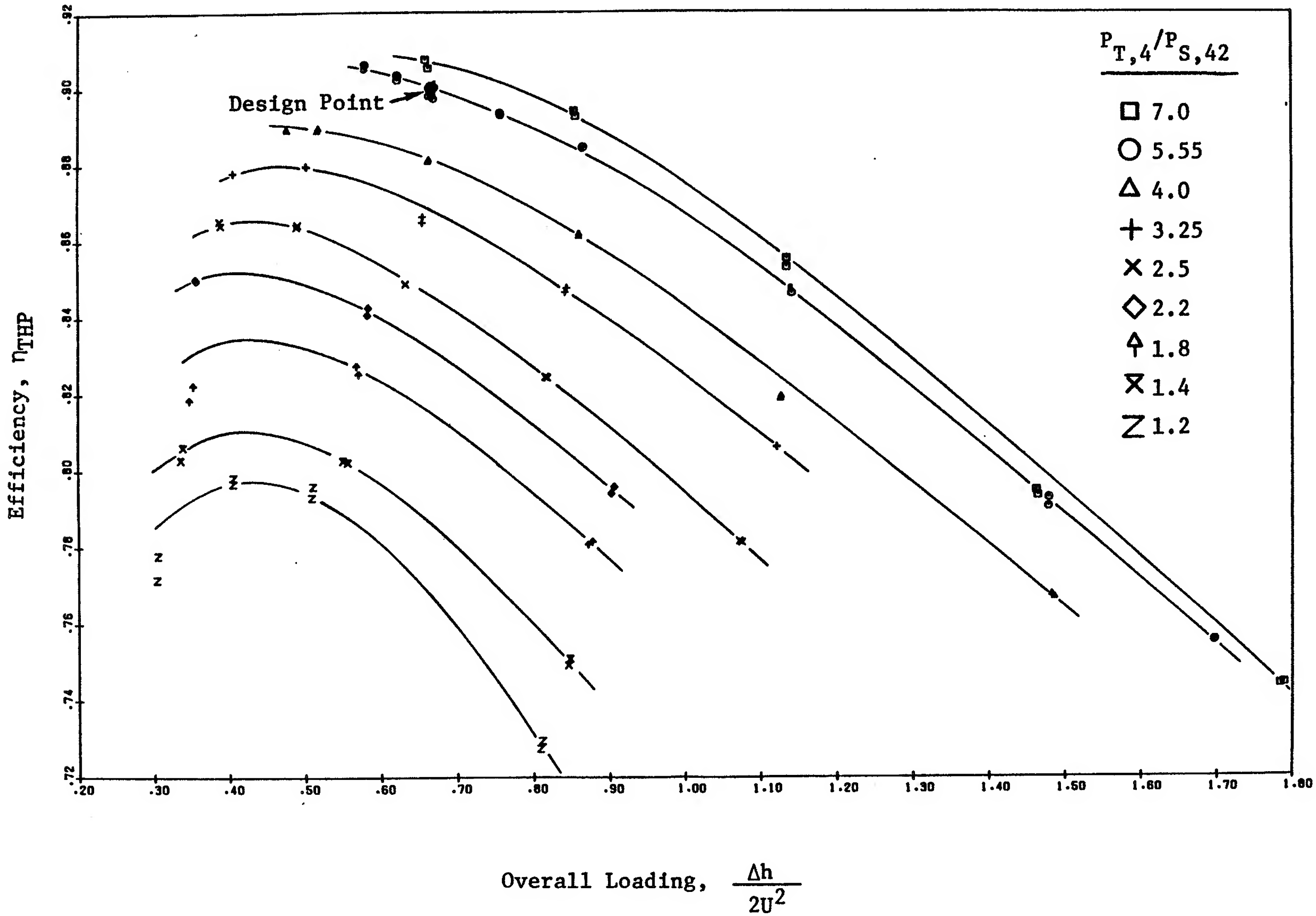

Figure 57. Efficiency (Thermo) vs. Loading (Power from shaft torque plus rotor coolant pumping).

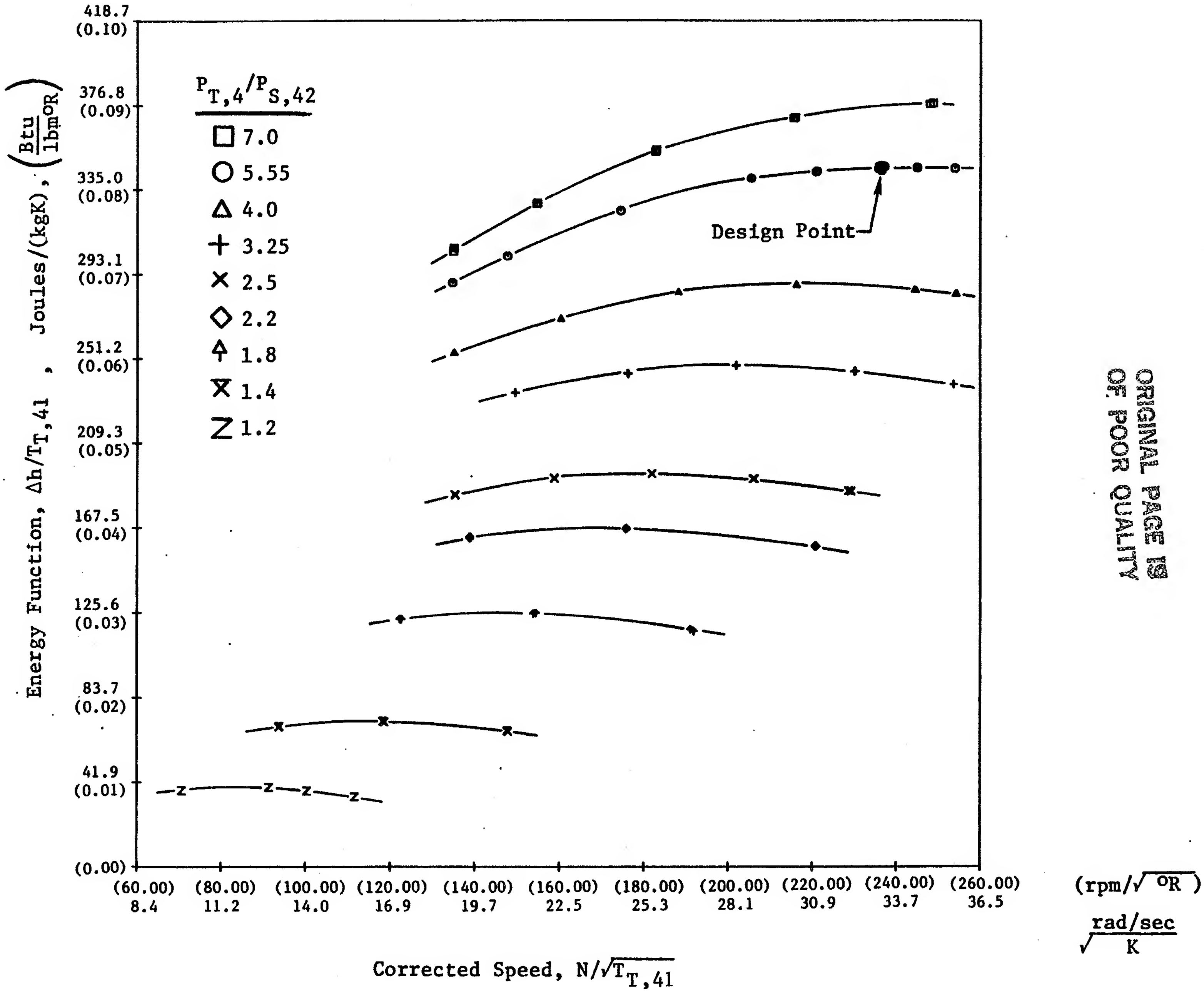

Figure 58. Energy Function vs. Corrected Speed (Power from shaft torque).

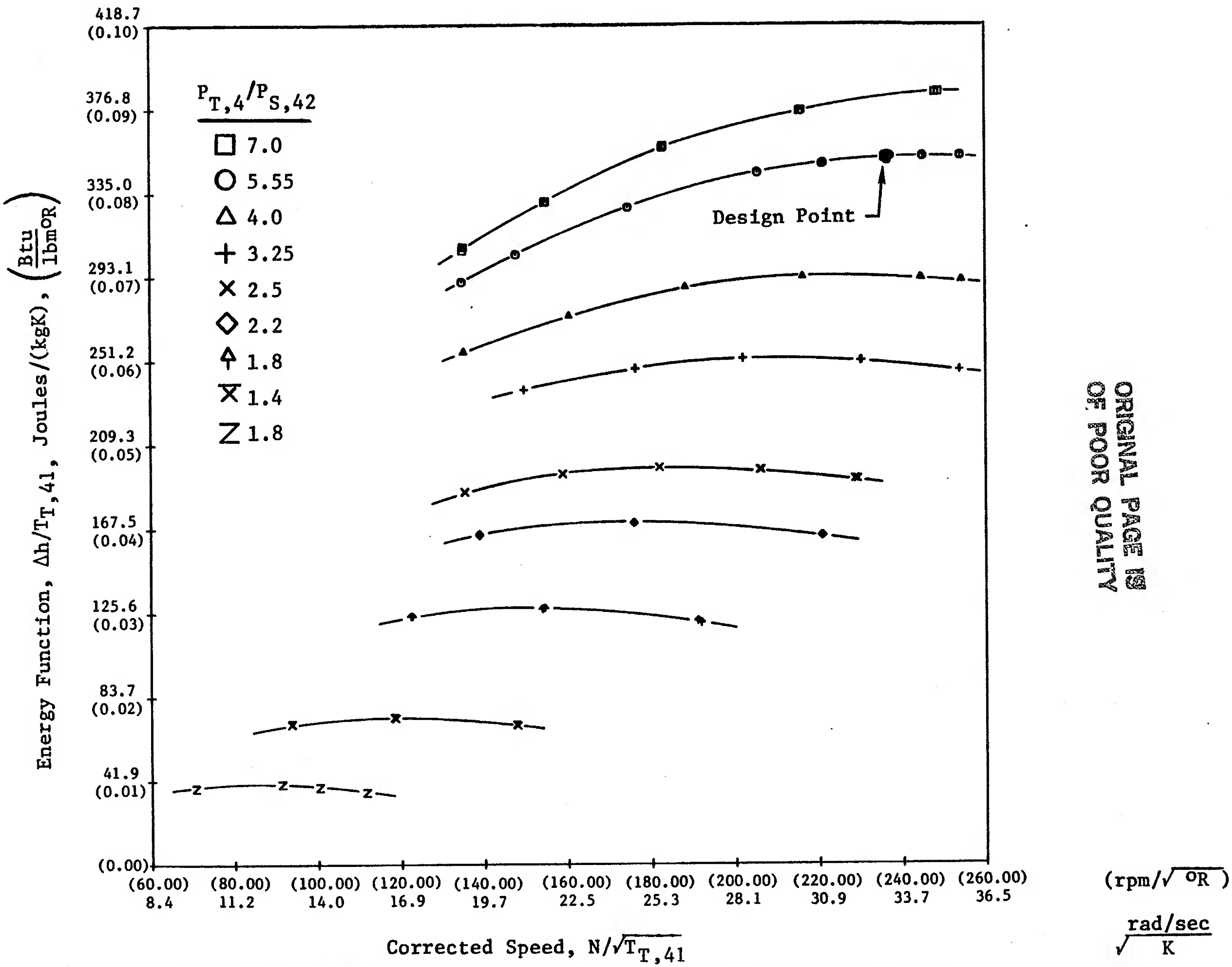

Figure 59. Energy Function vs. Corrected Speed (Power from shaft torque plus rotor coolant pumping).

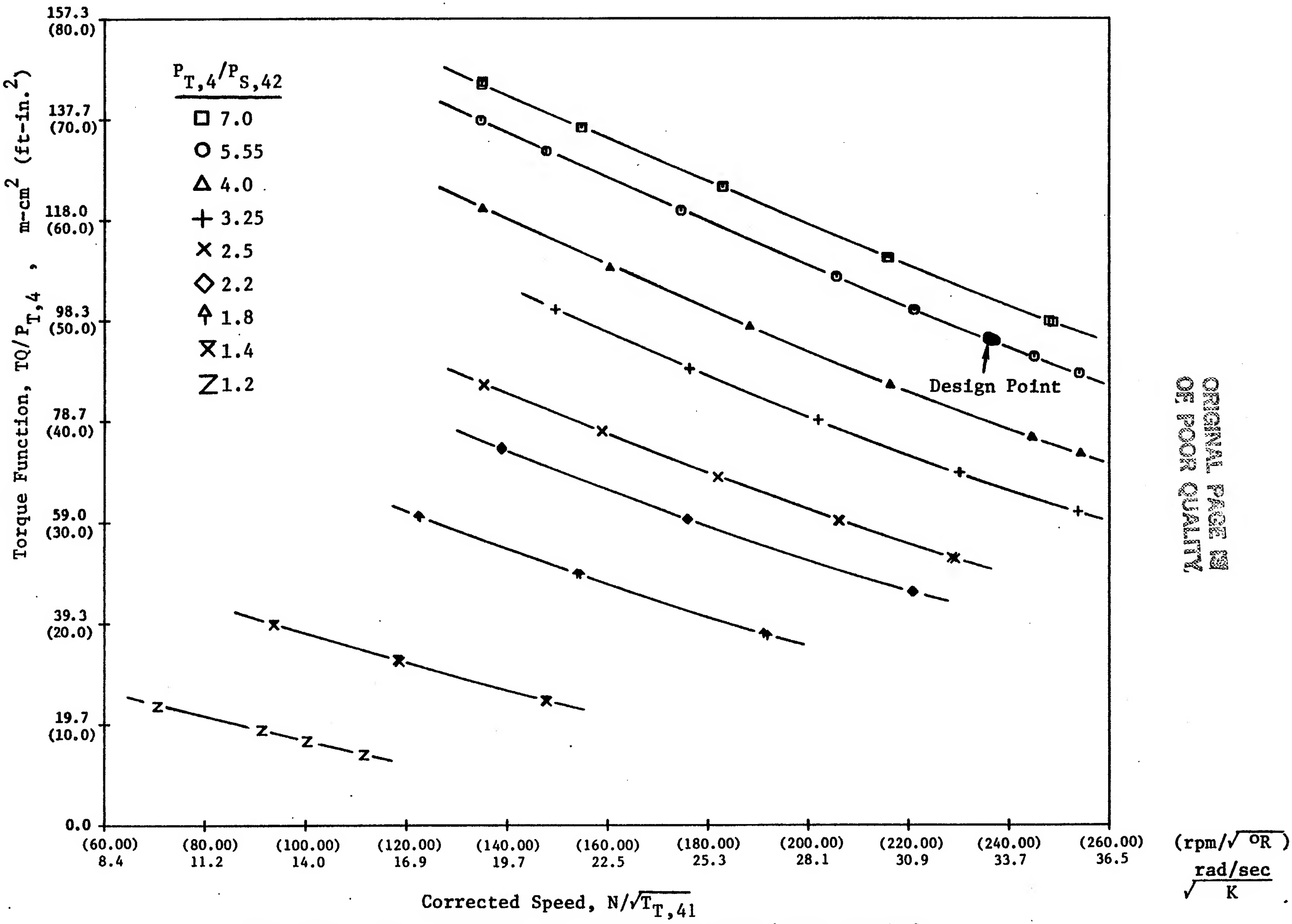

Figure 60. Torque Function vs. Corrected Speed (Based on shaft torque plus rotor coolant pumping).

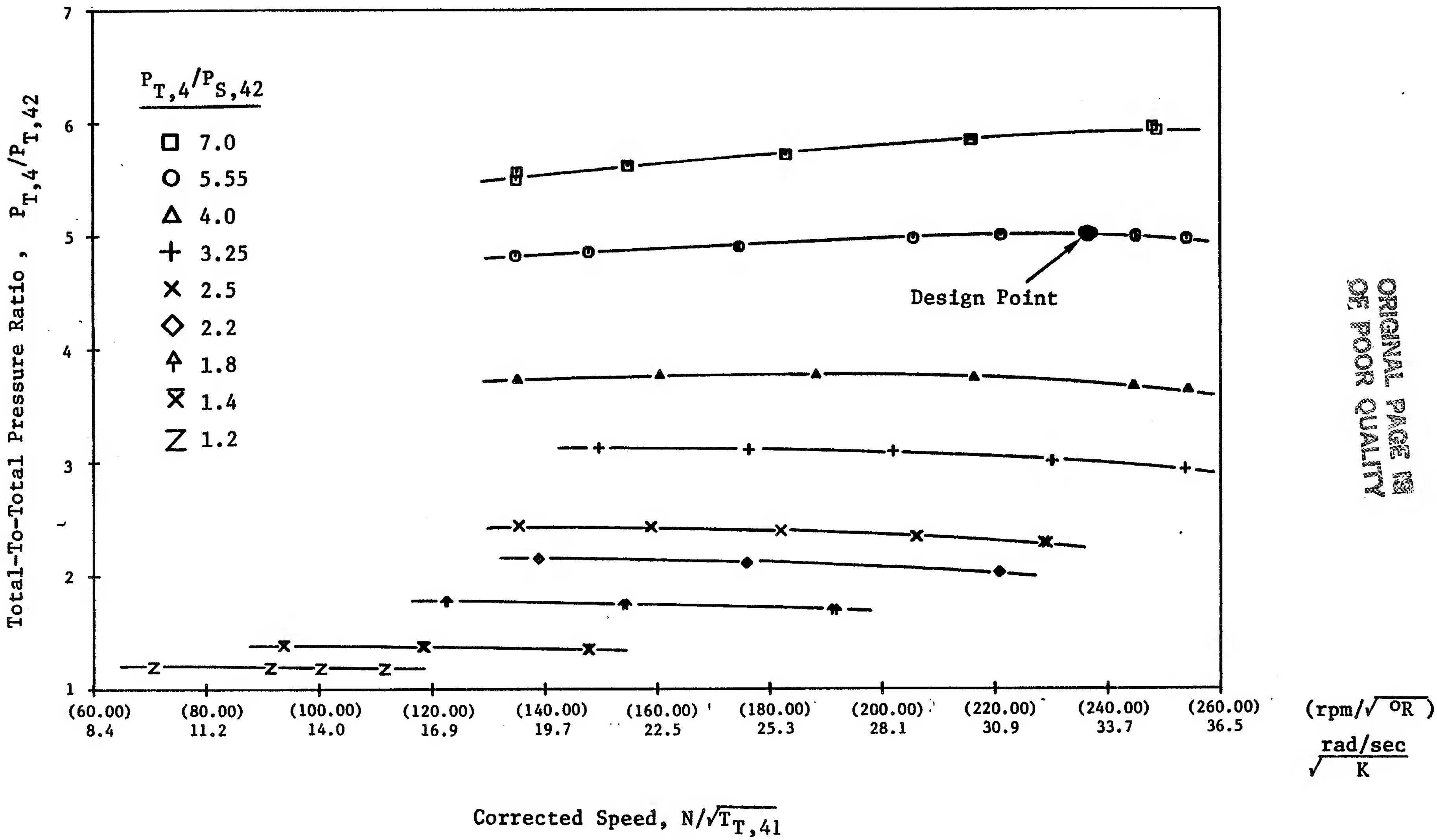

Figure 61. Total-to-Total Pressure Ratio vs. Corrected Speed.

ORIGINAL PAGE IS OF POOR QUALITY

Turbine flow function is presented in Figure 62 for the five higher pressure ratios and in Figure 63 for the four lower pressure ratios. At design point, the measured flow function is 18.19 which slightly exceeds the design intent of 18.026 by 0.9 percent. In Figure 62, two trends are noted. First, for a constant total-to-static pressure ratio and decreasing speed, flow function is seen to increase, as is normal, but them falls off at the lowest speed. A probable explanation for the fall-off is that the flow coefficient for one or more bladerows downstream of the stage one nozzle decreases (reducing effective flow area) due to incipient separation as loading and incidence increase at lower speeds. A second trend is seen at constant speed and increasing pressure ratio. For this situation, flow function increases up to a presume ratio of 5.5, but then drops off at the highest pressure ratio of 7.0. The difference in flow function is on the order of 0.1% and is probably due to the amount of leakage flow up the forward face of the rotor. This flow was seen to have an effect on turbine flow function and will be addressed in Section 6.2.5.

Stage one reaction, defined as the ratio of the static enthalpy drop across the rotor to the total-to-static enthalpy drop across the stage, is presented in Figure 64 and 65 for hub and tip respectively. The typical trend for reaction is to decrease with decreasing speed. This is observed to be the case at higher speeds for a given pressure ratio but not at lower speeds. Again, this may be due to separation in one or more bladerows at far offdesign operating points and also to the amount of wheel space leakage flow injected between the first stage nozzle and rotor. The effect of this flow on stage one reaction will be discussed in Section 6.2.5.

Static pressure drop through the turbine at design point conditions is illustrated in Figure 66. Good agreement with design intent was observed. It is noted that there is no value for the static pressure at the outer wall at vane two exit. Although this instrumentation was installed, apparently all pressure leads were damaged during assembly of the nozzle to the support casing.

Turbine exit swirl for the range of conditions investigated is presented in Figure 67. (Positive swirl is backward running.) These data were derived from two sources: (1) continuity calculation using measured flows, average

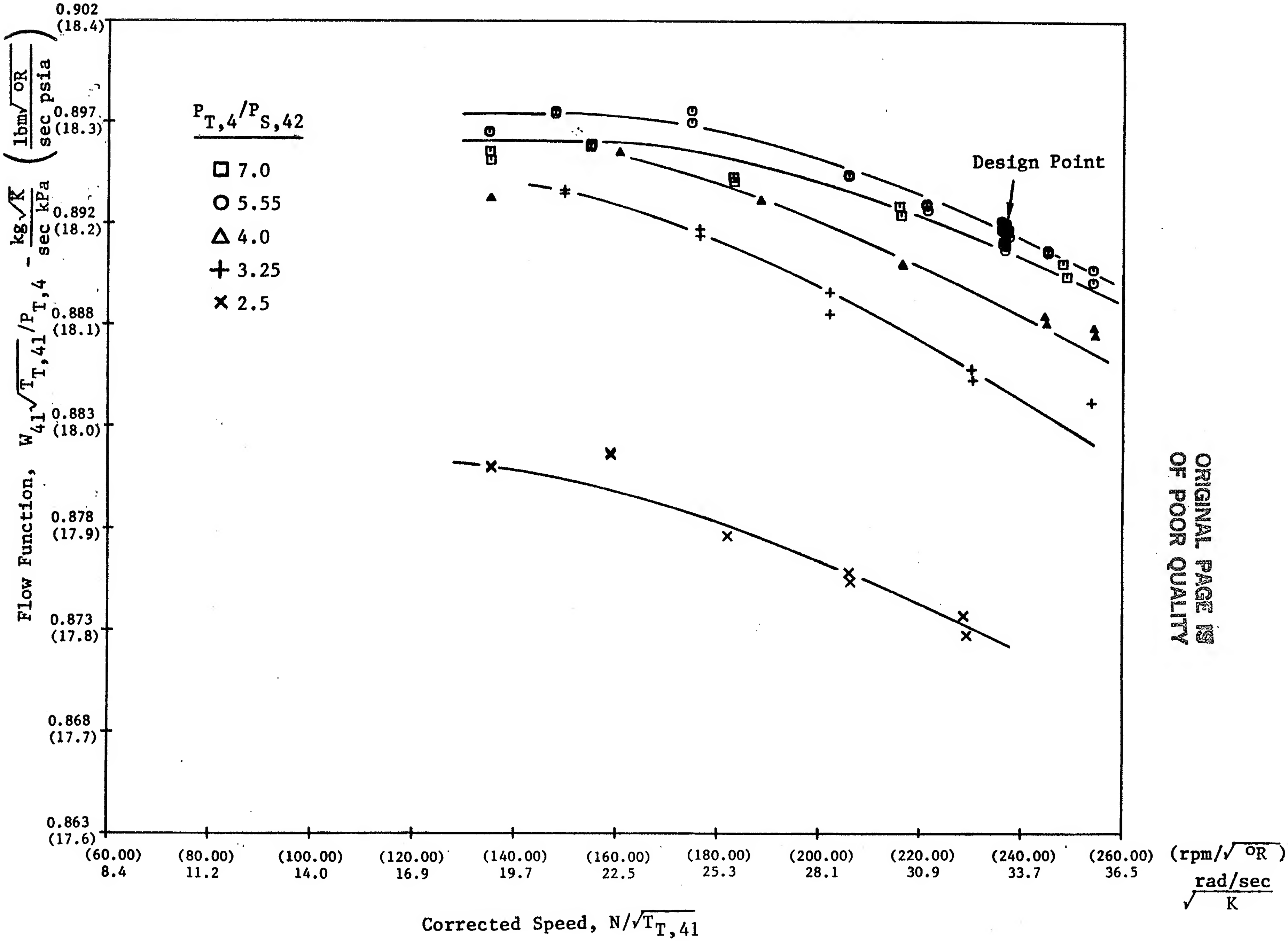

Figure 62. Flow Function vs. Corrected Speed (Five Higher Pressure Ratios).

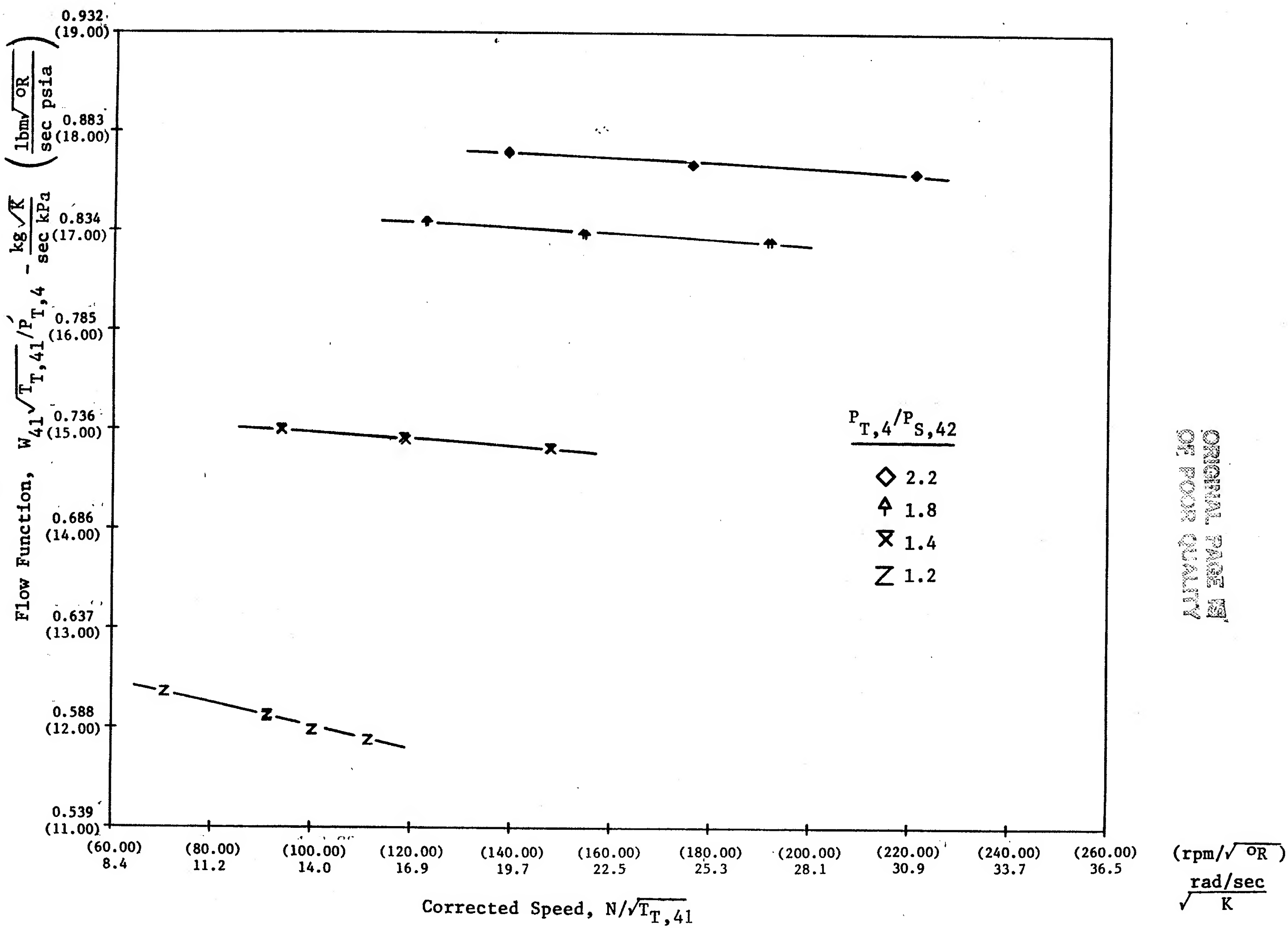

Figure 63. Flow Function vs. Corrected Speed (Four Lower Pressure Ratios).

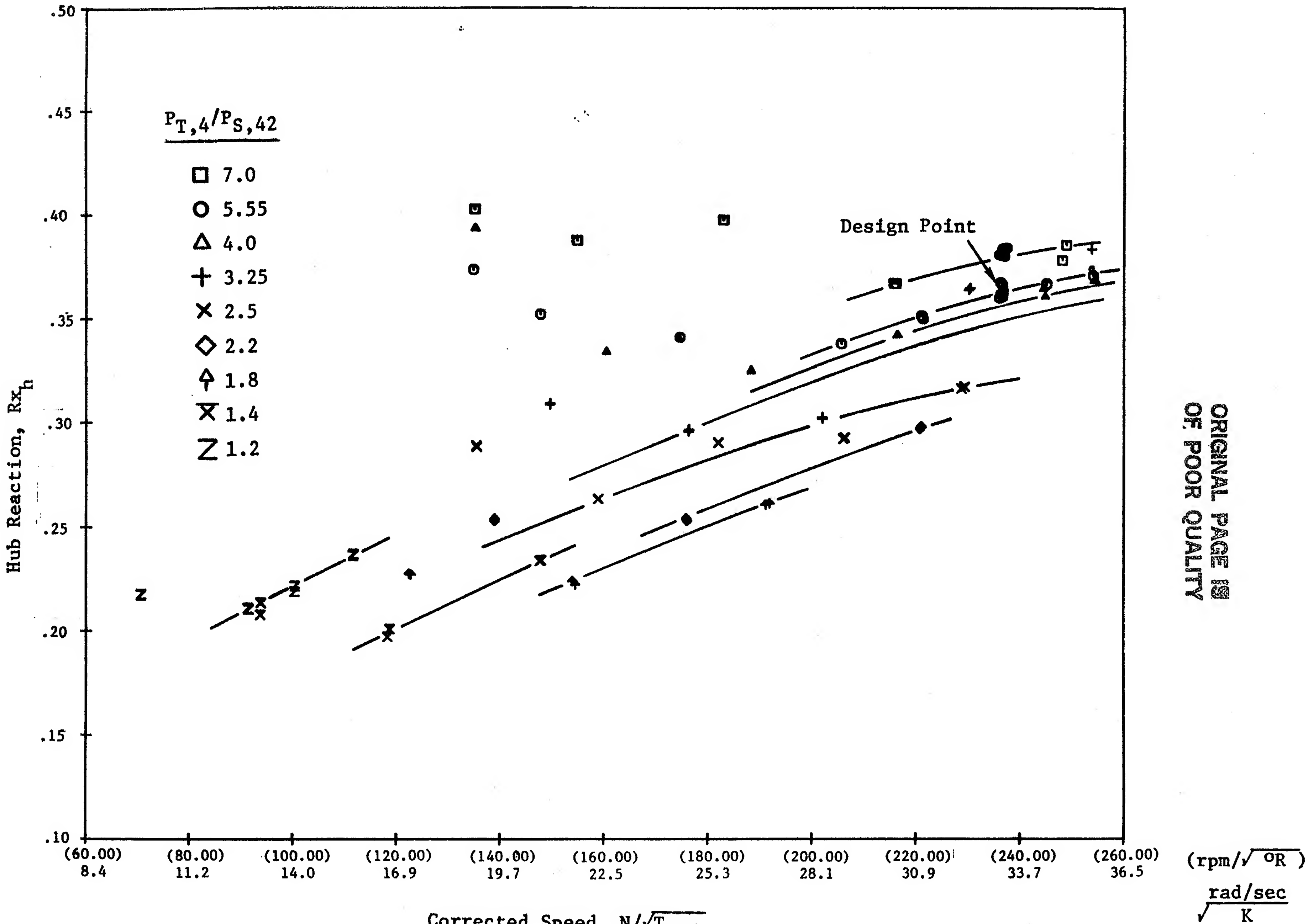

Figure 64. Stage One Hub Reaction vs. Corrected Speed. Solid Lines Show Expected Trend.

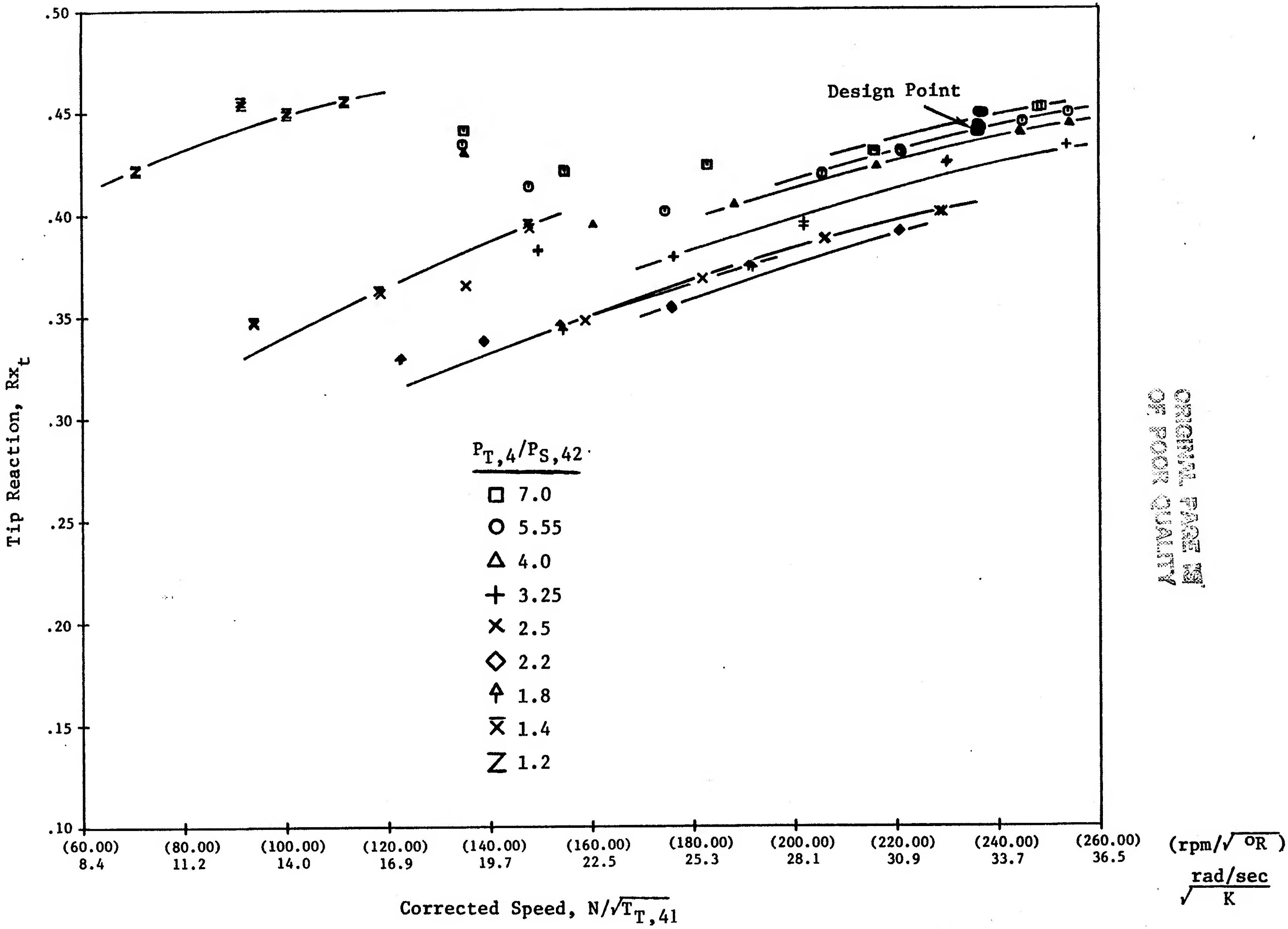

Figure 65. Stage One Tip Reaction vs. Corrected Speed. Solid Lines Show Expected Trend.

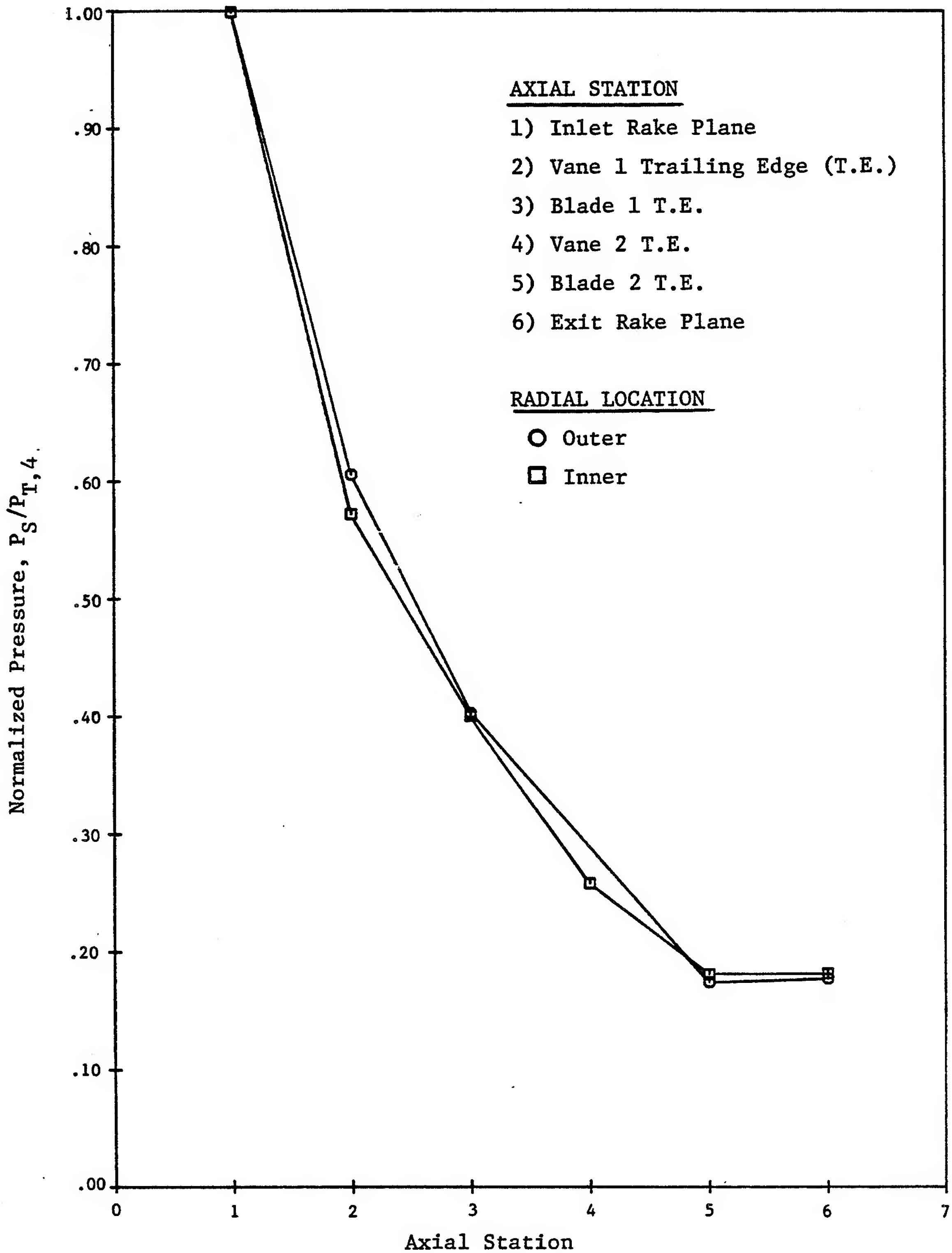

Figure 66. Static Pressure vs. Axial Station at Design Point Conditions

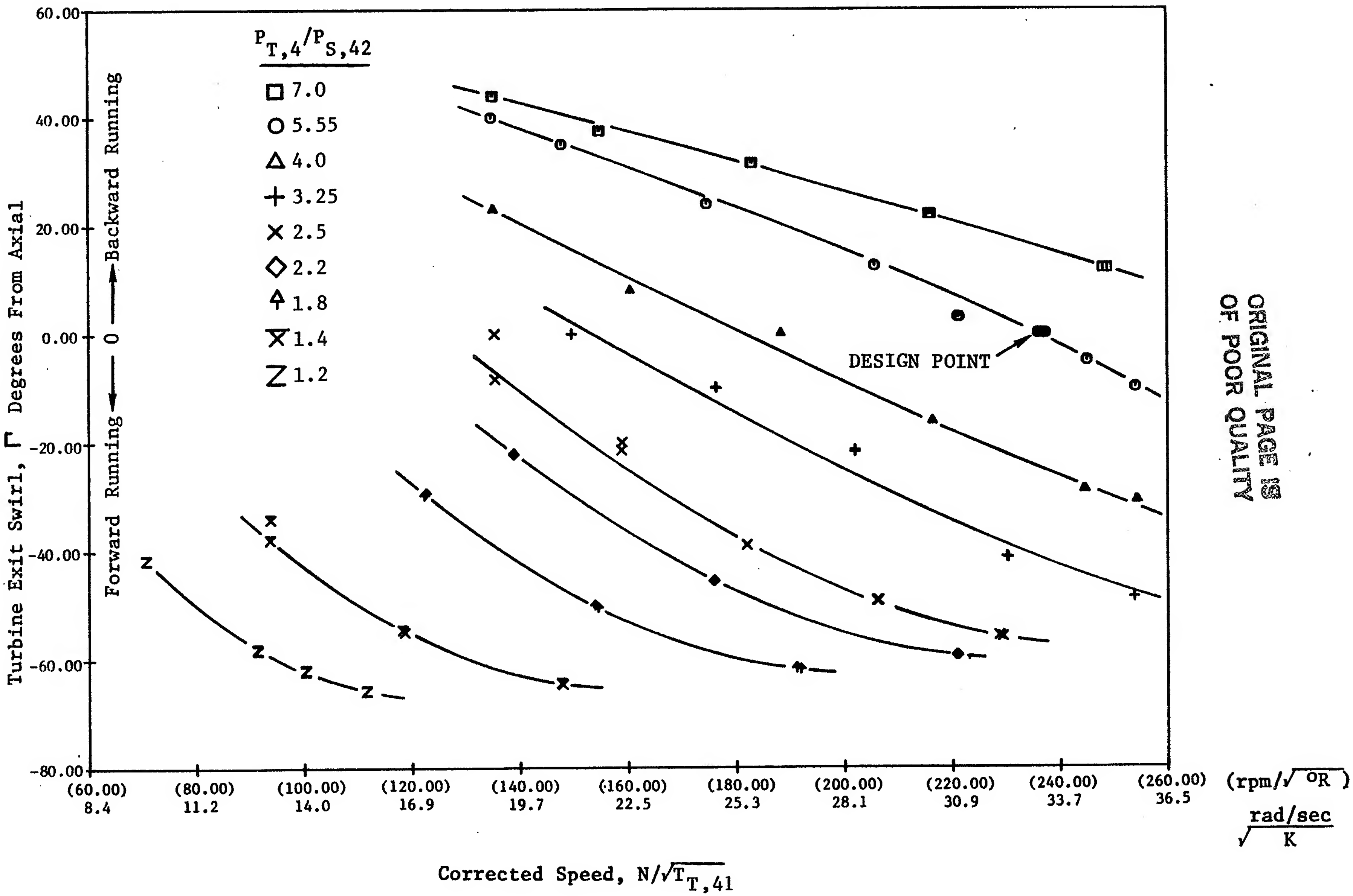

Figure 67. Turbine Exit Swirl vs. Corrected Speed.

exit static pressure, average exit rake total pressure and average exit rake total temperature; and (2) radial traverses. The reasons for using two sources were that the continuity calculation was insensitive between plus and minus ten degrees and the direction of the swirl (backward or forward running) cannot be determined from continuity, and the fact that traverses were not obtained at all points. In particular, no traversing was done at the four lower pressure ratios. This was due to an interference between the traversing probe and an arc rake after the rakes had been rotated to be more aligned with expected levels of swirl. Levels and trends agree well with expected values.

A tabulation of the pertinent data parameters is presented in Appendix G.

6.2.2 Stage Exit Survey

A set of detailed traverses was taken at design point operating conditions. Circumferential traverses covering two stage two vane spacings were taken at twenty-one radial locations to measure absolute levels of total temperature, total pressure, and flow angle. The radial variation of these parameters is shown in Figure 68. Arc rake averages of pressure and temperature show good agreement with the traverse data. Design intent swirl profile is compared to measured values and good agreement is observed over most of the annulus with some overturning in the hub region. In the case of the swirl profile, design intent is at blade trailing edge plane.

Contour plots were constructed from the circumferential traverses and are presented in Figures 69 through 71 for pressure, swirl and temperature respectively. Stage two vane wakes are observed at approximately twenty-five and sixty-five percent of circumferential arc. The circumferential travel was 18 degrees of arc.

6.2.3 Reynolds Number Variation

Energy averaged Reynolds number, based on vane throat dimension, was varied from 115,000 to 186,000 where rig design point Reynolds number is 176,000. Reynolds number was varied by changing inlet pressure while holding inlet temperature constant. The effect of Reynolds number on efficiency (thermodynaminc with pump work) is shown in Figure 72. It is observed that

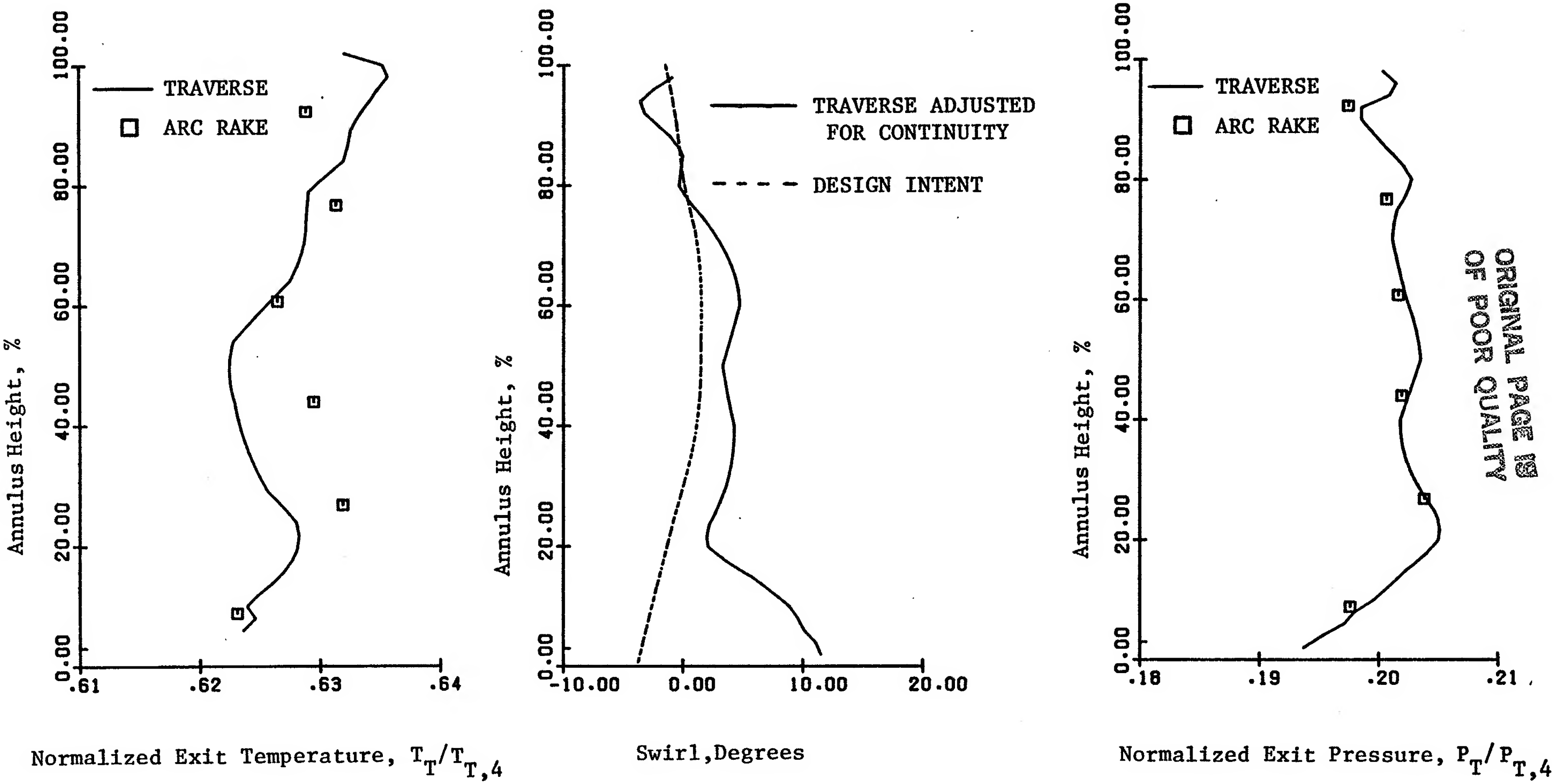

Figure 68. Turbine Exit Radial Profiles

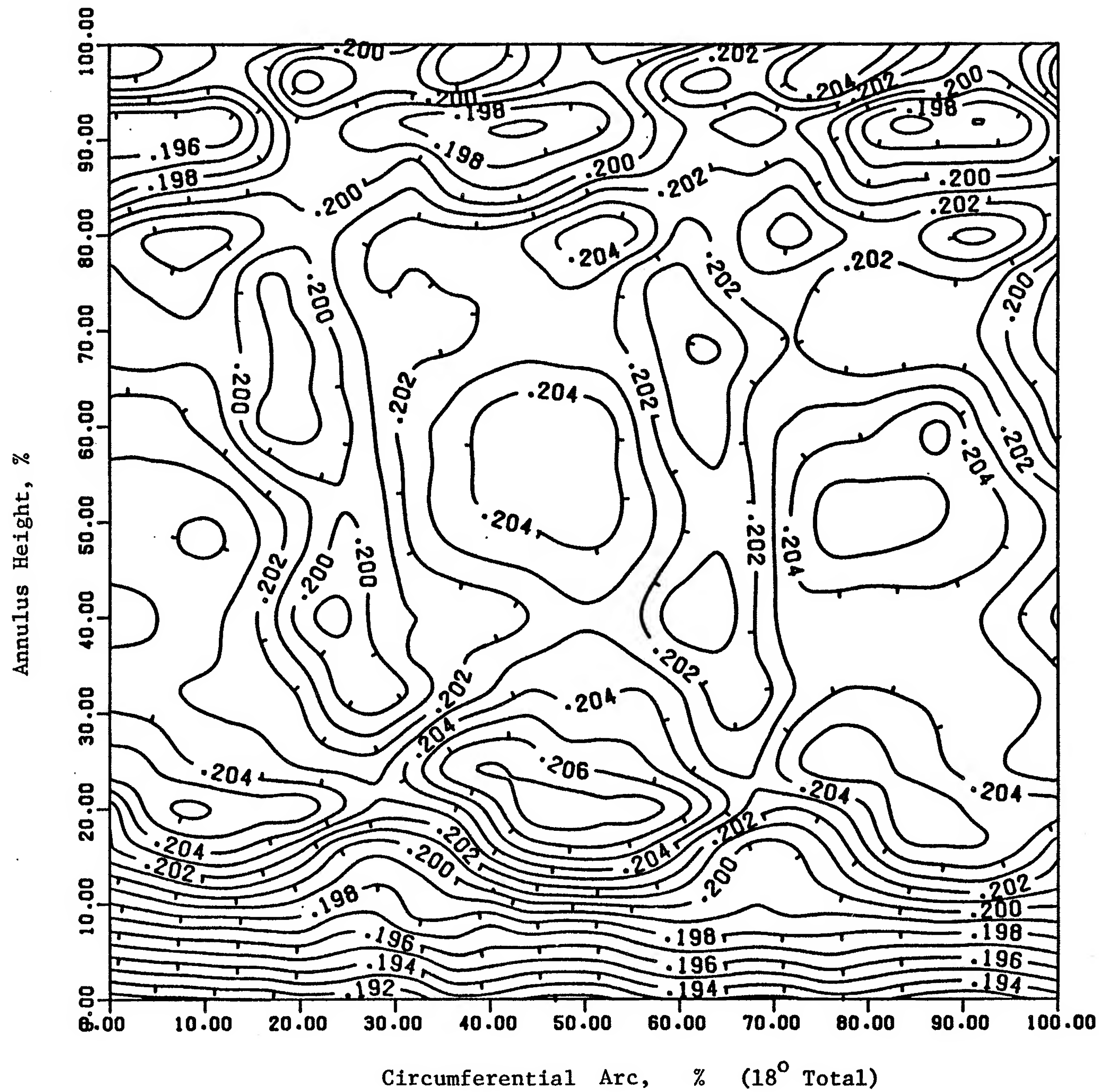

Figure 69. Turbine Exit Normalized Pressure ($P_T/P_{T,4}$) Contours at Design Point

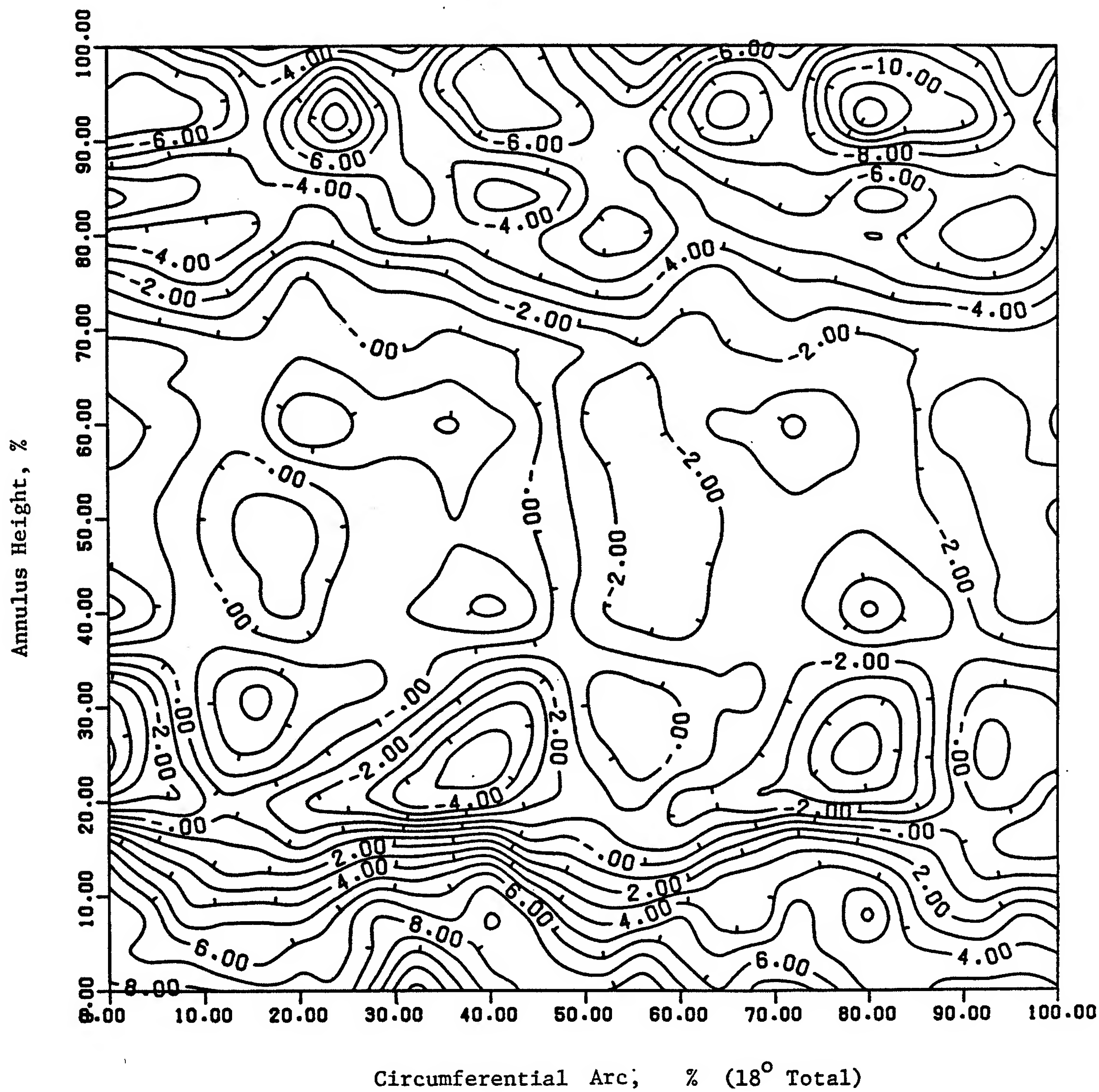

Figure 70. Turbine Exit Absolute Flow Angle Contours at Design Point

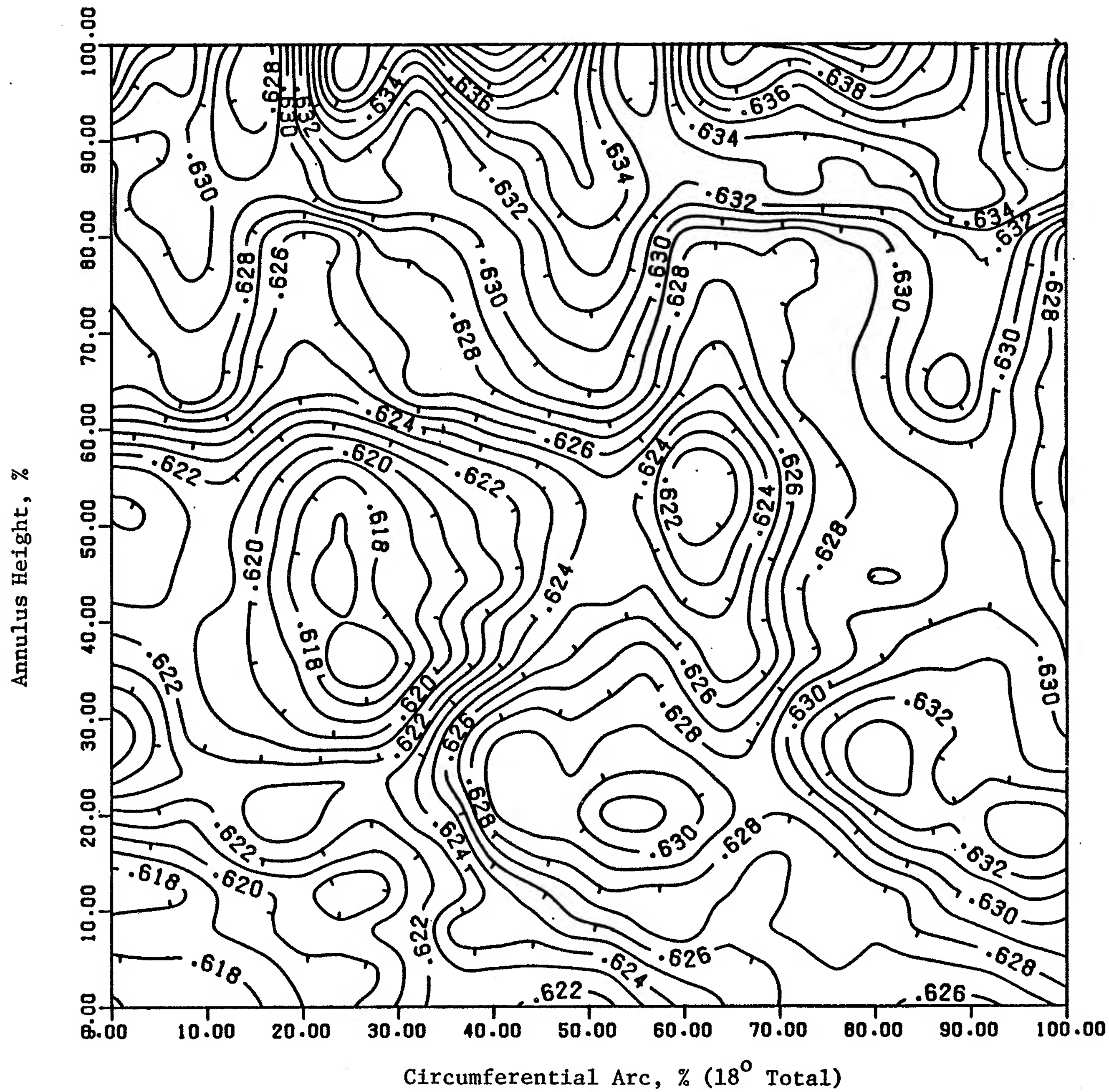

Figure 71. Turbine Exit Normalized Temperature ($T_T/T_{T,4}$) Contours at Design Point

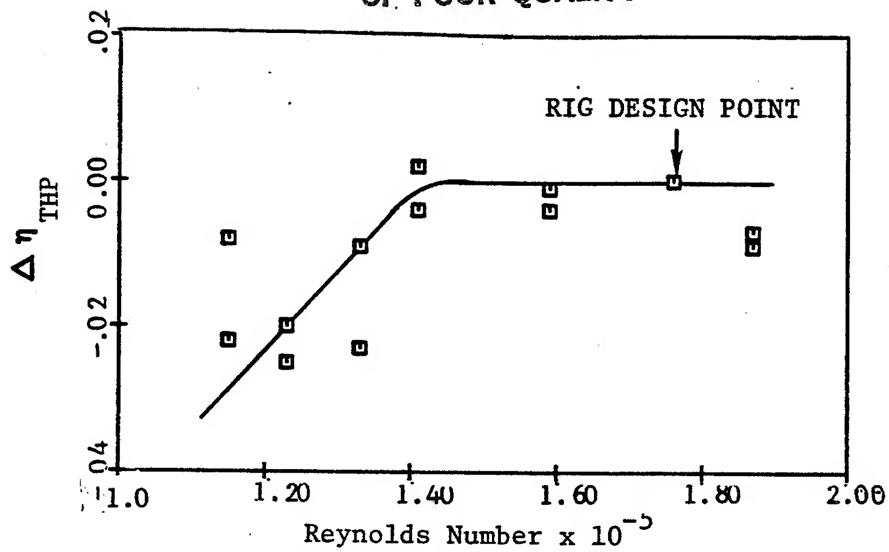

Figure 72. Efficiency Variation with Reynolds Number

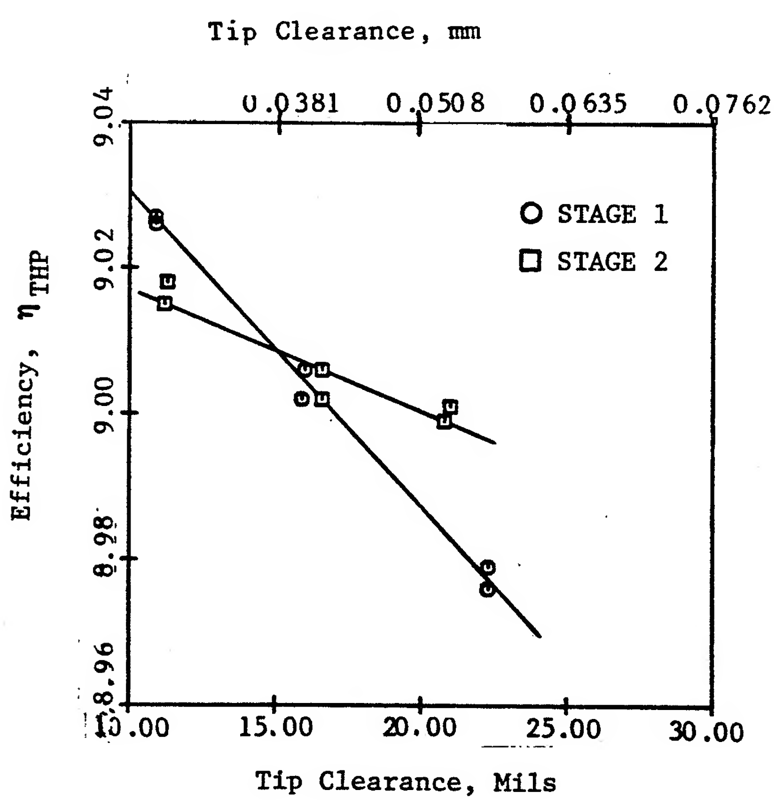

Figure 73. Efficiency vs. Tip Clearance

the rig design point is beyond the critical Reynolds number. Since the Reynolds number at all significant engine operating points is above critical, no efficiency correction is required.

6.2.4 Tip Clearance Variation

Blade tip clearance was varied on each stage independently. The range of clearance variation was from 0.028 cm (0.011 in.) to 0.056 cm (0.022 in.), where the nominal was 0.041 cm (0.016 in.). The minimum clearance was set so as to not rub the shroud and damage the blade hardware. The maximum clearance resulted when a temperature limit on a sealing ring in the clearance control air circuit was reached. The effect on overall turbine efficiency for stage one clearance is 0.0074 per one percent of blade height. Effect of stage two tip clearance is 0.0047 per one percent blade height. The observed trends are presented in Figure 73 for the thermodynamic with pumping definition of efficiency. As previously stated in Section 5.2, this variation was done at design point conditions except for reduced rotor coolant temperature. It is noted that the clearance effect on turbine efficiency of stage one is approximately fifty-seven percent greater than that of stage two. In view of the 57/43 work split for the 2 stage turbine, this general trend was expected.

6.2.5 Cooling Flow Variation

The following cooling flows were varied: stage one nozzle, rotor inducer, simulated compressor discharge leakage, and stage two vane. Flow rates were changed by increasing or decreasing the particular coolant circuit supply pressure. All variations were done at design point conditions. The effect of these variations on turbine efficiency (thermodynamic plus pump power) is shown in Figure 74. In each case the "zero" delta efficiency is defined where design intent coolant supply pressure was set. Flows are expressed as percent of stage one nozzle exit flow (W_{41}).

Stage one stator cooling flows were increased from 8.1% W_{41} (coolant supply pressure at design intent) to 8.8% with no change in turbine efficiency observed. This can be attributed to the fact that the increased coolant pressure tends to "supercharge" the flow and counters the increased mixing

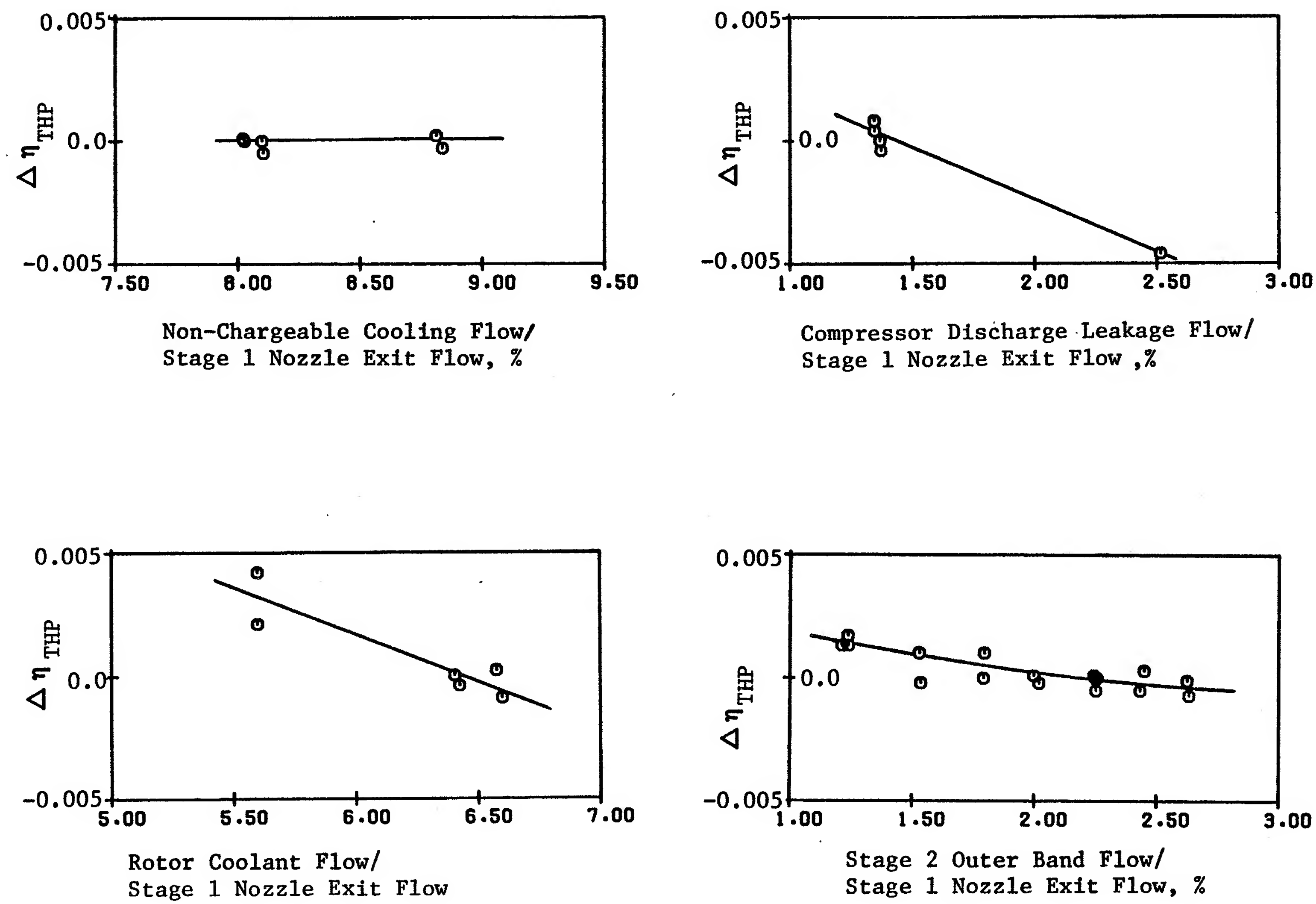

Figure 74. Effect of Cooling Flow Variation on Efficiency

losses of the additional coolant. This agrees well with prediction where an increase of 0.03 points was estimated and is consistent with annular cascade test results of Figure 40.

Simulated compressor discharge leakage was increased from 1.35% to 2.5% which resulted in a decrease in turbine efficiency of nearly one-half percent. This is approximately 0.2 points larger than predicted. This increase in flow was also seen to have a significant effect on both turbine flow function and stage one reaction as shown in Figure 75. Flow function decreases approximately 0.25% (from 18.165 to 18.12) and reaction increases from 0.37 to 0.44 at the hub. Somewhat less of an increase in tip reaction is also noted. These effects are a result of a reduction in stator one effective area due to the increased leakage flow blockage. The changes in flow function and reaction due to the increase in simulated compressor discharge leakage is of sufficient magnitude to account for the apparent anomalies in Figures 62, 64 and 65 for flow function, hub reaction and tip reaction respectively.

Rotor coolant flow was reduced to 5.6% and increased to 6.6% from a base of 6.4% (Figure 74). As expected, turbine efficiency increased 0.32 points with the reduction in rotor cooling flow and decreased 0.06 points with the increase in cooling flow and agrees well with prediction.

An estimate was made of what efficiency would have resulted if design intent rotor cooling flow was achieved at the correct supply pressure. This is based on the test results with the effect of the lower coolant supply pressure factored out. In terms of the thermodynamic definition of efficiency with credit for rotor coolant pumping, n_{THP}, and additional 0.3 points is estimated. For the General Electric cycle definition, n_{GE}, virtually no change is expected.

Stage two vane coolant flow was varied from 1.2% to 2.6%; flowrate at design coolant supply pressure was 2.25%. The total change in efficiency was on the order of 0.2 points. A trend of decreasing efficiency with increasing flowrate is observed as expected. Predicted values were +0.1 points at 1.2% and -0.1 points at 2.6%.

ORIGINAL PAGE IS
OF POOR QUALITY

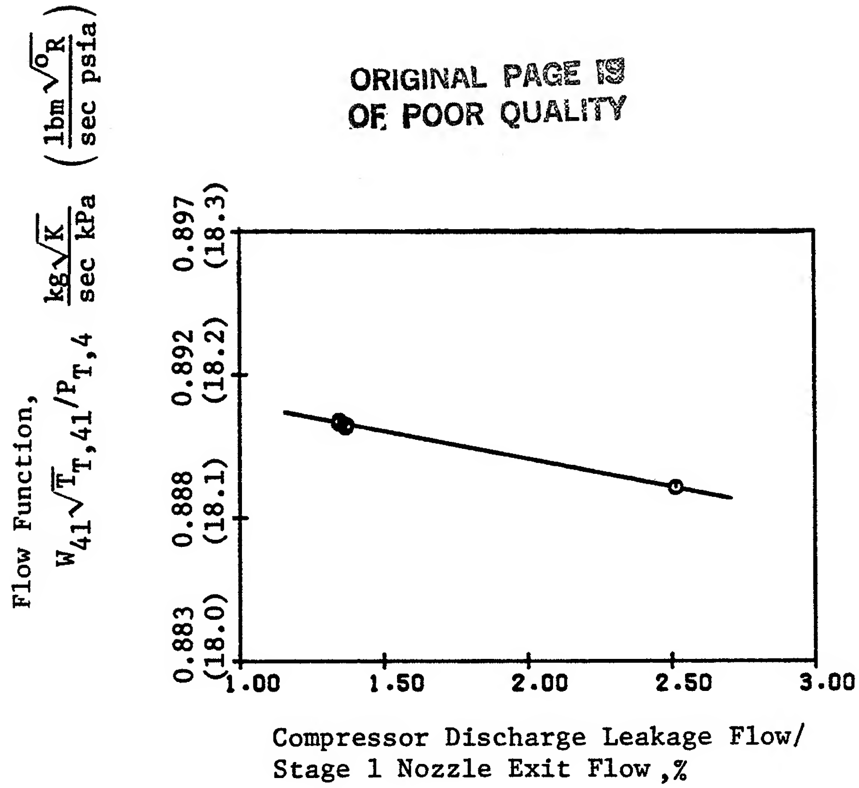

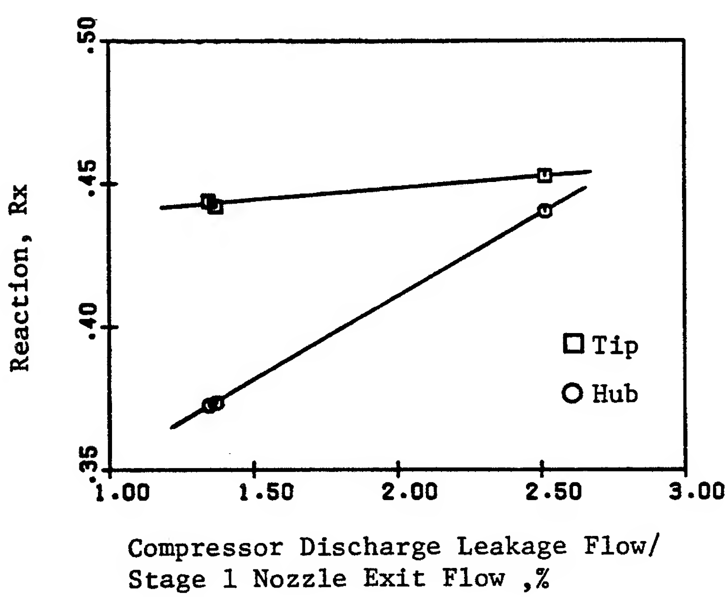

Figure 75. Effect of Simulated Compressor Discharge Leakage on Flow Function and Reaction

7.0 CONCLUSIONS

Full scale rig testing with simulated cooling flows has verified the aerodynamic design of the high pressure turbine for the General Electric Energy Efficient Engine. Rig thermodynamic efficiency with credit for rotor coolant pumping was demonstrated to be 90.0%. In terms of General Electric cycle definition, this efficiency was 92.5%, exceeding ICLS goal by 0.6 points and the FPS goal by 0.1 points.

The performance of the turbine was mapped over a wide range of operating conditions to evaluate off-design capabilities. Adequate definition of the off-design performance characteristic was accomplished. At very low pressure ratios (sub-idle and start region), the turbine exceeded expectations by two to five points in efficiency.

Rotor tip clearances were successfully varied independently on each stage to obtain the effect on two stage turbine efficiency.

Reynolds number was varied over a range of 115,000 to 186,000. It was verified that significant turbine operating points are at Reynolds numbers greater than critical and that no efficiency correction is required.

All cooling flow circuits were varied and changes in turbine efficiency agreed well with prediction.

Annular cascade testing of two stage one vane candidates showed the base configuration to have better performance than the lower unguided turning configuration by 0.48 percent in vane kinetic energy efficiency. Predicted level of efficiency would be met with trailing edge slots drilled per design intent.

Efficiency goals for the high pressure turbine in the FPS have been met.

8.0 REFERENCES

1. Halila, E.E., Lenahan, D.T., and Thomas, T.T., "Energy Efficient Engine High Pressure Turbine Test Hardware Detailed Design Report", NASA CR-167955.

APPENDICES

APPENDIX A

AIRFOIL COORDINATES

Typical Airfoil Coordinate Definition

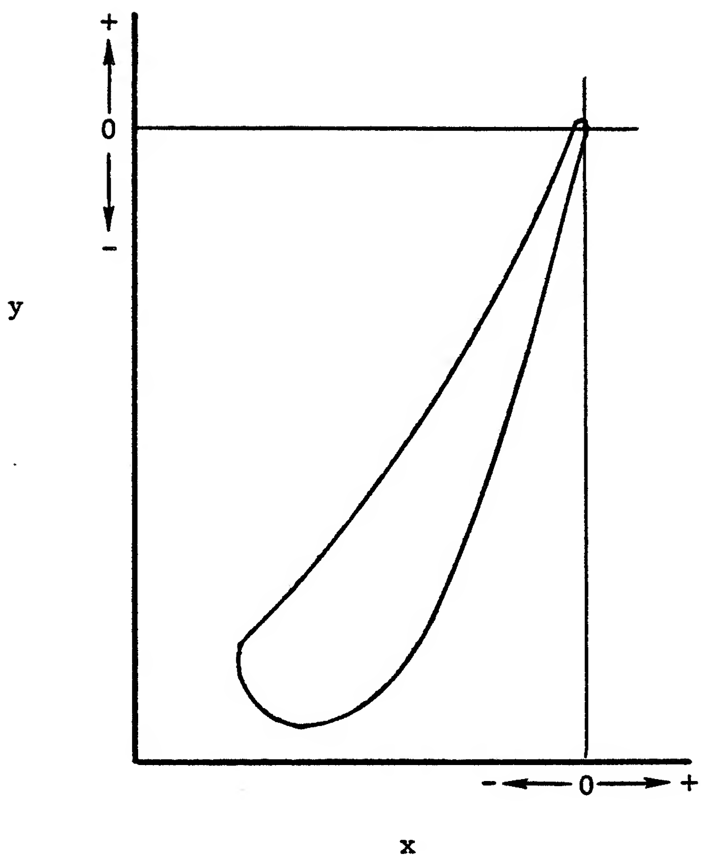

X = Axial distance

Y = Tangential distance on radius

SUCTION SURFACE COORDINATES

PT.	X	Y	PT.	X	Y
1	-12.949311	-18.491997	42	-6.302391	-18.508307
2	-13.014145	-18.637451	43	-6.043191	-18.087966
3	-13.060081	-18.783015	44	-5.783990	-17.635204
4	-13.087528	-18.928686	45	-5.524789	-17.149553
5	-13.096202	-19.074464	46	-5.265588	-16.631778
6	-13.094451	-19.128685	47	-5.006387	-16.082417
7	-13.089885	-19.182922	48	-4.747187	-15.502349
8	-13.083085	-19.237173	49	-4.487986	-14.892743
9	-13.075554	-19.291427	50	-4.228785	-14.254215
10	-13.067484	-19.345685	51	-3.969584	-13.586929
11	-13.057946	-19.399951	52	-3.710383	-12.891267
12	-13.046259	-19.454229	53	-3.451183	-12.167556
13	-13.032628	-19.508519	54	-3.191982	-11.416392
14	-13.018450	-19.562812	55	-2.932781	-10.638920
15	-13.004502	-19.617103	56	-2.673580	-9.837220
16	-12.989823	-19.671399	57	-2.414379	-9.014562
17	-12.973824	-19.725702	58	-2.155179	-8.174962
18	-12.956734	-19.780010	59	-1.895978	-7.322318
19	-12.589152	-20.492955	60	-1.636777	-6.460058
20	-12.221571	-20.907595	61	-1.377576	-5.590808
21	-11.853989	-21.179417	62	-1.118375	-4.715737
22	-11.486407	-21.357978	63	-0.859175	-3.832921
23	-11.227206	-21.444828	64	-0.599974	-2.936548
24	-10.958006	-21.494044	65	-0.340773	-2.020067
25	-10.708805	-21.517666	66	-0.253179	-1.706302
26	-10.449604	-21.518070	67	-0.165585	-1.389960
27	-10.190403	-21.494884	68	-0.077991	-1.068811
28	-9.931203	-21.451423	69	0.009603	-0.740281
29	-9.672002	-21.387636	70	0.097197	-0.400206
30	-9.412801	-21.304597	71	0.184792	-0.043980
31	-9.153600	-21.201770	72	0.188966	-0.019791
32	-8.894399	-21.079329	73	0.189972	0.004731
33	-8.635199	-20.935980	74	0.187794	0.029175
34	-8.375998	-20.771165	75	0.182468	0.053131
35	-8.116797	-20.583659	76	0.174083	0.076196
36	-7.857596	-20.371500	77	0.162779	0.097984
37	-7.598395	-20.134159	78	0.148746	0.118128
38	-7.339194	-19.868904	79	0.132217	0.136291
39	-7.079994	-19.575184	80	0.113471	0.152167
40	-6.820793	-19.251315	81	0.092820	0.165491
41	-6.561592	-18.895593	82	0.070611	0.176037

PRESSURE SURFACE COORDINATES

PT.	X	Y	PT.	X	Y
83	0.047216	0.183629	123	-6.561592	-11.029343
84	0.023026	0.188138	124	-6.820793	-11.386360
85	-0.001553	0.189490	125	-7.079994	-11.738000
86	-0.026109	0.187661	126	-7.339194	-12.083879
87	-0.050231	0.182681	127	-7.598395	-12.423695
88	-0.073514	0.174633	128	-7.857596	-12.757027
89	-0.095569	0.163652	129	-8.116797	-13.084601
90	-0.116025	0.149922	130	-8.375998	-13.405879
91	-0.134539	0.133673	131	-8.635199	-13.722966
92	-0.150801	0.115178	132	-8.894399	-14.035432
93	-0.164538	0.094745	133	-9.153600	-14.345715
94	-0.193910	0.003247	134	-9.412801	-14.653858
95	-0.223283	-0.053901	135	-9.672002	-14.961177
96	-0.252655	-0.113932	136	-9.931203	-15.267179
97	-0.282028	-0.177720	137	-10.190403	-15.571901
98	-0.311400	-0.241855	138	-10.449604	-15.872428
99	-0.340773	-0.307068	139	-10.708805	-16.168200
100	-0.599974	-0.863073	140	-10.968006	-16.454952
101	-0.859175	-1.402345	141	-11.227206	-16.731870
102	-1.118375	-1.937034	142	-11.486407	-16.998446
103	-1.377576	-2.462909	143	-11.797863	-17.304954
104	-1.636777	-2.978862	144	-12.109318	-17.602627
105	-1.895978	-3.484983	145	-12.420773	-17.896405
106	-2.155179	-3.980920	146	-12.732228	-18.194148
107	-2.414379	-4.466231	147	-12.747580	-18.209788
108	-2.673580	-4.940662	148	-12.762559	-18.225698
109	-2.932781	-5.404243	149	-12.777158	-18.241886
110	-3.191982	-5.857514	150	-12.791319	-18.258392
111	-3.451183	-6.300999	151	-12.805035	-18.275223
112	-3.710383	-6.735004	152	-12.818439	-18.292280
113	-3.969584	-7.160073	153	-12.831587	-18.309525
114	-4.228785	-7.576902	154	-12.844396	-18.327017
115	-4.487986	-7.985707	155	-12.856845	-18.344771
116	-4.747187	-8.387099	156	-12.869056	-18.362698
117	-5.006387	-8.781797	157	-12.881095	-18.380751
118	-5.265588	-9.169753	158	-12.892946	-18.398941
119	-5.524789	-9.552010	159	-12.904601	-18.417274
120	-5.783990	-9.928782	160	-12.916064	-18.435746
121	-6.043191	-10.300467	161	-12.927338	-18.454357
122	-6.302391	-10.667312	162	-12.938421	-18.473107

Stage 1 Vane Base Airfoil Coordinates (10X), inches

Radius = 12.825 inches

SUCTION SURFACE COORDINATES						PRESSURE SURFACE COORDINATES					
PT.	X	Y	PT.	X	Y	PT.	X	Y	PT.	X	Y
1	-12.942957	-19.799971	42	-6.312592	-19.852351	83	0.040791	0.185776	123	-6.572194	-11.955824
2	-13.013612	-19.953000	43	-6.052990	-19.422969	84	0.016146	0.189543	124	-6.831797	-12.334520
3	-13.064935	-20.105434	44	-5.793388	-18.956640	85	-0.008776	0.190049	125	-7.091399	-12.707168
4	-13.097440	-20.257288	45	-5.533785	-18.453685	86	-0.033545	0.187283	126	-7.351001	-13.073563
5	-13.111089	-20.408559	46	-5.274183	-17.915023	87	-0.057735	0.181294	127	-7.610603	-13.433851
6	-13.110943	-20.476942	47	-5.014581	-17.342881	88	-0.080928	0.172185	128	-7.870206	-13.787884
7	-13.106848	-20.545204	48	-4.754979	-16.738790	89	-0.102726	0.160114	129	-8.129808	-14.136202
8	-13.099622	-20.613369	49	-4.495376	-16.104472	90	-0.122752	0.145287	130	-8.389410	-14.478579
9	-13.090294	-20.681469	50	-4.235774	-15.440556	91	-0.140663	0.127962	131	-8.649012	-14.816192
10	-13.078575	-20.749495	51	-3.976172	-14.746072	92	-0.156149	0.108435	132	-8.908615	-15.148799
11	-13.063840	-20.817429	52	-3.716570	-14.019245	93	-0.168944	0.087044	133	-9.168217	-15.477708
12	-13.046160	-20.885271	53	-3.456967	-13.258736	94	-0.197744	-0.002012	134	-9.427819	-15.802881
13	-13.025968	-20.953036	54	-3.197365	-12.464388	95	-0.226543	-0.064700	135	-9.687421	-16.125017
14	-13.003759	-21.020739	55	-2.937763	-11.638025	96	-0.255342	-0.129176	136	-9.947024	-16.443793
15	-12.979899	-21.088391	56	-2.678161	-10.783344	97	-0.284142	-0.196822	137	-10.206626	-16.759222
16	-12.954256	-21.155988	57	-2.418558	-9.904717	98	-0.312941	-0.264790	138	-10.466228	-17.069736
17	-12.926634	-21.223524	58	-2.158956	-9.005728	99	-0.341740	-0.333592	139	-10.725830	-17.375046
18	-12.896968	-21.290996	59	-1.899354	-8.088330	100	-0.601343	-0.936988	140	-10.985433	-17.672894
19	-12.548885	-21.898292	60	-1.639752	-7.153419	101	-0.860945	-1.524639	141	-11.245035	-17.963017
20	-12.200803	-22.269748	61	-1.380149	-6.201463	102	-1.120547	-2.107268	142	-11.504637	-18.245342
21	-11.852720	-22.518510	62	-1.120547	-5.233051	103	-1.380149	-2.680952	143	-11.819782	-18.577701
22	-11.504637	-22.684880	63	-0.860945	-4.248126	104	-1.639752	-3.244199	144	-12.134926	-18.903065
23	-11.245035	-22.770484	64	-0.601343	-3.244450	105	-1.899354	-3.796756	145	-12.450071	-19.225145
24	-10.985433	-22.820995	65	-0.341740	-2.219621	106	-2.158956	-4.338122	146	-12.765215	-19.549276
25	-10.725830	-22.845917	66	-0.253893	-1.868701	107	-2.418558	-4.867640	147	-12.777618	-19.562641
26	-10.466228	-22.847495	67	-0.166045	-1.515489	108	-2.678161	-5.384844	148	-12.789746	-19.576202
27	-10.205626	-22.826589	68	-0.078198	-1.158975	109	-2.937763	-5.889666	149	-12.801595	-19.589961
28	-9.947024	-22.784890	69	0.009650	-0.797049	110	-3.197365	-6.382517	150	-12.813138	-19.603937
29	-9.687421	-22.723023	70	0.097497	-0.426094	111	-3.456967	-6.864143	151	-12.824369	-19.618133
30	-9.427819	-22.641474	71	0.185345	-0.041901	112	-3.716570	-7.335151	152	-12.835344	-19.632512
31	-9.168217	-22.540171	72	0.189215	-0.017240	113	-3.976172	-7.796085	153	-12.846089	-19.647053
32	-8.908615	-22.419021	73	0.189826	0.007717	114	-4.235774	-8.247611	154	-12.856587	-19.661770
33	-8.649012	-22.277191	74	0.187168	0.032541	115	-4.495376	-8.690095	155	-12.866840	-19.676660
34	-8.389410	-22.114122	75	0.181286	0.056803	116	-4.754979	-9.123951	156	-12.876910	-19.691680
35	-8.129808	-21.928319	76	0.172281	0.080087	117	-5.014581	-9.549795	157	-12.886827	-19.706808
36	-7.870206	-21.718725	77	0.160309	0.101992	118	-5.274183	-9.967814	158	-12.895586	-19.722049
37	-7.610603	-21.483099	78	0.145577	0.122140	119	-5.533785	-10.378614	159	-12.906181	-19.737406
38	-7.351001	-21.220293	79	0.128338	0.140186	120	-5.793388	-10.782546	160	-12.915616	-19.752876
39	-7.091399	-20.927305	80	0.108889	0.155817	121	-6.052990	-11.179904	161	-12.924890	-19.768461
40	-6.831797	-20.603391	81	0.087566	0.168766	122	-6.312592	-11.570915	162	-12.934003	-19.784159
41	-6.572194	-20.245184	82	0.064735	0.178810						

Stage 1 Vane Base Airfoil Coordinates (10X), inches

Radius = 13.612 inches

SUCTION SURFACE COORDINATES

PT.	X	Y	PT.	X	Y
1	-12.936602	-21.127869	42	-6.322793	-21.220362
2	-13.012840	-21.287954	43	-6.062789	-20.783871
3	-13.069766	-21.446915	44	-5.802786	-20.305617
4	-13.107378	-21.604753	45	-5.542782	-19.786800
5	-13.125677	-21.761466	46	-5.282778	-19.228510
6	-13.127529	-21.845534	47	-5.022774	-18.634851
7	-13.123761	-21.929275	48	-4.762771	-18.008075
8	-13.115957	-22.012782	49	-4.502767	-17.350513
9	-13.105007	-22.096105	50	-4.242763	-16.662804
10	-13.089524	-22.179165	51	-3.982760	-15.942713
11	-13.069571	-22.261964	52	-3.722756	-15.186055
12	-13.045741	-22.344538	53	-3.462752	-14.389634
13	-13.019129	-22.426950	54	-3.202749	-13.552444
14	-12.988881	-22.509151	55	-2.942745	-12.677064
15	-12.955045	-22.591142	56	-2.682741	-11.768975
16	-12.918536	-22.672979	57	-2.422737	-10.833757
17	-12.879393	-22.754662	58	-2.162734	-9.874481
18	-12.837202	-22.836169	59	-1.902730	-8.890903
19	-12.508619	-23.320608	60	-1.642726	-7.881071
20	-12.180035	-23.640960	61	-1.382723	-6.843028
21	-11.851451	-23.862068	62	-1.122719	-5.776701
22	-11.522867	-24.013570	63	-0.862715	-4.684132
23	-11.262864	-24.097165	64	-0.602712	-3.567110
24	-11.002860	-24.148772	65	-0.342708	-2.427912
25	-10.742856	-24.174976	66	-0.254607	-2.037768
26	-10.482853	-24.177862	67	-0.166506	-1.645667
27	-10.222849	-24.159666	68	-0.078405	-1.251978
28	-9.962845	-24.120241	69	0.009696	-0.855125
29	-9.702842	-24.060968	70	0.097797	-0.452133
30	-9.442838	-23.981669	71	0.185898	-0.039269
31	-9.182834	-23.882798	72	0.189465	-0.014253
32	-8.922830	-23.763958	73	0.189680	0.011015
33	-8.662827	-23.624840	74	0.186541	0.036088
34	-8.402823	-23.464886	75	0.180103	0.060522
35	-8.142819	-23.282314	76	0.170479	0.083887
36	-7.882815	-23.077085	77	0.157840	0.105767
37	-7.622812	-22.845054	78	0.142408	0.125777
38	-7.362808	-22.586859	79	0.124458	0.143562
39	-7.102804	-22.296770	80	0.104307	0.158808
40	-6.842800	-21.975099	81	0.082311	0.171245
41	-6.582797	-21.616639	82	0.058859	0.180653

PRESSURE SURFACE COORDINATES

PT.	X	Y	PT.	X	Y
83	0.034366	0.186866	123	-6.582797	-12.911101
84	0.009265	0.189774	124	-6.842800	-13.311446
85	-0.016000	0.189325	125	-7.102804	-13.705032
86	-0.040982	0.185528	126	-7.362808	-14.091858
87	-0.065238	0.178449	127	-7.622812	-14.472574
88	-0.088342	0.168214	128	-7.882815	-14.847331
89	-0.109882	0.155003	129	-8.142819	-15.216465
90	-0.129479	0.139051	130	-8.402823	-15.580097
91	-0.146786	0.120640	131	-8.662827	-15.938357
92	-0.161497	0.100094	132	-8.922830	-16.291213
93	-0.173351	0.077779	133	-9.182834	-16.638699
94	-0.201577	-0.007902	134	-9.442838	-16.980683
95	-0.229803	-0.076366	135	-9.702842	-17.317168
96	-0.258029	-0.145373	136	-9.962845	-17.648023
97	-0.286255	-0.216872	137	-10.222849	-17.973236
98	-0.314482	-0.288661	138	-10.482853	-18.292761
99	-0.342708	-0.361002	139	-10.742856	-18.606612
100	-0.602712	-1.013322	140	-11.002860	-18.914808
101	-0.862715	-1.651120	141	-11.262864	-19.217695
102	-1.122719	-2.283436	142	-11.522867	-19.515698
103	-1.382723	-2.906725	143	-11.841701	-19.874716
104	-1.642726	-3.519072	144	-12.160535	-20.228854
105	-1.902730	-4.119839	145	-12.479369	-20.580418
106	-2.162734	-4.708367	146	-12.798202	-20.931869
107	-2.422737	-5.283758	147	-12.807594	-20.942515
108	-2.682741	-5.845312	148	-12.816820	-20.953279
109	-2.942745	-6.392851	149	-12.825882	-20.964158
110	-3.202749	-6.926640	150	-12.834778	-20.975154
111	-3.462752	-7.447666	151	-12.843510	-20.986266
112	-3.722756	-7.956873	152	-12.852057	-20.997509
113	-3.982760	-8.454797	153	-12.860383	-21.008908
114	-4.242763	-8.942072	154	-12.868581	-21.020397
115	-4.502767	-9.419224	155	-12.876652	-21.031977
116	-4.762771	-9.886447	156	-12.884594	-21.043647
117	-5.022774	-10.344233	157	-12.892408	-21.055408
118	-5.282778	-10.793033	158	-12.900094	-21.067258
119	-5.542782	-11.232961	159	-12.907652	-21.079200
120	-5.802786	-11.664517	160	-12.915082	-21.091231
121	-6.062789	-12.087874	161	-12.922383	-21.103354
122	-6.322793	-12.503240	162	-12.929557	-21.115566

Stage 1 Vane Base Airfoil Coordinates (10X) , inches

Radius = 14.40 inches

SUCTION SURFACE COORDINATES

PT.	X	Y	PT.	X	Y
1	-12.930217	-19.354575	42	-6.307253	-18.964441
2	-13.010558	-19.520508	43	-6.047861	-18.484285
3	-13.062741	-19.682486	44	-5.788469	-17.964422
4	-13.086768	-19.840509	45	-5.529077	-17.406503
5	-13.091432	-19.995811	46	-5.269684	-16.813921
6	-13 087802	-20.082001	47	-5.010292	-16.190830
7	-13.078033	-20.167337	48	-4.750900	-15.538470
8	-13.062304	-20.251619	49	-4.491508	-14.855622
9	-13.042436	-20.335728	50	-4.232116	-14.146109
10	-13.019042	-20.419141	51	-3.972724	-13.411351
11	-12.991006	-20.501903	52	-3.713332	-12.659957
12	-12.958366	-20.584017	53	-3.453940	-11.897461
13	-12.921837	-20.665385	54	-3.194548	-11.123473
14	-12.882101	-20.746703	55	-2.935155	-10.333581
15	-12.838393	-20.827263	56	-2.675763	-9.524851
16	-12.791446	-20.907367	57	-2.416371	-8.699468
17	-12.742139	-20.987140	58	-2.156979	-7.861456
18	-12.689717	-21.066475	59	-1.897587	-7.012364
19	-12.391062	-21.436821	60	-1.638195	-6.155925
20	-12.092406	-21.694109	61	-1.378803	-5.302683
21	-11.793751	-21.878202	62	-1.119411	-4.453942
22	-11.495095	-22.010190	63	-0.860019	-3.604297
23	-11.235703	-22.093143	64	-0.600627	-2.733097
24	-10.976311	-22.150148	65	-0.341235	-1.665042
25	-10.716919	-22.182647	66	-0.253532	-1.574704
26	-10.457527	-22.191645	67	-0.165829	-1.281192
27	-10.198135	-22.178150	68	-0.078126	-0.986629
28	-9.938743	-22.142655	69	0.009577	-0.691106
29	-9.679350	-22.086164	70	0.097280	-0.381971
30	-9.419958	-22.008271	71	0.184983	-0.043375
31	-9.160566	-21.908676	72	0.189069	-0.018788
32	-8.901174	-21.785616	73	0.189901	0.006122
33	-8.641782	-21.640565	74	0.187466	0.030927
34	-8.382390	-21.468534	75	0.181805	0.055200
35	-8.122998	-21.269430	76	0.173015	0.078523
36	-7.863606	-21.040964	77	0.161248	0.100494
37	-7.604214	-20.782155	78	0.146706	0.120737
38	-7.344821	-20.490296	79	0.129640	0.138901
39	-7.085429	-20.165185	80	0.110342	0.154676
40	-6.826037	-19.803366	81	0.089146	0.167788
41	-6.566645	-19.403726	82	0.066416	0.178014

PRESSURE SURFACE COORDINATES

PT.	X	Y	PT.	X	Y
83	0.042543	0.185176	123	-6.566645	-11.673133
84	0.017938	0.189151	124	-6.826037	-12.064484
85	-0.006976	0.189872	125	-7.085429	-12.449409
86	-0.031770	0.187325	126	-7.344821	-12.827408
87	-0.056017	0.181555	127	-7.604214	-13.198881
88	-0.079300	0.172660	128	-7.863606	-13.564098
89	-0.101218	0.160794	129	-8.122998	-13.923632
90	-0.121395	0.146162	130	-8.382390	-14.277818
91	-0.139483	0.129014	131	-8.641782	-14.626334
92	-0.155170	0.109646	132	-8.901174	-14.969367
93	-0.168187	0.088391	133	-9.160566	-15.305530
94	-0.197029	-0.025939	134	-9.419958	-15.634390
95	-0.223870	-0.097031	135	-9.679350	-15.954489
96	-0.254711	-0.155817	136	-9.938743	-16.265489
97	-0.283552	-0.215990	137	-10.198135	-16.566736
98	-0.312393	-0.276919	138	-10.457527	-16.859031
99	-0.341235	-0.333036	139	-10.716919	-17.142615
100	-0.600627	-0.886362	140	-10.976311	-17.417768
101	-0.860019	-1.424928	141	-11.235703	-17.684619
102	-1.119411	-1.963928	142	-11.495095	-17.942642
103	-1.378603	-2.503301	143	-11.801226	-18.235798
104	-1.638195	-3.044718	144	-12.107356	-18.519887
105	-1.897587	-3.577397	145	-12.413487	-18.797321
106	-2.156979	-4.100015	146	-12.719517	-19.072175
107	-2.416371	-4.610233	147	-12.734858	-19.086659
108	-2.675763	-5.107540	148	-12.749713	-19.101431
109	-2.933155	-5.593574	149	-12.764184	-19.116490
110	-3.194548	-6.070599	150	-12.778270	-19.131835
111	-3.453940	-6.540140	151	-12.791864	-19.147548
112	-3.713332	-7.003560	152	-12.804609	-19.163894
113	-3.972724	-7.460795	153	-12.817133	-19.180404
114	-4.232116	-7.911386	154	-12.829436	-19.197080
115	-4.491508	-8.354727	155	-12.841518	-19.213920
116	-4.750900	-8.790445	156	-12.853379	-19.230925
117	-5.010292	-9.218802	157	-12.865019	-19.248095
118	-5.269684	-9.640128	158	-12.876438	-19.265429
119	-5.529077	-10.055963	159	-12.887636	-19.282929
120	-5.788469	-10.466699	160	-12.898613	-19.300593
121	-6.047861	-10.873437	161	-12.909369	-19.318422
122	-6.307253	-11.275613	162	-12.919903	-19.336416

Stage 1 Vane Lut Airfoil Coordinates (10X), inches

Radius = 12.825 inches

SUCTION SURFACE COORDINATES

PT.	X	Y	PT.	X	Y
1	-13.113632	-20.552516	42	-6.395740	-20.585848
2	-13.191887	-20.721208	43	-6.132815	-20.092617
3	-13.244186	-20.885838	44	-5.869891	-19.553080
4	-13.272940	-21.046782	45	-5.606966	-18.968540
5	-13.280586	-21.204424	46	-5.344041	-18.342449
6	-13.275037	-21.306874	47	-5.081116	-17.680420
7	-13.262555	-21.408223	48	-4.818191	-16.986319
8	-13.244839	-21.508764	49	-4.555266	-16.261248
9	-13.221721	-21.608454	50	-4.292341	-15.506794
10	-13.192856	-21.707247	51	-4.029417	-14.725310
11	-13.159112	-21.805277	52	-3.766492	-13.924446
12	-13.120900	-21.902607	53	-3.503567	-13.103031
13	-13.078251	-21.999243	54	-3.240642	-12.259814
14	-13.031682	-22.095265	55	-2.977717	-11.392910
15	-12.981586	-22.190736	56	-2.714792	-10.505217
16	-12.928198	-22.285692	57	-2.451868	-9.602876
17	-12.871941	-22.380198	58	-2.188943	-8.639239
18	-12.812882	-22.474266	59	-1.926018	-7.763373
19	-12.523221	-22.858906	60	-1.663093	-6.826519
20	-12.233559	-23.140350	61	-1.400168	-5.886790
21	-11.943898	-23.352753	62	-1.137243	-4.949913
22	-11.654237	-23.513394	63	-0.874319	-4.006643
23	-11.391312	-23.624010	64	-0.611394	-3.042129
24	-11.120387	-23.703815	65	-0.348469	-2.064774
25	-10.865462	-23.754799	66	-0.259588	-1.735034
26	-10.602538	-23.778324	67	-0.170707	-1.403677
27	-10.339613	-23.775602	68	-0.081825	-1.071836
28	-10.076688	-23.748054	69	0.007056	-0.739538
29	-9.813763	-23.696447	70	0.095937	-0.399751
30	-9.550838	-23.621405	71	0.184818	-0.044174
31	-9.287913	-23.523091	72	0.189034	-0.019180
32	-9.024989	-23.401218	73	0.189901	0.006153
33	-8.762064	-23.255223	74	0.187405	0.031377
34	-8.499139	-23.084057	75	0.181589	0.056047
35	-8.236214	-22.886537	76	0.172558	0.079724
36	-7.973289	-22.660695	77	0.160470	0.101992
37	-7.710364	-22.405683	78	0.145540	0.122455
38	-7.447440	-22.117790	79	0.128033	0.140753
39	-7.184515	-21.795358	80	0.108259	0.156560
40	-6.921590	-21.434602	81	0.086569	0.169599
41	-6.658665	-21.032161	82	0.063347	0.179638

PRESSURE SURFACE COORDINATES

PT.	X	Y	PT.	X	Y
83	0.039004	0.186500	123	-6.658665	-12.481453
84	0.013972	0.190063	124	-6.921590	-12.891469
85	-0.011305	0.190265	125	-7.184515	-13.295599
86	-0.035380	0.187104	126	-7.447440	-13.693789
87	-0.060809	0.180634	127	-7.710364	-14.085573
88	-0.084157	0.170970	128	-7.973289	-14.470844
89	-0.106013	0.158285	129	-8.236214	-14.849339
90	-0.125939	0.142802	130	-8.499139	-15.220333
91	-0.143730	0.124796	131	-8.762064	-15.585966
92	-0.158924	0.104586	132	-9.024989	-15.944415
93	-0.171301	0.082530	133	-9.287913	-16.296386
94	-0.200829	-0.030393	134	-9.550838	-16.641645
95	-0.230357	-0.105264	135	-9.813763	-16.979563
96	-0.259885	-0.170444	136	-10.076688	-17.309484
97	-0.289413	-0.236940	137	-10.339613	-17.630279
98	-0.318341	-0.303914	138	-10.602538	-17.941247
99	-0.348469	-0.370998	139	-10.865462	-18.241216
100	-0.611394	-0.959997	140	-11.128387	-18.530634
101	-0.874319	-1 536311	141	-11.391312	-18.808201
102	-1.137243	-2.119736	142	-11.654237	-19.078167
103	-1.400168	-2.714139	143	-11.962761	-19.385303
104	-1.663093	-3.308339	144	-12.271284	-19.686281
105	-1.926018	-3.890997	145	-12.579808	-19.981368
106	-2.188943	-4.457503	146	-12.888332	-20.265576
107	-2.451868	-5.008750	147	-12.904223	-20.280384
108	-2.714792	-5.544931	148	-12.919772	-20.295460
109	-2.977717	-6.068210	149	-12.934995	-20.310792
110	-3.240642	-6.580255	150	-12.949387	-20.326384
111	-3.503567	-7.081718	151	-12.964370	-20.342297
112	-3.766492	-7.573463	152	-12.978403	-20.358563
113	-4.029417	-8.055946	153	-12.992097	-20.375095
114	-4.292341	-8.529160	154	-13.005525	-20.391837
115	-4.555266	-8.994195	155	-13.018675	-20.408797
116	-4.818191	-9.451604	156	-13.031536	-20.425983
117	-5.081116	-9.902120	157	-13.044114	-20.443392
118	-5.344041	-10.346242	158	-13.056409	-20.461023
119	-5.606966	-10.784583	159	-13.068420	-20.478876
120	-5.869891	-11.217168	160	-13.080148	-20.496953
121	-6.132815	-11.644224	161	-13.091593	-20.515251
122	-6.395740	-12.065714	162	-13.102754	-20.533772

Stage 1 Vane Lut Airfoil Coordinates (10X) , inches

Radius = 13.612 inches

SUCTION SURFACE COORDINATES

PT.	X	Y	PT.	X	Y
1	-13.297047	-21.751557	42	-6.484227	-22.259871
2	-13.372479	-21.921818	43	-6.217770	-21.755452
3	-13.426350	-22.088449	44	-5.951312	-21.197654
4	-13.456658	-22.251448	45	-5.684855	-20.587376
5	-13.469403	-22.410815	46	-5.418397	-19.928114
6	-13.463007	-22.530835	47	-5.151940	-19.227080
7	-13.446235	-22.649107	48	-4.885482	-18.491056
8	-13.427859	-22.767110	49	-4.619025	-17.722616
9	-13.401186	-22.883715	50	-4.352567	-16.924195
10	-13.365545	-22.998978	51	-4.086109	-16.097928
11	-13.327314	-23.113469	52	-3.819652	-15.245107
12	-13.283756	-23.227231	53	-3.553194	-14.363394
13	-13.234651	-23.340058	54	-3.286737	-13.448460
14	-13.181358	-23.452181	55	-3.020279	-12.501273
15	-13.125062	-23.563797	56	-2.753821	-11.531250
16	-13.064857	-23.674756	57	-2.487364	-10.548930
17	-13.001887	-23.785248	58	-2.220906	-9.556887
18	-12.936047	-23.895257	59	-1.954449	-8.551411
19	-12.655380	-24 293217	60	-1.687991	-7.530934
20	-12.374713	-24.599761	61	-1.421534	-6.500765
21	-12.094046	-24.842455	62	-1.155076	-5.468243
22	-11.813379	-25.034118	63	-0.888618	-4.429928
23	-11.546921	-25.175000	64	-0.622161	-3.367496
24	-11.280464	-25.279828	65	-0.355703	-2.274365
25	-11.014006	-25.351193	66	-0.265644	-1.902727
26	-10.747549	-25.390836	67	-0.175584	-1.531232
27	-10.481091	-25.400240	68	-0.085525	-1.159892
28	-10.214634	-25.381803	69	0.004534	-0.783665
29	-9.948176	-25.336042	70	0.094594	-0.416874
30	-9.681718	-23.264730	71	0.184653	-0.044757
31	-9.415261	-25.168323	72	0.188938	-0.019484
32	-9.148803	-25.047746	73	0.189901	0.006143
33	-8.882346	-24.902843	74	0.187344	0.031659
34	-8.615888	-24.733658	75	0.181374	0.056593
35	-8.349431	-24.539508	76	0.172101	0.080507
36	-8.082973	-24.318738	77	0.159592	0.102949
37	-7.316515	-24.069251	78	0.144375	0.123515
38	-7.550058	-23.787838	79	0.126427	0.141831
39	-7.283600	-23.470687	80	0.106177	0.157564
40	-7.017143	-23.114089	81	0.083992	0.170427
41	-6.750685	-22.710922	82	0.060277	0.180185

PRESSURE SURFACE COORDINATES

PT.	X	Y	PT.	X	Y
83	0.035465	0.186661	123	-6.750685	-13.300360
84	0.010006	0.189736	124	-7.017143	-13.728420
85	-0.015635	0.189356	125	-7.283600	-14.151244
86	-0.040991	0.185526	126	-7.550058	-14.569275
87	-0.065600	0.178316	127	-7.816515	-14.981080
88	-0.089015	0.167858	128	-8.082973	-15.386132
89	-0.110808	0.154343	129	-8.349431	-15.783226
90	-0.130582	0.139015	130	-8.615888	-16.171727
91	-0.147978	0.119174	131	-8.882346	-16.552714
92	-0.162678	0.098162	132	-9.148803	-16.925926
93	-0.174415	0.075362	133	-9.415261	-17.293146
94	-0.204630	-0.035177	134	-9.681718	-17.654365
95	-0.234844	-0.113760	135	-9.948176	-18.009889
96	-0.265059	-0.185658	136	-10.214634	-18.358710
97	-0.295274	-0.258779	137	-10.481091	-18.699175
98	-0.325489	-0.332065	138	-10.747549	-19.028899
99	-0.353703	-0.405373	139	-11.014006	-19.345137
100	-0.622161	-1.035854	140	-11.280464	-19.648515
101	-0.888618	-1.650458	141	-11.546921	-19.936141
102	-1.155076	-2.279519	142	-11.813379	-20.217600
103	-1.421534	-2.929341	143	-12.124296	-20.538250
104	-1.687991	-3.580829	144	-12.435213	-20.856053
105	-1.954449	-4.215464	145	-12.746130	-21.168864
106	-2.220906	-4.828067	146	-13.057047	-21.461557
107	-2.487364	-5.420620	147	-13.073580	-21.476620
108	-2.753821	-5.996426	148	-13.089826	-21.491917
109	-3.020279	-6.558016	149	-13.105788	-21.507450
110	-3.286737	-7.105743	150	-13.121464	-21.523219
111	-3.553194	-7.639485	151	-13.136899	-21.539187
112	-3.819652	-8.159539	152	-13.152147	-21.555311
113	-4.086109	-8.666309	153	-13.167048	-21.571721
114	-4.352567	-9.162197	154	-13.181604	-21.588117
115	-4.619025	-9.648285	155	-13.195814	-21.605399
116	-4.885482	-10.126799	156	-13.209678	-21.622667
117	-5.151940	-10.598997	157	-13.223197	-21.640222
118	-5.418397	-11.065558	158	-13.236369	-21.658062
119	-5.684855	-11.526055	159	-13.249196	-21.676189
120	-5.951312	-11.980100	160	-13.261678	-21.694602
121	-6.217770	-12.426934	161	-13.273813	-21.713301
122	-6.484227	-12.867117	162.	-13.285603	-21.732286

Stage 1 Vane Lut Airfoil Coordinates (10X), inches

Radius = 14.400 inches

SUCTION SURFACE COORDINATES

PT.	X	Y	PT.	X	Y
1	-5.140494	-0.136228	42	0.350044	2.999538
2	-5.235531	0.004528	43	0.565623	2.855710
3	-5.288572	0.147249	44	0.781202	2.696068
4	-5.314007	0.291261	45	0.996781	2.512956
5	-5.318106	0.436272	46	1.212360	2.311299
6	-5.316315	0.476823	47	1.427939	2.091152
7	-5.313033	0.521443	48	1.643518	1.852515
8	-5.308261	0.564133	49	1.859097	1.590063
9	-5.301997	0.606092	50	2.074676	1.305524
10	-5.294261	0.649721	51	2.290255	0.999871
11	-5.285771	0.692584	52	2.505834	0.672754
12	-5.276041	0.735506	53	2.721413	0.323088
13	-5.265070	0.778486	54	2.936992	-0.046462
14	-5.252859	0.821524	55	3.152570	-0.438297
15	-5.239587	0.864611	56	3.368149	-0.847570
16	-5.225306	0.907746	57	3.583728	-1.274374
17	-5.209908	0.950933	58	3.799307	-1.720078
18	-5.193394	0.994172	59	4.014886	-2.184684
19	-4.883430	1.611906	60	4.230465	-2.657629
20	-4.577465	2.045373	61	4.446044	-3.142337
21	-4.260501	2.387461	62	4.661623	-3.640508
22	-3.961536	2.660682	63	4.877202	-4.147542
23	-3.745957	2.838360	64	5.092781	-4.659508
24	-3.530378	2.987761	65	5.303360	-5.180191
25	-3.314799	3.115315	66	5.419168	-5.450856
26	-3.099220	3.227980	67	5.522975	-5.722041
27	-2.883641	3.324920	68	5.640783	-5.994916
28	-2.668062	3.404873	69	5.751591	-6.269482
29	-2.452483	3.471350	70	5.852398	-6.545557
30	-2.236904	3.523150	71	5.973206	-6.823128
31	-2.021325	3.560004	72	5.980948	-6.847085
32	-1.805746	3.582818	73	5.985454	-6.871856
33	-1.590167	3.591323	74	5.996646	-6.897006
34	-1.374568	3.585334	75	5.994502	-6.922092
35	-1.159009	3.564828	76	5.979059	-6.946674
36	-0.943430	3.529704	77	5.970414	-6.970321
37	-0.727851	3.479757	78	5.958719	-6.992617
38	-0.512272	3.415095	79	5.944178	-7.013171
39	-0.296693	3.335719	80	5.927047	-7.031622
40	-0.081114	3.239758	81	5.907626	-7.047846
41	0.134465	3.127555	82	5.886258	-7.060961

PRESSURE SURFACE COORDINATES

PT.	X	Y	PT.	X	Y
83	5.863318	-7.071335	123	0.134465	-1.349190
84	5.839205	-7.078583	124	-0.081114	-1.251061
85	5.814346	-7.082580	125	-0.296693	-1.158585
86	5.789178	-7.083255	126	-0.512272	-1.071701
87	5.764141	-7.080596	127	-0.727851	-0.991252
88	5.739676	-7.074650	128	-0.943430	-0.916014
89	5.716211	-7.065322	129	-1.159009	-0.845899
90	5.694160	-7.053371	130	-1.374588	-0.780907
91	5.673909	-7.038411	131	-1.590167	-0.721428
92	5.655813	-7.020905	132	-1.805746	-0.666977
93	5.640192	-7.001159	133	-2.021325	-0.617297
94	5.584886	-6.920846	134	-2.236904	-0.572388
95	5.529581	-6.840478	135	-2.452483	-0.532193
96	5.474276	-6.760055	136	-2.668062	-0.496796
97	5.418971	-6.679577	137	-2.883641	-0.466239
98	5.363666	-6.599045	138	-3.099220	-0.440101
99	5.308360	-6.518458	139	-3.314799	-0.419018
100	5.092781	-6.203495	140	-3.530378	-0.403847
101	4.877202	-5.885720	141	-3.745957	-0.395535
102	4.661623	-5.571445	142	-3.961536	-0.390059
103	4.446044	-5.257657	143	-4.110301	-0.388217
104	4.230465	-4.952578	144	-4.259065	-0.386940
105	4.014886	-4.654459	145	-4.407830	-0.387540
106	3.799307	-4.368324	146	-4.556594	-0.383620
107	3.583728	-4.096248	147	-4.596512	-0.382221
108	3.368149	-3.836775	148	-4.635750	-0.379212
109	3.152570	-3.590719	149	-4.674309	-0.374501
110	2.936992	-3.358080	150	-4.712189	-0.368386
111	2.721413	-3.141272	151	-4.749390	-0.360569
112	2.505834	-2.936096	152	-4.785912	-0.351149
113	2.290255	-2.742198	153	-4.821755	-0.340126
114	2.074676	-2.561894	154	-4.857102	-0.327934
115	1.859097	-2.393143	155	-4.891843	-0.314311
116	1.643518	-2.233014	156	-4.925771	-0.298769
117	1.427939	-2.081508	157	-4.958096	-0.281308
118	1.212360	-1.940656	158	-4.991187	-0.261928
119	0.996781	-1.808611	159	-5.022676	-0.240628
120	0.781202	-1.633253	160	-5.053350	-0.217408
121	0.565623	-1.564582	161	-5.083212	-0.192268
122	0.350044	-1.452951	162	-5.112260	-0.165208

Stage 1 Blade Airfoil Coordinates (10X), inches

Radius = 12.731 inches

SUCTION SURFACE COORDINATES

PT.	X	Y	PT.	X	Y
1	-5.258417	0.595922	42	0.209663	2.944553
2	-5.362502	0.732809	43	0.425295	2.762122
3	-5.424432	0.875621	44	0.640928	2.562310
4	-5.453530	1.023049	45	0.856560	2.345131
5	-5.461378	1.173464	46	1.072193	2.110587
6	-5.460690	1.202943	47	1.287826	1.857761
7	-5.453219	1.232332	48	1.503458	1.583543
8	-5.456966	1.262232	49	1.719091	1.290372
9	-5.453931	1.292041	50	1.934723	0.978248
10	-5.450113	1.321960	51	2.150356	0.647108
11	-5.445526	1.351908	52	2.365988	0.236878
12	-5.440407	1.382090	53	2.581621	-0.072373
13	-5.434587	1.412291	54	2.797253	-0.460647
14	-5.428040	1.442593	55	3.012886	-0.867944
15	-5.420768	1.472098	56	3.228518	-1.292444
16	-5.412774	1.503505	57	3.444151	-1.733800
17	-5.404057	1.534113	58	3.659784	-2.193045
18	-5.394617	1.564822	59	3.875416	-2.670177
19	-5.071709	2.263659	60	4.091048	-3.161523
20	-4.748802	2.699115	61	4.306681	-3.665605
21	-4.425895	3.016525	62	4.522314	-4.184704
22	-4.102988	3.263797	63	4.737946	-4.710820
23	-3.887256	3.410319	64	4.953579	-5.264392
24	-3.671723	3.520609	65	5.169212	-5.819520
25	-3.456090	3.622144	66	5.280407	-6.110355
26	-3.240458	3.704931	67	5.391602	-6.404372
27	-3.024825	3.768971	68	5.502797	-6.701495
28	-2.809193	3.814263	69	5.613993	-7.000143
29	-2.593560	3.849164	70	5.725188	-7.301449
30	-2.377928	3.860733	71	5.836383	-7.605278
31	-2.162295	3.872860	72	5.843391	-7.623331
32	-1.946663	3.861596	73	5.847174	-7.634097
33	-1.731030	3.837266	74	5.847665	-7.679146
34	-1.515398	3.798313	75	5.844856	-7.704042
35	-1.299765	3.744836	76	5.838795	-7.728351
36	-1.084132	3.676336	77	5.829589	-7.751652
37	-0.868500	3.593346	78	5.817397	-7.773539
38	-0.652867	3.494012	79	5.802432	-7.793632
39	-0.437235	3.379467	80	5.784953	-7.811581
40	-0.221602	3.249708	81	5.765264	-7.027074
41	-0.005970	3.104737	82	5.743708	-7.839841

PRESSURE SURFACE COORDINATES

PT.	X	Y	PT.	X	Y
83	5.720659	-7.849662	123	-0.005970	-0.882253
84	5.696519	-7.856364	124	-0.221602	-0.727541
85	5.671706	-7.859832	125	-0.437235	-0.583097
86	5.646653	-7.860006	126	-0.652867	-0.448236
87	5.621795	-7.856381	127	-0.868500	-0.322566
88	5.597565	-7.850513	128	-1.084132	-0.206086
89	5.574382	-7.841012	129	-1.299765	-0.098798
90	5.552652	-7.828543	130	-1.515398	-0.000636
91	5.532751	-7.813324	131	-1.731030	0.088297
92	5.515025	-7.795619	132	-1.946663	0.167995
93	5.499783	-7.775735	133	-2.162295	0.238459
94	5.444688	-7.695087	134	-2.377928	0.300747
95	5.389593	-7.614277	135	-2.593560	0.353020
96	5.334497	-7.533303	136	-2.809193	0.395269
97	5.279402	-7.452166	137	-3.024825	0.426958
98	5.224307	-7.370865	138	-3.240458	0.448204
99	5.169212	-7.289402	139	-3.456090	0.460653
100	4.953579	-6.969002	140	-3.671723	0.462461
101	4.737946	-6.639338	141	-3.887256	0.449740
102	4.522314	-6.311225	142	-4.102988	0.441592
103	4.306681	-5.986125	143	-4.254770	0.430420
104	4.091049	-5.662287	144	-4.403552	0.419302
105	3.875416	-5.334372	145	-4.558334	0.411957
106	3.659784	-5.014036	146	-4.710117	0.411722
107	3.444151	-4.701281	147	-4.746189	0.411187
108	3.228518	-4.396105	148	-4.781807	0.412007
109	3.012886	-4.096510	149	-4.816969	0.414182
110	2.797253	-3.803307	150	-4.851677	0.417711
111	2.581621	-3.518313	151	-4.865929	0.422595
112	2.365988	-3.243968	152	-4.919726	0.428833
113	2.150356	-2.979030	153	-4.953143	0.436204
114	1.934723	-2.724040	154	-4.986322	0.444283
115	1.719091	-2.478352	155	-5.018912	0.454118
116	1.503459	-2.243226	156	-5.050912	0.465702
117	1.287826	-2.018080	157	-5.082324	0.479043
118	1.072193	-1.803116	158	-5.113146	0.494130
119	0.856560	-1.598334	159	-5.143378	0.510937
120	0.640928	-1.404265	160	-5.173022	0.529590
121	0.425295	-1.220625	161	-5.202076	0.549347
122	0.209663	-1.046615	162	-5.230541	0.572057

Stage 1 Blade Airfoil Coordinates (10X), inches

Radius = 13.571 inches

SUCTION SURFACE COORDINATES

PT.	X	Y	PT.	X	Y
1	-5.376128	1.735771	42	0.209051	2.557211
2	-5.419189	1.819716	43	0.424619	2.327819
3	-5.444962	1.903916	44	0.640187	2.082685
4	-5.457868	1.988305	45	0.855756	1.822852
5	-5.458817	2.072871	46	1.071324	1.547878
6	-5.457612	2.098560	47	1.286892	1.257761
7	-5.455537	2.124252	48	1.502460	0.954075
8	-5.452590	2.149977	49	1.718028	0.635371
9	-5.448772	2.175704	50	1.933597	0.304430
10	-5.444083	2.201445	51	2.149165	-0.040164
11	-5.438816	2.227194	52	2.364733	-0.398100
12	-5.433217	2.252948	53	2.580301	-0.769420
13	-5.426970	2.278711	54	2.795870	-1.153888
14	-5.420077	2.304484	55	3.011438	-1.551531
15	-5.412536	2.330267	56	3.227006	-1.952401
16	-5.404347	2.356059	57	3.442574	-2.386500
17	-5.395511	2.381860	58	3.658143	-2.822582
18	-5.386028	2.407671	59	3.873711	-3.271117
19	-5.065100	3.003115	60	4.089279	-3.732268
20	-4.744171	3.364969	61	4.304847	-4.204363
21	-4.423243	3.625078	62	4.520416	-4.685155
22	-4.102314	3.816893	63	4.735984	-5.176440
23	-3.886746	3.916130	64	4.951552	-5.675100
24	-3.671178	3.993459	65	5.167120	-6.170048
25	-3.455609	4.047932	66	5.277646	-6.438441
26	-3.240041	4.087191	67	5.388171	-6.700576
27	-3.024473	4.107821	68	5.498696	-6.961215
28	-2.808205	4.112199	69	5.609221	-7.222266
29	-2.593336	4.100811	70	5.719746	-7.403594
30	-2.377768	4.074163	71	5.830272	-7.744029
31	-2.162200	4.032432	72	5.838549	-7.767797
32	-1.946632	3.975567	73	5.843612	-7.792451
33	-1.731063	3.903395	74	5.845372	-7.817558
34	-1.515495	3.817240	75	5.843798	-7.842677
35	-1.299927	3.715301	76	5.838918	-7.867368
36	-1.084359	3.597363	77	5.830817	-7.891197
37	-0.868790	3.464687	78	5.819638	-7.913748
38	-0.653222	3.315426	79	5.805577	-7.934620
39	-0.437654	3.150271	80	5.788879	-7.953452
40	-0.222086	2.968748	81	5.769839	-7.969912
41	-0.006517	2.770965	82	5.748791	-7.983711

PRESSURE SURFACE COORDINATES-

PT.	X	Y	PT.	X	Y
83	5.726103	-7.994607	123	-0.006517	-0.818394
84	5.702175	-8.002408	124	-0.222086	-0.620959
85	5.677425	-8.006079	125	-0.437654	-0.433645
86	5.652288	-8.008238	126	-0.653222	-0.257197
87	5.627205	-8.006163	127	-0.868790	-0.090481
88	5.602617	-8.000792	128	-1.084359	0.067171
89	5.578954	-7.992217	129	-1.299927	0.215036
90	5.556632	-7.980590	130	-1.515495	0.354287
91	5.536043	-7.966115	131	-1.731063	0.485353
92	5.517548	-7.949046	132	-1.946632	0.608181
93	5.501471	-7.929531	133	-2.162200	0.722075
94	5.445746	-7.853540	134	-2.377768	0.823832
95	5.390021	-7.777167	135	-2.593336	0.928748
96	5.334296	-7.700364	136	-2.808205	1.018618
97	5.278571	-7.623729	137	-3.024473	1.100200
98	5.222845	-7.546664	138	-3.240041	1.171869
99	5.167120	-7.469235	139	-3.455609	1.233337
100	4.951552	-7.167141	140	-3.671178	1.284537
101	4.735984	-6.863098	141	-3.886746	1.324955
102	4.520416	-6.555766	142	-4.102314	1.356271
103	4.304847	-6.247874	143	-4.307968	1.378316
104	4.089279	-5.939367	144	-4.513621	1.397185
105	3.873711	-5.630760	145	-4.719275	1.419802
106	3.658143	-5.324674	146	-4.924928	1.456071
107	3.442574	-5.020116	147	-4.957138	1.463380
108	3.227006	-4.718708	148	-4.988385	1.471757
109	3.011438	-4.421555	149	-5.019571	1.481201
110	2.795870	-4.123118	150	-5.049795	1.491714
111	2.580301	-3.839236	151	-5.079358	1.503295
112	2.364733	-3.554675	152	-5.108256	1.515943
113	2.149165	-3.274924	153	-5.136781	1.529198
114	1.933597	-2.999237	154	-5.164559	1.543652
115	1.718028	-2.728444	155	-5.191521	1.559427
116	1.502460	-2.464199	156	-5.217665	1.576520
117	1.286692	-2.205724	157	-5.242993	1.594931
118	1.071324	-1.952504	158	-5.267710	1.614327
119	0.855756	-1.708065	159	-5.291570	1.635104
120	0.640187	-1.472406	160	-5.314342	1.657637
121	0.424619	-1.244237	161	-5.336026	1.681926
122	0.209051	-1.026171	162	-5.358621	1.707971

Stage 1 Blade Airfoil Coordinates (10X) ,inches

Radius = 14.410 inches

SUCTION SURFACE COORDINATES

PT.	X	Y	PT.	X	Y
1	-17.502286	-15.266567	42	-8.488698	-17.634830
2	-17.525151	-15.353746	43	-8.142224	-17.351857
3	-17.539410	-15.437642	44	-7.795750	-17.038839
4	-17.546352	-15.518746	45	-7.449276	-16.687872
5	-17.546522	-15.597267	46	-7.102802	-16.304417
6	-17.537134	-15.709865	47	-6.756328	-15.886059
7	-17.516626	-15.818222	48	-6.409853	-15.428842
8	-17.487207	-15.923178	49	-6.063379	-14.935334
9	-17.449637	-16.025025	50	-5.716905	-14.405536
10	-17.405806	-16.124483	51	-5.370431	-13.840060
11	-17.355507	-16.221474	52	-5.023957	-13.239672
12	-17.301112	-16.316902	53	-4.677482	-12.603793
13	-17.241548	-16.410358	54	-4.331008	-11.934453
14	-17.178446	-16 502465	55	-3.984534	-11.230807
15	-17.112138	-16.593348	56	-3.638060	-10.492685
16	-17.042107	-16.682811	57	-3.291586	-9.709340
17	-16.969785	-16.771400	58	-2.945111	-8.886272
18	-16.894786	-16.858968	59	-2.598637	-8.020456
19	-16.525635	-17.247974	60	-2.252163	-7.109666
20	-16.156484	-17.573762	61	-1.905689	-6.155534
21	-15.787332	-17.861675	62	-1.559215	-5.177572
22	-15.418181	-18.103673	63	-1.212740	-4.170307
23	-15.071707	-18.311940	64	-0.866266	-3.133559
24	-14.725233	-18.478802	65	-0.519792	-2.111373
25	-14.378759	-18.620065	66	-0.403208	-1.765829
26	-14.032284	-18.742450	67	-0.286623	-1.419485
27	-13.685810	-18.839960	68	-0.170039	-1.077831
28	-13.339336	-18.912598	69	-0.053433	-0.737906
29	-12.992862	-18.965003	70	0.063130	-0.399185
30	-12.646388	-18.999082	71	0.179714	-0.061668
31	-12.299914	-19.010831	72	0.186383	-0.036899
32	-11.953440	-19.001052	73	0.189954	-0.011459
33	-11.606966	-18.969866	74	0.189469	0.014191
34	-11.260491	-18.917229	75	0.185831	0.039582
35	-10.914017	-18.843123	76	0.178806	0.064251
36	-10.567543	-18.747549	77	0.168523	0.087750
37	-10.221069	-18.626704	78	0.155168	0.109649
38	-9.874595	-18.480784	79	0.138985	0.129550
39	-9.528121	-18.311132	80	0.120269	0.147090
40	-9.181647	-18.117020	81	0.099331	0.161949
41	-8.835173	-17.889885	82	0.076042	0.173856

PRESSURE SURFACE COORDINATES

PT.	X	Y	PT.	X	Y
83	0.052528	0.182595	123	-8.835173	-11.409414
84	0.027453	0.188006	124	-9.181647	-11.665326
85	0.001880	0.189991	125	-9.528121	-11.904488
86	-0.023728	0.188513	126	-9.874595	-12.130353
87	-0.048903	0.183599	127	-10.221069	-12.342922
88	-0.073187	0.175339	128	-10.567543	-12.542196
89	-0.096137	0.163883	129	-10.914017	-12.723703
90	-0.117335	0.149441	130	-11.260491	-12.891407
91	-0.136394	0.132275	131	-11.606966	-13.049002
92	-0.152968	0.112698	132	-11.953440	-13.196489
93	-0.166754	0.091067	133	-12.299914	-13.333866
94	-0.225593	-0.016163	134	-12.646388	-13.458653
95	-0.284433	-0.123039	135	-12.992862	-13.569469
96	-0.343273	-0.229560	136	-13.339336	-13.674003
97	-0.402112	-0.335725	137	-13.685810	-13.772254
98	-0.460952	-0.441535	138	-14.032284	-13.864224
99	-0.519792	-0.546990	139	-14.378759	-13.947671
100	-0.866266	-1.160747	140	-14.725233	-14.024230
101	-1.212740	-1.762187	141	-15.071707	-14.098371
102	-1.559215	-2.352213	142	-15.418181	-14.170095
103	-1.905689	-2.929692	143	-15.599907	-14.206748
104	-2.252163	-3.494042	144	-15.781633	-14.242736
105	-2.598637	-4.045262	145	-15.963360	-14.278533
106	-2.945111	-4.585359	146	-16.145086	-14.315067
107	-3.291586	-5.111746	147	-16.247406	-14.338966
108	-3.638060	-5.623073	148	-16.347266	-14.366373
109	-3.984534	-6.119340	149	-16.444214	-14.397936
110	-4.331008	-6.602919	150	-16.539190	-14.432309
111	-4.677482	-7.070647	151	-16.632296	-14.469351
112	-5.023957	-7.522045	152	-16.723546	-14.509039
113	-5.370431	-7.957115	153	-16.812566	-14.551909
114	-5.716905	-8.375856	154	-16.900150	-14.596828
115	-6.063379	-8.770202	155	-16.984401	-14.646499
116	-6.409853	-9.164223	156	-17.065469	-14.700712
117	-6.756328	-9.533962	157	-17.143003	-14.758681
118	-7.102802	-9.887418	158	-17.217556	-14.823471
119	-7.449276	-10.224593	159	-17.287515	-14.893529
120	-7.795750	-10.544296	160	-17.351580	-14.971994
121	-8.142224	-10.848031	161	-17.409513	-15.059205
122	-8.488698	-11.136403	162	-17.460337	-15.156556

Stage 2 Vane Airfoil Coordinates (10X), inches

Radius = 12.290 inches

SUCTION SURFACE COORDINATES

PT.	X	Y	PT.	X	Y
1	-18.482700	-15.642400	42	-8.701757	-17.851505
2	-18.515603	-15.734322	43	-8.324820	-17.515865
3	-18.538097	-15.823651	44	-7.947882	-17.149190
4	-18.551014	-15.910597	45	-7.570945	-16.749287
5	-18.557187	-15.995862	46	-7.194008	-16.317750
6	-18.556556	-16.097007	47	-6.817070	-15.853871
7	-18.548003	-16.196179	48	-6.440133	-15.356081
8	-18.531551	-16.293385	49	-6.063195	-14.825396
9	-18.508627	-16.388978	50	-5.686258	-14.258728
10	-18.479333	-16.482986	51	-5.309321	-13.656664
11	-18.444482	-16.575610	52	-4.932383	-13.014526
12	-18.405045	-16.667092	53	-4.555446	-12.331770
13	-18.361280	-16.757496	54	-4.178509	-11.608601
14	-18.314256	-16.847089	55	-3.801571	-10.837677
15	-18.263915	-16.935855	56	-3.424634	-10.022544
16	-18.210895	-17.023955	57	-3.047696	-9.160843
17	-18.154751	-17.111277	58	-2.670759	-8.252621
18	-18.095400	-17.197800	59	-2.293822	-7.300721
19	-17.631676	-17.767897	60	-1.916884	-6.305382
20	-17.167953	-18.224562	61	-1.539947	-5.276666
21	-16.704229	-18.594451	62	-1.163009	-4.213700
22	-16.240505	-18.895605	63	-0.786072	-3.134179
23	-15.863568	-19.109602	64	-0.409135	-2.040186
24	-15.486631	-19.275544	65	-0.032197	-0.946143
25	-15.109693	-19.413484	66	0.094719	-0.579514
26	-14.732756	-19.525151	67	0.221635	-0.212936
27	-14.355818	-19.606339	68	0.348551	0.153272
28	-13.978881	-19.663440	69	0.475467	0.515956
29	-13.601943	-19.696692	70	0.602384	0.877366
30	-13.225006	-19.704287	71	0.729300	1.237500
31	-12.848069	-19.688639	72	0.736202	1.262525
32	-12.471131	-19.649384	73	0.739628	1.288258
33	-12.094194	-19.586088	74	0.739515	1.314217
34	-11.717257	-19.498158	75	0.735864	1.339919
35	-11.340319	-19.385374	76	0.728744	1.364883
36	-10.963382	-19.248029	77	0.718287	1.388643
37	-10.586444	-19.086123	78	0.704689	1.410757
38	-10.209507	-18.895253	79	0.688204	1.430810
39	-9.832569	-18.677151	80	0.669139	1.448429
40	-9.455632	-18.432303	81	0.647851	1.463285
41	-9.078695	-18.157566	82	0.624736	1.475101

PRESSURE SURFACE COORDINATES

PT.	X	Y	PT.	X	Y
83	0.600227	1.483655	123	-9.078695	-11.497548
84	0.574780	1.488789	124	-9.455632	-11.793264
85	0.548871	1.490406	125	-9.832569	-12.071554
86	0.522983	1.488476	126	-10.209507	-12.332944
87	0.497600	1.483036	127	-10.586444	-12.579202
88	0.473195	1.474186	128	-10.963382	-12.810327
89	0.450225	1.462093	129	-11.340319	-13.023597
90	0.429117	1.446981	130	-11.717257	-13.222889
91	0.410266	1.429133	131	-12.094194	-13.409249
92	0.394024	1.408082	132	-12.471131	-13.582679
93	0.380694	1.385606	133	-12.848069	-13.739650
94	0.311880	1.266923	134	-13.225006	-13.885326
95	0.243064	1.146729	135	-13.601943	-14.020855
96	0.174249	1.026026	136	-13.978881	-14.146238
97	0.105433	0.904814	137	-14.355818	-14.258666
98	0.036618	0.783094	138	-14.732756	-14.362879
99	-0.032197	0.660864	139	-15.109693	-14.459633
100	-0.409135	-0.032685	140	-15.486631	-14.548167
101	-0.786072	-0.710064	141	-15.863568	-14.630019
102	-1.163009	-1.366455	142	-16.240505	-14.706399
103	-1.539947	-2.007922	143	-16.414954	-14.739897
104	-1.916884	-2.634535	144	-16.589403	-14.772221
105	-2.293822	-3.246644	145	-16.763851	-14.803447
106	-2.670759	-3.843472	146	-16.938300	-14.833600
107	-3.047696	-4.425017	147	-17.044501	-14.851859
108	-3.424634	-4.991764	148	-17.150361	-14.870788
109	-3.801571	-5.544775	149	-17.255439	-14.891171
110	-4.178509	-6.081068	150	-17.359932	-14.912689
111	-4.555446	-6.600644	151	-17.463261	-14.936434
112	-4.932383	-7.103512	152	-17.564551	-14.964068
113	-5.309321	-7.591029	153	-17.663804	-14.995594
114	-5.686258	-8.060935	154	-17.761914	-15.029302
115	-6.063195	-8.513229	155	-17.857064	-15.068661
116	-6.440133	-8.947912	156	-17.949360	-15.113471
117	-6.817070	-9.364666	157	-18.039478	-15.162440
118	-7.194008	-9.763973	158	-18.125406	-15.219408
119	-7.570945	-10.145871	159	-18.207291	-15.284098
120	-7.947882	-10.510359	160	-18.285639	-15.355542
121	-8.324820	-10.856537	161	-18.358059	-15.438304
122	-8.701757	-11.185306	162	-18.424829	-15.531857

Stage 2 Vane Airfoil Coordinates (10X), inches

Radius = 13.635 inches

SUCTION SURFACE COORDINATES

PT.	X	Y	PT.	X	Y
1	-19.567800	-16.203500	42	-8.928748	-18.385532
2	-19.570087	-16.250330	43	-8.520761	-18.033902
3	-19.586001	-16.296307	44	-8.112773	-17.649821
4	-19.591541	-16.341430	45	-7.704786	-17.231427
5	-19.594708	-16.385700	46	-7.296798	-16.779721
6	-19.594650	-16.494176	47	-6.888811	-16.292898
7	-19.583952	-16.598827	48	-6.480823	-15.770463
8	-19.563851	-16.700095	49	-6.072836	-15.213049
9	-19.536073	-16.798603	50	-5.664848	-14.613460
10	-19.501562	-16.894689	51	-5.256861	-13.974031
11	-19.461423	-16.988751	52	-4.848873	-13.290217
12	-19.415108	-17.080592	53	-4.440885	-12.556676
13	-19.365211	-17.171145	54	-4.032898	-11.770082
14	-19.311023	-17.260155	55	-3.624910	-10.924921
15	-19.253285	-17.347888	56	-3.216923	-10.022179
16	-19.192545	-17.434541	57	-2.808935	-9.057752
17	-19.129329	-17.520304	58	-2.400948	-8.036089
18	-19.063700	-17.605200	59	-1.992960	-6.967292
19	-18.569000	-18.171791	60	-1.584973	-5.856587
20	-18.076100	-18.639942	61	-1.176985	-4.719135
21	-17.582299	-19.029839	62	-0.768998	-3.558898
22	-17.088499	-19.351600	63	-0.361010	-2.383907
23	-16.680512	-19.580042	64	0.046977	-1.192198
24	-16.272524	-19.767903	65	0.454965	0.014707
25	-15.864537	-19.925330	66	0.592737	0.427766
26	-15.456549	-20.048942	67	0.730510	0.843910
27	-15.048561	-20.145141	68	0.868282	1.262717
28	-14.640574	-20.215036	69	1.006055	1.684289
29	-14.232586	-20.256395	70	1.143828	2.111439
30	-13.824599	-20.273314	71	1.281600	2.542500
31	-13.416611	-20.264933	72	1.287690	2.567419
32	-13.008624	-20.230675	73	1.290367	2.592931
33	-12.600636	-20.170722	74	1.289584	2.618571
34	-12.192649	-20.085192	75	1.285353	2.643871
35	-11.784661	-19.973965	76	1.277754	2.668372
36	-11.376674	-19.834329	77	1.266923	2.691625
37	-10.968686	-19.667284	78	1.253059	2.713208
38	-10.560699	-19.472065	79	1.236414	2.732726
39	-10.152711	-19.246569	80	1.217291	2.749825
40	-9.744723	-18.990630	81	1.196040	2.764191
41	-9.336736	-18.705048	82	1.173047	2.775564

PRESSURE SURFACE COORDINATES

PT.	X	Y	PT.	X	Y
83	1.148731	2.783736	123	-9.336736	-11.381916
84	1.123537	2.788559	124	-9.744723	-11.705280
85	1.097922	2.789944	125	-10.152711	-12.010718
86	1.072354	2.787865	126	-10.560699	-12.296585
87	1.047300	2.782362	127	-10.968686	-12.564932
88	1.023215	2.773533	128	-11.376674	-12.817161
89	1.000539	2.761541	129	-11.784661	-13.053188
90	0.979604	2.746604	130	-12.192649	-13.270273
91	0.961032	2.728994	131	-12.600636	-13.473947
92	0.944922	2.709032	132	-13.008624	-13.664209
93	0.931648	2.687001	133	-13.416611	-13.837556
94	0.852201	2.531913	134	-13.824599	-13.999863
95	0.772754	2.377626	135	-14.232586	-14.152126
96	0.693307	2.224224	136	-14.640574	-14.292107
97	0.613859	2.071706	137	-15.048561	-14.422072
98	0.534412	1.920071	138	-15.456549	-14.545034
99	0.454965	1.769321	139	-15.864537	-14.660863
100	0.046977	1.009095	140	-16.272524	-14.768043
101	-0.361010	0.276338	141	-16.680512	-14.869944
102	-0.768998	-0.435687	142	-17.088499	-14.966865
103	-1.176985	-1.128941	143	-17.279449	-15.009976
104	-1.584973	-1.799380	144	-17.470400	-15.052228
105	-1.992960	-2.450736	145	-17.661350	-15.093357
106	-2.400948	-3.087075	146	-17.852300	-15.133600
107	-2.808935	-3.708397	147	-17.976172	-15.159720
108	-3.216923	-4.315218	148	-18.099564	-15.186611
109	-3.624910	-4.909535	149	-18.221671	-15.215561
110	-4.032098	-5.486831	150	-18.343099	-15.245599
111	-4.440885	-6.047045	151	-18.462408	-15.278941
112	-4.848873	-6.590199	152	-18.579084	-15.316695
113	-5.256861	-7.118555	153	-18.693597	-15.357822
114	-5.664848	-7.628742	154	-18.805592	-15.403082
115	-6.072836	-8.120405	155	-18.913307	-15.455014
116	-6.480023	-8.593540	156	-19.017068	-15.512097
117	-6.888811	-9.048581	157	-19.117992	-15.576296
118	-7.296798	-9.485165	158	-19.212117	-15.650113
119	-7.704786	-9.902830	159	-19.301509	-15.731520
120	-8.112773	-10.301574	160	-19.382975	-15.825635
121	-8.520761	-10.681398	161	-19.456476	-15.932520
122	-8.928748	-11.040625	162	-19.519306	-16.056517

Stage 2 Vane Airfoil Coordinates (10X), inches

Radius = 14.980 inches

SUCTION SURFACE COORDINATES

PT.	X	Y	PT.	X	Y
1	-6.373520	0.656610	42	0.226345	2.645723
2	-6.414879	0.727896	43	0.481247	2.475633
3	-6.442473	0.800475	44	0.736148	2.290310
4	-6.456304	0.874346	45	0.991050	2.090005
5	-6.456372	0.949510	46	1.245951	1.874898
6	-6.455779	0.965035	47	1.500852	1.644987
7	-6.454767	0.980600	48	1.755754	1.400274
8	-6.453339	0.996203	49	2.010655	1.139037
9	-6.451492	1.011046	50	2.265557	0.862364
10	-6.449227	1.027529	51	2.520458	0.570282
11	-6.446545	1.043250	52	2.775360	0.262793
12	-6.443504	1.059005	53	3.030261	-0.060118
13	-6.440409	1.074765	54	3.285162	-0.398527
14	-6.437000	1.090555	55	3.540064	-0.752378
15	-6.433276	1.106374	56	3.794965	-1.121671
16	-6.429239	1.122223	57	4.049867	-1.506292
17	-6.424887	1.138101	58	4.304768	-1.904451
18	-6.420221	1.154010	59	4.559670	-2.317284
19	-6.033086	1.950528	60	4.814571	-2.744788
20	-5.645952	2.405939	61	5.069473	-3.185327
21	-5.258818	2.737119	62	5.324374	-3.637634
22	-4.871684	2.991866	63	5.579276	-4.102980
23	-4.616782	3.130929	64	5.834177	-4.578264
24	-4.361081	3.243881	65	6.089079	-5.063022
25	-4.106979	3.340856	66	6.193746	-5.265103
26	-3.852078	3.418477	67	6.298412	-5.468063
27	-3.597176	3.479244	68	6.403079	-5.672276
28	-3.342275	3.526128	69	6.507746	-5.877902
29	-3.087373	3.557012	70	6.612413	-6.084940
30	-2.832472	3.572404	71	6.717079	-6.293390
31	-2.577570	3.574120	72	6.732951	-6.331044
32	-2.322669	3.561043	73	6.743732	-6.370459
33	-2.067768	3.533752	74	6.749235	-6.410949
34	-1.812866	3.492077	75	6.749365	-6.451811
35	-1.557965	3.435990	76	6.744120	-6.492336
36	-1.303063	3.365727	77	6.733590	-6.531818
37	-1.048162	3.281387	78	6.717958	-6.569572
38	-0.793260	3.182841	79	6.697496	-6.604943
39	-0.538359	3.070090	80	6.672560	-6.637314
40	-0.283457	2.942983	81	6.643583	-6.666125
41	-0.028556	2.801506	82	6.611068	-6.690874

PRESSURE SURFACE COORDINATES

PT.	X	Y	PT.	X	Y
83	6.575580	-6.711132	123	-0.028556	-0.925081
84	6.537737	-6.726546	124	-0.283457	-0.778339
85	6.498194	-6.736848	125	-0.538359	-0.639574
86	6.457640	-6.741860	126	-0.793260	-0.508790
87	6.416780	-6.741495	127	-1.048162	-0.385986
88	6.376322	-6.735758	128	-1.303063	-0.271020
89	6.336970	-6.724751	129	-1.557965	-0.163973
90	6.299408	-6.708662	130	-1.812866	-0.065039
91	6.264208	-6.687773	131	-2.067768	0.025784
92	6.232221	-6.662447	132	-2.322669	0.108495
93	6.203764	-6.633122	133	-2.577570	0.183262
94	6.184650	-6.610863	134	-2.832472	0.250004
95	6.165536	-6.588623	135	-3.087373	0.308431
96	6.146421	-6.566402	136	-3.342275	0.358544
97	6.127307	-6.544201	137	-3.597176	0.400239
98	6.108193	-6.522018	138	-3.852078	0.432699
99	6.089079	-6.499855	139	-4.106979	0.457852
100	5.834177	-6.205447	140	-4.361881	0.475699
101	5.579276	-5.914609	141	-4.616782	0.483058
102	5.324374	-5.628561	142	-4.871684	0.489473
103	5.069473	-5.346734	143	-5.145718	0.486209
104	4.814571	-5.069946	144	-5.419752	0.482006
105	4.559670	-4.798342	145	-5.693786	0.474861
106	4.304768	-4.531923	146	-5.967821	0.472510
107	4.049867	-4.269988	147	-5.996302	0.473165
108	3.794965	-4.013144	148	-6.024223	0.475057
109	3.540064	-3.762137	149	-6.051582	0.478186
110	3.285162	-3.516966	150	-6.078379	0.482552
111	3.030261	-3.277595	151	-6.104616	0.488154
112	2.775360	-3.043033	152	-6.130291	0.494994
113	2.520458	-2.815240	153	-6.155521	0.502815
114	2.265557	-2.594216	154	-6.180402	0.511405
115	2.010655	-2.378941	155	-6.204598	0.521504
116	1.755754	-2.170684	156	-6.228110	0.533111
117	1.500852	-1.970007	157	-6.250937	0.546228
118	1.245951	-1.776909	158	-6.273079	0.560853
119	0.991050	-1.591106	159	-6.294536	0.576987
120	0.736148	-1.412693	160	-6.315309	0.594629
121	0.481247	-1.242221	161	-6.335398	0.613781
122	0.226345	-1.079683	162	-6.354801	0.634441

Stage 2 Blade Airfoil Coordinates (10X), inches

Radius = 12.25 inches

SUCTION SURFACE COORDINATES

PT.	X	Y	PT.	X	Y
1	-5.925176	2.319816	42	0.224491	2.328202
2	-5.939076	2.361600	43	0.460785	2.124270
3	-5.948961	2.402586	44	0.697079	1.906732
4	-5.954830	2.442533	45	0.933373	1.675288
5	-5.956683	2.481522	46	1.169667	1.429599
6	-5.954748	2.517438	47	1.405960	1.169468
7	-5.950666	2.552841	48	1.642254	0.894651
8	-5.945270	2.587931	49	1.878548	0.604944
9	-5.937401	2.622430	50	2.114842	0.300383
10	-5.927169	2.656366	51	2.351136	-0.019063
11	-5.914575	2.689737	52	2.587430	-0.353241
12	-5.899770	2.722582	53	2.823724	-0.702053
13	-5.883880	2.755167	54	3.060018	-1.065235
14	-5.866909	2.787494	55	3.296312	-1.442478
15	-5.848115	2.819386	56	3.532606	-1.833445
16	-5.827835	2.850923	57	3.768899	-2.237085
17	-5.806383	2.882181	58	4.005193	-2.653239
18	-5.783576	2.913116	59	4.241487	-3.079684
19	-5.463028	3.222294	60	4.477781	-3.516579
20	-5.142481	3.425484	61	4.714075	-3.961127
21	-4.821934	3.579436	62	4.950369	-4.413412
22	-4.501387	3.691915	63	5.186662	-4.871088
23	-4.265093	3.754021	64	5.422956	-5.333239
24	-4.028799	3.799048	65	5.659250	-5.798603
25	-3.792505	3.827716	66	5.736029	-5.950092
26	-3.556211	3.842382	67	5.812808	-6.101801
27	-3.319917	3.842725	68	5.889587	-6.253731
28	-3.083624	3.830023	69	5.966367	-6.405605
29	-2.847330	3.804182	70	6.043146	-6.557549
30	-2.611036	3.765039	71	6.119924	-6.709584
31	-2.374742	3.715014	72	6.131349	-6.736520
32	-2.138448	3.651878	73	6.139098	-6.764733
33	-1.902154	3.576381	74	6.143035	-6.793725
34	-1.665860	3.488540	75	6.143090	-6.822983
35	-1.429566	3.388193	76	6.139262	-6.851990
36	-1.193272	3.275830	77	6.131619	-6.880232
37	-0.956978	3.149736	78	6.120295	-6.907210
38	-0.720685	3.011400	79	6.105492	-6.932447
39	-0.484391	2.860181	80	6.087471	-6.955496
40	-0.248097	2.695974	81	6.066551	-6.975950
41	-0.011803	2.518710	82	6.043101	-6.993448

PRESSURE SURFACE COORDINATES

PT.	X	Y	PT.	X	Y
83	6.017537	-7.007679	123	-0.011803	-1.168934
84	5.990311	-7.018391	124	-0.248097	-0.979782
85	5.961904	-7.025397	125	-0.484391	-0.795591
86	5.932818	-7.028570	126	-0.720685	-0.616488
87	5.903569	-7.027857	127	-0.956978	-0.442501
88	5.874673	-7.023268	128	-1.193272	-0.273866
89	5.846641	-7.014805	129	-1.429566	-0.110076
90	5.819970	-7.002857	130	-1.665860	0.048868
91	5.795131	-6.987396	131	-1.902154	0.202723
92	5.772563	-6.968775	132	-2.138448	0.351791
93	5.752665	-6.947325	133	-2.374742	0.496353
94	5.737096	-6.928444	134	-2.611036	0.636405
95	5.721527	-6.909584	135	-2.847330	0.771950
96	5.705958	-6.890746	136	-3.083624	0.902996
97	5.690388	-6.871930	137	-3.319917	1.029611
98	5.674819	-6.853135	138	-3.556211	1.151785
99	5.659250	-6.834362	139	-3.792505	1.269242
100	5.422956	-6.552080	140	-4.028799	1.381884
101	5.186662	-6.274866	141	-4.265093	1.489913
102	4.950369	-6.002389	142	-4.501387	1.593447
103	4.714075	-5.734725	143	-4.795909	1.716203
104	4.477781	-5.471418	144	-5.090431	1.833112
105	4.241487	-5.213337	145	-5.384953	1.948747
106	4.005193	-4.959071	146	-5.679476	2.081316
107	3.768899	-4.708487	147	-5.698206	2.090939
108	3.532606	-4.461715	148	-5.716478	2.101034
109	3.296312	-4.219387	149	-5.734292	2.111601
110	3.060018	-3.980236	150	-5.751740	2.122545
111	2.823724	-3.744262	151	-5.768900	2.133785
112	2.587430	-3.511464	152	-5.785451	2.145654
113	2.351136	-3.281831	153	-5.801391	2.158151
114	2.114842	-3.055367	154	-5.816722	2.171276
115	1.878548	-2.832099	155	-5.831590	2.184878
116	1.642254	-2.612028	156	-5.846085	2.198863
117	1.405960	-2.394434	157	-5.859781	2.213672
118	1.169667	-2.180496	158	-5.872678	2.229305
119	0.933373	-1.970440	159	-5.884776	2.245760
120	0.697079	-1.763697	160	-5.896075	2.263039
121	0.460785	-1.560691	161	-5.906574	2.281141
122	0.224491	-1.362437	162	-5.916274	2.300067

Stage 2 Blade Airfoil Coordinates (10X), inches

Radius = 13.625 inches

SUCTION SURFACE COORDINATES

PT.	X	Y	PT.	X	Y
1	-5.224293	4.340588	42	0.322067	1.742200
2	-5.219653	4.358210	43	0.533990	1.473725
3	-5.214390	4.375430	44	0.745913	1.196079
4	-5.208505	4.392248	45	0.957836	0.909022
5	-5.201997	4.408664	46	1.169758	0.613330
6	-5.194865	4.424677	47	1.381681	0.308770
7	-5.187111	4.440289	48	1.593604	-0.003711
8	-5.178735	4.455499	49	1.805527	-0.324287
9	-5.169735	4.470306	50	2.017449	-0.651818
10	-5.160113	4.484712	51	2.229372	-0.986352
11	-5.149867	4.498715	52	2.441295	-1.326822
12	-5.139274	4.512494	53	2.653218	-1.673109
13	-5.128172	4.525944	54	2.865140	-2.024602
14	-5.116532	4.539047	55	3.077063	-2.381100
15	-5.104354	4.551803	56	3.288986	-2.742490
16	-5.091638	4.564212	57	3.500909	-3.108636
17	-5.078385	4.576274	58	3.712831	-3.479559
18	-5.064593	4.587988	59	3.924754	-3.855138
19	-4.777541	4.752642	60	4.136677	-4.235122
20	-4.490490	4.823709	61	4.348599	-4.619328
21	-4.203439	4.839615	62	4.560522	-5.006807
22	-3.916388	4.815120	63	4.772445	-5.397394
23	-3.704465	4.779469	64	4.984368	-5.790072
24	-3.492542	4.724647	65	5.196291	-6.184199
25	-3.280620	4.657193	66	5.282910	-6.345609
26	-3.068697	4.574927	67	5.369530	-6.507244
27	-2.856774	4.480081	68	5.456149	-6.668051
28	-2.644851	4.374569	69	5.542768	-6.830557
29	-2.432929	4.257229	70	5.629388	-6.992377
30	-2.221006	4.130118	71	5.716007	-7.154312
31	-2.009083	3.992328	72	5.729922	-7.185181
32	-1.797160	3.843801	73	5.739537	-7.217647
33	-1.585238	3.684542	74	5.744677	-7.251115
34	-1.373315	3.513976	75	5.745247	-7.284970
35	-1.161392	3.331878	76	5.741238	-7.318592
36	-0.949469	3.138200	77	5.732722	-7.351364
37	-0.737546	2.932794	78	5.719855	-7.382685
38	-0.525624	2.716057	79	5.702874	-7.411979
39	-0.313701	2.488127	80	5.682090	-7.438710
40	-0.101778	2.249678	81	5.657885	-7.462387
41	0.110145	2.000778	82	5.630702	-7.482577

PRESSURE SURFACE COORDINATES

PT.	X	Y	PT.	X	Y
83	5.601040	-7.498908	123	0.110145	-1.418499
84	5.569444	-7.511081	124	-0.101778	-1.193767
85	5.536492	-7.518872	125	-0.313701	-0.971683
86	5.502790	-7.522140	126	-0.525624	-0.750258
87	5.468955	-7.520823	127	-0.737546	-0.529425
88	5.435609	-7.514947	128	-0.949469	-0.309093
89	5.403363	-7.504618	129	-1.161392	-0.089342
90	5.372808	-7.490026	130	-1.373315	0.129616
91	5.344505	-7.471440	131	-1.585238	0.347813
92	5.318973	-7.449199	132	-1.797160	0.565200
93	5.296681	-7.423712	133	-2.009083	0.781744
94	5.279950	-7.401702	134	-2.221006	0.997167
95	5.263218	-7.379713	135	-2.432929	1.211993
96	5.246486	-7.357746	136	-2.644851	1.426308
97	5.229754	-7.335800	137	-2.856774	1.639871
98	5.213023	-7.313876	138	-3.068697	1.853161
99	5.196291	-7.291973	139	-3.280620	2.066201
100	4.984368	-7.016421	140	-3.492542	2.279328
101	4.772445	-6.744408	141	-3.704465	2.491610
102	4.560522	-6.475874	142	-3.916388	2.703046
103	4.348599	-6.210503	143	-4.227214	3.011252
104	4.136677	-5.948385	144	-4.538040	3.315042
105	3.924754	-5.689143	145	-4.848866	3.620289
106	3.712831	-5.432972	146	-5.159693	3.996580
107	3.500909	-5.179449	147	-5.170846	4.015435
108	3.288986	-4.928632	148	-5.181117	4.034448
109	3.077063	-4.680411	149	-5.190507	4.053627
110	2.865140	-4.434529	150	-5.199002	4.072974
111	2.653218	-4.191189	151	-5.206722	4.092466
112	2.441295	-3.950105	152	-5.213552	4.112126
113	2.229372	-3.711010	153	-5.219437	4.131962
114	2.017449	-3.474519	154	-5.224349	4.151982
115	1.805527	-3.239796	155	-5.228406	4.172162
116	1.593604	-3.006613	156	-5.231627	4.192499
117	1.381681	-2.774970	157	-5.233867	4.213020
118	1.169758	-2.545339	158	-5.235013	4.233747
119	0.957836	-2.317402	159	-5.235064	4.254680
120	0.745913	-2.090513	160	-5.234018	4.275848
121	0.533990	-1.864671	161	-5.231874	4.297222
122	0.322067	-1.639878	162	-5.228632	4.318802

Stage 2 Blade Airfoil Coordinates (10X), inches

Radius = 15.000 inches

APPENDIX B

Significance of the Blade-Jet Speed Ratio

The blade-jet speed ratio is defined as the ratio of the average pitch-line wheel speed, U, to the velocity, C_o, which would theoretically be obtained by expanding the turbine flow from stage inlet total enthalpy to the ideal stage exit enthalpy. This can be expressed in terms of quantities measurable directly in the rig as follows:

$$\frac{U}{C_o} = \frac{\sqrt{\sum_{i=1}^{n} r_{p,i}^2 N_i^2}}{\sqrt{2\, C_p\, T_{T,41}\left[1 - \left(\frac{P_{S,42}}{P_{T,4}}\right)^{\frac{\gamma-1}{\gamma}}\right]}} = \frac{(\text{Constant}) \times (N/\sqrt{T_{T,41}})}{\left[1 - \left(\frac{P_{S,42}}{P_{T,4}}\right)^{\frac{\gamma-1}{\gamma}}\right]^{1/2}}$$

where

i = stage indicator

n = number of stages

For a given set of turbine inlet conditions, we see that the blade-jet speed ratio is a function of pressure ratio and speed only. Consequently, once the rig has been set at the desired total-to-static pressure ratio, the second independent parameter in the test matrix, U/C_o, may be set by adjusting rig speed.

APPENDIX C

Reynolds Number Calculation

The standard expression for Reynolds number is:

$$Re = \frac{\rho\ V\ l}{\mu} \tag{C1}$$

For application to a turbine stage, ρV is replaced by W/A, where A is defined as the vane flow area, or

$$W/A = W/(n\ d_o\ h) \tag{C2}$$

where n = number of vanes

d_o = throat dimension of vanes

h = trailing edge height of vanes

Combining (C1) and C2) yields

$$Re = \frac{Wl}{\mu n\ d_o\ h} \tag{C3}$$

Defining the characteristic length, l, to be the vane throat dimension, d_o, equation (C3) reduces to

$$Re = \frac{W}{\mu\ n\ h} \tag{C4}$$

For multistage turbines, the individual stage Reynolds numbers are energy weighted. The energy averaged Reynolds numer is deined as

$$\overline{Re} = \frac{\sum_{i=1}^{n} (\Delta h)_i\ Re_i}{\sum_{i=1}^{n} (\Delta h)_i} \tag{C5}$$

where N = total number of stages

$(\Delta h)_i$ = energy extraction of i^{th} stage

Re_i = Reynolds number of i^{th} stage.

From equation (C4), observe that Reynolds number can be modulated by changing the flow, W. In order to change Reynolds number in the rig and still retain the required flow function, $W_{41}\sqrt{T_{T,41}}/P_{T,4}$, inlet total temperature was held constant while inlet total pressure was varied in direct proportion to the desired change in Reynolds number.

Table C-1 compares the Reynolds number for the rig test at 50 psia inlet pressure with those of ICLS. Included for reference is the takeoff Reynolds number.

Table C-1. Reynolds Number

	Two Stage Group
Re for Rig at $P_{T_o} = 50$	1.76×10^5
Re for ICLS at max climb	2.50×10^5
Re for ICLS at takeoff	4.66×10^5

APPENDIX D

Nozzle Efficiency Definition

Nozzle performance is expressed in terms of kinetic energy efficiency

$$\eta_v = \left(\frac{V_1}{V_{1,\ isen}} \right)^2$$

where V_1 = actual vane exit velocity

$V_{1,isen}$ = isentropic velocity at vane exit.

This can be expressed as

$$\eta_v = \frac{1 - \left(P_{S,1}/P_{T,1}\right)^{\frac{\gamma - 1}{\gamma}}}{1 - \left(P_{S,1}/P_{T,0}\right)^{\frac{\gamma - 1}{\gamma}}}$$

This equation is used to calculate performance at any radial position traversed. The overall nozzle performance is obtained by using the same basic equations for radially mass averaged parameters.

APPENDIX E

DATA TABULATIONS FOR ANNULAR CASCADE TESTS

Appendix E.

Data Tabulation For Annular Cascade Tests.

BASE VANE - COOLED

RDG	$P_{T,0}/P_{S,1}$	W_0	$T_{T,0}$	$P_{T,0}$	W_c	P_c	$T_{T,c}$	η_{PITCH}	$\eta_{OVERALL}$
2	1.628	24.602	1294.1	49.771	1.053	50.583	686.5	.9510	.9359
4	1.867	25.765	1289.8	50.029	1.073	50.738	682.9	.9460	.9335
7	1.482	26.204	1293.6	49.758	1.070	50.761	676.7	.9521	-
8	1.729	27.138	1295.5	49.983	1.069	50.746	682.4	.9518	-
9	1.795	27.211	1294.6	49.840	1.069	50.632	683.5	.9520	-
10	1.922	27.355	1291.4	49.800	1.120	50.687	677.4	.9495	-
11	2.003	27.494	1295.5	49.885	1.121	50.695	676.4	.9427	-
12	2.104	27.640	1292.1	50.033	1.127	50.785	674.4	.9402	-
15	2.508	27.642	1295.9	49.868	1.178	50.617	667.8	.9290	.9157
17	1.631	27.686	1291.1	49.869	1.071	50.721	677.3	.9532	-
18	1.629	28.042	1291.6	50.038	.764	50.158	734.0	.9543	.9358

LUT VANE - COOLED

RDG	$P_{T,0}/P_{S,1}$	W_0	$T_{T,0}$	$P_{T,0}$	W_c	P_c	$T_{T,c}$	η_{PITCH}	$\eta_{OVERALL}$
47	1.672	25.178	1291.8	50.235	.790	51.107	702.0	.9504	.9314
49	2.397	25.655	1295.6	50.020	.815	50.884	715.8	.9444	.9262
52	1.794	25.349	1281.3	49.558	.810	50.518	700.0	.9523	-
53	1.800	25.542	1287.7	49.917	.817	50.801	700.4	.9498	-
54	2.106	25.556	1291.0	49.810	.837	50.734	698.6	.9526	-
55	2.010	25.626	1288.0	49.827	.837	50.644	696.5	.9429	-
56	2.234	25.672	1278.3	49.794	.877	50.672	689.5	.9480	-
57	2.659	25.643	1285.8	49.845	.922	50.715	683.2	.9311	-
58	2.158	25.666	1284.4	49.792	.866	50.719	687.7	.9480	.9355
60	1.664	25.382	1280.0	49.927	.791	50.843	704.9	.9513	-

BASE VANE - SOLID

RDG	$P_{T,0}/P_{S,0}$	W_0	$T_{T,0}$	$P_{T,0}$	W_c	P_c	$T_{T,c}$	η_{PITCH}	$\eta_{OVERALL}$
67	1.664	25.095	1277.6	50.200	.786	50.428	765.7	.9766	.9667
69	1.660	25.235	1281.4	50.482	.904	50.629	715.3	.9757	-
70	2.427	25.482	1277.4	50.125	.989	50.383	717.6	.9590	.9451
72	2.610	25.040	1282.4	50.089	.975	50.175	721.9	.9481	-
73	2.247	25.268	1280.9	49.992	.974	50.221	722.5	.9670	-
74	2.162	25.182	1282.0	49.853	.975	50.142	724.5	.9703	-
75	2.075	25.213	1281.8	49.888	.939	50.103	728.7	.9727	-
76	1.878	25.116	1281.4	49.794	.892	49.935	735.1	.9784	-
77	1.789	25.035	1282.1	49.832	.888	49.990	738.1	.9773	-
78	1.493	24.151	1282.9	49.977	.830	50.201	747.8	.9782	-
79	1.660	24.890	1283.5	49.968	.869	50.209	744.5	.9772	-
80	1.982	25.219	1282.2	49.954	.928	50.256	736.1	.9784	.9678

BASE VANE - LAST ROW OF S.S. HOLES SEALED

85	1.661	24.848	1278.9	50.018	.966	50.801	737.8	.9585	.9445

BASE VANE - T.E. SEALED 1st TEST

93	1.670	25.018	1284.1	49.967	.810	50.630	-	.9624	-

BASE VANE - T.E. SEALED 2nd TEST

99	1.661	25.128	1274.5	49.963	.759	50.730	641.7	.9670	-

APPENDIX F

Turbine Efficiency Definitions

- GE Definition

$$\eta_{GE} = \frac{H}{W_{41} \Delta h_a}$$

- Thermodynamic Efficiency

$$\eta_{TH} = \frac{H}{W_{41} \Delta h_a + \Sigma W_c \Delta h_{a,c}}$$

- Thermodynamic Efficiency with rotor coolant pump power credited to turbine

$$\eta_{THP} = \frac{H + H'}{W_{41} \Delta h_a + \Sigma W_c \Delta h_{a,c}}$$

The coolant available energy was calculated by expanding the flow isentropically from the source pressure and temperature. In the case of rotor coolant, the source pressure was the pressure upstreat of the inducer (tangential accelerator).

The power to pump the rotor coolant from its entry on the rotor to its injection into the flowpath was calculated as:

$$H' = W_c \left[U^2_{equ} - \left(UV_u\right)_{ind} \right] \text{, Watts}$$

Since flowrate, speed, and inducer radius were known from measurements, the "equivalent" radius and tangential velocity at the inducer could be determined. The total rotor coolant flow was considered to enter the flowpath at six locations. For stage one, these were blade tip, blade pitchline, and blade hub. For stage two, blade tip, 88%, and hub were used. The total power required to pump the rotor coolant is equal to the sum of the powers to pump the six individual flows. By equating the total to the sum, an "equivalent" radius can be calculated. The "equivalent" radius was determined to be 35.194 cm (13.856 in.).

The ideal absolute velocity leaving the inducer nozzle can be calculated from the pressure ratio across the inducer and the temperature. The actual velocity was calculated assuming an efficiency of 0.90 (reasonable for small height, low aspect ratio nozzle). To calculate the tangential component, the flow angle must be determined. Using the measured inducer nozzle area and assuming a flow coefficient of 0.90, a flow angle of 72.5° was calculated.

The variation of inducer pressure ratio (inlet to exit) over the range of test conditions is presented in Figure F-1. The calculated inducer tangential velocity is shown in Figure F-2 where it is normalized by the inducer wheel speed. These tangential velocities were used in calculating the power to pump the rotor coolant.

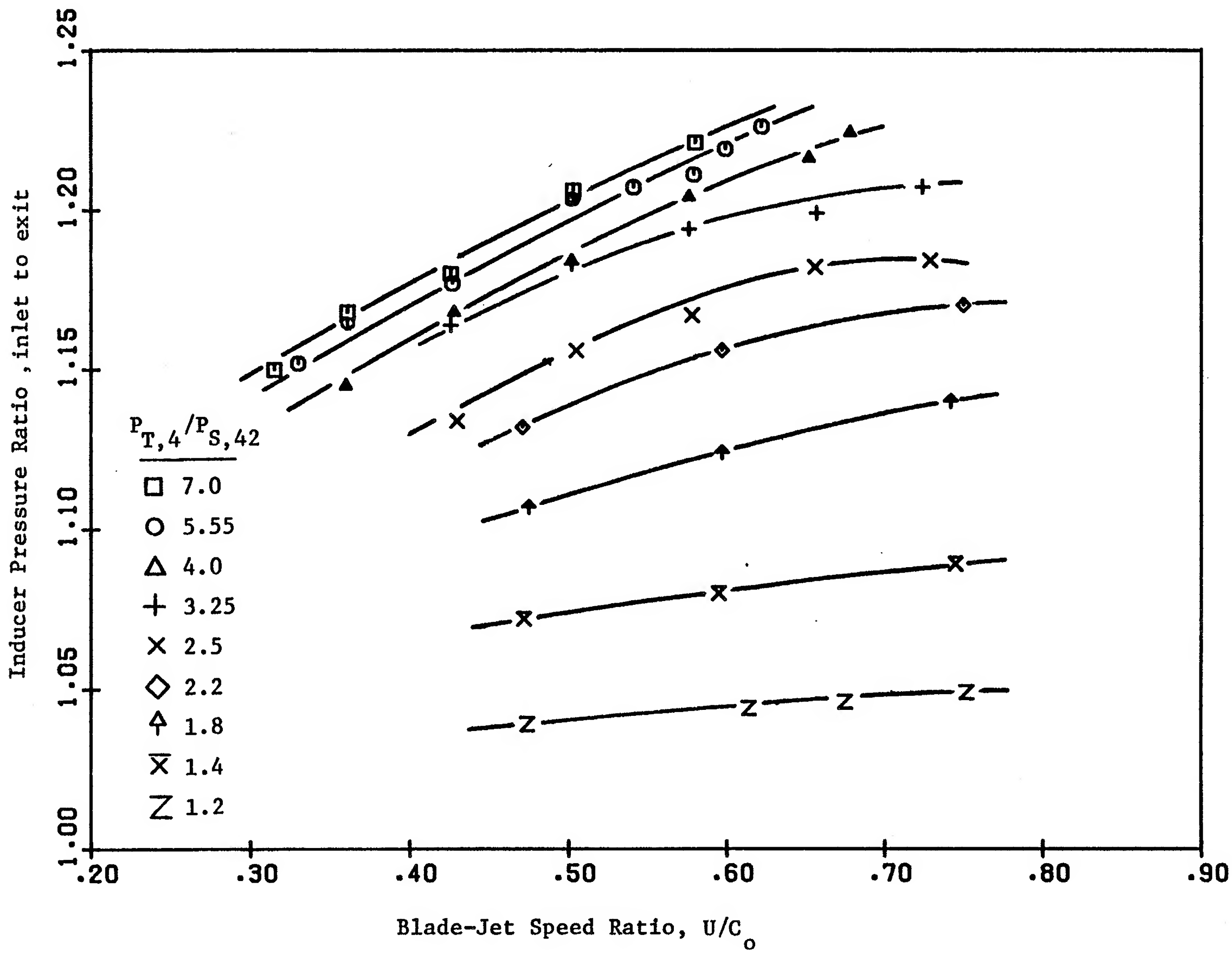

Figure F-1. Inducer Pressure Ratio vs. Blade-Jet Speed Ratio

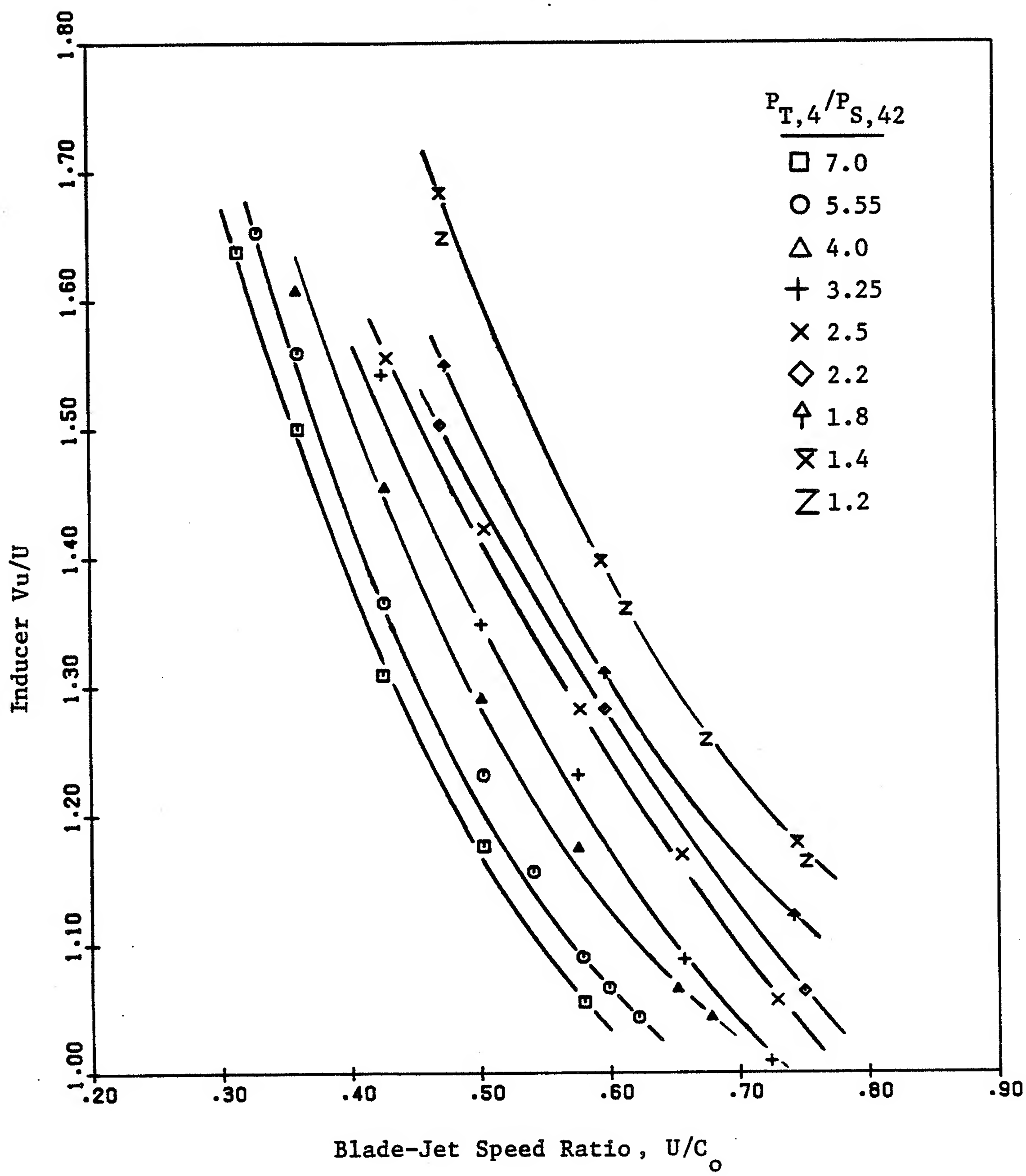

Figure F-2. Inducer Tangential Velocity vs. Blade-Jet Speed Ratio

APPENDIX G

DATA TABULATION FOR

TURBINE RIG TEST

<u>Definition of Units</u>

P_T	expressed in psia
P_c	expressed in psia
$P_{T,0}$	expressed in psia
T_T	expressed in °R
$T_{T,c}$	expressed in °R
$T_{T,0}$	expressed in °R
W_c	expressed in lbm/sec
W_0	expressed in lbm/sec
W	expressed in lbm/sec

PERFORMANCE

RDG.	$P_{T,4}/P_{S,42}$	$P_{T,4}/P_{T,42}$	$N/\sqrt{T_{T,41}}$ rpm/$\sqrt{°R}$	U/C_o	$W_{41}\sqrt{T_{T,41}}/P_{T,4}$ $\frac{lbm\sqrt{°R}}{sec\ psia}$	$\Delta h/T_{T,41}$ Btu/(lbm °R) Measured	w/Pumping
50	7.02834	5.96044	248.063	0.577954	18.1611	0.901403E-01	0.918039E-01
51	6.97168	5.92759	248.841	0.580725	18.1481	0.902224E-01	0.918962E-01
52	7.00776	5.84139	215.683	0.502722	18.2173	0.884295E-01	0.895998E-01
53	7.01421	5.84409	216.067	0.503532	18.2082	0.885481E-01	0.897193E-01
54	7.04109	5.71261	183.071	0.426131	18.2411	0.847048E-01	0.854668E-01
55	7.05666	5.71373	182.881	0.425427	18.2455	0.845146E-01	0.852758E-01
56	6.93434	5.61300	154.920	0.361385	18.2779	0.784176E-01	0.789060E-01
57	6.94595	5.61835	154.714	0.360767	18.2755	0.783128E-01	0.788009E-01
58	6.97230	5.55887	135.157	0.314848	18.2624	0.731284E-01	0.734627E-01
59	6.81745	5.49050	134.985	0.315834	18.2709	0.727290E-01	0.730637E-01
10	5.59431	5.01834	235.966	0.576662	18.1969	0.827960E-01	0.842694E-01
11	5.58517	5.01413	235.982	0.576845	18.1935	0.827070E-01	0.841818E-01
12	5.56754	4.99914	236.307	0.578105	18.1837	0.824074E-01	0.838692E-01
13	5.56257	4.99302	236.266	0.578091	18.1792	0.823942E-01	0.838575E-01
14	5.57039	4.99801	221.059	0.540661	18.2195	0.820805E-01	0.833207E-01
15	5.57163	4.99738	221.030	0.540581	18.2181	0.820820E-01	0.833201E-01
29	5.55308	4.98844	236.725	0.579519	18.1783	0.825137E-01	0.839822E-01
31	5.55963	4.98176	245.127	0.599973	18.1724	0.825706E-01	0.841765E-01
32	5.57751	4.99909	245.125	0.599483	18.1716	0.825828E-01	0.841904E-01
33	5.57874	4.99416	245.087	0.599355	18.1743	0.826531E-01	0.842599E-01
34	5.55603	4.97211	254.049	0.622011	18.1425	0.825600E-01	0.843167E-01
35	5.55635	4.96152	254.043	0.621938	18.1551	0.824952E-01	0.842398E-01
36	5.57658	5.00242	221.256	0.540869	18.2135	0.821805E-01	0.834183E-01
38	5.55671	4.97298	205.630	0.503076	18.2469	0.812797E-01	0.823116E-01
39	5.57590	4.97396	205.568	0.502549	18.2485	0.813273E-01	0.823575E-01
40	5.55852	4.89893	174.576	0.427022	18.3110	0.775100E-01	0.781796E-01
41	5.54813	4.89037	174.612	0.427251	18.2994	0.775370E-01	0.782097E-01
42	5.58128	4.85091	147.790	0.361137	18.3106	0.721602E-01	0.725920E-01
43	5.58848	4.85613	147.772	0.360904	18.3080	0.721721E-01	0.726019E-01
44	5.56246	4.81942	134.814	0.329603	18.2897	0.690018E-01	0.693333E-01
45	5.57066	4.82200	134.839	0.329583	18.2906	0.690026E-01	0.693351E-01
47	5.56070	4.98494	236.621	0.578940	18.1837	0.822159E-01	0.836788E-01
48	5.56337	4.99979	236.228	0.578005	18.1813	0.824784E-01	0.839531E-01
49	5.55852	4.99390	236.503	0.578895	18.1838	0.825400E-01	0.840169E-01
185	5.57315	5.00567	236.780	0.579326	18.2007	0.826393E-01	0.841138E-01
186	5.58174	5.00875	236.434	0.578247	18.1950	0.827352E-01	0.842090E-01
187	5.57707	5.01065	236.561	0.578602	18.1990	0.826366E-01	0.841061E-01
188	5.58062	5.01554	237.151	0.580069	18.1918	0.828146E-01	0.842904E-01
189	5.58520	5.01447	237.250	0.580214	18.1952	0.827370E-01	0.842116E-01
190	5.58425	5.01468	236.950	0.579480	18.1909	0.827896E-01	0.842639E-01
191	5.58415	5.01364	237.374	0.580545	18.1877	0.827294E-01	0.842050E-01
206	5.58295	5.01434	236.470	0.578284	18.2011	0.825966E-01	0.840679E-01
208	5.58407	5.01866	236.435	0.578106	18.1931	0.826949E-01	0.841656E-01
209	5.58768	5.02264	236.925	0.579286	18.1959	0.827675E-01	0.842350E-01
217	5.57343	5.00344	235.912	0.576809	18.2028	0.824510E-01	0.839098E-01
67	4.01443	3.63000	254.482	0.678244	18.0893	0.676516E-01	0.694299E-01
68	4.01804	3.63000	254.214	0.677324	18.0966	0.676299E-01	0.694061E-01
69	4.01473	3.66000	244.508	0.651476	18.1084	0.681370E-01	0.697495E-01
70	4.01036	3.66000	244.856	0.652720	18.1011	0.680861E-01	0.696990E-01
71	4.01867	3.73875	216.316	0.576120	18.1602	0.687085E-01	0.698852E-01
72	4.01738	3.73757	216.457	0.576626	18.1584	0.686525E-01	0.698334E-01
73	4.01227	3.76519	188.322	0.501644	18.2226	0.677999E-01	0.686255E-01
74	4.01037	3.76360	188.326	0.501784	18.2219	0.678225E-01	0.686484E-01
75	4.01033	3.76233	160.502	0.427598	18.2691	0.646772E-01	0.652188E-01
76	4.00782	3.75989	160.459	0.427562	18.2701	0.647077E-01	0.652470E-01
77	4.01799	3.72609	135.082	0.359541	18.2241	0.606199E-01	0.609619E-01
78	4.01225	3.72395	135.268	0.360214	18.2242	0.606503E-01	0.609924E-01
16	3.26216	3.09273	202.002	0.575678	18.1110	0.592252E-01	0.602171E-01

PERFORMANCE

RDG.	$P_{T,4}/P_{S,42}$	$P_{T,4}/P_{T,42}$	$N/\sqrt{T_{T,41}}$ rpm/$\sqrt{°R}$	U/C_o	$W_{41}\sqrt{T_{T,41}}/P_{T,4}$ $\frac{\text{lbm}\sqrt{°R}}{\text{sec psia}}$	$\Delta h/T_{T,41}$ Btu/(lbm °R) Measured	w/Pumping
17	3.26273	3.09240	201.979	0.575526	18.1323	0.591488E-01	0.601386E-01
18	3.25952	3.10639	176.362	0.502612	18.1878	0.582029E-01	0.589208E-01
19	3.25973	3.10653	176.262	0.502324	18.1946	0.582919E-01	0.590059E-01
20	3.26360	3.12317	149.624	0.426088	18.2292	0.559908E-01	0.564369E-01
21	3.26234	3.12322	149.629	0.426141	18.2326	0.559840E-01	0.564284E-01
219	3.25681	3.00435	230.070	0.656281	18.0566	0.584970E-01	0.598881E-01
220	3.25883	3.00473	230.334	0.656910	18.0460	0.585331E-01	0.599223E-01
222	3.25774	2.93471	253.760	0.723635	18.0239	0.570078E-01	0.587619E-01
22	2.50665	2.42638	158.935	0.505012	17.9723	0.458405E-01	0.463682E-01
23	2.51282	2.43047	158.829	0.504091	17.9744	0.459079E-01	0.464343E-01
181	2.51315	2.43909	135.474	0.430092	17.9599	0.438965E-01	0.442440E-01
182	2.51460	2.44370	135.382	0.429680	17.9613	0.439665E-01	0.443136E-01
224	2.51038	2.39468	182.014	0.577915	17.8930	0.464039E-01	0.471631E-01
225	2.50123	2.34225	206.012	0.655247	17.8570	0.458093E-01	0.468779E-01
226	2.50164	2.34293	206.326	0.656267	17.8480	0.458045E-01	0.468670E-01
227	2.49716	2.28590	229.318	0.730199	17.7956	0.443510E-01	0.457334E-01
228	2.50169	2.29096	228.718	0.727468	17.8148	0.443971E-01	0.457744E-01
229	2.20542	2.02822	220.986	0.750610	17.5826	0.378099E-01	0.390622E-01
230	2.20626	2.02835	220.720	0.749360	17.5790	0.378142E-01	0.390746E-01
231	2.20829	2.11084	175.983	0.596996	17.6694	0.398998E-01	0.406065E-01
232	2.20471	2.10756	175.809	0.597168	17.6639	0.399045E-01	0.406134E-01
233	2.20928	2.15170	138.902	0.471186	17.7942	0.389264E-01	0.393031E-01
234	2.20535	2.14834	138.909	0.471808	17.7803	0.387620E-01	0.391376E-01
235	1.80770	1.74502	154.468	0.598183	16.9650	0.299649E-01	0.304843E-01
236	1.80618	1.74467	153.903	0.596370	16.9716	0.298911E-01	0.304072E-01
237	1.80695	1.77262	122.708	0.475474	17.0906	0.292273E-01	0.295070E-01
238	1.80599	1.77149	122.375	0.474148	17.0872	0.292566E-01	0.295357E-01
239	1.80616	1.69461	191.851	0.743444	16.8920	0.278230E-01	0.287280E-01
240	1.80691	1.69685	191.124	0.740564	16.8908	0.280240E-01	0.289413E-01
241	1.40668	1.37741	118.246	0.593443	14.9171	0.172132E-01	0.174930E-01
242	1.40501	1.37535	118.643	0.596730	14.8962	0.171253E-01	0.174040E-01
243	1.40408	1.38810	93.7277	0.471742	15.0019	0.165513E-01	0.166986E-01
244	1.40361	1.38911	93.8171	0.472374	14.9914	0.166227E-01	0.167692E-01
245	1.40294	1.35168	147.644	0.743993	14.8173	0.160917E-01	0.165947E-01
246	1.40286	1.35087	147.911	0.745165	14.8091	0.160082E-01	0.165099E-01
247	1.20611	1.19067	91.4197	0.614250	12.1344	0.939882E-02	0.956051E-02
248	1.20494	1.18975	91.2987	0.614554	12.1128	0.940476E-02	0.956450E-02
249	1.20611	1.19820	70.6717	0.474213	12.3618	0.902636E-02	0.910499E-02
250	1.20568	1.19777	70.6947	0.474567	12.3620	0.900419E-02	0.908275E-02
251	1.20500	1.18541	100.363	0.675175	11.9800	0.896460E-02	0.916613E-02
252	1.20492	1.18508	100.283	0.674422	11.9800	0.896510E-02	0.916613E-02
253	1.20488	1.17901	111.553	0.751502	11.8800	0.828045E-02	0.855043E-02
254	1.20416	1.17855	111.627	0.752220	11.8800	0.825614E-02	0.852740E-02

RDG.	Average Clearance (inches x 10^3) Stg 1	Stg 2	η_{GE} Measured	η_{TH} Measured	η_{GE} Corrected to 0.016 in. Tip Clearance	η_{TH} Corrected to 0.016 in. Tip Clearance	η_{THP} Corrected to 0.016 in. Tip Clearance
50	15.8	14.0	0.931205	0.889413	0.9308	0.8890	0.9054
51	15.6	12.8	0.934408	0.891723	0.9337	0.8910	0.9076
52	18.6	17.2	0.921593	0.879795	0.9229	0.8811	0.8927
53	19.1	17.7	0.922733	0.880790	0.9244	0.8825	0.8941
54	14.9	15.4	0.891618	0.848337	0.8910	0.8477	0.8554
55	14.4	15.7	0.889492	0.846229	0.8887	0.8454	0.8531
56	12.0	13.4	0.831982	0.792163	0.8298	0.7900	0.7949
57	11.9	13.5	0.830461	0.790751	0.8283	0.7885	0.7935
58	13.8	14.2	0.779266	0.742298	0.7780	0.7410	0.7444
59	13.4	14.4	0.779350	0.742065	0.7780	0.7407	0.7441
10	16.3	15.5	0.925915	0.885437	0.9259	0.8854	0.9012
11	15.7	15.5	0.925307	0.884742	0.9251	0.8845	0.9003
12	15.6	15.2	0.923374	0.882624	0.9231	0.8823	0.8980
13	16.1	15.4	0.923767	0.882784	0.9237	0.8827	0.8984
14	17.0	16.9	0.919800	0.879300	0.9204	0.8799	0.8932
15	16.8	17.0	0.919901	0.879258	0.9205	0.8799	0.8931
29	16.9	15.7	0.925547	0.884607	0.9258	0.8849	0.9007
31	17.3	16.0	0.926771	0.885645	0.9274	0.8862	0.9035
32	17.0	16.8	0.925318	0.884442	0.9258	0.8849	0.9022
33	17.0	16.3	0.926545	0.885547	0.9270	0.8860	0.9033
34	16.5	15.5	0.927575	0.886053	0.9277	0.8862	0.9050
35	16.7	16.0	0.927900	0.887200	0.9282	0.8875	0.9063
36	16.9	14.6	0.920500	0.880100	0.9207	0.8803	0.8936
38	16.7	15.2	0.913092	0.872980	0.9133	0.8732	0.8843
39	16.8	15.1	0.913539	0.873382	0.9137	0.8736	0.8846
40	16.9	14.5	0.877200	0.839000	0.8773	0.8391	0.8463
41	17.2	14.6	0.878328	0.839852	0.8786	0.8402	0.8474
42	18.0	15.0	0.820781	0.785185	0.8215	0.7859	0.7906
43	22.7	16.3	0.820467	0.785191	0.8235	0.7882	0.7929
44	16.4	14.8	0.787424	0.752113	0.7874	0.7521	0.7557
45	16.8	13.5	0.787220	0.751951	0.7872	0.7520	0.7556
47	17.9	15.0	0.922503	0.881825	0.9231	0.8824	0.8981
48	17.4	14.0	0.923983	0.883550	0.9243	0.8839	0.8996
49	17.3	14.2	0.925269	0.884645	0.9256	0.8849	0.9008
185	15.9	15.9	0.925449	0.884206	0.9254	0.8842	0.9000
186	15.9	15.7	0.926178	0.884879	0.9261	0.8848	0.9005
187	15.7	15.8	0.924939	0.883936	0.9248	0.8838	0.8996
188	15.6	15.7	0.926557	0.885155	0.9263	0.8849	0.9006
189	15.4	15.8	0.925811	0.884435	0.9255	0.8841	0.8999
190	15.7	15.9	0.926327	0.884905	0.9262	0.8848	0.9006
191	15.5	16.0	0.925814	0.884497	0.9256	0.8843	0.9001
206	15.1	15.5	0.924137	0.883064	0.9236	0.8826	0.8983
208	15.3	15.4	0.924842	0.883639	0.9244	0.8832	0.8990
209	15.2	15.2	0.925390	0.884248	0.9249	0.8837	0.8994
217	14.3	15.2	0.923428	0.881793	0.9226	0.8818	0.8974
67	16.7	12.2	0.907800	0.856069	0.9075	0.8664	0.8892
68	16.4	12.4	0.907400	0.855864	0.9070	0.8661	0.8889
69	16.4	13.6	0.909400	0.862551	0.9032	0.8689	0.8895
70	16.4	13.4	0.909000	0.862355	0.9088	0.8682	0.8888
71	16.5	14.6	0.904835	0.866378	0.9048	0.8664	0.8812
72	16.6	14.5	0.904307	0.865837	0.9043	0.8658	0.8807
73	16.1	14.7	0.888962	0.850939	0.8888	0.8507	0.8611
74	16.5	14.8	0.889496	0.851455	0.8895	0.8515	0.8618
75	15.3	14.1	0.848429	0.812392	0.8478	0.8118	0.8186
76	15.6	14.3	0.849242	0.813015	0.8487	0.8125	0.8193
77	16.6	15.0	0.800037	0.762537	0.8001	0.7626	0.7669
78	16.6	14.9	0.800777	0.763187	0.8009	0.7633	0.7676
16	17.3	15.5	0.888800	0.851800	0.8893	0.8523	0.8665
17	17.4	15.6	0.887700		0.8882		
18	18.2	17.4	0.870573		0.8718		

ORIGINAL PAGE IS OF POOR QUALITY

PERFORMANCE

RDG.	Average Clearance (inches x 10^3) Stg 1	Stg 2	η_{GE} Measured	η_{TH} Measured	η_{GE} Corrected to 0.016 in. Tip Clearance	η_{TH} Corrected to 0.016 in. Tip Clearance	η_{THP} Corrected to 0.016 in. Tip Clearance
20	16.9	15.7	0.833973	0.799300	0.8344	0.7996	0.8060
21	16.8	15.3	0.897626	0.799431	0.8343	0.7997	0.8061
219	15.6	13.8	0.898119	0.859650	0.8970	0.8591	0.8795
220	15.0	13.8	0.891092	0.860120	0.8973	0.8593	0.8797
222	15.8	10.9	0.848879	0.852674	0.8901	0.8517	0.8779
22	16.4	16.0	0.848694	0.814941	0.8491	0.8151	0.8245
23	16.5	15.9	0.808698	0.814738	0.8489	0.8149	0.8243
181							
182							
224	15.6	14.7	0.808459	0.835148	0.8707	0.8351	0.8488
225	16.4	16.0	0.870743	0.844500	0.8796	0.8447	0.8644
226	15.8	16.4	0.879400	0.844123	0.8792	0.8442	0.8638
227	17.6	16.5	0.879093	0.838500	0.8744	0.8393	0.8654
228	18.4	15.5	0.873600	0.837328	0.8735	0.8383	0.8643
229	15.7	14.3	0.872518	0.823300	0.8567	0.8229	0.8502
230	15.7	14.1	0.857100	0.822800	0.8567	0.8224	0.8498
231	16.2	14.5	0.857100	0.826223	0.8605	0.8260	0.8407
232	15.7	14.4	0.860734	0.828263	0.8621	0.8279	0.8426
233	15.6	13.8	0.862460	0.788650	0.8201	0.7881	0.7957
234	15.4	14.1	0.820745	0.787019	0.8182	0.7864	0.7940
235	17.0	14.5	0.818778	0.813100	0.8456	0.8132	0.8273
236	16.9	14.5	0.845500	0.811110	0.8438	0.8112	0.8252
237	15.7	14.2	0.843695	0.773610	0.8033	0.7732	0.7806
238	15.7	14.1	0.803748	0.774300	0.8050	0.7739	0.7813
239	16.1	14.0	0.805400	0.793011	0.8252	0.7927	0.8185
240	15.8	13.9	0.825528	0.796700	0.8291	0.7962	0.8223
241	16.2	15.6	0.829600	0.789313	0.8187	0.7893	0.8021
242	15.7	15.7	0.818717	0.789988	0.8180	0.7898	0.8026
243	16.8	15.1	0.818182	0.742406	0.7696	0.7426	0.7492
244	17.5	14.9	0.769449	0.743819	0.7716	0.7443	0.7509
245	16.6	13.9	0.771139	0.781757	0.8111	0.7817	0.8061
246	15.9	14.1	0.811233	0.778688	0.8083	0.7784	0.8028
247	17.2	15.1	0.808571	0.779327	0.8049	0.7796	0.7930
248	18.3	15.9	0.804564	0.781700	0.8097	0.7827	0.7959
249	18.4	14.5	0.808700	0.722400	0.7474	0.7232	0.7295
250	17.9	14.0	0.746600	0.720761	0.7465	0.7213	0.7275
251	17.1	13.5	0.745959	0.779000	0.8068	0.7791	0.7967
252	17.3	13.5	0.806700	0.780500	0.8086	0.7807	0.7982
253	21.1	16.1	0.808400	0.727217	0.7782	0.7534	0.7779
254	15.4	10.0	0.776000	0.748300	0.7739	0.7470	0.7717

RDG.	Inlet P_T	Inlet T_T	Inlet W	Vane 1 Exit W	Vane 1 Exit T_T	Loading, ψ_P Meas.	Loading, ψ_P With Pumping	$TQ/P_{T,4}$ ft. in^2 With Pumping	Reaction, R_x Hub	Reaction, R_x Tip	Exit Swirl Γ, degrees
50	50.2355	1281.20	24.0062	25.9994	1231.35	0.651698	0.663726	49.9341	0.378538	0.451309	12.0000
51	50.1864	1275.00	24.0256	26.0146	1225.75	0.648219	0.660245	49.7922	0.385983	0.451903	12.0000
52	50.2421	1281.47	24.0687	26.0825	1231.42	0.845698	0.856891	56.2251	0.367242	0.430330	22.0000
53	50.2428	1276.49	24.1093	26.1158	1227.08	0.843827	0.854988	56.1718	0.367122	0.429920	22.0000
54	50.2288	1275.84	24.1571	26.1599	1226.70	1.12439	1.13451	63.2678	0.397818	0.423448	31.5000
55	50.2356	1278.41	24.1446	26.1452	1228.99	1.12421	1.13434	63.2074	0.397661	0.423651	31.5000
56	50.2521	1275.89	24.2151	26.2261	1226.57	1.45361	1.46266	69.1644	0.387768	0.420428	37.5000
57	50.2585	1278.88	24.1879	26.1966	1229.34	1.45553	1.46460	69.1552	0.388045	0.421167	37.5000
58	50.8430	1275.27	24.5249	26.5033	1227.37	1.78097	1.78911	73.7460	0.402937	0.440768	44.0000
59	50.8355	1278.53	24.5055	26.4779	1230.51	1.77577	1.78394	73.4733	0.402854	0.441001	44.0000
10	50.1630	1280.95	24.0150	26.0136	1231.29	0.661546	0.673318	48.2804	0.360272	0.440729	00.0000
11	50.1760	1280.66	24.0198	26.0188	1230.98	0.660747	0.672529	48.2181	0.360328	0.440347	00.0000
12	50.2020	1277.34	24.0532	26.0488	1228.09	0.656544	0.668191	47.9471	0.362096	0.440859	00.0000
13	50.1770	1277.90	24.0400	26.0207	1228.91	0.656667	0.668329	47.9368	0.362241	0.442280	00.0000
14	50.1840	1276.81	24.0925	26.0983	1227.38	0.747267	0.758558	51.0175	0.351563	0.430316	3.0000
15	50.1690	1276.89	24.0818	26.0879	1227.44	0.747472	0.758747	51.0219	0.351551	0.430717	3.0000
29	50.1789	1276.87	24.0368	26.0317	1227.85	0.655070	0.666728	47.9127	0.363311	0.440224	00.0000
31	50.1955	1278.32	24.0238	26.0172	1229.23	0.611355	0.623245	46.3624	0.367252	0.444687	-5.0000
32	50.2223	1278.19	24.0431	26.0286	1229.35	0.611456	0.623359	46.3683	0.366923	0.444873	-5.0000
33	50.2234	1278.78	24.0438	26.0268	1229.94	0.612166	0.624067	46.4208	0.366655	0.444211	-5.0000
34	50.2212	1275.58	24.0498	26.0055	1227.54	0.569097	0.581206	44.7349	0.373517	0.449146	-10.000
35	50.2266	1277.07	24.0397	26.0176	1228.37	0.568675	0.580702	44.7285	0.371225	0.448948	-10.000
36	50.2140	1275.93	24.1336	26.1019	1227.71	0.746843	0.758092	51.0151	0.350170	0.429495	3.0000
38	50.2128	1277.25	24.1525	26.1404	1228.53	0.855181	0.866038	54.2648	0.338078	0.419517	12.5000
39	50.2153	1277.31	24.1506	26.1447	1228.45	0.856201	0.867047	54.3161	0.338158	0.418580	12.5000
40	50.2077	1277.44	24.2541	26.2207	1229.34	1.13145	1.14123	60.9234	0.341206	0.401313	24.0000
41	50.2032	1277.57	24.2211	26.2019	1229.34	1.13138	1.14120	60.8945	0.341207	0.401097	24.0000
42	50.1960	1276.10	24.2454	26.2292	1227.94	1.46980	1.47860	66.8193	0.352322	0.413133	35.0000
43	50.1883	1276.59	24.2294	26.2182	1228.23	1.47041	1.47917	66.8270	0.352522	0.413568	35.0000
44	50.1840	1277.52	24.1922	26.1793	1229.21	1.68905	1.69716	69.8825	0.373612	0.434349	40.0000
45	50.1994	1277.04	24.2278	26.1880	1229.27	1.68844	1.69658	69.8747	0.373870	0.433822	40.0000
47	50.2285	1277.33	24.0904	26.0525	1229.03	0.653282	0.664906	47.7747	0.360919	0.439271	00.0000
48	50.2404	1284.20	24.0117	25.9983	1234.43	0.657547	0.669304	48.0046	0.367743	0.443056	00.0000
49	50.2165	1281.10	24.0408	26.0199	1231.54	0.656508	0.668255	47.9918	0.366800	0.442952	00.0000
185	50.2070	1278.06	23.9176	26.1142	1224.47	0.655764	0.667464	48.0357	0.383498	0.448548	00.0000
186	50.2157	1281.76	23.8746	26.0762	1227.70	0.658445	0.670174	48.1452	0.384022	0.449033	00.0000
187	50.2173	1280.00	23.8913	26.1023	1225.87	0.656955	0.668637	48.0713	0.383603	0.449050	00.0000
188	50.2350	1275.95	23.9324	26.1389	1222.34	0.655101	0.666775	48.0379	0.384291	0.448670	00.0000
189	50.2350	1274.60	23.9490	26.1567	1221.12	0.653940	0.665595	47.9817	0.384318	0.448807	00.0000
190	50.2257	1277.20	23.9237	26.1171	1223.79	0.656012	0.667694	48.0609	0.384284	0.448955	00.0000
191	50.2286	1273.52	23.9557	26.1498	1220.45	0.653193	0.664843	47.9331	0.384460	0.448848	00.0000
206	50.1953	1279.83	23.9194	26.0835	1226.84	0.657143	0.668849	48.0736	0.380655	0.442473	00.0000
208	50.2053	1279.75	23.9186	26.0760	1226.96	0.658122	0.669827	48.1154	0.380648	0.441945	00.0000
209	50.2053	1274.19	23.9835	26.1308	1222.20	0.655975	0.667605	48.0629	0.380323	0.441646	00.0000
217	50.1372	1282.91	23.8751	26.0191	1230.30	0.659095	0.670757	48.1012	0.381033	0.439306	00.0000
67	50.1755	1274.42	23.9195	25.9385	1224.44	0.464743	0.476959	36.6660	0.368867	0.443214	-31.0000
68	50.1777	1276.76	23.9089	25.9266	1226.66	0.465576	0.477804	36.7070	0.368633	0.443580	-31.0000
69	50.2036	1278.49	23.8906	25.9471	1227.59	0.507046	0.519046	38.3781	0.364813	0.439667	-29.0000
70	50.2019	1274.48	23.9399	25.9678	1224.56	0.505226	0.517194	38.2801	0.361095	0.438946	-29.0000
71	50.2143	1278.20	23.9964	26.0184	1228.38	0.653255	0.664443	43.5883	0.342150	0.422578	-16.2395
72	50.2215	1276.01	24.0252	26.0387	1226.59	0.651871	0.663084	43.5234	0.342393	0.422565	-16.2900
73	50.1375	1276.98	24.0371	26.0838	1226.89	0.850508	0.860864	49.3343	0.325282	0.404350	00.0000
74	50.1373	1276.80	24.0408	26.0836	1226.81	0.850758	0.861118	49.3480	0.325076	0.404316	00.0000
75	50.1415	1276.15	24.1159	26.1579	1226.38	1.11696	1.12631	55.1523	0.334339	0.394650	8.0000
76	50.1387	1271.51	24.1571	26.2044	1222.03	1.11809	1.12741	55.1940	0.334172	0.394554	8.0000
77	50.1942	1277.40	24.0783	26.1103	1227.37	1.47800	1.48634	61.1031	0.393802	0.430022	23.0000
78	50.1878	1273.74	24.1087	26.1436	1223.94	1.47466	1.48298	61.0496	0.393695	0.429268	23.0000
16	50.1640	1276.67	23.9378	25.9666	1224.16	0.645723	0.656537	40.1087	0.302028	0.395592	-21.4883

ORIGINAL PAGE IS OF POOR QUALITY

PERFORMANCE

RDG.	Inlet P_T	Inlet T_T	Inlet W	Vane 1 Exit W	Vane 1 Exit T_T	Loading, ψ_P Meas.	Loading, ψ_P With Pumping	$TQ/P_{T,4}$ ft. in^2 With Pumping	Reaction, R_x Hub	Reaction, R_x Tip	Exit Swirl Γ, degrees
17	50.1560	1276.35	23.9338	25.9753	1225.83	0.645036	0.655831	40.1123	0.302652	0.393535	-21.8271
18	50.1470	1277.23	24.0082	26.0480	1226.03	0.832501	0.842769	45.1437	0.296743	0.378837	-10.0309
19	50.1440	1278.13	24.0032	26.0488	1226.72	0.834721	0.844945	45.2515	0.295889	0.378522	-9.89170
20	50.1380	1277.06	24.0596	26.0924	1226.98	1.11266	1.12153	51.0825	0.309008	0.381673	00.0000
21	50.1530	1277.90	24.0642	26.0957	1227.87	1.11245	1.12128	51.0837	0.309598	0.382424	00.0000
219	50.1515	1280.63	23.6549	25.8684	1225.47	0.491658	0.503350	34.9197	0.364241	0.424124	-41.1852
220	50.1622	1278.35	23.6698	25.8792	1223.53	0.490836	0.502485	34.8791	0.365091	0.425136	-41.3592
222	50.1280	1280.63	23.6061	25.8030	1226.07	0.393856	0.405975	31.0080	0.383945	0.433077	-48.6772
22	50.1520	1277.95	23.7282	25.7206	1228.06	0.807349	0.816643	38.9545	0.263639	0.347729	-19.9700
23	50.1600	1278.75	23.7327	25.7183	1228.96	0.809615	0.818899	39.0407	0.263366	0.347632	-21.4238
181	50.2099	1275.58	23.7461	25.7592	1225.53	1.06407	1.07249	43.5770	0.288728	0.364927	-8.30888
182	50.2114	1277.01	23.7409	25.7468	1226.97	1.06721	1.07564	43.6787	0.289146	0.365025	00.0000
224	50.1738	1282.68	23.4466	25.6124	1228.63	0.623156	0.633351	34.4457	0.290588	0.368078	-38.9744
225	50.0971	1277.01	23.4050	25.5875	1222.32	0.480196	0.491399	30.1815	0.292513	0.387175	-49.2477
226	50.0998	1276.76	23.3926	25.5808	1221.87	0.478687	0.489791	30.1202	0.292977	0.387773	-49.2085
227	50.1311	1276.78	23.3389	25.5190	1222.11	0.376152	0.387821	26.3700	0.317500	0.400571	-55.9090
228	50.1406	1280.56	23.3434	25.5135	1225.74	0.377575	0.389288	26.4884	0.316754	0.400612	-55.7217
229	50.1916	1273.64	23.1131	25.2764	1218.99	0.344451	0.355859	23.0922	0.298230	0.391452	-59.3490
230	50.1929	1276.90	23.0850	25.2390	1222.17	0.345321	0.356830	23.1173	0.297216	0.390825	-59.3650
231	50.1875	1278.96	23.1912	25.3413	1224.55	0.573167	0.583319	30.2902	0.252974	0.353370	-45.5647
232	50.1562	1277.76	23.1971	25.3235	1223.98	0.574369	0.584572	30.3159	0.254139	0.354658	-45.6436
233	50.1786	1285.81	23.2948	25.4517	1230.72	0.897586	0.906272	37.4068	0.252957	0.337902	-22.2356
234	50.1757	1285.46	23.2792	25.4324	1230.52	0.893711	0.902371	37.2184	0.253984	0.337369	-22.0435
235	50.1777	1284.59	22.1956	24.2819	1229.03	0.558707	0.568390	24.8744	0.222324	0.342976	-50.4335
236	50.1844	1289.39	22.1704	24.2491	1233.64	0.561432	0.571125	24.9118	0.223967	0.345466	-50.0012
237	50.1940	1285.15	22.3666	24.4621	1229.80	0.863569	0.871832	30.5328	0.227221	0.329153	-29.3727
238	50.1932	1284.92	22.3684	24.4572	1229.75	0.869144	0.877433	30.6366	0.227511	0.328623	-29.7787
239	50.2121	1279.86	22.1652	24.2329	1225.08	0.336301	0.347240	18.7921	0.261292	0.373569	-61.8477
240	50.2026	1287.91	22.0884	24.1547	1232.39	0.341311	0.352483	18.9906	0.260643	0.374168	-61.6243
241	50.2204	1281.19	19.5112	21.4197	1223.21	0.547699	0.556602	16.3952	0.197262	0.362449	-54.5461
242	50.2190	1271.39	19.5691	21.4649	1214.59	0.541253	0.550062	16.2343	0.200955	0.361263	-54.9578
243	50.2225	1284.26	19.6048	21.5074	1227.20	0.838196	0.845655	19.8569	0.207888	0.347361	-37.8862
244	50.2173	1280.81	19.6164	21.5171	1224.12	0.840209	0.847616	19.9080	0.213581	0.346354	-34.1283
245	50.2112	1286.74	19.3261	21.2246	1228.74	0.328413	0.338679	12.3730	0.233808	0.395126	-64.3313
246	50.2183	1282.28	19.3548	21.2491	1224.90	0.325530	0.335731	12.2808	0.234157	0.393042	-64.5486
247	50.2346	1278.60	15.8048	17.4709	1217.34	0.500316	0.508923	9.42778	0.210518	0.453594	-58.2492
248	50.2221	1282.42	15.7496	17.4083	1221.14	0.501959	0.510485	9.42868	0.210950	0.455252	-58.0537
249	50.1811	1285.97	16.0861	17.7160	1226.06	0.804028	0.811032	11.8314	0.217275	0.421219	-41.6199
250	50.1718	1286.29	16.0798	17.7116	1226.25	0.801533	0.808526	11.7997	0.217900	0.422130	-41.6533
251	50.1718	1282.09	15.9952	17.6252	1222.23	0.395941	0.404874	8.33634	0.221613	0.450004	-61.8398
252	50.1635	1283.86	15.9842	17.6171	1223.85	0.396600	0.405494	8.34539	0.219079	0.448555	-62.0417
253	50.1631	1283.55	15.9825	17.6271	1222.84	0.296032	0.305684	6.99739	0.236326	0.455699	-65.7565
254	50.1665	1281.86	15.9885	17.6352	1221.12	0.294775	0.304508	6.97129	0.237271	0.454853	-65.6592

PERFORMANCE Flowpath Static Pressures (psia)

RDG.	Inlet Rake Plane Outer	Inlet Rake Plane Inner	Vane 1 Exit Outer	Vane 1 Exit Inner	Blade 1 Exit Outer	Blade 1 Exit Inner	Vane 2 Exit Inner	Blade 2 Exit Outer	Blade 2 Exit Inner	Exit Rake Plane Outer	Exit Rake Plane Inner
50	50.1513	50.1793	30.5932	28.8259	20.1368	20.0346	12.8061	6.81699	7.23909	7.02623	7.26890
51	50.1051	50.1320	30.6052	29.0225	20.1408	20.0453	12.8074	6.86549	7.29701	7.08265	7.31456
52	50.1605	50.1831	30.0665	28.5103	20.2126	20.0127	12.7558	6.84705	7.24130	7.06876	7.27023
53	50.1509	50.1799	30.0611	28.5076	20.2072	20.0074	12.7558	6.85244	7.24265	7.06473	7.26127
54	50.1436	50.1770	29.8499	29.2925	20.1642	19.9741	12.7677	6.78484	7.16159	7.08330	7.18404
55	50.1512	50.1813	29.8659	29.3006	20.1829	19.9920	12.7825	6.78125	7.15351	7.08330	7.15449
56	50.1591	50.1935	29.7926	28.9829	20.1871	19.9132	13.1930	6.98749	7.21560	7.26878	7.22491
57	50.1666	50.1978	29.8086	28.9977	20.1871	19.9256	13.1930	6.97491	7.19943	7.26341	7.20790
58	50.7469	50.7780	30.3826	29.4835	19.9645	19.8195	13.5922	7.06571	7.19503	7.38258	7.20171
59	50.7469	50.7770	30.3947	29.4889	19.9766	19.8320	13.6057	7.26328	7.36341	7.55046	7.36289
10	50.0852	50.1077	30.3143	28.3358	20.1825	20.0397	12.9287	8.72400	9.03993	8.85671	9.07686
11	50.0905	50.1281	30.3156	28.3479	20.1905	20.0469	12.9341	8.72400	9.04531	8.87282	9.09476
12	50.1174	50.1453	30.3517	28.4247	20.2012	20.0736	12.9542	8.76700	9.08302	8.91309	9.12071
13	50.0933	50.1309	30.3766	28.4269	20.1874	20.0768	12.9538	8.75400	9.07446	8.90726	9.13368
14	50.0997	50.1245	30.0654	28.0983	20.2169	20.0161	12.9000	8.75700	9.09332	8.90592	9.11220
15	50.0686	50.1105	30.0694	28.0956	20.2115	20.0161	12.9067	8.75900	9.08389	8.89384	9.11489
29	50.0940	50.1230	30.3418	28.4524	20.2114	20.0699	12.9617	8.74711	9.11204	8.94472	9.12773
31	50.1182	50.1461	30.4735	28.5650	20.2162	20.0766	12.9720	8.80408	9.08731	8.93349	9.12366
32	50.1396	50.1772	30.4703	28.5509	20.1902	20.0608	12.9457	8.77555	9.03814	8.91538	9.09347
33	50.1363	50.1707	30.4529	28.5468	20.1862	20.0608	12.9498	8.76657	9.04891	8.90196	9.10332
34	50.1392	50.1747	30.6013	28.7396	20.1876	20.0707	12.9554	8.80897	9.04508	8.95045	9.12764
35	50.1478	50.1747	30.5705	28.6588	20.1635	20.0493	12.9540	8.83950	9.09355	8.92897	9.15001
36	50.1352	50.1643	30.0683	28.0932	20.2077	20.0293	12.9205	8.72962	9.09230	8.90219	9.10668
38	50.1352	50.1664	29.7410	27.7268	20.1462	19.9686	12.8653	8.76014	9.11788	8.91964	9.15321
39	50.1320	50.1632	29.7130	27.7268	20.1448	19.9668	12.8599	8.76193	9.14212	8.90487	9.10668
40	50.1163	50.1550	29.2710	27.6718	20.1718	19.8059	12.8910	8.76702	9.10995	8.93994	9.12519
41	50.1238	50.1550	29.2696	27.6758	20.1798	19.8113	12.8923	8.79574	9.13284	8.97484	9.12250
42	50.1074	50.1483	29.4649	27.8027	20.0127	19.6197	13.2747	8.78970	9.03209	8.97373	9.01355
43	50.1020	50.1354	29.4556	27.7878	19.9900	19.5982	13.2666	8.76456	9.01458	8.95762	9.00371
44	50.1026	50.1348	29.7647	28.1736	19.6385	19.3864	13.4891	8.80277	9.00162	9.02795	9.01587
45	50.1069	50.1445	29.7620	28.1857	19.6465	19.3900	13.4972	8.80098	8.99623	9.01318	9.00960
47	50.1430	50.1785	30.3510	28.4051	20.2260	20.0685	12.9576	8.79234	9.12001	8.93925	9.12629
48	50.1664	50.1943	30.4316	28.5862	20.2331	20.0917	12.9877	8.75474	9.10171	8.93034	9.13081
49	50.1331	50.1674	30.4209	28.5552	20.2238	20.0863	12.9891	8.75115	9.09363	8.92497	9.14333
185	50.1255	50.1588	30.5444	29.0064	20.2443	20.1266	12.9650	8.78041	9.08294	8.90648	9.11097
186	50.1320	50.1631	30.5551	29.0199	20.2470	20.1283	12.9609	8.76963	9.07487	8.88366	9.10918
187	50.1330	50.1696	30.5497	29.0064	20.2390	20.1248	12.9569	8.76245	9.07083	8.89574	9.11276
188	50.1466	50.1853	30.5644	29.0413	20.2536	20.1341	12.9555	8.75920	9.06937	8.88758	9.11580
189	50.1488	50.1853	30.5657	29.0360	20.2496	20.1269	12.9555	8.76279	9.06937	8.88087	9.10774
190	50.1541	50.1756	30.5680	29.0383	20.2479	20.1315	12.9564	8.75659	9.06900	8.88051	9.10783
191	50.1476	50.1766	30.5653	29.0410	20.2412	20.1261	12.9497	8.74761	9.06766	8.88186	9.10783
206	50.1197	50.1423	30.3877	28.9117	20.2519	20.0993	12.9524	8.73504	9.07843	8.87649	9.10514
208	50.1143	50.1433	30.3877	28.9225	20.2586	20.1047	12.9551	8.72966	9.07304	8.86575	9.11588
209	50.1251	50.1508	30.3837	28.9103	20.2479	20.0922	12.9564	8.72606	9.07304	8.86037	9.10962
217	50.0371	50.0822	30.2989	28.9043	20.2579	20.0866	12.9612	8.74743	9.06972	8.88925	9.10225
67	50.0933	50.1223	30.9481	29.2468	20.9527	20.8862	14.8638	12.4255	12.3587	12.5283	12.4693
68	50.0933	50.1320	30.9508	29.2454	20.9487	20.8952	14.8571	12.4255	12.3601	12.5176	12.4586
69	50.1139	50.1472	30.8713	29.1680	20.9855	20.9163	14.8860	12.3966	12.4025	12.5129	12.4968
70	50.1214	50.1450	30.8646	29.0994	20.9855	20.9413	14.9035	12.4236	12.4132	12.5223	12.5138
71	50.1390	50.1659	30.4537	28.6217	21.0154	20.9364	14.9148	12.3523	12.4931	12.4476	12.5429
72	50.1401	50.1659	30.4617	28.6298	21.0194	20.9364	14.9188	12.3541	12.4971	12.4530	12.5491
73	50.0461	50.0794	29.8240	28.0461	20.8556	20.7735	14.7784	12.2907	12.5478	12.4203	12.5718
74	50.0547	50.0848	29.8266	28.0501	20.8596	20.7842	14.7824	12.2943	12.5532	12.4257	12.5781
75	50.0524	50.0847	29.5992	28.0875	20.8887	20.5497	14.7390	12.2702	12.6039	12.4253	12.5809
76	50.0578	50.0868	29.6005	28.0942	20.8860	20.5586	14.7457	12.2845	12.6147	12.4333	12.5871
77	50.1062	50.1406	30.2831	29.5542	20.5300	20.4569	15.2179	12.2576	12.6268	12.4253	12.5594
78	50.1094	50.1384	30.2751	29.5595	20.5434	20.4658	15.2246	12.2702	12.6416	12.4427	12.5746
16	50.0684	50.1082	30.8101	28.8343	22.4762	22.3821	17.2356	15.2430	15.3019	15.3751	15.3800

ORIGINAL PAGE IS
OF POOR QUALITY

PERFORMANCE Flowpath Static Pressures (psia)

RDG.	Inlet Rake Plane		Vane 1 Exit		Blade 1 Exit		Vane 2 Exit	Blade 2 Exit		Exit Rake Plane	
	Outer	Inner	Outer	Inner	Outer	Inner	Inner	Outer	Inner	Outer	Inner
17	50.0759	50.1017	30.7887	28.8451	22.4815	22.3660	17.2343	15.2480	15.3073	15.3657	15.3791
18	50.0488	50.0918	30.3136	28.6002	22.3508	22.2442	17.1862	15.2100	15.3937	15.3339	15.4357
19	50.0607	50.1004	30.2936	28.5908	22.3401	22.2585	17.1875	15.2120	15.3896	15.3326	15.4331
20	50.0595	50.0874	30.2905	28.6618	22.2126	21.9687	17.0688	15.1606	15.4323	15.2960	15.4296
21	50.0687	50.1042	30.3208	28.6735	22.2229	21.9629	17.0778	15.1670	15.4399	15.3076	15.4390
219	50.0641	50.0996	31.4452	30.2874	22.4419	22.3902	17.1914	15.3527	15.2039	15.4680	15.3299
220	50.0781	50.1060	31.4665	30.3144	22.4245	22.3920	17.1888	15.3455	15.2012	15.4626	15.3228
222	50.0451	50.0698	31.5665	30.6333	22.2731	22.2071	17.0420	15.3928	15.0799	15.5254	15.2493
22	50.0769	50.1026	31.9699	30.4924	25.4508	25.3488	21.3770	19.8870	19.9674	19.9931	20.0221
23	50.0833	50.1155	31.9538	30.4789	25.4268	25.3363	21.3313	19.8490	19.9405	19.9476	19.9757
181	50.1218	50.1584	32.2144	30.8893	25.2518	25.1796	21.3190	19.8167	20.0357	19.9544	20.0034
182	50.1229	50.1562	32.1957	30.8718	25.2210	25.1457	21.3002	19.7880	20.0169	19.9289	20.0070
224	50.0837	50.1214	32.3704	31.1315	25.4587	25.4614	21.3497	19.9119	19.8407	20.0264	19.9466
225	50.0152	50.0453	32.6756	31.0205	25.3271	25.2955	21.2417	20.0211	19.7554	20.1517	19.9063
226	50.0227	50.0506	32.6850	31.0299	25.3245	25.2955	21.2336	20.0121	19.7474	20.1517	19.9018
227	50.0472	50.0805	32.8591	31.3859	25.1526	25.0853	21.0837	20.1484	19.6861	20.2968	19.8537
228	50.0579	50.0923	32.8564	31.3604	25.1432	25.0692	21.0797	20.1162	19.6687	20.2566	19.8288
229	50.1121	50.1444	34.0118	32.5012	27.0151	26.9483	23.4942	22.8665	22.3081	23.0066	22.5099
230	50.1100	50.1433	34.0024	32.5052	27.0165	26.9750	23.4888	22.8683	22.3135	22.9986	22.5019
231	50.1204	50.1516	33.5607	32.0585	27.4764	27.4787	23.8437	22.7010	22.5596	22.8062	22.6475
232	50.0785	50.1054	33.5874	32.0733	27.4831	27.4787	23.8611	22.7046	22.5663	22.8330	22.6662
233	50.0973	50.1284	33.2861	31.9903	27.5517	27.4060	23.9140	22.5708	22.7064	22.6836	22.7416
234	50.0973	50.1295	33.2968	32.0118	27.5838	27.4114	23.9422	22.6120	22.7373	22.7264	22.7772
235	50.0953	50.1243	36.2116	34.8178	31.4106	31.4262	28.5775	27.7627	27.5775	27.8397	27.6757
236	50.1157	50.1404	36.2529	34.8555	31.4133	31.4404	28.6003	27.7556	27.5829	27.8691	27.7007
237	50.1095	50.1503	36.0791	34.8915	31.5438	31.4178	28.7033	27.6506	27.7343	27.7698	27.7868
238	50.1245	50.1503	36.0898	34.9104	31.5612	31.4303	28.7141	27.6703	27.7383	27.7859	27.7992
239	50.1432	50.1668	36.4662	35.0639	30.9830	30.9473	28.2565	27.9402	27.3504	28.0399	27.5610
240	50.1346	50.1550	36.4449	35.0505	30.9629	30.9527	28.2538	27.9205	27.3451	28.0198	27.5476
241	50.1608	50.1888	40.9766	39.9497	37.9386	37.9680	36.1799	35.7003	35.5658	35.7793	35.6236
242	50.1469	50.2017	41.0152	40.0048	37.9920	37.9875	36.1772	35.7647	35.6033	35.8514	35.6342
243	50.1721	50.1926	40.9053	40.1267	38.0675	38.0475	36.3403	35.7230	35.7516	35.7707	35.7672
244	50.1732	50.1861	40.9013	40.1307	38.0688	37.9799	36.3550	35.7087	35.6953	35.7721	35.7823
245	50.1703	50.1843	41.1268	40.0394	37.5952	37.6165	35.9730	35.9390	35.4581	35.9804	35.5995
246	50.1747	50.1983	41.1295	40.0515	37.6085	37.6183	35.9770	35.9783	35.4634	35.9937	35.6004
247	50.1996	50.2178	44.7661	44.0998	42.8856	42.9278	41.8879	41.6672	41.5354	41.7051	41.5948
248	50.2049	50.2060	44.7781	44.1146	42.8909	42.9438	41.9187	41.6815	41.5501	41.7291	41.6313
249	50.1462	50.1623	44.5595	44.1497	42.8951	42.9435	41.9309	41.5775	41.5824	41.6039	41.6079
250	50.1462	50.1623	44.5702	44.1524	42.9044	42.9417	41.9376	41.5811	41.5905	41.6119	41.6141
251	50.1549	50.1711	44.6733	44.0506	42.7461	42.7896	41.8254	41.6820	41.4689	41.7203	41.5527
252	50.1388	50.1517	44.6600	44.0412	42.7501	42.7985	41.8187	41.6963	41.4810	41.7177	41.5465
253	50.1416	50.1502	44.6209	44.0125	42.6349	42.6470	41.6883	41.7923	41.4390	41.7639	41.5025
254	50.1415	50.1587	44.6405	44.0336	42.6586	42.6586	41.7134	41.8148	41.4601	41.7943	41.5275

PERFORMANCE

Coolant Circuits

RDG.	Nozzle 1 Outer W_c Nozzle	Nozzle 1 Outer W_c Shroud	Nozzle 1 Outer P_c	Nozzle 1 Outer $T_{T,c}$	Nozzle 1 Inner W_c	Nozzle 1 Inner P_c	Nozzle 1 Inner $T_{T,c}$	Compressor Discharge Leakage W_c	Compressor Discharge Leakage P_c	Compressor Discharge Leakage $T_{T,c}$
50	1.14265	0.129376	50.0761	624.136	0.850488	51.0809	584.620	0.350135	40.1799	590.542
51	1.13933	0.129055	50.0009	624.617	0.849614	51.0218	584.865	0.382229	40.2418	600.244
52	1.16305	0.129500	50.1509	628.004	0.850731	51.0697	584.770	0.441506	40.7174	609.134
53	1.15627	0.129354	50.1374	629.079	0.850292	51.0644	584.739	0.442990	40.6825	609.363
54	1.14831	0.129718	50.0700	627.546	0.854438	51.0883	588.509	0.745691	41.7393	588.793
55	1.14213	0.129587	50.0378	624.914	0.858498	51.0883	588.485	0.744259	41.7527	588.711
56	1.15614	0.129832	50.0930	624.548	0.854835	51.1059	589.378	0.750009	42.0742	588.917
57	1.15334	0.129845	50.0957	624.434	0.855341	51.1140	589.260	0.751547	42.1146	588.834
58	1.13422	0.130627	50.5884	626.242	0.844239	51.5904	589.544	0.812690	42.9734	588.510
59	1.13254	0.130387	50.5266	626.242	0.839924	51.5743	589.600	0.822791	43.0568	587.818
10	1.14936	0.128881	50.0749	629.697	0.849162	51.0825	586.256	0.302624	40.0012	592.917
11	1.14871	0.128786	50.0454	628.621	0.850292	51.0905	586.280	0.303726	40.0335	593.203
12	1.14347	0.128831	50.0857	629.765	0.852113	51.1066	586.920	0.353488	40.5042	594.610
13	1.12859	0.128539	50.0154	628.919	0.852090	51.1008	587.647	0.354359	40.5522	595.971
14	1.15612	0.129154	50.0772	627.523	0.849652	51.0928	587.647	0.353737	40.6302	596.464
15	1.15518	0.129037	50.0315	627.637	0.850945	51.0874	587.711	0.354547	40.5952	596.715
29	1.15042	0.128257	50.1267	633.953	0.844432	51.0026	587.513	0.345082	40.2440	598.218
31	1.15099	0.128154	50.1370	634.777	0.842342	51.0236	587.031	0.338321	40.3404	593.061
32	1.14307	0.127941	50.1068	635.691	0.842470	51.0391	586.968	0.327584	40.1218	593.138
33	1.13995	0.127922	50.1041	635.463	0.843026	51.0525	586.912	0.328305	40.1433	593.068
34	1.11616	0.127770	50.0505	634.479	0.839540	51.0473	586.604	0.326242	40.0574	593.143
35	1.13575	0.128086	50.1231	633.678	0.842171	51.0554	586.580	0.292739	39.5275	591.225
36	1.13102	0.128249	50.0278	632.786	0.837241	51.0138	587.568	0.352616	40.5861	594.969
38	1.13663	0.128428	50.0573	632.832	0.851220	51.0756	587.971	0.350714	40.7018	595.100
39	1.13344	0.128388	50.0519	633.152	0.860662	51.1239	588.145	0.350354	40.7072	595.243
40	1.12778	0.128393	49.9970	632.008	0.838815	50.9938	587.624	0.430208	41.7011	596.463
41	1.14306	0.127934	50.1314	638.081	0.837696	50.9857	587.655	0.430472	41.7281	596.486
42	1.14757	0.127880	50.0591	637.292	0.836160	50.9752	588.074	0.430924	42.2231	596.851
43	1.15114	0.128076	50.1020	637.044	0.837655	50.9779	587.995	0.431831	42.1344	596.866
44	1.16106	0.128068	50.1563	637.878	0.825972	50.9435	590.797	0.564023	42.6136	616.434
45	1.14050	0.128601	50.0112	633.607	0.819648	50.9274	591.482	0.562662	42.6835	617.182
47	1.13539	0.128556	50.0527	629.674	0.826741	50.9931	589.939	0.328341	40.2318	595.683
48	1.13971	0.129584	50.0653	628.141	0.846840	51.0756	583.348	0.350647	40.2391	589.322
49	1.12973	0.129452	50.0170	623.793	0.849405	51.0433	581.822	0.348311	40.1557	587.815
185	1.30983	0.130030	50.3625	636.639	0.886812	51.0879	591.730	0.355185	40.2406	598.711
186	1.31122	0.130025	50.3652	636.864	0.890321	51.1363	591.893	0.355590	40.2890	598.925
187	1.31609	0.130052	50.3786	636.098	0.894902	51.1470	591.986	0.356344	40.2245	599.136
188	1.32407	0.130340	50.4524	636.233	0.882413	51.1053	591.994	0.366155	40.3441	599.377
189	1.32342	0.130235	50.4228	636.481	0.884302	51.1026	592.118	0.365212	40.3199	599.379
190	1.30986	0.130022	50.3916	636.909	0.883583	51.1062	592.126	0.367370	40.3773	599.449
191	1.31174	0.129981	50.3862	636.886	0.882303	51.0982	592.219	0.366773	40.3289	599.458
206	1.30329	0.129571	50.3217	637.270	0.860836	50.9961	589.947	0.359396	40.2079	597.839
208	1.29916	0.129687	50.3620	637.224	0.858218	50.9934	591.505	0.356969	40.2321	599.026
209	1.29282	0.129588	50.3298	637.608	0.854457	50.9719	591.722	0.355229	40.1352	599.172
217	1.28967	0.129091	50.2364	640.176	0.854311	50.9431	593.949	0.388831	40.5125	602.955
67	1.15232	0.128940	50.0245	623.381	0.866696	51.0213	590.640	0.309308	39.7274	594.211
68	1.15345	0.128903	50.0541	624.434	0.864277	51.0428	590.593	0.310269	39.7274	594.269
69	1.18406	0.129481	50.2213	629.720	0.872420	51.0730	590.984	0.345707	40.3522	596.965
70	1.15816	0.128328	50.1085	628.621	0.869710	51.0865	590.867	0.313207	39.8142	595.254
71	1.15139	0.128504	50.1224	631.665	0.870650	51.0789	591.078	0.347850	40.3338	597.284
72	1.14871	0.128442	50.1036	631.505	0.864783	51.0735	590.953	0.347830	40.4038	597.176
73	1.16428	0.128185	50.0386	634.754	0.882459	51.0542	590.976	0.414149	41.1483	598.810
74	1.16030	0.128231	50.0520	634.434	0.882450	51.0649	590.945	0.413733	41.1376	598.778
75	1.15689	0.128233	50.0342	635.349	0.885050	51.0605	590.617	0.446889	41.7625	599.199
76	1.16039	0.128227	50.0234	635.029	0.886872	51.0659	590.624	0.446042	41.7464	599.017
77	1.15785	0.128078	50.0960	630.269	0.874148	51.0605	586.541	0.839958	42.8087	586.172
78	1.15891	0.128079	50.0852	629.949	0.876054	51.0578	586.296	0.839766	42.8195	585.855
16	1.16840	0.128839	50.1329	573.324	0.860379	51.1243	588.390	0.356876	41.0222	596.806

PERFORMANCE

RDG.	Coolant Circuits Nozzle 1 Outer W_c Nozzle	W_c Shroud	P_c	$T_{T,c}$	Nozzle 1 Inner W_c	P_c	$T_{T,c}$	Compressor Discharge Leakage W_c	P_c	$T_{T,c}$
17	1.18107	0.128996	50.1813	626.882	0.860394	51.1350	588.319	0.357119	41.1540	596.715
18	1.16315	0.129075	50.0983	626.242	0.876703	51.1300	564.263	0.357037	41.1355	573.446
19	1.16852	0.129220	50.1305	626.356	0.877053	51.1461	564.069	0.339282	41.0225	572.367
20	1.18046	0.129397	50.1987	626.150	0.852383	51.0611	590.780	0.412836	42.3548	597.972
21	1.18055	0.129061	50.1203	626.905	0.850941	51.0848	591.916	0.412112	42.2064	599.021
219	1.32996	0.128914	50.4166	630.544	0.883483	50.9513	586.661	0.414171	40.3808	615.339
220	1.32563	0.129078	50.4623	630.612	0.883747	50.9566	587.495	0.425747	40.4346	616.514
222	1.32586	0.128482	50.3922	633.757	0.870970	50.8892	591.796	0.410960	39.9394	621.807
22	1.14426	0.126944	50.1386	624.846	0.848131	51.0978	591.908	0.404824	42.5825	597.669
23	1.13873	0.126975	50.1413	624.662	0.846858	51.1005	591.769	0.404208	42.5878	597.710
181	1.20763	0.128363	50.3776	628.118	0.805473	51.0224	588.620	0.563795	42.9749	614.691
182	1.21333	0.128501	50.3830	626.859	0.792582	50.9472	588.683	0.564726	42.9507	614.874
224	1.29475	0.128545	50.2982	636.713	0.871032	50.9537	597.154	0.439972	41.4054	624.281
225	1.32035	0.128814	50.3016	630.921	0.862213	50.8309	585.839	0.311694	40.8117	588.358
226	1.32773	0.129040	50.3338	629.269	0.860429	50.8255	586.156	0.312587	40.7687	589.422
227	1.31095	0.127927	50.4943	632.011	0.869179	50.9161	587.458	0.357261	41.1096	596.202
228	1.30102	0.127413	50.3573	632.864	0.869098	50.9161	583.445	0.356554	40.9455	591.899
229	1.30923	0.127600	50.3873	628.187	0.854051	50.9596	588.691	0.359634	41.5377	595.512
230	1.29804	0.127610	50.4061	628.782	0.855930	50.9515	588.706	0.365436	41.5995	596.524
231	1.29830	0.128034	50.4305	631.001	0.851851	50.9464	590.381	0.371092	42.1592	598.376
232	1.27610	0.127127	50.2236	631.139	0.850290	50.8953	589.892	0.364293	42.1162	597.643
233	1.29966	0.128523	50.3047	626.402	0.857274	50.9361	591.028	0.431989	42.9960	598.806
234	1.29938	0.128633	50.3450	626.653	0.853784	50.9361	592.560	0.431146	42.9880	600.044
235	1.24478	0.122310	50.3511	632.672	0.841463	50.9636	588.145	0.394063	43.5802	595.363
236	1.23743	0.122142	50.3349	633.702	0.841274	50.9824	588.746	0.394067	43.5883	595.495
237	1.25865	0.122398	50.3239	632.878	0.836761	50.9553	590.248	0.411033	44.0667	598.127
238	1.25208	0.122379	50.3373	632.786	0.836707	50.9499	590.397	0.411233	44.0989	598.600
239	1.23074	0.121450	50.2474	632.924	0.837015	50.9943	588.951	0.375528	42.9764	600.742
240	1.23077	0.121747	50.3065	633.084	0.835565	50.9916	589.655	0.375471	42.9602	601.076
241	1.12180	0.107466	50.3419	625.807	0.786683	51.0136	580.660	0.371278	45.6252	589.982
242	1.10930	0.107216	50.3231	624.594	0.786574	51.0512	578.993	0.373021	45.6978	588.784
243	1.12020	0.106593	50.3871	636.571	0.782385	51.0023	587.339	0.369805	46.0306	596.147
244	1.12012	0.106397	50.3495	636.594	0.780591	51.0023	587.300	0.369470	46.0280	596.141
245	1.11377	0.106836	50.4369	635.760	0.784700	51.0199	585.656	0.370618	45.2283	594.788
246	1.11403	0.106899	50.4476	635.349	0.780317	51.0199	587.782	0.369277	45.1987	596.802
247	0.962893	0.869807E-01	50.4779	635.811	0.703198	51.0314	583.498	0.361887	47.6805	590.849
248	0.939012	0.866234E-01	50.4725	639.951	0.699762	51.0314	584.810	0.357928	47.7370	591.327
249	0.331151	0.865569E-01	50.3128	632.603	0.698693	50.9684	583.158	0.356608	47.8782	590.312
250	0.932061	0.364741E-01	50.3074	632.260	0.699669	50.9764	583.205	0.355830	47.8728	590.396
251	0.926587	0.866188E-01	50.3602	636.204	0.703444	50.9862	579.886	0.358727	47.5897	586.357
252	0.931686	0.863463E-01	50.3333	638.306	0.701256	50.9782	580.186	0.357374	47.5870	587.497
253	0.939009	0.867713E-01	50.3732	633.976	0.705563	50.9831	577.080	0.359752	47.5542	583.652
254	0.940246	0.867447E-01	50.3849	633.130	0.706459	50.9840	575.049	0.360132	47.5525	581.345

PERFORMANCE

Coolant Circuits

RDG	Inducer W_c	Inducer $P_{c,in}$	Inducer $P_{c,out}$	Inducer $T_{T,c}$	Nozzle 2 Outer W_c	Nozzle 2 Outer P_c	Nozzle 2 Outer $T_{T,c}$
50	1.69476	49.4598	40.4857	618.343	0.583629	23.6773	640.530
51	1.69327	49.4939	40.5538	618.335	0.589734	23.7861	639.464
52	1.65847	49.5883	41.1254	618.547	0.558424	23.2739	643.991
53	1.65677	49.5597	41.0859	618.616	0.559784	23.2417	643.855
54	1.58834	49.6875	42.1176	620.495	0.548112	23.1072	646.096
55	1.59003	49.6911	42.1068	620.548	0.560265	23.4483	645.833
56	1.55182	49.6281	42.5063	621.775	0.537620	22.9783	651.175
57	1.55338	49.6747	42.5440	621.675	0.539418	23.0052	651.363
58	1.50630	49.9999	43.4682	622.832	0.534207	22.9484	650.703
59	1.51245	50.1056	43.5381	622.955	0.546395	23.2627	650.141
10	1.69930	49.6262	40.5446	619.715	0.577137	23.4720	641.632
11	1.70073	49.6494	40.5697	619.571	0.575808	23.6037	641.975
12	1.66640	49.5312	40.8602	620.306	0.586072	23.5137	641.705
13	1.66603	49.6078	40.9530	621.464	0.598425	23.4138	641.136
14	1.65916	49.5594	40.9888	621.503	0.576073	23.9443	640.497
15	1.65717	49.5308	41.0336	621.450	0.582486	24.0800	641.374
29	1.67066	49.4433	40.6933	621.514	0.579754	23.5467	641.567
31	1.68098	49.5198	40.6766	621.224	0.582707	23.7248	642.808
32	1.68663	49.4502	40.5459	621.195	0.576657	23.6436	645.420
33	1.68575	49.4627	40.5675	621.379	0.577476	23.5992	645.140
34	1.69509	49.4530	40.4269	621.020	0.599661	23.9620	642.207
35	1.69408	49.1628	40.0377	620.968	0.582996	23.5766	643.129
36	1.64888	49.4634	40.9914	621.966	0.570905	23.5001	642.655
38	1.64855	49.5906	41.2317	622.255	0.576891	23.5793	642.482
39	1.64854	49.5924	41.2119	622.240	0.580904	23.6639	641.687
40	1.58134	49.6405	42.1601	622.496	0.564525	23.3847	645.679
41	1.58188	49.6692	42.1799	622.381	0.567082	23.4250	645.665
42	1.55150	49.7581	42.7225.	622.832	0.569107	23.5381	649.563
43	1.54221	49.6291	42.6328	622.977	0.556052	23.1418	651.008
44	1.49358	49.6654	43.1299	626.911	0.558815	23.2203	650.094
45	1.50106	49.8016	43.2214	627.521	0.558679	23.2109	649.486
47	1.66965	49.4347	40.6577	623.852	0.584319	23.7923	643.316
48	1.68185	49.4365	40.6363	617.079	0.581478	23.7136	642.844
49	1.68221	49.3595	40.5484	615.820	0.592121	23.9057	641.334
185	1.67359	49.1093	40.6620	624.415	0.583519	23.7703	639.304
186	1.67565	49.1613	40.6997	624.522	0.583976	23.8670	639.408
187	1.66944	49.0412	40.6333	624.737	0.574579	23.6118	639.789
188	1.66752	49.0917	40.7251	624.540	0.583629	23.7702	638.202
189	1.66637	49.0738	40.7090	625.099	0.586083	23.8561	638.225
190	1.66759	49.1178	40.7512	625.136	0.579504	23.7470	638.857
191	1.66462	49.0712	40.7154	624.992	0.580086	23.6422	638.712
206	1.67160	49.0372	40.6149	623.545	0.577029	23.5939	639.995
208	1.67146	49.0766	40.6526	624.801	0.573258	23.5858	640.967
209	1.66491	48.9548	40.5378	624.854	0.571319	23.5388	640.597
217	1.65740	49.0477	40.7690	627.287	0.573393	23.5972	644.716
67	1.70905	49.2953	40.2421	623.690	0.613642	25.2359	641.820
68	1.70888	49.2666	40.2493	623.888	0.610346	24.9378	642.506
69	1.68916	49.4814	40.8014	624.125	0.558641	24.1650	645.882
70	1.69421	49.2055	40.3800	624.128	0.606987	24.8606	642.959
71	1.65188	49.2311	40.9130	624.499	0.578614	24.6167	643.618
72	1.65844	49.2974	40.9381	624.370	0.578651	24.5966	643.771
73	1.60894	49.3596	41.6818	624.520	0.575130	24.3946	645.066
74	1.60916	49.3506	41.6800	624.505	0.575657	24.4027	644.890
75	1.56470	49.4125	42.3067	624.687	0.574831	24.3150	648.769
76	1.56393	49.3802	42.2780	624.534	0.579407	24.3123	648.490
77	1.49708	49.5666	43.3035	620.474	0.567017	24.1673	649.777
78	1.49611	49.5702	43.2945	620.122	0.565061	24.2089	649.077
16	1.62472	49.6384	41.6023	622.436	0.587115	25.9485	646.853

PERFORMANCE

Coolant Circuits

RDG	Inducer W_c	Inducer $P_{c,in}$	Inducer $P_{c,out}$	Inducer $T_{T,c}$	Nozzle 2 Outer W_c	Nozzle 2 Outer P_c	Nozzle 2 Outer $T_{T,c}$
17	1.63686	49.6976	41.5592	622.161	0.568643	26.2318	646.470
18	1.62783	49.4551	41.8814	600.913	0.580395	25.9072	647.801
19	1.63154	49.5985	41.8455	600.844	0.603328	25.6816	647.087
20	1.54034	49.9649	42.8828	625.065	0.598355	25.5859	649.140
21	1.53243	49.6653	42.7192	626.506	0.585213	25.9373	649.843
219	1.66086	49.0533	40.8928	618.944	0.606693	26.3757	637.269
220	1.65248	49.0407	40.9502	619.614	0.608810	26.0361	637.215
222	1.66422	48.7744	40.4021	623.605	0.627151	26.3728	637.038
22	1.50743	49.7365	43.0127	626.766	0.568939	28.3787	656.308
23	1.50615	49.8117	43.0773	626.963	0.570026	28.1867	656.664
181	1.45604	49.4030	43.5503	625.566	0.552894	28.1168	657.914
182	1.45531	49.3887	43.5449	625.695	0.547933	28.0564	657.932
224	1.55012	49.0199	41.9944	629.515	0.580609	28.5313	648.227
225	1.60856	48.9320	41.3954	618.517	0.606208	28.7428	643.559
226	1.60892	48.9123	41.3793	618.785	0.604586	28.7629	643.159
227	1.62458	49.2044	41.5498	620.035	0.618992	28.3797	644.480
228	1.61797	49.0074	41.4153	616.567	0.623715	28.9326	643.723
229	1.57132	49.0902	41.9339	621.954	0.614419	30.7675	643.953
230	1.57023	49.1547	42.0128	622.230	0.649542	30.6508	644.520
231	1.52664	49.3744	42.7114	624.073	0.602358	30.3719	652.068
232	1.53459	49.3225	42.6558	623.462	0.598978	30.7771	650.084
233	1.44664	49.3015	43.5491	625.646	0.571303	30.3173	656.205
234	1.44190	49.3122	43.5652	627.239	0.569385	30.3522	655.898
235	1.41350	49.4965	44.0562	623.796	0.566303	33.8503	659.493
236	1.41325	49.5109	44.0598	624.320	0.578193	34.1655	659.220
237	1.34754	49.5133	44.7397	627.016	0.543414	33.7722	667.056
238	1.34770	49.5312	44.6967	627.458	0.541099	33.7936	667.007
239	1.47398	49.3893	43.2856	624.238	0.623991	34.3450	652.600
240	1.46947	49.3947	43.3376	624.645	0.612698	34.2216	654.381
241	1.18529	49.7212	46.0643	621.134	0.471553	39.4658	679.581
242	1.18357	49.6245	45.8869	619.902	0.465073	39.4363	681.256
243	1.14231	49.8586	46.5136	627.113	0.444603	39.3821	690.241
244	1.14215	49.8855	46.4921	627.214	0.443990	39.3835	689.919
245	1.23854	49.6738	45.5975	624.438	0.516829	39.6637	671.756
246	1.23263	49.6433	45.5706	625.946	0.518709	39.6597	671.547
247	0.918375	50.1609	48.0828	626.231	0.357765	43.7209	705.320
248	0.922240	50.2612	48.1150	627.385	0.360291	43.7584	706.500
249	0.866014	50.1587	48.2831	628.130	0.347702	43.6916	711.568
250	0.867076	50.1444	48.2903	628.015	0.346219	43.6929	711.836
251	0.936955	50.0879	47.8987	622.826	0.382450	43.7844	702.137
252	0.933702	50.0969	47.8969	623.612	0.382886	43.7911	701.843
253	0.962470	50.0875	47.7549	620.820	0.384746	43.6915	704.059
254	0.962353	50.0777	47.7559	618.850	0.384524	43.7193	703.982

COOLING FLOW VARIATION

Rdg	$P_{T,4}/P_{S,42}$	$P_{T,4}/P_{T,42}$	$N/\sqrt{T_{T,41}}$ rpm/$\sqrt{°R}$	U/C_o	$W_{41}\sqrt{T_{T,41}}/P_{T,4}$ $\frac{lbm\sqrt{°R}}{sec\ psia}$	$\Delta h/T_{T,41}$ Btu/(lbm °R) Measured	$\Delta h/T_{T,41}$ Btu/(lbm °R) w/Pumping
111	5.57269	5.00357	236.998	0.579579	18.1669	0.823321E-01	0.838170E-01
112	5.58017	5.00984	236.704	0.578774	18.1677	0.824878E-01	0.839703E-01
113	5.57257	5.01067	236.919	0.579454	18.1728	0.823347E-01	0.838191E-01
114	5.57038	5.00545	236.712	0.578956	18.1623	0.822758E-01	0.837568E-01
115	5.57994	5.00861	236.933	0.579388	18.1654	0.824174E-01	0.839002E-01
116	5.56298	4.99786	236.882	0.579623	18.1709	0.822935E-01	0.837767E-01
117	5.56606	5.00074	236.793	0.579276	18.1664	0.821988E-01	0.836805E-01
118	5.56590	4.99614	236.968	0.579677	18.1647	0.824610E-01	0.839430E-01
119	5.56637	4.99322	237.215	0.580322	18.1669	0.822377E-01	0.837238E-01
120	5.57850	5.00579	237.121	0.579716	18.1613	0.827172E-01	0.841966E-01
121	5.56856	4.99660	237.030	0.579819	18.1614	0.827535E-01	0.842332E-01
122	5.56273	4.98710	237.023	0.579821	18.1578	0.826596E-01	0.841396E-01
123	5.56092	4.98769	237.021	0.579922	18.1611	0.826788E-01	0.841537E-01
124	5.57252	4.99952	236.860	0.579250	18.1643	0.824240E-01	0.839015E-01
125	5.56844	4.99771	237.092	0.579978	18.1711	0.824548E-01	0.839323E-01
126	5.57082	4.99774	237.193	0.580073	18.1665	0.825872E-01	0.840640E-01
127	5.57535	4.99889	236.963	0.579430	18.1676	0.825638E-01	0.840422E-01
129	5.55460	4.98404	236.738	0.579423	18.1208	0.823603E-01	0.838277E-01
130	5.54622	4.97641	236.645	0.579333	18.1556	0.823839E-01	0.838990E-01
131	5.53682	4.96990	236.742	0.579834	18.1626	0.824259E-01	0.839367E-01
132	5.56578	5.00038	236.634	0.578834	18.1790	0.826989E-01	0.839918E-01
133	5.56068	4.99510	236.718	0.579170	18.1902	0.824596E-01	0.837547E-01
134	5.57808	5.00203	237.162	0.579865	18.1688	0.825533E-01	0.840233E-01
135	5.57756	5.00248	237.183	0.579940	18.1666	0.826764E-01	0.841431E-01
138	5.54823	4.98272	236.681	0.579362	18.1626	0.824362E-01	0.839054E-01
139	5.55401	4.98147	236.272	0.578227	18.1649	0.824070E-01	0.838759E-01

Rdg	Average Clearance (inches x 10^3) Stg 1	Stg 2	η_{GE} Measured	η_{TH} Measured	η_{GE} Corrected to 0.016 in. Tip Clearance	η_{TH} Corrected	η_{THP} Corrected
111	18.1	14.0	0.922234	0.884147	0.9228	0.8847	0.9007
112	18.2	14.6	0.923381	0.885484	0.9242	0.8863	0.9022
113	18.0	14.3	0.921595	0.883564	0.9222	0.8842	0.9001
114	17.7	13.5	0.921425	0.882533	0.9217	0.8828	0.8987
115	17.8	13.5	0.922741	0.883732	0.9231	0.8841	0.9000
116	18.3	13.3	0.922299	0.882490	0.9228	0.8830	0.8989
117	18.2	13.3	0.920959	0.881226	0.9215	0.8817	0.8976
118	18.3	13.3	0.924347	0.883650	0.9248	0.8841	0.9000
119	18.3	13.1	0.922097	0.881614	0.9226	0.8821	0.8980
120	19.1	12.5	0.926320	0.884188	0.9271	0.8350	0.9008
121	18.4	13.9	0.927555	0.885400	0.9283	0.8861	0.9019
122	18.8	13.7	0.927371	0.884435	0.9282	0.8852	0.9011
123	18.5	13.6	0.927537	0.884682	0.9282	0.8854	0.9012
124	18.3	13.7	0.923580	0.882110	0.9242	0.8827	0.8985
125	18.6	13.8	0.924104	0.882803	0.9248	0.8835	0.8993
126	18.6	14.0	0.925632	0.884415	0.9264	0.8852	0.9010
127	19.1	13.6	0.925217	0.883936	0.9262	0.8849	0.9008
129	18.6	15.3	0.924264	0.879181	0.9253	0.8802	0.8958
130	18.8	13.6	0.925203	0.882256	0.9260	0.8831	0.8993
131	18.9	13.5	0.926289	0.883450	0.9272	0.8843	0.9005
132	17.5	12.5	0.926542	0.889664	0.9266	0.8898	0.9037
133	17.5	12.7	0.924357	0.887580	0.9245	0.8877	0.9016
134	17.9	13.3	0.924860	0.883385	0.9252	0.8837	0.8994
135	18.1	13.2	0.926213	0.884779	0.9266	0.8852	0.9009
138	18.0	13.5	0.925222	0.883682	0.9257	0.8842	0.8999
139	18.2	13.4	0.924924	0.883292	0.9255	0.8839	0.8996

COOLING FLOW VARIATION

Rdg	Inlet P_T	Inlet T_T	Inlet W	Vane 1 Exit W	Vane 1 Exit T_T	Loading, ψ_P Meas.	Loading, ψ_P With Pumping	$TQ/P_{T,4}$ ft. in^2 With Pumping	Reaction, R_x Hub	Reaction, R_x Tip	Exit Swirl Γ, degrees
111	50.1851	1274.80	23.9598	26.0732	1222.71	0.652122	0.663883	47.7333	0.382288	0.448137	0.
112	50.1938	1276.62	23.9403	26.0639	1224.12	0.654983	0.666755	47.8824	0.382786	0.447831	0.
113	50.1902	1276.10	23.9600	26.0707	1223.99	0.652576	0.664341	47.7659	0.382753	0.448405	0.
114	50.1942	1274.79	23.9703	26.0665	1223.16	0.653256	0.665015	47.7446	0.379684	0.446769	0.
115	50.1867	1273.86	23.9788	26.0762	1222.30	0.653158	0.664909	47.7899	0.379885	0.446957	0.
116	50.1828	1275.55	23.9632	26.0666	1223.76	0.652456	0.664216	47.7444	0.377536	0.446243	0.
117	50.1819	1276.57	23.9458	26.0498	1224.68	0.652194	0.663951	47.6954	0.377487	0.446102	0.
118	50.1770	1274.90	23.9537	26.0615	1223.12	0.653310	0.665051	47.8054	0.376047	0.444844	0.
119	50.1837	1275.39	23.9608	26.0618	1223.71	0.650185	0.661934	47.6367	0.376402	0.444787	0.
120	50.1819	1275.50	23.9589	26.0493	1224.04	0.654492	0.666197	47.9098	0.372707	0.443364	0.
121	50.1938	1275.23	23.9801	26.0500	1224.57	0.655285	0.667002	47.9494	0.372216	0.442764	0.
122	50.1225	1276.60	23.8968	26.0072	1224.63	0.654578	0.666298	47.8880	0.371789	0.442410	0.
123	50.1211	1276.07	23.9110	26.0141	1224.36	0.654740	0.666420	47.9051	0.371412	0.442185	0.
124	50.1198	1277.25	23.8999	26.0075	1225.34	0.653615	0.665332	47.8025	0.374400	0.443869	0.
125	50.1329	1276.41	23.9238	26.0319	1224.61	0.652575	0.664268	47.7911	0.374588	0.444202	0.
126	50.1431	1274.01	23.9397	26.0554	1222.27	0.653068	0.664746	47.8335	0.372156	0.443956	0.
127	50.1365	1276.51	23.9163	26.0277	1224.71	0.654150	0.665863	47.8706	0.372590	0.443597	0.
129	50.1823	1277.05	23.8933	25.9696	1226.10	0.653778	0.665427	47.6706	0.440304	0.452683	0.
130	50.1947	1277.84	23.9532	26.0119	1227.42	0.654483	0.666519	47.8216	0.379433	0.444199	0.
131	50.1876	1277.03	23.9658	26.0257	1226.71	0.654281	0.666273	47.8420	0.378699	0.444139	0.
132	50.1630	1278.38	23.9429	26.0303	1227.29	0.657044	0.667316	47.9382	0.367157	0.441546	0.
133	50.1730	1277.63	23.9674	26.0590	1226.59	0.654681	0.664963	47.8157	0.366860	0.441300	0.
134	50.1885	1279.09	23.7767	26.0812	1222.37	0.652973	0.664600	47.8228	0.375966	0.445532	0.
135	50.1950	1278.03	23.7915	26.0904	1221.54	0.653831	0.665430	47.8810	0.375325	0.445228	0.
138	50.1907	1278.24	23.9386	26.0262	1226.83	0.654699	0.666368	47.8364	0.373326	0.442123	0.
139	50.1945	1282.76	23.9004	25.9861	1231.10	0.656736	0.668442	47.9084	0.373353	0.441896	0.

COOLING FLOW VARIATION - Flowpath Static Pressures (psia)

Rdg	Inlet Rake Plane Outer	Inlet Rake Plane Inner	Vane 1 Exit Outer	Vane 1 Exit Inner	Blade 1 Exit Outer	Blade 1 Exit Inner	Vane 2 Exit Inner	Blade 2 Exit Outer	Blade 2 Exit Inner	Exit Rake Plane Outer	Exit Rake Plane Inner
111	50.1028	50.1393	30.3633	28.6943	19.9838	19.7656	12.8671	8.68646	9.10616	8.89882	9.11226
112	50.1082	50.1415	30.3432	28.6903	19.9758	19.7478	12.8604	8.66491	9.08461	8.88405	9.10600
113	50.1092	50.1350	30.3659	28.7010	19.9771	19.7585	12.8671	8.66491	9.08731	8.89747	9.11584
114	50.1060	50.1339	30.3713	28.7078	20.0373	19.8638	12.8953	8.67748	9.08596	8.90687	9.11495
115	50.1049	50.1393	30.3726	28.7145	20.0320	19.8656	12.8927	8.67928	9.08192	8.89210	9.09615
116	50.1016	50.1328	30.3936	28.7195	20.0919	19.9504	12.9246	8.71617	9.09367	8.90517	9.13651
117	50.0984	50.1253	30.3883	28.7168	20.0905	19.9486	12.9206	8.70360	9.08425	8.90651	9.12488
118	50.0989	50.1290	30.3901	28.7281	20.1379	20.0080	12.9439	8.74000	9.09686	8.91103	9.11911
119	50.1064	50.1354	30.3901	28.7375	20.1392	20.0080	12.9426	8.75616	9.09955	8.91372	9.11732
120	50.1020	50.1342	30.4149	28.7301	20.2202	20.1153	12.9755	8.75455	9.07191	8.88618	9.10499
121	50.1121	50.1369	30.4194	28.7306	20.2354	20.1266	12.9841	8.78020	9.08049	8.91758	9.10999
122	50.0397	50.0719	30.3789	28.7072	20.2457	20.1422	12.9877	8.79409	9.09348	8.90504	9.11580
123	50.0375	50.0676	30.3749	28.7018	20.2417	20.1440	12.9903	8.79049	9.09618	8.90772	9.11848
124	50.0369	50.0638	30.3646	28.7036	20.1685	20.0516	12.9491	8.74608	9.08184	8.88804	9.10015
125	50.0734	50.0810	30.3727	28.7063	20.1658	20.0481	12.9518	8.74429	9.08588	8.90147	9.10462
126	50.0705	50.0845	30.3671	28.6468	20.1576	20.0469	12.9489	8.75033	9.08968	8.89318	9.10887
127	50.0501	50.0877	30.3644	28.6563	20.1710	20.0469	12.9475	8.75751	9.09507	8.88782	9.09724
129	50.1009	50.1289	30.7556	30.6195	20.3273	20.2172	13.0522	8.76177	9.11503	8.91712	9.15160
130	50.1020	50.1353	30.4564	28.9065	20.2230	20.1047	12.9971	8.79947	9.12984	8.94263	9.15786
131	50.1031	50.1278	30.4470	28.8796	20.2149	20.0976	12.9971	8.80127	9.13523	8.96008	9.16860
132	50.0772	50.1062	30.2623	28.4738	20.0888	19.9861	12.9119	8.76634	9.10389	8.90602	9.11947
133	50.0836	50.1180	30.2637	28.4779	20.0941	19.9968	12.9173	8.77711	9.11601	8.91810	9.12752
134	50.1063	50.1428	30.3816	28.7463	20.1868	20.0690	12.9634	8.73483	9.06521	8.88893	9.10596
135	50.1095	50.1461	30.3762	28.7274	20.1828	20.0619	12.9607	8.74561	9.07329	8.89296	9.10596
138	50.1059	50.1327	30.3666	28.7124	20.1973	20.0710	12.9727	8.78720	9.11218	8.93706	9.15543
139	50.1091	50.1381	30.3573	28.7165	20.1946	20.0746	12.9781	8.79258	9.11756	8.93572	9.13932

COOLING FLOW VARIATION Coolant Circuits

Rdg	Nozzle 1 Outer W_c Nozzle	Nozzle 1 Outer W_c Shroud	Nozzle 1 Outer P_c	Nozzle 1 Outer $T_{T,c}$	Nozzle 1 Inner W_c	Nozzle 1 Inner P_c	Nozzle 1 Inner $T_{T,c}$	Compressor Discharge Leakage W_c	Compressor Discharge Leakage P_c	Compressor Discharge Leakage $T_{T,c}$
111	1.23987	0.129701	50.3924	628.278	0.873529	51.0560	582.162	0.357480	40.1549	591.699
112	1.24829	0.129712	50.4139	628.141	0.875347	51.0910	582.099	0.350984	40.1145	591.520
113	1.24494	0.129751	50.4220	628.324	0.865802	51.0131	582.194	0.358985	40.1898	591.916
114	1.23295	0.129605	50.3951	628.713	0.863216	51.0023	582.992	0.366411	40.2705	592.833
115	1.23608	0.129495	50.3629	628.965	0.861274	50.9943	582.889	0.365700	40.2517	592.508
116	1.24468	0.129710	50.4391	629.285	0.858685	50.9872	584.051	0.364187	40.2608	593.476
117	1.24620	0.129772	50.4552	629.949	0.857856	50.9818	583.948	0.363754	40.2392	593.529
118	1.24908	0.129695	50.4369	630.635	0.858767	50.9877	584.731	0.364163	40.2182	594.184
119	1.24191	0.129531	50.3993	630.200	0.859079	50.9957	584.707	0.364344	40.2505	594.144
120	1.23854	0.129553	50.4040	628.896	0.851857	50.9628	586.043	0.362832	40.1664	595.346
121	1.22476	0.128272	50.3749	634.860	0.845173	50.9391	586.209	0.362993	40.1911	595.461
122	1.24613	0.129276	50.3960	631.230	0.864266	51.0085	587.884	0.356790	40.1046	596.848
123	1.24265	0.129192	50.3610	631.436	0.860452	50.9843	588.098	0.355320	40.0400	596.953
124	1.24112	0.129197	50.3561	632.489	0.866445	51.0144	587.236	0.366271	40.2207	596.300
125	1.23632	0.129133	50.3534	632.809	0.871743	51.0385	587.489	0.365203	40.1535	596.315
126	1.23895	0.129155	50.3559	633.130	0.876786	51.0786	587.734	0.350351	40.1263	593.147
127	1.23612	0.129115	50.3639	634.548	0.875209	51.1001	588.066	0.350282	40.1667	593.337
129	1.21640	0.128597	50.3449	635.006	0.859894	51.0461	591.932	0.652991	40.3144	587.119
130	1.21738	0.128478	50.3288	638.351	0.841296	50.9602	588.738	0.391829	41.2585	597.119
131	1.22063	0.128427	50.3153	639.275	0.839286	50.9279	588.793	0.389809	41.1644	597.297
132	1.22609	0.128922	50.3727	637.878	0.861320	51.0337	590.993	0.351741	36.4167	626.859
133	1.23216	0.128967	50.3889	638.847	0.859468	51.0310	590.946	0.351580	36.4490	627.123
134	1.37571	0.132931	51.2718	630.017	0.928782	51.4276	591.365	0.354917	40.1960	597.605
135	1.37134	0.132799	51.2315	629.560	0.927512	51.4142	591.668	0.353549	40.1315	598.031
138	1.25029	0.130475	50.4213	629.445	0.837304	50.9909	592.001	0.356036	40.2107	598.715
139	1.24842	0.130478	50.4428	632.306	0.837322	51.0231	591.932	0.356540	40.2564	598.982

Rdg	Inducer W_c	Inducer $P_{c,in}$	Inducer $P_{c,out}$	Inducer $T_{T,c}$	Nozzle 2 Outer W_c	Nozzle 2 Outer P_c	Nozzle 2 Outer $T_{T,c}$
111	1.67888	49.0963	40.5628	616.408	0.322828	19.8033	677.486
112	1.68147	49.1196	40.5503	616.103	0.315733	19.7455	678.826
113	1.67900	49.1375	40.5987	616.225	0.322224	19.8288	679.158
114	1.67680	49.1464	40.6579	617.105	0.398305	20.7090	664.455
115	1.67638	49.1411	40.6435	617.097	0.400076	20.7037	664.232
116	1.67730	49.1492	40.6499	618.093	0.467798	21.7231	653.448
117	1.67615	49.1241	40.6212	618.085	0.466530	21.7043	653.479
118	1.67433	49.1103	40.6253	618.714	0.525962	22.6626	645.485
119	1.67641	49.1569	40.6217	618.691	0.520566	22.6223	645.448
120	1.66941	49.0352	40.5394	619.878	0.633612	24.6296	633.013
121	1.67191	49.0859	40.5686	619.993	0.637982	24.6785	633.358
122	1.67252	49.0711	40.5072	621.393	0.684488	25.6703	628.757
123	1.66757	48.9851	40.4354	621.768	0.682668	25.6059	628.948
124	1.66890	49.1003	40.6027	620.880	0.585539	23.7155	638.212
125	1.66612	49.0125	40.5435	621.064	0.585344	23.7115	638.953
126	1.66790	49.0346	40.5173	621.233	0.580894	23.6549	639.361
127	1.67143	49.0920	40.5585	621.294	0.582573	23.6670	639.578
129	1.65412	49.0568	40.6560	622.951	0.579000	23.7057	641.900
130	1.71627	50.3645	41.6225	621.543	0.578821	23.6560	641.847
131	1.71089	50.2463	41.5257	621.703	0.579305	23.6479	642.009
132	1.45702	44.1710	36.7880	628.905	0.589360	23.7873	639.873
133	1.45876	44.1979	36.8401	628.972	0.586312	23.7389	640.315
134	1.66319	49.0658	40.5664	624.487	0.584903	23.7608	640.100
135	1.65931	48.9833	40.5161	624.810	0.583449	23.7003	640.117
138	1.66652	49.1108	40.6007	625.697	0.583781	23.7525	641.297
139	1.66923	49.1860	40.6671	625.873	0.586536	23.7821	641.695

REYNOLDS NUMBER VARIATION

Rdg	$P_{T,4}/P_{S,42}$	$P_{T,4}/P_{T,42}$	$N/\sqrt{T_{T,41}}$ rpm/$\sqrt{°R}$	U/C_o	$W_{41}\sqrt{T_{T,41}}/P_{T,4}$ $\frac{lbm\sqrt{°R}}{sec\ psia}$	$\Delta h/T_{T,41}$ Btu/(lbm °R) Measured	w/Pumping
142	5.58631	5.02745	236.887	0.579441	18.1502	0.830335E-01	0.844806E-01
143	5.59349	5.03320	237.096	0.579864	18.1416	0.830553E-01	0.845077E-01
144	5.56649	4.98279	236.790	0.579427	18.1137	0.825693E-01	0.840333E-01
145	5.56746	4.98298	236.761	0.579380	18.1150	0.825434E-01	0.840067E-01
146	5.56961	5.00373	236.409	0.577957	18.1014	0.828167E-01	0.842734E-01
147	5.57235	5.00103	236.391	0.577867	18.1057	0.827257E-01	0.841778E-01
148	5.58059	5.00238	236.258	0.577658	18.0909	0.825967E-01	0.840332E-01
149	5.57734	5.00264	236.214	0.577433	18.0949	0.825630E-01	0.839994E-01
152	5.55067	4.96512	236.124	0.577901	18.0738	0.822686E-01	0.837151E-01
153	5.55602	4.97780	236.145	0.577907	18.0599	0.824778E-01	0.839143E-01
154	5.55496	4.97426	236.213	0.578737	18.1246	0.823196E-01	0.837640E-01
155	5.57748	5.00897	236.248	0.578308	18.1264	0.827390E-01	0.841813E-01
156	5.57901	5.00435	236.192	0.577704	18.1409	0.829063E-01	0.843717E-01
157	5.57349	4.99183	236.358	0.578274	18.1366	0.827585E-01	0.842236E-01

Rdg	Average Clearance (inches x 10^3) Stg 1	Stg 2	η_{GE} Measured	η_{TH} Measured	η_{GE} Corrected to 0.016 in. Tip Clearance	η_{TH}	η_{THP}
142	16.3	16.5	0.927879	0.883909	0.9281	0.8841	0.8995
143	16.3	16.6	0.927630	0.883624	0.9278	0.8838	0.8993
144	16.0	15.0	0.926703	0.884197	0.9265	0.8840	0.8997
145	16.1	15.8	0.926377	0.883964	0.9264	0.8840	0.8996
146	17.3	15.7	0.927523	0.884639	0.9280	0.8851	0.9007
147	15.7	15.7	0.926766	0.884073	0.9266	0.8839	0.8994
148	15.3	15.6	0.925179	0.882677	0.9248	0.8823	0.8976
149	15.3	15.4	0.924763	0.882164	0.9244	0.8818	0.8971
152	17.1	15.5	0.924895	0.882254	0.9253	0.8827	0.8982
153	16.7	15.6	0.926070	0.883805	0.9263	0.8840	0.8994
154	16.0	15.6	0.924588	0.882217	0.9245	0.8821	0.8976
155	16.5	15.5	0.926129	0.883670	0.9262	0.8838	0.8992
156	17.6	16.2	0.928473	0.884999	0.9292	0.8857	0.9013
157	16.7	16.5	0.927987	0.884516	0.9284	0.8849	0.9006

REYNOLDS NUMBER VARIATION

Rdg.	Inlet P_T	Inlet T_T	Inlet W	Vane 1 Exit W	Vane 1 Exit T_T	Loading, ψ_P Meas.	Loading, ψ_P With Pumping	$TQ/P_{T,4}$ ft. in^2 With Pumping	Reaction, R_x Hub	Reaction, R_x Tip	Exit Swirl Γ, degrees
142	53.1707	1275.18	25.3800	27.5772	1224.64	0.658293	0.669766	48.0896	0.411907	0.452670	0.
143	53.1727	1273.57	25.3888	27.5808	1223.25	0.657308	0.668802	48.0398	0.412756	0.452488	0.
144	45.2455	1276.62	21.5684	23.3954	1227.17	0.655151	0.666767	47.7583	0.395172	0.450257	0.
145	45.2459	1277.67	21.5579	23.3890	1228.04	0.655107	0.666720	47.7525	0.395611	0.450816	0.
146	40.1803	1279.78	19.1013	20.7469	1228.98	0.659234	0.670830	47.9395	0.396713	0.450738	0.
147	40.1789	1279.04	19.1074	20.7579	1228.18	0.658608	0.670169	47.8999	0.397044	0.450992	0.
148	35.1905	1279.11	16.7372	18.1587	1229.15	0.658326	0.669776	47.8057	0.393524	0.451652	0.
149	35.1900	1280.01	16.7323	18.1570	1229.88	0.658301	0.669754	47.8058	0.393636	0.451450	0.
152	32.6719	1279.33	15.5315	16.8371	1230.02	0.656452	0.667994	47.6064	0.394207	0.450737	0.
153	32.6735	1279.66	15.5194	16.8225	1230.39	0.658006	0.669466	47.6789	0.393473	0.449293	0.
154	37.6471	1280.75	17.9558	19.4401	1231.97	0.656368	0.667885	47.7503	0.391734	0.448991	0.
155	37.6474	1279.99	17.9626	19.4479	1231.25	0.659511	0.671007	47.9856	0.391721	0.449188	0.
156	50.1520	1279.27	23.8882	25.9542	1228.79	0.661163	0.672850	48.1443	0.393350	0.446864	0.
157	50.1510	1277.73	23.9004	25.9602	1227.59	0.659058	0.670725	48.0146	0.392900	0.446830	0.

Flowpath Static Pressures (psia)

Rdg	Inlet Rake Plane Outer	Inlet Rake Plane Inner	Vane 1 Exit Outer	Vane 1 Exit Inner	Blade 1 Exit Outer	Blade 1 Exit Inner	Vane 2 Exit Inner	Blade 2 Exit Outer	Blade 2 Exit Inner	Exit Rake Plane Outer	Exit Rake Plane Inner
142	53.0872	53.1248	32.4811	31.5485	21.4126	21.3306	13.7317	9.24475	9.58092	9.37084	9.66524
143	53.0915	53.1216	32.4784	31.5714	21.4140	21.3288	13.7263	9.20884	9.55130	9.34802	9.66434
144	45.1479	45.1695	27.5354	26.3981	18.1154	18.0797	11.7089	7.97264	8.27299	8.06418	8.19219
145	45.1479	45.1652	27.5461	26.4048	18.1181	18.0797	11.7089	7.99239	8.27568	8.06149	8.19219
146	40.0733	40.1250	24.4776	23.4925	16.0937	16.0700	10.4107	7.05078	7.31750	7.11145	7.31696
147	40.0841	40.1250	24.4776	23.4965	16.0870	16.0664	10.4080	7.05437	7.31750	7.10474	7.31606
148	35.1840	35.1840	21.4577	20.5303	14.0706	14.0817	9.13618	6.17464	6.44366	6.22123	6.39052
149	35.1840	35.1840	21.4523	20.5317	14.0706	14.0817	9.13618	6.17284	6.44366	6.22123	6.39769
152	32.6011	32.6022	19.9268	19.0663	13.0746	13.0607	8.51146	5.80063	6.00724	5.82632	5.94591
153	32.5882	32.6032	19.8960	19.0528	13.0692	13.0607	8.51685	5.77727	6.03958	5.81557	5.94591
154	37.6061	37.6104	22.9280	21.9363	15.0852	15.0718	9.79461	6.63812	6.88690	6.70892	6.84550
155	37.5985	37.6104	22.9280	21.9336	15.0785	15.0682	9.78922	6.56806	6.85053	6.65250	6.84729
156	50.0688	50.0957	30.4757	29.2386	20.1554	20.0635	12.9978	8.79390	9.10093	8.86948	9.10933
157	50.0699	50.0903	30.4784	29.2332	20.1540	20.0688	12.9991	8.82084	9.12113	8.88693	9.10933

REYNOLDS NUMBER VARIATION

Coolant Circuits

	Nozzle 1 Outer				Nozzle 1 Inner			Compressor Discharge Leakage		
	W_c		P_c	$T_{T,c}$	W_c	P_c	$T_{T,c}$	W_c	P_c	$T_{T,c}$
Rdg	Nozzle	Shroud								
142	1.31626	0.137164	53.4073	635.918	0.880930	54.0304	592.164	0.613877	43.5283	618.505
143	1.31341	0.137193	53.4100	635.418	0.878543	54.0304	592.118	0.621480	43.5767	613.951
144	1.09285	0.114958	45.3308	639.500	0.734167	45.9545	593.608	0.394268	36.2175	627.025
145	1.09591	0.114943	45.3308	639.703	0.735166	45.9545	593.755	0.396330	36.2175	627.245
146	0.996020	0.103175	40.4063	630.795	0.649569	40.8044	594.329	0.354710	32.3810	629.552
147	1.00048	0.103209	40.4171	630.887	0.649984	40.8125	594.415	0.353865	32.3272	629.492
148	0.844161	0.897459E-01	35.2943	633.953	0.577328	35.8111	594.818	0.307070	28.3230	630.843
149	0.844557	0.897210E-01	35.2916	634.297	0.580147	35.8138	594.865	0.313611	28.3203	632.387
152	0.775245	0.826926E-01	32.7357	639.725	0.530401	33.1719	593.064	0.286859	26.3766	633.144
153	0.773492	0.825738E-01	32.7142	640.176	0.529535	33.1719	592.987	0.280450	26.2796	631.575
154	0.899027	0.956142E-01	37.7083	636.098	0.585281	38.1550	592.467	0.325214	30.2434	628.767
155	0.900841	0.957220E-01	37.7352	636.098	0.584505	38.1550	592.498	0.331197	30.2299	630.089
156	1.22822	0.127831	50.3859	642.925	0.837714	51.0253	593.072	0.440809	40.2425	623.807
157	1.22488	0.127752	50.3725	644.029	0.834972	51.0253	593.258	0.440655	40.2344	624.151

	Inducer				Nozzle 2 Outer		
Rdg	W_c	$P_{c,in}$	$P_{c,out}$	$T_{T,c}$	W_c	P_c	$T_{T,c}$
142	1.70630	51.9424	43.6234	625.523	0.615877	25.0970	636.969
143	1.70817	52.0176	43.7112	625.077	0.615877	25.0715	636.806
144	1.49203	44.2176	36.5781	629.799	0.520176	21.3692	644.009
145	1.49197	44.2194	36.5638	630.078	0.518955	21.3840	644.361
146	1.32163	39.4656	32.6727	633.094	0.449982	18.8799	650.791
147	1.31842	39.4082	32.6279	633.110	0.445128	18.8100	651.107
148	1.13949	34.4374	28.5959	635.249	0.396672	16.6661	657.033
149	1.13970	34.4374	28.5959	635.378	0.394654	16.6352	657.280
152	1.06729	32.1487	26.6523	635.728	0.365067	15.4667	661.469
153	1.05975	32.0266	26.5284	635.984	0.366736	15.4573	661.594
154	1.22953	36.8579	30.5172	632.986	0.423590	17.8049	655.267
155	1.22683	36.7987	30.4939	633.107	0.420486	17.7122	655.358
156	1.66643	49.1838	40.6469	626.444	0.582331	23.7346	640.572
157	1.66454	49.1372	40.6002	626.848	0.582594	23.7722	640.446

CLEARANCE VARIATION

Rdg	$P_{T,4}/P_{S,42}$	$P_{T,4}/P_{T,42}$	$N/\sqrt{T_{T,41}}$ rpm/$\sqrt{°R}$	U/C_o	$W_{41}\sqrt{T_{T,41}}/P_{T,4}$ $\frac{lbm\sqrt{°R}}{sec\ psia}$	$\Delta h/T_{T,41}$ Btu/(lbm °R) Measured	$\Delta h/T_{T,41}$ Btu/(lbm °R) w/Pumping
192	5.57872	5.00208	237.434	0.580749	18.2038	0.823673E-01	0.839516E-01
193	5.58020	5.00336	237.210	0.580193	18.2034	0.824243E-01	0.840083E-01
194	5.58834	5.00879	237.444	0.580612	18.1873	0.826492E-01	0.842340E-01
195	5.58643	5.00922	237.130	0.579880	18.1893	0.826542E-01	0.842389E-01
196	5.57600	4.99343	237.700	0.581520	18.2315	0.820825E-01	0.836766E-01
197	5.57617	5.00239	237.488	0.581028	18.2276	0.821368E-01	0.837303E-01
200	5.58540	5.01365	237.190	0.580087	18.2046	0.824570E-01	0.840450E-01
201	5.58683	5.01082	237.244	0.580194	18.2064	0.824142E-01	0.840020E-01
202	5.58344	5.00751	237.313	0.580339	18.2063	0.825304E-01	0.841177E-01
203	5.58026	5.00799	237.202	0.580204	18.2026	0.825627E-01	0.841497E-01

Rdg.	Average Clearance (inches x 10^3) Stg 1	Stg 2	η_{GE} Measured	η_{TH} Measured	η_{THP} Calculated
192	15.9	16.6	0.922878	0.883213	0.900202
193	16.0	16.6	0.923362	0.883634	0.900616
194	10.9	16.0	0.925435	0.885685	0.902668
195	10.9	16.0	0.925392	0.885660	0.902640
196	22.3	16.2	0.920479	0.880798	0.897904
197	22.3	16.3	0.920234	0.880496	0.897578
200	16.8	21.0	0.922788	0.883071	0.900077
201	16.6	20.8	0.922578	0.882890	0.899900
202	16.1	11.2	0.924200	0.884443	0.901454
203	15.4	11.3	0.924486	0.884804	0.901812

Rdg	Inlet P_T	Inlet T_T	Inlet W	Vane 1 Exit W	Vane 1 Exit T_T	Loading, ψ_P Meas.	Loading, ψ_P With Pumping	$TQ/P_{T,4}$ ft. in^2 With Pumping	Reaction, R_x Hub	Reaction, R_x Tip	Exit Swirl Γ, degrees
192	50.2276	1273.81	23.9413	26.2101	1216.94	0.650007	0.662510	47.8190	0.384711	0.463883	0.
193	50.2272	1276.02	23.9192	26.1885	1218.87	0.651685	0.664209	47.8954	0.385056	0.464140	0.
194	50.2218	1273.57	23.9183	26.1889	1216.43	0.652178	0.664684	47.9346	0.390698	0.474176	0.
195	50.2209	1276.95	23.8876	26.1590	1219.44	0.653948	0.666486	48.0062	0.390554	0.473908	0.
196	50.2147	1273.64	23.9651	26.2471	1216.60	0.646311	0.658863	47.6818	0.377933	0.440906	0.
197	50.2087	1275.96	23.9339	26.2162	1218.65	0.647896	0.660465	47.7447	0.377907	0.441939	0.
200	50.2156	1276.88	23.8982	26.1805	1219.23	0.652056	0.664613	47.9238	0.386560	0.465142	0.
201	50.2123	1276.34	23.9007	26.1878	1218.63	0.651419	0.663970	47.8931	0.387129	0.465472	0.
202	50.2113	1274.65	23.9314	26.1986	1217.56	0.651963	0.664502	47.9449	0.383086	0.455975	0.
203	50.2077	1276.44	23.9079	26.1739	1219.18	0.652826	0.665375	47.9756	0.382877	0.456021	0.

CLEARANCE VARIATION

Flowpath Static Pressures (psia)

Rdg	Inlet Rake Plane Outer	Inlet Rake Plane Inner	Vane 1 Exit Outer	Vane 1 Exit Inner	Blade 1 Exit Outer	Blade 1 Exit Inner	Vane 2 Exit Inner	Blade 2 Exit Outer	Blade 2 Exit Inner	Exit Rake Plane Outer	Exit Rake Plane Inner
192	50.1465	50.1765	30.9202	29.0312	20.2181	20.1324	13.0099	8.75578	9.09288	8.89626	9.11060
193	50.1422	50.1776	30.9256	29.0393	20.2221	20.1342	12.9951	8.73423	9.08211	8.89492	9.10702
194	50.1394	50.1684	31.1143	29.1596	20.0941	20.1008	12.9713	8.73111	9.07719	8.88061	9.09316
195	50.1394	50.1684	31.0996	29.1583	20.0954	20.1097	12.9700	8.73111	9.07854	8.88195	9.09764
196	50.1281	50.1592	30.3949	28.8746	20.3837	20.1673	13.0431	8.73161	9.08442	8.90392	9.10708
197	50.1227	50.1560	30.4189	28.8732	20.3837	20.1691	13.0445	8.72263	9.08173	8.89318	9.11513
200	50.1331	50.1675	30.9013	29.0512	20.1671	20.1095	12.9452	8.75429	9.07119	8.87462	9.10641
201	50.1321	50.1643	30.9027	29.0620	20.1590	20.1059	12.9492	8.75788	9.07523	8.87328	9.10194
202	50.1308	50.1641	30.7389	29.0061	20.2841	20.1614	13.0494	8.69160	9.08526	8.88192	9.10387
203	50.1308	50.1609	30.7389	28.9980	20.2908	20.1632	13.0507	8.69160	9.08526	8.88461	9.11013

CLEARANCE VARIATION

Coolant Circuits

Rdg	Nozzle 1 Outer W_c Nozzle	Nozzle 1 Outer W_c Shroud	Nozzle 1 Outer P_c	Nozzle 1 Outer $T_{T,c}$	Nozzle 1 Inner W_c	Nozzle 1 Inner P_c	Nozzle 1 Inner $T_{T,c}$	Compressor Discharge Leakage W_c	Compressor Discharge Leakage P_c	Compressor Discharge Leakage $T_{T,c}$
192	1.36955	0.129948	50.3818	633.793	0.899271	51.0293	531.445	0.377233	40.2492	543.874
193	1.36888	0.129921	50.3738	633.130	0.900404	51.0374	531.067	0.378657	40.2815	543.906
194	1.37123	0.130020	50.3689	630.292	0.899431	51.0163	530.534	0.376587	40.2335	543.040
195	1.36984	0.130078	50.3769	630.109	0.901564	51.0190	530.452	0.377610	40.2685	542.971
196	1.37705	0.130201	50.3478	635.782	0.904996	51.0330	530.313	0.382425	40.2986	543.249
197	1.37817	0.130133	50.3505	635.601	0.904152	51.0437	530.264	0.382523	40.3147	543.252
200	1.37893	0.130226	50.4099	632.031	0.903391	51.0574	530.009	0.383071	40.3284	542.496
201	1.38279	0.130272	50.4206	631.825	0.904329	51.0493	529.976	0.383791	40.3176	542.886
202	1.36981	0.130232	50.3823	631.436	0.897429	51.0136	529.623	0.380434	40.2604	542.496
203	1.36899	0.130229	50.3823	631.299	0.896966	51.0271	529.722	0.380612	40.2711	542.630

Rdg	Inducer Wc	Inducer $P_{c,in}$	Inducer $P_{c,out}$	Inducer $T_{T,c}$	Nozzle 2 Outer W_c	Nozzle 2 Outer P_c	Nozzle 2 Outer $T_{T,c}$
192	1.76099	49.0077	40.6105	570.681	0.573907	23.5384	635.529
193	1.76356	49.0686	40.6356	570.353	0.576378	23.5707	635.126
194	1.75911	48.9759	40.5931	569.697	0.583221	23.6517	630.042
195	1.76181	49.0118	40.6182	569.635	0.585024	23.6786	629.916
196	1.77036	49.0947	40.6491	569.249	0.579494	23.6643	637.077
197	1.77124	49.1287	40.6671	569.298	0.578981	23.6925	638.206
200	1.76422	49.0349	40.6736	569.522	0.580433	23.6095	635.103
201	1.76359	49.0420	40.6790	569.178	0.579214	23.6068	634.894
202	1.76502	49.0171	40.6074	569.041	0.576775	23.6168	633.272
203	1.76443	49.0368	40.6271	569.137	0.574530	23.6181	633.456

ORIGINAL PAGE IS
OF POOR QUALITY

DISTRIBUTION

NASA Headquarters
600 Independence Avenue, SW
Washington, DC 20546
Attention: RTP-6/R.S. Colladay
RTP-6/C.C. Rosen
RTP-6/J. Facey (2 copies)
RTM-6/L. Harris

NASA-Lewis Research Center
21000 Brookpark Road
Cleveland, OH 44135
Attention:

D.L. Nored	MS 301-2	
C.C. Ciepluch	MS 301-4	(18 copies)
J.W. Schaefer	MS 301-4	
P.G. Batterton	MS 301-4	
G.K. Sievers	MS 301-2	
M.A. Beheim	MS 3-5	
M.J. Hartmann	MS 3-7	
R.A. Rudey	MS 86-5	
W.C. Strack	MS 501-10	
T.P. Moffitt	MS 77-2	
R.E. Jones	MS 86-6	
L.J. Kiraly	MS 23-2	
D.C. Mikkelson	MS 86-1	
A. Long	MS 500-305	
J.F. Groeneweg	MS 54-3	
W.M. Braithwaite	MS 500-208	
J.C. Williams	MS 500-211	
R.L. Davies	MS 106-1	
R.H. Johns	MS 49-6	
L.J. Kaszubinski	MS 86-2	
J.F. Sellers	MS 100-1	
J.R. Mihaloew	MS 100-1	
L. Reid	MS 5-9	
D.W. Drier	MS 86-2	
R.W. Niedzwiecki	MS 86-6	
AFSC Liaison Office	MS 501-3	
ARMY R&T Propulsion Lab	MS 302-2	

NASA Ames Research Center
Moffett Field, CA 94035
Attention: 202-7/M.H. Waters

NASA Langley Research Center
Langley Field, VA 23365
Attention: R. Leonard
D. Maiden
L.J. Williams

NASA Dryden Flight Research Center
P.O. Box 273
Edwards, CA 93523
Attention: J.A. Albers

Department of Defense
Washington, DC 20301
Attention: R. Standahar 3D1089 Pentagon

Wright-Patterson Air Force Base
Dayton, OH 45433
Attention: APL Chief Scientist AFWAL/PS
E.E. Abell ASD/YZE
H.I. Bush AFWAL/POT
E.E. Bailey (NASA Liaison) AFWAL/NASA
R.P. Carmichael ASD/XRHI
R. Ellis ASD/YZN
W.H. Austin, Jr. ASD/ENF

Eustis Directorate
U.S. Army Air Mobility
R&D Laboratory
Fort Eustis, VA 23604
Attention: J. Lane, SAVDL-EU-Tapp

NAVY Department
Naval Air Systems Command
Washington, DC 20361
Attention: W. Koven AIR-03E
J.L. Byers AIR-53602
E.A. Lichtman AIR-330E
G. Derderian AIR-5362C

NAVAL Air Propulsion Test Center
Trenton, NJ 08628
Attention: J.J. Curry
A.A. Martino

U.S. Naval Air Test Center
Code SY-53
Patuxent River, MD 20670
Attention: E.A. Lynch

USAVRAD Command
P.O. Box 209
St. Louis, MO 63166
Attention: Robert M. Titus

Detroit Diesel Allison Div. G.M.C.
333 West First St.
Dayton, OH 45202
Attention: F.H. Walters

Department of Transportation
NASA/DOT Joint Office of
Noise Abatement
Washington, D.C. 20590
Attention: C. Foster

Federal Aviation Administration
Noise Abatement Division
Washington, DC 20590
Attention: E. Sellman AEE-120

Rohr Corporation
P.O. Box 1516
Chuyla Vista, CA 92012
Attention: James C. Fuscoe

TRW Equipment
TRW Inc.
23555 Euclid Ave.
Cleveland, Ohio 44117
Attention: I. Toth

Federal Aviation Administration
12 New England Executive Park
Burlington, MA 18083
Attention: Jack A. Sain, ANE-200

Curtiss Wright Corporation
Woodridge, NJ 07075
Attention: S. Lombardo
S. Moskowitz

AVCO/Lycoming
550 S. Main Street
Stratford, CN 06497
Attention: H. Moellmann

Williams Research Co.
2280 W. Maple Road
Walled Lake, MI 48088
Attention: R. VanNimwegen
R. Horn

Teledyne CAE, Turbine Engines
1330 Laskey Road
Toledo, OH 43612
Attention: R.H. Gaylord

Pratt & Whitney Aircraft Group/UTC
Government Products Division
P.O. Box 2691
West Palm Beach, FL 33402
Attention: B.A. Jones

Boeing Commercial Airplane Co.
P.O. Box 3707
Seattle, WA 98124
Attention: P.E. Johnson MS 9H-46
D.C. Nordstrom MS-73-01

Brunswick Corporation
2000 Brunswick Lane
Deland, FL 32720
Attention: A. Erickson

Delta Airlines, Inc.
Hartsfield-Atlanta International Airport
Atlanta, GA 30320
Attention: C.C. Davis

FluiDyne Engineering Corp.
5900 Olson Memorial Highway
Minneapolis, MN 55422
Attention: J.S. Holdhusen

Massachusetts Inst. of Technology
Dept. of Astronautics & Aeronautics
Cambridge, MA 02139
Attention: Mames Mar

Detroit Diesel Allison Div. G.M.C.
P.O. Box 894
Indianapolis, IN 46202
Attention: W.L. McIntire

The Garrett Corporation
AIResearch Manufacturing Co.
Torrance, CA 90509
Attention: F.E. Faulkner

The Garrett Corporation
AIResearch Manufacturing Co.
402 S. 36 Street
Phoenix, AZ 85034
Attention: Library

General Electric Co./AEG
1000 Western Avenue
Lynn, MA 01910
Attention: R.E. Nietzel

Pratt & Whitney Aircraft Group/UTC
Commercial Products Division
East Hartford, CT 06108
Attention: W. Gardner (3 copies)
I. Mendelson

Douglas Aircraft Co.
McDonnell Douglas Corp.
3855 Lakewood Boulevard
Long Beach, CA 90846
Attention: R.T. Kawai Code 36-41
M. Klotzsche 36-41

AIResearch Manufacturing Co.
111 South 34th Street
P.O. Box 5217
Phoenix, AZ 85010
Attention: C.E. Corrigan
(930120/503-4F)

American Airlines
Maint. & Engrg. Center
Tulsa, OK 74151
Attention: W.R. Neeley

Lockheed California Co.
Burbank, CA 91502
Attention: J.F. Stroud, Dept. 75-42
R. Tullis, Dept. 74-21

Grumman Aerospace Corp.
South Oyster Bay Road
Bethpage, NY 11714
Attention: C. Hoeltzer